Changes in RNA regulatory processes during mammalian ageing

Submitted by Benjamin Pereira Lee, to the University of Exeter as a thesis for the degree of Doctor of Philosophy in Medical Studies, December 2019.

I certify that all material in this thesis which is not my own work has been identified and that no material has previously been submitted and approved for the award of a degree by this or any other University.

(Signature) …… 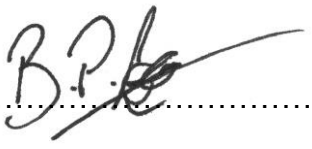 ……

Abstract

Ageing is defined as a system-wide, gradual loss in overall organ and tissue function across the lifespan of an organism, and in humans is the single largest risk factor for most chronic diseases. Thanks to ongoing improvements in healthcare, human life expectancy is steadily rising, but the proportion of life spent free of chronic disease (known as healthspan) is not extending concurrently in our increasingly aged population. Socio-economic costs are growing, both in terms of healthcare spending and quality of life. A central goal of ageing research therefore is to find methods of extending healthspan. However, ageing is a complex, heterogeneous process and the underlying mechanisms of ageing and determinants of lifespan/healthspan are still not well understood.

RNA regulators of gene expression are important factors in the ageing process, and I hypothesise that they may have potential to affect healthspan, or act as biomarkers of ageing. In this thesis, I have examined some of these RNA regulatory factors and their associations with ageing and lifespan in mammals. In order to do this, I assessed the expression patterns of RNA regulatory factors in two mouse models and a human cohort. In one mouse model, I found that both mRNA splicing regulatory factors and microRNAs are associated with strain-specific longevity during normal ageing, and that it is possible that these regulators play a causal role in determining strain lifespan. In the second mouse model, I showed these splicing factors to be associated with dietary restriction (a known treatment for extension of lifespan) and provided evidence that they could be mechanistically involved in the lifespan response to dietary restriction. I also showed that expression levels of these splicing factors were associated with cognitive decline and reduction in physical ability in humans.

These results indicate that correct RNA regulation is a key component of the ageing process and suggests that the factors that govern these processes may represent useful future targets for healthpan intervention in ageing people.

List of Contents

List of Tables

List of Figures

List of Supplementary Information

Author’s Declaration

Prior to submission of this thesis, each data chapter has been published in a primary research journal. As these publications are all collaborative works there are multiple named authors, however the author of this thesis is lead author on each of these publications and was responsible for the majority of each piece of work. In the interest of clarity, for each chapter a section is included detailing author contributions.

Abbreviations

ΔC_T	Delta C_T value
$\Delta\Delta C_T$	Delta Delta C_T value
3'	3-prime end of DNA or RNA molecule
5'	5-prime end of DNA or RNA molecule
18S	18S ribosomal RNA (*Mammalian)*
ABCR	ATP Binding Cassette Subfamily A Member 4
Acvr2a	Activin A Receptor Type 2A (*M.musculus*)
Ago2	Argonaute 2
AKAP17A	A-Kinase Anchoring Protein 17A (NB. Also known as Splicing Factor, Arginine/Serine-Rich 17A)
AL	*Ad libitum*
AMV	Avian Myeloblastosis Virus
ANCOVA	Analysis Of Covariance
ANKRD1	Ankyrin Repeat Domain 1
ATM	Ataxia Telangiectasia Mutated (*H. Sapiens*)
BER	Base Excision Repair
CDKN2A	Cyclin Dependent Kinase Inhibitor 2
cDNA	Complementary DNA
C. elegans	*Caenorhabditis elegans*
CHEK2	Checkpoint Kinase 2 (*H. Sapiens*)
CpG	Cytosine-phosphate-Guanine dinucleotide
C_{rt}	Cycle Relative Threshold
C_T	Cycle Threshold
daf-2	Abnormal Dauer Formation 2 (*C.elegans*)
daf-16	Abnormal Dauer Formation 16 (*C.elegans*)
dH_2O	Distilled Ultrapure Water
DNA	Deoxyribonucleic Acid
dNTP	Deoxynucleoside Triphosphate
DR	Dietary Restriction

ds-DNA	Double-Stranded DNA
Dusp5	Dual Specificity Phosphatase 5 (*M.musculus*)
EC	Endogenous Control
ECM	Extracellular Matrix
EDTA	Ethylenediaminetetraacetic acid
ENG	Endoglin
EPESE-SPPB	Epidemiologic Studies of the Elderly – Short Physical Performance Battery
ERCC6	ERCC Excision Repair 6, Chromatin Remodeling Factor
ERCC8	ERCC Excision Repair 8, CSA Ubiquitin Ligase Complex Subunit
ESE	Exonic Splicing Enhancer
ESS	Exonic Splicing Silencer
FDR	False Discovery Rate
Fgf7	Fibroblast Growth Factor 7 (*M.musculus*)
FN1	Fibronectin 1 (*H. Sapiens*)
FOXO/FoxO	Forkhead Box O1 (*H.Sapiens/M.musculus*)
FU3	Follow-up 3 of the InCHIANTI study of ageing
FU4	Follow-up 4 of the InCHIANTI study of ageing
Gabarapl1	Gamma-Aminobutyric Acid Receptor-Associated Protein-Like 1 (*M.musculus*)
GH	Growth Hormone
GOI	Gene Of Interest
GTP	Guanosine Triphosphate
GUSB/Gusb	Glucuronidase Beta (*H. Sapiens/M.musculus*)
hnRNP	Heterogeneous Nuclear Ribonucleoprotein
HNRNPA0/Hnrnpa0	Heterogeneous Nuclear Ribonucleoprotein A0 (*H. Sapiens/M.musculus*)
HNRNPA1/Hnrnpa1	Heterogeneous Nuclear Ribonucleoprotein A1 (*H. Sapiens/M.musculus*)
HNRNPA2B1/Hnrnpa2b1	Heterogeneous Nuclear Ribonucleoprotein A2/B1 (*H. Sapiens/M.musculus*)

HNRNPD/Hnrnpd	Heterogeneous Nuclear Ribonucleoprotein D (*H. Sapiens/M.musculus*)
HNRNPH3/Hnrnph3	Heterogeneous Nuclear Ribonucleoprotein H3 (*H. Sapiens/M.musculus*)
HNRNPK/Hnrnpk	Heterogeneous Nuclear Ribonucleoprotein K (*H. Sapiens/M.musculus*)
HNRNPM/Hnrnpm	Heterogeneous Nuclear Ribonucleoprotein M (*H. Sapiens/M.musculus*)
HNRNPUL2/Hnrnpul2	Heterogeneous Nuclear Ribonucleoprotein U Like 2 (*H. Sapiens/M.musculus*)
HR	Homologous Recombination
H. sapiens	*Homo sapiens*
IDH3B/Idh3b	Isocitrate Dehydrogenase (NAD(+)) 3 Non-Catalytic Subunit Beta (*H. Sapiens/M.musculus*)
IGF-1	Insulin-like Growth Factor 1
IIS	Insulin and Insulin-like Growth Factor Signalling Cascade
IL1B	Interleukin 1β (*H. Sapiens*)
IL6	Interleukin 6 (*H. Sapiens*)
IMP3	IMP U3 Small Nucleolar Ribonucleoprotein 3
ISE	Intronic Splicing Enhancer
ISS	Intronic Splicing Silencer
lincRNA	Long Intergenic Non-Coding RNA
LMNA	Lamin A/C (*H. Sapiens*)
lncRNA	Long Non-Coding RNA
LSM2	LSM2 Homolog, U6 Small Nuclear RNA And MRNA Degradation Associated
LSM14A	LSM14A MRNA Processing Body Assembly Factor
MAPK	Mitogen-Activated Protein Kinase 1 (*H. Sapiens*)
MAPT	Microtubule Associated Protein Tau
MGB	Minor Groove Binding domain
miRNA	MicroRNA

Mmp9	Matrix Metallopeptidase 9 (*M.musculus*)
M-MuLV or MMLV	Moloney Murine Leukemia Virus
MMSE	Mini Mental State Exam
mRNA	Messenger RNA
mtDNA	Mitochondrial DNA
mTOR	Mechanistic Target of Rapamycin (*H. Sapiens*)
mTORC1	Mechanistic Target of Rapamycin Complex 1
mTORC2	Mechanistic Target of Rapamycin Complex 2
M. musculus	*Mus musculus*
MYC	V-Myc Avian Myelocytomatosis Viral Oncogene Homolog (*H. Sapiens*)
NAD	Nicotinamide Adenine Dinucleotide
ncRNA	Non-Coding RNA
NER	Nucleotide Excision Repair
NFKB1	Nuclear Factor Kappa-light-chain-enhancer of activated B cells Subunit 1 (*H. Sapiens*)
NFQ	Non-Fluorescent Quencher
NF-κB	Nuclear Factor Kappa-light-chain-enhancer of activated B cells
NHEJ	Non-homologous End Joining
PCR	Polymerase Chain Reaction
piRNA	Piwi-Interacting RNA
PNISR/Pnisr	PNN Interacting Serine And Arginine Rich Protein (NB. New designation of SFRS18/Sfrs18) (*H. Sapiens/M.musculus*)
PolyA	Poly-adenine
PPIA/Ppia	Peptidylprolyl Isomerase A (*H. Sapiens/M.musculus*)
PPT	Purdue Pegboard Test
pre-mRNA	Precursor Messenger RNA
Pten	Phosphatase And Tensin Homolog
qRT-PCR	Quantitative Real-Time Polymerase Chain Reaction

Ran	Ras-related Nuclear Protein
RISC	RNA Induced Silencing Complex
RNA	Ribonucleic Acid
RNP	Ribonucleoprotein
ROS	Reactive Oxygen Species
Rps6ka3	Ribosomal Protein S6 Kinase A3 (*M.musculus*)
RT	Reverse Transcription
SASP	Senescence Associated Secretory Phenotype
siRNA	Small Interfering RNA
SF1	Splicing Factor 1
SF3B1/Sf3b1	Splicing Factor 3b Subunit 1 (*H. Sapiens/M.musculus*)
SFRS18/Sfrs18	Splicing Factor, Arginine/Serine-Rich 18 (NB. Nomenclature has changed to PNISR/Pnisr) (*H. Sapiens/M.musculus*)
Smad4	SMAD Family Member 4 (*M.musculus*)
snoRNA	Small Nucleolar RNA
snRNA	Small Nuclear RNA
snRNP	Small Nuclear Ribonucleoproteins
SR	Serine and Arginine Rich
SRSF1/Srsf1	Serine And Arginine Rich Splicing Factor 1 (*H. Sapiens/M.musculus*)
SRSF2/Srsf2	Serine And Arginine Rich Splicing Factor 2 (*H. Sapiens/M.musculus*)
SRSF3/Srsf3	Serine And Arginine Rich Splicing Factor 3 (*H. Sapiens/M.musculus*)
SRSF6/Srsf6	Serine And Arginine Rich Splicing Factor 6 (*H. Sapiens/M.musculus*)
SRSF7/Srsf7	Serine And Arginine Rich Splicing Factor 7 (*H. Sapiens/M.musculus*)
SS	Splice Site
STAT1	Signal Transducer And Activator Of Transcription 1 (*H. Sapiens*)

SYBR Green I	N',N'-dimethyl-N-[4-[(E)-(3-methyl-1,3-benzothiazol-2-ylidene)methyl]-1-phenylquinolin-1-ium-2-yl]-N-propylpropane-1,3-diamine
TAC	Taqman™ Array Cards
***Taq* polymerase**	*Thermus aquaticus* DNA polymerase
TGF-beta	Transforming Growth Factor Beta 1 (*H. Sapiens*)
T_m	Melting Temperature
TMT	Trail Making Test
TNF	Tumor Necrosis Factor (*H. Sapiens*)
TRA2β/Tra2β	Transformer 2 Beta Homolog (*H. Sapiens/M.musculus*)
TRP53	Tumor Protein P53 (*H. Sapiens*)
ULT	Ultra-Low Temperature
UTR	Untranslated Region
UV	Ultraviolet
VCAN	Versican (*H. Sapiens*)
VILO™	Variable In, Linear Out
WRN	Werner Syndrome RecQ Like Helicase
XPC	XPC Complex Subunit, DNA Damage Recognition And Repair Factor
Zfhx3	Zinc Finger Homeobox 3 (*M.musculus*)

Acknowledgements

I would firstly like to thank my supervisors, Professor Lorna Harries and Professor David Melzer, for giving me the opportunity to pursue this research, their invaluable guidance throughout the duration of my PhD, and for continuing to be excellent (and very understanding) line managers in my role as a part-time Research Technician during this time.

I must also thank my examiners; Professor David Elliot, Professor Katie Lunnon and my non-examining chair, Dr. Jon Brown. In part for agreeing to assess this work, but primarily for their patience - I realise that this thesis has been a very long time in the making.

I have had an amazing team around me which has been overwhelmingly helpful in ways too numerous to list. In particular the past and present members (and honorary members) of Team RNA; Laura Bramwell, Dr. James Brewer, Ryan Frankum, Shahnaz Haque, Dr. Alice Holly, Dr. Nicola Jeffery, Dr. Eva Latorre, Dr. Jon Locke, Jed Lye, Emad Manni, Dr. Luke Pilling, Dr. Cyrielle Tonneau, and all the other researchers at the University of Exeter who have played a part in my studies.

I must also thank the project students, placement students and technicians who I have had the pleasure of supervising and/or working alongside during their time with our team, and who helped generate parts of the data presented in this thesis; Greg Barr, Federica Bighi, Dr. Ivana Burić, Florence Emond, Jemma Garratt, Anupriya George-Pandeth, Emily Goodman, Dr. Robert Morse and John Watt.

This work would not have been possible without the many collaborations and generous provision of samples from fellow researchers at the Nathan Shock

Center of Excellence in the Basic Biology of Aging, the Institute of Biodiversity Animal Health & Comparative Medicine at the University of Glasgow and the InCHIANTI study of Aging, for which I am also very grateful.

I would also like to thank the funding bodies that enabled me to carry out this PhD. My studies have been generously supported by Exeter University Departmental funds, and the work contained in this thesis was funded from several sources: the NIH-NIA Intramural Research Program, the Wellcome Trust, the Velux Stiftung Foundation and the University of Glasgow.

Finally, I would not have been able to do any of this without the support of my long-suffering family, so this thesis is dedicated to Faith, Eleanor, Samuel, Ilda and Craig.

Chapter 1

Introduction

1.1 Impact of an ageing population

It is widely recognised that human life expectancy is increasing worldwide (Figure 1.1a)[1], and as a consequence there is a strong trend towards greater numbers of elderly individuals in the general population[1]. Although the lower-income countries lag behind those with higher income, the same trend is beginning to show in the projected figures for the year 2100[1]. Globally, this increase in numbers of the elderly is almost universally coupled with a downturn in birth rates, resulting in a progressively larger old-age dependency ratio (Figure 1.1b)[1]. The importance of this increase in the dependency ratio becomes apparent when we consider the socio-economic impact of a populace that is projected to be increasingly biased in numbers of older individuals. As can be seen in Figure 1.1c, according to the 2018 figures from the Office of Budget Responsibility, in the UK the overwhelming majority (≈75%) of expenditure in terms of health and adult social care is concentrated in the 65-and-over age group[2]. Given this fact, along with the predicted increase in the elderly and reduction in numbers of working-age individuals, it is not unreasonable to conclude that increased strain will be placed on healthcare providers and their funding systems in the foreseeable future.

Of course, the view presented above is purely economical and does not consider the human and quality of life aspects of such a change in demographics. There is little doubt that ageing is the largest single risk factor for a host of common ailments including cancer, cardiovascular disease, neurodegeneration etc.[3]; the observed trend towards increased numbers of more elderly individuals goes hand-in-hand with increased incidence of such diseases and so decreased quality of life.

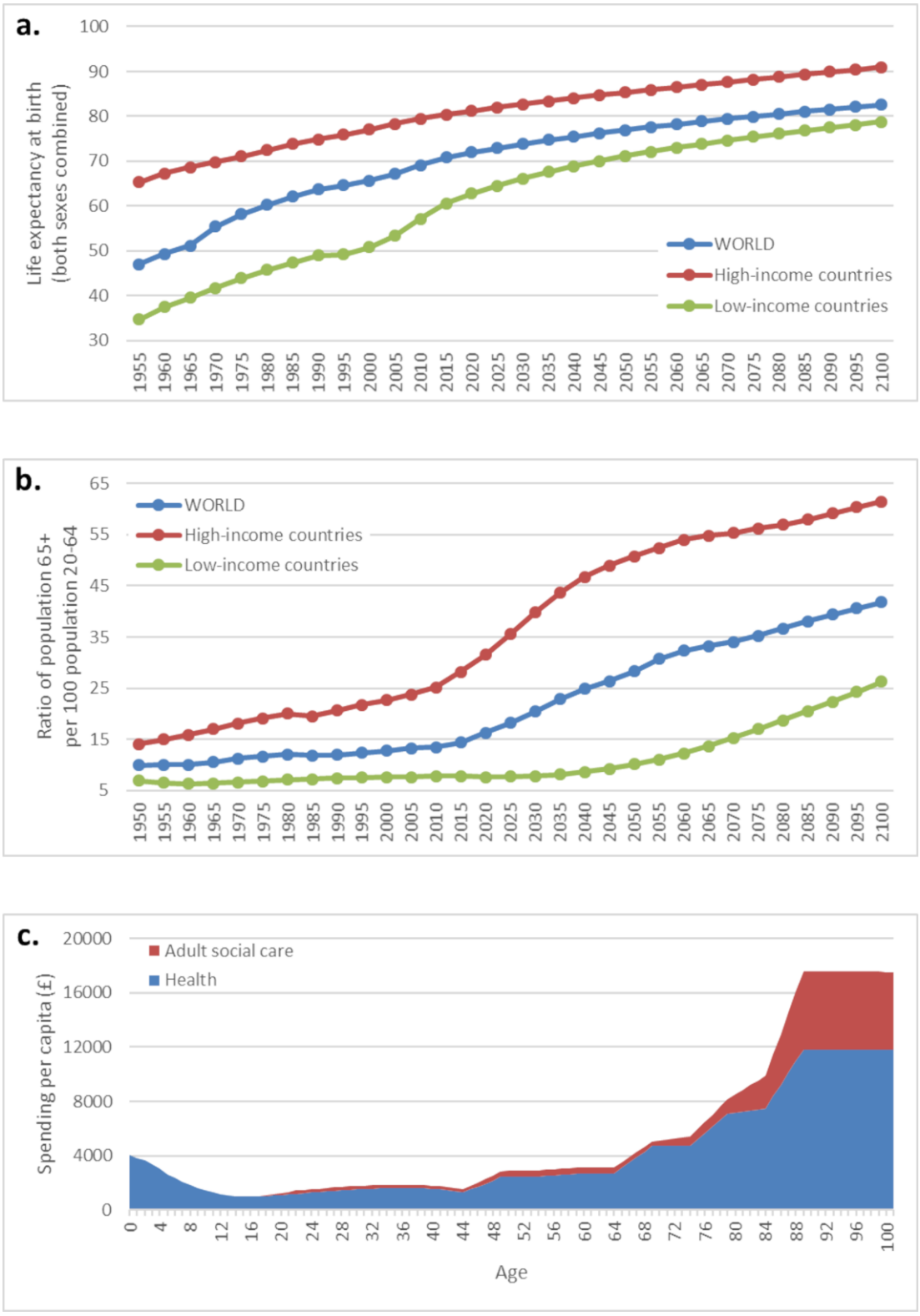

Figure 1.1: Historic and predicted population dynamics

Shown here are plots of worldwide life expectancy and dependency ratios, along with recent UK healthcare spending. Panel **a** shows worldwide life expectancy in years at birth from 1955 to 2100. Panel **b** shows worldwide dependency ratio calculated as the number of over 65s per 100 "working age" individuals (20-64 years old). Panel **c** shows stacked plots of 2018 figures for healthcare spending and adult social care spending by age group, in pounds per capita in the UK. Data for panels **a** & **b** were taken from the United Nations World Population Prospects 2017[1], while data for panel **c** were taken from the Office of Budget Responsibility (OBR) Fiscal Sustainability Report, July 2018[2].

Gerontologists have therefore been working for many years towards a greater understanding of the ageing process and the underlying determinants of later life health, in a bid to improve outcomes and potentially alleviate some of the future negative socio-economic impact.

1.2 Mechanisms of ageing

Ageing is generally defined as a progressive loss of physiological function leading to reduced survival and is a process which affects most living organisms[4]. However, the fact that there are some exceptions to this observation whereby certain species appear to show negligible ageing (data from AnAge database[5]), coupled with the fact that large amounts of variation in lifespan exist between biologically very similar organisms, rules out the idea that ageing is simply a result of wear-and-tear over time[6]. There is still debate surrounding the basic causes of ageing and discussion also continues into the reason why organisms age at all. Several theories exist which each go some way toward an answer to these questions. These theories are not mutually exclusive[7], and it seems plausible that a unifying theory of ageing mechanisms could include aspects drawn from many. In the next sections, I will discuss the development of evolutionary theories of ageing, followed by a brief description of the popular mechanistic hypotheses thought to contribute to ageing, grouped into the error-based theories and programmed theories.

1.3 Evolutionary theories of ageing

Theories relating to the evolution of ageing have been discussed since the mid-19th century shortly after the publication of Darwin's *On the Origin of Species*[8], since it was not immediately apparent how observations of ageing processes and

species-specific lifespan could comfortably fit Darwin's natural selection hypothesis. Around the turn of the century, August Weismann presented a series of hypotheses in an effort to explain ageing in the context of natural selection (reviewed by Kirkwood & Cremer[9]). His initial ideas were centred around species-level selection and proposed that once an individual had performed "its share in this work *[…towards the maintenance of the species…]* it has fulfilled its duty and it may die"[9]. This was later shown to be a somewhat circular argument and did not account for within-species selection, so is now largely disregarded as a workable theory. However, two of Weismann's central arguments proved to be pivotal to subsequent theories of ageing: the first was the recognition that there is a fundamental difference between the 'immortal' germ line and 'mortal' soma[10], while the second was the suggestion of a limit to the reproductive potential of somatic cells. His views were opposed by other scholars at the time and did not attain wide recognition, however although his theories were incomplete in certain respects, these concepts provided a basis for several strands of the later theories of ageing, including disposable soma, programmed longevity and replicative senescence (see sections 1.3.3, 1.5.1 and 1.6.1).

Modern evolutionary theories of ageing generally fit into one of three categories; mutation accumulation, antagonistic pleiotropy and disposable soma. Although there have been a number of refinements to these theories, the basic arguments as initially described in each case are still valid.

1.3.1 Mutation accumulation

In the years following Weismann's death in 1914, few hypotheses regarding the mechanism of ageing were proposed, and it was not until 1952 that a further in-depth examination of the evolution of ageing was undertaken by Peter Medawar.

In a lecture given at University College London (later published as 'An Unsolved Problem of Biology'[11]), he proposed a theory which underpins all modern evolutionary theories of ageing, in that the forces of natural selection decline with age, particularly after the organism has reached an age at which it would have the ability to reproduce.

The basic premise is that since all organisms will eventually die, whether through disease, starvation, cold, predation, accident etc., traits conferring an early-life advantage will be actively selected for, rather than those with late-life beneficial effects, simply due to progressively smaller numbers of individuals on which natural selection can act. He also argued that this effect would only be apparent after reaching reproductive age, as natural selection can only act upon inherited traits. For example, a mutant allele causing death before reproductive age would be very strongly selected against, as few (if any) individuals would survive long enough to pass this to their offspring, whereas a mutant allele with fatal effect after reproduction would have reduced selection pressure upon it, as it would be inherited by the offspring and would thus only affect the organism's ability to have more descendants.

In short, Medawar suggested that declining survivorship and fertility during normal lifespan causes selection forces to progressively weaken until there is little or no opposition to the accumulation of mutant alleles with deleterious effects in late life, and that ageing is effectively a by-product of the build-up of these late-acting harmful mutations.

1.3.2 Antagonistic pleiotropy

George Williams' paper of 1957[6] expanded on Medawar's hypothesis, adding the concept of antagonistic pleiotropy. Pleiotropy occurs when one gene affects two

seemingly unrelated traits. In the context of antagonistic pleiotropy in relation to ageing theory, a special kind of effect is assumed whereby an allele of a gene has opposite effects on evolutionary fitness at different ages. With this assumption in mind alongside Medawar's idea of selection pressure declining over time, it becomes evident that an allele which has a beneficial early-life effect would be positively selected for despite any late-life deleterious effects, and vice versa. Logically, this would lead to a similar accumulation of late-life harmful effect alleles as proposed in Medawar's theory, but also provides a more robust explanation for the persistence of such harmful alleles in a population. Several genes have since been shown to act in this manner, with late-life links to increased risk of cancer, Huntingdon's disease and osteoporosis but early-life advantages in terms of increased fertility and decreased risk of other illnesses[12].

1.3.3 Disposable soma

The disposable soma theory of ageing was first proposed in the late 1970s by Thomas Kirkwood[13,14], although the basis of his theory owes something to the earlier ideas of Weismann, Medawar and Williams. This hypothesis relies on recognition that somatic cells and reproductive cells in a multicellular organism have diverging requirements in order to maximise whole-organism fitness. Effectively this can be thought of as the soma playing a support role in order for the reproductive cells to fulfil their ultimate purpose of continuing the germ line through reproduction. A second observation fundamental to the disposable soma theory is that organisms have a requirement to allocate resources in such a way that maximises their evolutionary fitness.

Given that each individual somatic cell has a limited life expectancy (as proposed by Medawar) and upon death all the resources invested into it are lost, logically

the amount of investment in the repair and maintenance of the soma will be some amount less than that required for it to last indefinitely. The optimal amount of investment will vary from species to species depending on the surrounding environment, but in all cases too low an investment will result in degradation of the soma before reproduction has taken place (which is clearly an unacceptable outcome in terms of fitness), while any investment in maintaining the soma over and above that required for it to reach its expected lifespan confers no additional advantage. In the latter situation it would actually improve overall fitness to reduce investment in somatic maintenance and use those resources elsewhere, for example faster growth or increased fecundity.

As with the preceding theories of ageing, the disposable soma hypothesis predicts that ageing is a result of an accumulation of harmful late-life traits, although it arrives at this point through a different mode of action, i.e. accumulation of cellular damage due to reduced maintenance rather than differential selective pressures on harmful alleles.

1.4 Error-based theories of ageing

1.4.1 Rate of living

The rate of living hypothesis is based on the observations made in 1908 by Max Rubner[15] that the lifespan of mammals increases with size, and that mass-specific metabolic rates decrease with size. Formalised by Raymond Pearl in 1928[16], the theory states that lifespan and metabolic rate are inversely correlated due to a limited supply of “inherent vitality” being available throughout life. While this theory still holds some attraction thanks to its apparent logic, there are many examples of animals which do not conform to the proposed negative correlation

between metabolism and lifespan[17], casting doubt on the validity of this theory as originally presented by Pearl. However, there have been substantial refinements to the basic theory which have led to the more widely accepted free radical and oxidative stress theories of ageing as I will discuss in the following sections.

1.4.2 Free radicals

In 1956, Denham Harman proposed a mechanism which could potentially explain the observations underlying the rate of living theory without relying on the assumption of a finite lifetime supply of energy. He argued that oxygen free radicals produced during normal metabolic oxygen consumption cause damage to biological molecules (proteins, nucleic acids and lipids etc.), leading to ageing and ultimately death through accumulation of this oxidative damage[18]. The fact that the production rate of free radicals is strongly correlated with metabolic activity provided the necessary link to the rate of living theory, however Harman's mechanistic insight did not address any of the shortcomings of the rate of living theory discussed in section 1.4.1.

1.4.3 Oxidative stress

The oxidative stress theory builds upon the free radical concept but includes some important refinements. Firstly, the recognition that other reactive molecules produced by normal metabolism can also cause oxidative damage; these damaging molecules along with the free radicals are collectively termed reactive oxygen species (ROS). Secondly, the fact that organisms have mechanisms to both prevent and repair oxidative damage caused by ROS[19]. These additional considerations give the oxidative stress model greater capacity to explain observations of ageing and lifespan, although a number of exceptions exist where this theory does not hold true[15]. Further research in this field has implicated

membrane fatty acid composition as a potential determinant of distinct species lifespans, which is plausible given the known variability in sensitivity to oxidative damage shown by different fatty acids[15,20].

1.4.4 Protein damage and autophagy

Protein damage has often been postulated as a driver of the ageing process. Perhaps the earliest instance is the cross-linking theory of Johan Bjorksten, originally proposed in the early 1940s and expanded in later work[21,22], essentially arguing that intra- or inter-molecular bonds between macromolecules (with particular reference to proteins) formed either through the action of naturally occurring small molecules or direct reaction between molecules, would lead to a build-up of immobilised, non-functional proteins, resulting in the ageing phenotype.

Leslie Orgel later developed a theory encompassing both DNA and protein machinery[23,24] which stated that errors in proteins (particularly those involved in translating genetic information) could potentially reduce their specificity, thereby causing increased error rates in subsequent protein synthesis. This would produce a positive feedback loop, eventually leading to an “error catastrophe” situation at which point the cell would no longer be viable. While careful not to claim that it was the direct cause of organismal ageing, he argued that this loss of viability could be contributing to the ageing process.

Since these early theories, there has been less focus on protein damage as a central cause of ageing in and of itself (indeed Orgel’s hypothesis has largely been disproven through experimental testing), however it is widely recognised that loss of proteostasis is a key element of the ageing phenotype[25] and also plays a major role in many age-related diseases[26].

One important aspect of the proteostasis network implicated in ageing and lifespan is autophagy – an evolutionarily conserved protein degradation system in eukaryotic cells allowing for the destruction of unnecessary or damaged cellular components[27]. In model organisms, autophagy has been found to decline with age, and experimental over- or under-expression of key components of the autophagy machinery have been shown to respectively increase or decrease lifespan (reviewed by Bareja *et al.*[28]), all of which suggests that autophagy is an important influence in the ageing phenotype.

1.4.5 DNA damage

Since DNA is central to all life, it was inevitable that it should be implicated in the ageing process. The first mentions of DNA having a role in the context of ageing were in a 1958 paper by Gioacchino Failla[29] and another a year later from Leo Szilard[30] which introduced the idea that DNA could potentially play an important role in ageing, however these early theories focused entirely on DNA mutations as the potential ageing mechanism.

It was later recognised that DNA alterations could take two distinct forms, and have varying effects dependant on the severity and genomic location[31-33]:

1. Mutations; defined as changes in the nucleotide sequence (deletions, insertions, substitutions or rearrangements) which can lead to functional changes to proteins.
2. DNA damage; defined as a change to the structure of the DNA molecule, which can cause changes to gene expression and cellular function, impairment of transcription, cell cycle arrest and can in certain cases lead to apoptosis.

The realisation that DNA damage (as described in point 2) can also lead to mutations during the process of DNA repair and/or replication led to an expansion in the framework of the DNA-oriented theories of ageing and a shift towards the now more widely accepted DNA damage theory of ageing (reviewed by Gensler & Bernstein[31], Vijg & Dollé[32], Hoeijmakers[33], Freitas & de Magalhães[34] and Ou & Schumacher[35]).

DNA damage can be caused by both exogenous influences, including chemicals, radiation, viruses etc. as well as endogenous factors such as spontaneous chemical reactions and ROS[34]. Damage can take the form of abasic sites, inter- and intra-strand crosslinks, bulky chemical adducts, UV-induced photoproducts, deamination or oxidative modifications of bases and DNA strand breaks. All of these types of damage have the potential to induce mutations through incorrect repair or replication of the damaged DNA, which can lead to cancer, cell-cycle arrest, senescence or apoptosis. It is also possible for certain types of DNA damage to act as barriers to transcription or arrest replication, which can cause cell death or senescence[33,34].

While it is estimated that many thousands of instances of DNA damage occur in every human cell on a daily basis[36], it is also the case that several highly conserved and effective DNA repair mechanisms exist to rapidly deal with the damage, maintaining genomic integrity within the cell thereby avoiding apoptosis or senescence. These include non-homologous end joining (NHEJ), homologous recombination (HR), base excision repair (BER), nucleotide excision repair (NER) and several other more specialised mechanisms (all of these genome maintenance pathways have been reviewed in depth by Hoeijmakers[33], Freitas & de Magalhães[34] and Ou & Schumacher[35]).

There is a compelling case for DNA damage to be regarded as a factor in the ageing process. Experiments in both model organisms[37] and in humans[38] have shown that DNA damage accumulates during life, and there is also evidence that activity of DNA repair pathways declines with age[39]. It is also notable that defective DNA repair genes are implicated in all known diseases characterised by accelerated ageing (known as progeroid syndromes). Werner Syndrome, Hutchison-Gilford Progeria, Xeroderma Pigmentosum, Bloom Syndrome, Cockayne Syndrome, Ataxia Telangiestasia and several others are all characterised by progeroid phenotypes, and in each case the gene(s) disrupted are known to be either directly involved in, or closely linked to, DNA repair pathways[39]. Finally, there have been numerous experiments showing that manipulation of genes in these pathways can cause changes in ageing and/or lifespan phenotypes in model organisms[39] lending further weight to the argument that DNA damage plays a significant role in the mechanisms of ageing.

All the above arguments refer to the nuclear DNA complement, however there is also some evidence that DNA damage in the mitochondrial genome (mtDNA) may also play a part in the ageing process. It has been shown that mtDNA mutations increase with age and that transgenic mice engineered for artificially high mtDNA mutation rates show shortened lifespan and premature ageing phenotypes. That being said, there is still debate as to whether such mtDNA damage is a causal factor or simply correlated with ageing[40].

1.5 Programmed theories of ageing

1.5.1 Programmed longevity

The idea of programmed longevity relies on the assumption that the declines seen in function and reproductive capacity during ageing are the result of genetically predetermined processes (in a similar manner to early life developmental processes) and therefore must fulfil some adaptive role in order to be favoured by natural selection[41]. Arguments in favour of an evolutionary advantage conferred by ageing as a fixed programme usually revolve around a perceived need to prevent over-population, to remove older individuals that may compete for resources with younger (fitter/more fertile) kin, or to promote turnover of generations, thus enhancing evolutionary change[42].

The theory of programmed longevity can be traced back to the work of Weismann[9] and his assertion that the contribution to survival of the species (i.e. reproduction) is the overriding reason for the existence of the individual. In general however, most gerontologists do not subscribe to the idea of programmed longevity as the fundamental mechanism of ageing due to its reliance on species-level or group-level selection, which is accepted to be a weaker evolutionary force than selection at the individual level[43].

Programmed longevity is an attractive premise as it offers a simple explanation for the observation that ageing is essentially universal and appears to be relatively uniform in its effects within species. It also theoretically allows for the existence of clearly defined ageing genes or pathways which could potentially be switched off, thereby opening the door to the concept of a ‘magic bullet’ cure for ageing which has its own rather obvious appeal[44]. However, it remains a

controversial standpoint, generating a huge amount of debate and little consensus between proponents from both sides of the argument[41,42,44-49].

1.5.2 Endocrine system

It has long been known that hormonal regulation is imperative to the maintenance of homeostasis and stress responses, and that during the ageing process there is a functional decline of the endocrine system in terms of hypothalamic sensitivity and responsiveness, hormone production and tissue sensitivity to hormonal signals[50-52]. Based on this knowledge, Vladimir Dilman proposed the Neuroendocrine Theory of Ageing[53,54] in which he argued that the ageing phenotype is driven by this decline in function, and by extension the loss of homeostasis caused by the decline. However, he also postulated that the progressive deterioration of endocrine function is a continuation of the necessary deviation from homeostasis required for growth and development during early life, and so can be categorised as a programmed cause of ageing. While Dilman's somewhat controversial theory is not widely accepted as likely to be a fundamental cause of ageing, there is ample evidence that the endocrine system has an critical role in the ageing process[55].

Age-related changes in levels of sex hormones are of course associated with the menopause in females and the less dramatic andropause in males, both of which have been linked to increased risk of several chronic diseases common in the elderly including osteoporosis, heart disease and declining cognitive function. Decreases in adrenal steroid hormones have been correlated with conditions such as depression, type 2 diabetes and Alzheimer's disease. Dysfunction of hormone production by the thyroid also results in increased risk of certain pathologies, e.g. atrial fibrillation, reduced bone-mineral density and dementia[56].

However, the most persuasive evidence for endocrine involvement in the underlying mechanisms of ageing is found in the nutrient sensing pathways:

1. Insulin and insulin-like growth factor signalling

The 'insulin and insulin-like growth factor signal cascade' (usually shortened to Insulin/IGF-1 signalling or IIS) is a well conserved system which regulates growth, metabolism and stress resistance in response to nutrient availability[57,58]. This pathway was first linked to ageing and lifespan in *Caenorhabditis elegans*; it was found that mutations in *daf-2* (an IIS receptor ortholog), in the presence of a functional *daf-16* gene (a downstream FOXO-family transcription factor which regulates hundreds of genes involved in stress resistance, immune function and metabolism[58]), led to a doubling of the animals' lifespan[59]. It was later shown that mutations in IIS receptor orthologs in *Drosophila melanogaster* and mice resulted in similar lifespan increases[60-62]. In mammals, IGF-1 production is regulated by growth hormone (GH) (which does not have an ortholog in the simple model organisms), and several mutant mouse strains exist with reduced GH signalling, all of which display increased lifespan[63]. Additionally, both upstream regulators and downstream effectors of the IIS have been shown to affect lifespan and the ageing process in model organisms[57].

2. Mechanistic target of rapamycin

The mechanistic (formerly "mammalian") target of rapamycin (mTOR) is a serine/threonine kinase which acts as the catalytic subunit in two protein complexes, mTOR Complex 1 (mTORC1) and mTOR Complex 2 (mTORC2)[64]. These two complexes have somewhat different functions; mTORC1 regulates protein synthesis, lipid, nucleotide and glucose metabolism, as well as protein turnover in response to levels of growth factors, nutrients, oxygen and DNA

damage. mTORC2 is involved in the regulation of other kinases in several pathways related to proliferation and survival, primarily in response to signals from the IIS. Both complexes are central effectors in a number of pathways critical to cell growth, proliferation and survival[65].

Once again, experiments in *C. elegans* first indicated that mTOR was involved in the ageing process, where it was found that RNAi knockdowns of the mTOR ortholog, *let-363,* more than doubled the worms' lifespan[66]. Subsequently, mutations in mTOR and other components of the mTORC1 pathway, as well as the use of rapamycin to directly target mTOR were shown to extend lifespan in yeast, fruit flies and mice (reviewed by Johnson *et al*.[64]). Finally, it has been shown that mTOR signalling is involved in the lifespan increases seen with dietary restriction in model organisms[65,67,68].

1.5.3 Immunosenescence and inflamm-ageing

Age-related changes in the immune system are well documented[69], and the progressive decline in naïve cells coupled with the increase in memory cells during this process would appear indicative of a 'programmed' function in ageing. These changes bring reduced ability to respond appropriately to infections and cancer, impaired wound-healing capacity and a predisposition towards increased tissue inflammation[70]. While the idea of a progressively weakening immune system would appear to be a reasonable mechanism for the development of ageing phenotypes *per se*, it is actually the case that few morbidities can be directly attributable to infection in the elderly and many age-related diseases start in young to middle age while the immune system remains efficient[71].

More likely as a direct candidate for mechanistic involvement in the ageing process is the chronic, sterile, low-grade inflammation seen during advancing

age, known as inflamm-ageing[72]. Certainly inflamm-ageing is a risk factor for many age-related diseases, e.g. heart failure, atherosclerosis, obesity, diabetes and neurodegenerative conditions[73], however there is ample evidence that the increasing inflammatory background associated with advancing age is at least in part a product of senescent cells[74] (see also section 1.6).

Once again, it is not clear whether immunosenescence and inflamm-ageing can be classified as root causes of the ageing phenotype, however they undoubtedly play an important role in the process.

1.6 Cellular senescence

In most of the mechanisms outlined above, the late-life accumulation of deleterious traits is thought to manifest a negative effect (at least partially) through cellular senescence. Cellular senescence is defined as a permanent† state of cell-cycle arrest in response to different damaging stimuli[75]. The basic premise was first proposed by Weismann, who suggested the existence of a limit to the reproductive potential of somatic cells[9], but it was not until Leonard Hayflick and Paul Moorhead showed this experimentally in their 1961 paper[76], and coined the term ‘cellular senescence’, that the idea became more widely accepted.

Senescent cells are known to be important in several biological processes, i.e. tumour suppression, wound healing, tissue repair and embryonic development, but in all these cases the presence of senescent cells is transient, and the cells are subsequently cleared by the immune system. During ageing however, there is a gradual accumulation of senescent cells, which is thought to be a potential source of late-life deleterious effects[74].

† This is the classical definition of senescence. As I will discuss in section 1.7.2, recent research from our group calls the permanence of senescence into question.

Apart from the suspension of the cell-cycle, senescence is characterised by altered cellular morphology, gene expression, metabolism, epigenome and secretory phenotype[77]. The senescence associated secretory phenotype (SASP) is a cocktail of pro-inflammatory cytokines, chemokines, growth factors and extracellular matrix-degrading proteins[78] which is thought to serve as a signal to enable immune clearance of senescent cells and/or promote tissue repair[77], however chronic SASP has been shown to induce senescence in neighbouring young cells as well as promoting chronic inflammation and tissue dysfunction[79]. Senescence can also affect cells that are normally non-proliferative (neurons, cardiomyocytes etc.) and while cell-cycle arrest is obviously not a defining feature of senescence in these cell types, they can display the other features of senescence, including secretion of SASP[80].

These features of senescent cells make them a good candidate for a driver of the ageing process as first proposed by Hayflick and Moorhead[76], however it was not until the emergence of two pieces of work by Darren Baker in 2011 and 2016 that this idea was supported empirically. In his first set of experiments, a novel transgene was introduced into BubR1 progeroid mice allowing drug-inducible selective elimination of senescent cells. Life-long removal of senescent cells resulted in delayed onset of age-related disorders, while late-life removal attenuated the progression of existing age-related pathologies[81]. In his later work using the same transgenic system, it was found that clearance of senescent cells in wild-type mice resulted in extended median lifespan and delayed the age-related deterioration of several organs[82].

Senescent cells have been implicated in a variety of age-related diseases, including cardiovascular disease, idiopathic pulmonary fibrosis, chronic obstructive pulmonary disease, insulin resistance, macular degeneration and

many more[83,84]. Along with the experimental evidence as described in the previous paragraph, there is a strong case for cellular senescence having a central role in the mechanism of ageing.

1.6.1 Replicative senescence

Replicative senescence, as originally described by Hayflick and Moorhead, is the suspension of cell cycle due to serial passage of cells in culture[76,85], however in their works at the time no mechanism was described for this phenomenon. It was later discovered that telomere length plays an important role in senescence, both *in vitro* and *in vivo*[86,87]. Telomeres are non-coding chromosomal 'caps' consisting of hundreds to thousands of TTAGGG repeats which, along with specific telomere-associated proteins, serve to protect the ends of chromosomes[88]. In most mammalian cells (with the notable exception of the germ-line cells), telomere length is genetically determined during development and is not extended during adulthood due to stringent repression of telomerase, a specialised ribonucleoprotein responsible for telomere maintenance and extension[89]. Successive rounds of cell division therefore result in gradual shortening of the telomeres, eventually leading to disruption of the protective cap which in turn elicits a DNA damage response, leading to cell-cycle arrest and senescence[87].

1.6.2 Stress-induced senescence

Senescence can also be induced by factors other than repeated cell divisions. Stressors such as DNA damage, oxidative stress and expression of oncogenes have all been shown to cause premature senescence through activation of the p53/p21 or p38/p16/Rb cell cycle arrest pathways[90-93]. It was originally thought that these causes were independent of telomere length, however more recent

evidence suggests that the routes to replicative and stress-induced senescence are not mutually exclusive[93].

1.7 The Hallmarks of ageing

1.7.1 Current perspective

In a landmark paper published in 2013, Carlos López-Otin *et al.* described a set of molecular and cellular hallmarks of ageing in an effort to outline the defining characteristics of ageing and the mechanisms involved[94]. The authors used a specific set of criteria to determine these hallmarks, as follows:

1. Each hallmark should manifest during normal ageing.
2. Each hallmark should accelerate ageing when experimentally aggravated.
3. Each hallmark should retard ageing when experimentally ameliorated.

The hallmarks that they identified as fulfilling all these criteria are summarised in Figure 1.2.

I have already described most of these hallmarks as they fall under one or more of the theories of ageing in the preceding sections, with the exception of ‘Epigenetic alterations’ and ‘Stem cell exhaustion’, which I shall address briefly here:

1. Epigenetic alterations

Several different epigenetic alterations have been implicated in the ageing process; however, these largely appear to exert their effects through one of the mechanisms described above.

Histone modifications meet the criteria for a hallmark, however they appear to act through regulation of genes in the IIS pathway described in section 1.5.2[95]. The

sirtuin class of deacetylases, which act on histone markers, have also been implicated in determination of lifespan, although again they seem to exert their influence through pathways such as IIS, NF-κB signalling, glucose homeostasis and genomic stability[94].

Figure 1.2: Hallmarks of ageing

The nine hallmarks of ageing proposed to determine the ageing phenotype, as described in Carlos López-Otin's 2013 publication (reproduced from López-Otin *et al.*[94], with permission from Elsevier; © 2013).

Patterns of DNA methylation at CpG dinucleotides change significantly during ageing. These changes are remarkably consistent to the extent that they can be used to predict biological age from the methylation status at a relatively small

subset of CpG sites. In 2013, Steve Horvath used this predictable shift in DNA methylation to develop an epigenetic clock[96] algorithm, which is highly accurate in its predictions of age across multiple tissues, using information from just 353 CpG sites. Other epigenetic clock models have since been developed with varying levels of accuracy in different tissues[97], and DNA methylation has also been found to be a promising marker for estimation of the number of stem cell divisions in tissues, a metric known as the 'mitotic clock', which is useful in both estimation of tissue ageing and also for predicting cancer risk[98]. However, while it is true that DNA methylation is strongly correlated with advancing age and may be seen to play an important role in the ageing process, it would appear to do so through the regulation of gene expression (see section 1.8.2). For example, around half of the 353 CpGs used in Horvath's clock are in gene promoter regions, and the remainder are in enhancer sequences[97]. It is also the case that there is currently no compelling evidence that these patterns of methylation change directly affect lifespan.

A number of microRNAs (miRNAs) have also been shown to associate with lifespan[99] (see also chapter 4[100]), however by the very nature of miRNAs as regulatory non-coding RNAs, their method of action is through the modulation of other mechanistic pathways. I discuss these in more detail in section 1.8.9.

2. Stem cell exhaustion

Declining ability to regenerate tissues is a defining characteristic of the ageing process, and one that is largely driven by reduced competence of stem cells. While this is without doubt a highly important factor in the development of age-associated phenotypes, the loss of stem cell capacity is thought to be driven by one or more of the age-associated damages as described previously[94].

1.7.2 Adding a 10th hallmark: Altered control of gene expression.

Our group's research and the work contained within this thesis have brought us to the conclusion that a 10th hallmark could potentially be added to the list as described by López-Otin *et al.*, namely 'Altered control of gene expression'.

Although altered control of gene expression is, to an extent, implied in the 'Epigenetic alterations' hallmark, we feel that it fulfils the criteria (as laid out in López-Otin's paper) in its own right.

It has been found in several studies that changes in levels of key regulators of gene expression are associated with normal ageing[101-103], lifespan (see chapters 3[104], 4[100] and 5[105]) and with future age-related clinical outcomes (chapter 6[106]). Much of our group's work has focused specifically on the factors regulating alternative mRNA splicing (see section 1.8.4), and we have also shown that it is possible to restore replicatively senescent cells to an apparently more youthful, proliferative state through modulation of splicing factor expression using resveratrol and its analogues, as well as specific hydrogen sulphide donors[107,108]. Given this evidence, it seems that there is a strong case for altered control of gene expression to be included as one of the fundamental hallmarks of ageing.

1.8 Control of gene expression

Not only does the control of gene expression satisfy the criteria of a hallmark of ageing, it is also known to be a key player in the development of ageing phenotypes. Adaptive, plastic patterns of gene expression are vital to maintenance of homeostasis and to effective cellular responses to stress[109], which are known to be highly important factors in the ageing process[110,111].

There are several ways by which gene expression can be regulated, which I will describe in turn:

1.8.1 Histone modifications

Human genomic DNA is packaged in the nucleus as chromatin, a highly compacted state necessary to retain order and enable the entire genome to fit inside. The basic unit of chromatin is the 'nucleosome core particle', in which 145-147 base pairs of DNA are wrapped around an octamer of histone proteins[112]. Nucleosomes tend to block transcription either physically or by making sections of DNA unavailable for transcription factor binding, however mechanisms exist which can alter nucleosome positioning and thus affect gene expression[113]. Apart from these remodelling mechanisms, individual histones can be post-translationally modified in many ways including methylation, acetylation, phosphorylation etc. which are able not only to affect gene expression, but can also have other downstream effects on pathways such as DNA repair and apoptosis[112].

1.8.2 DNA methylation

DNA methylation is well known to affect gene expression. The majority of DNA methylation in mammals can be defined as the presence of a methyl group on the cytosine of a CpG dinucleotide. CpGs tend to be concentrated in CpG islands, found commonly around promotor sites. CpG islands are predominantly hypomethylated in the case of actively transcribed genes and conversely are hypermethylated when a gene is silenced[114]. There is also increasing evidence that DNA methylation within the gene body can also impact on gene expression[115].

1.8.3 Transcriptional regulation

An important aspect of gene expression lies in the control of transcription of the genomic DNA to RNA. This can be at the level of chromatin state and thus availability of a gene for transcription[112], sequence and strength of promoter elements[116], DNA polymerase activity[117], presence or binding of transcriptional enhancers[118], genomic landscape[119] and post-transcriptional alterations[120]. The fact that such levels of fine control over expression exist is testament to the vital role that tight regulation of expression plays in maintenance of a stable cellular environment while also allowing for adaptive responses to external challenges.

1.8.4 mRNA processing

Once transcribed, a precursor mRNA (pre-mRNA) must be processed into a mature mRNA for correct and efficient translation. The DNA templates (and therefore the transcribed pre-mRNAs) of the vast majority of eukaryotic genes contain both non-coding intronic sequences and coding exonic sequences. In order to produce a mature mRNA, the introns must be removed by RNA splicing, a 5' cap is added, and the molecule is polyadenylated via addition of a polyA tail at the 3' end (see Figure 1.3). All these steps are subject to regulatory processes that can impact the eventual expression profile of the gene[121-123].

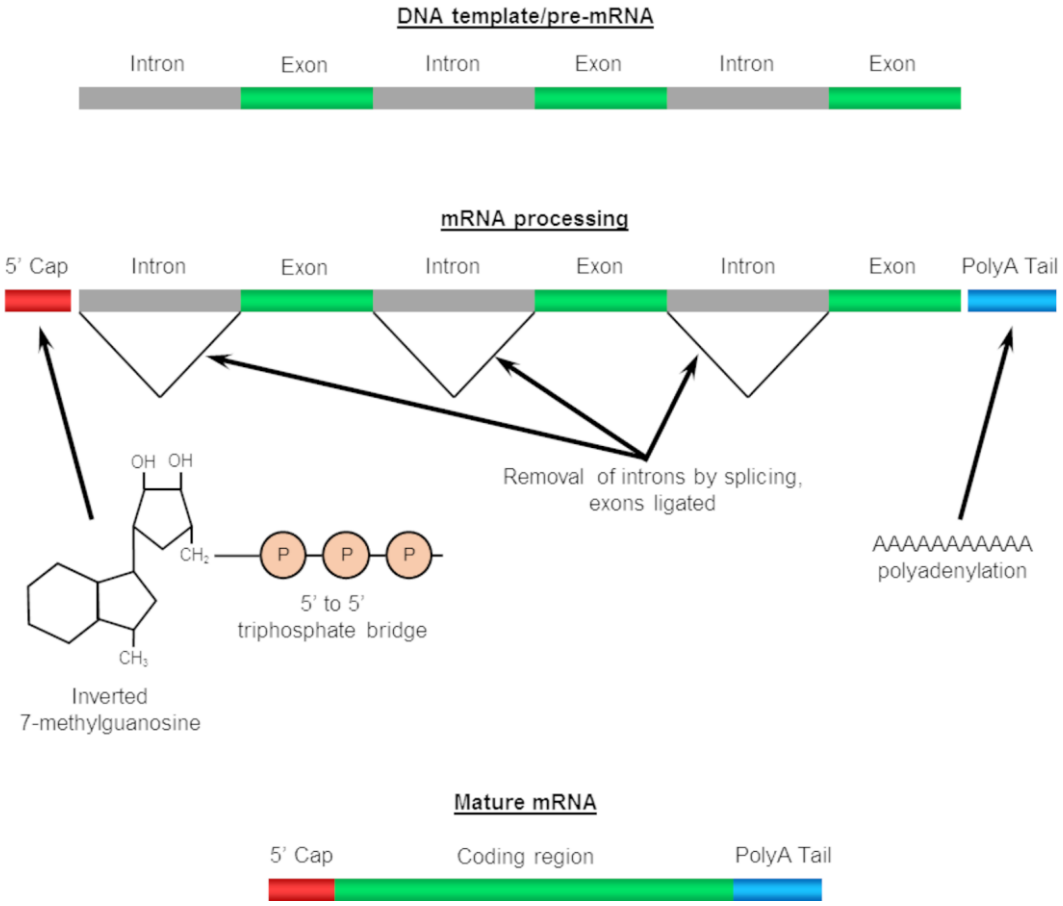

Figure 1.3 mRNA processing

Shown here are the steps involved in processing of a pre-mRNA transcript to a mature mRNA molecule; removal of introns by splicing, addition of 5' cap and polyadenylation.

1.8.5 RNA splicing

As mentioned in section 1.8.4, most eukaryotic genes contain non-coding introns which are spliced out during mRNA processing, and the coding exons are ligated to form the mature mRNA. RNA splicing is catalysed by the spliceosome, a large, dynamic ribonucleoprotein (RNP) complex which is recruited to splice sites through recognition of short, highly conserved sequences at the 5' splice site (SS), 3' SS, branch site and polypyrimidine tract[124,125]. Splice site choice is also determined by a set of *cis*-acting auxiliary splice site elements and *trans*-acting

splicing factors which act to increase or decrease the likelihood of a particular splice event going ahead. The *cis*-acting sequence elements are known as exonic splicing enhancers (ESE), exonic splicing silencers (ESS), intronic splicing enhancers (ISE) and intronic splicing silencers (ISS). The *trans*-acting splicing factors are split into two classes, the serine/arginine rich (SR) proteins and the heterogeneous nuclear ribonucleoproteins (hnRNP). Generally, the SR proteins bind to ESE and ISE sequences and are splice enhancing, while the hnRNPs bind to ESS and ISS sequences and are splice inhibitory. However, there are incidences where these splicing factors can in fact exert effects in the opposite direction, indeed it is usually the combinatorial effect of binding multiple different splicing factors (both enhancers and inhibitors) and thus the exact balance achieved at any given splice site that ultimately determines the outcome of the splicing event[126].

There are in fact two spliceosome complexes in eukaryotes, the U2-dependent and the U12-dependent spliceosome. The U12-dependent spliceosome is often referred to as the 'minor' spliceosome, as U12-type introns account for less than 0.5% of introns in any given genome[127]. While slightly less efficient than U2-dependent splicing, the U12-dependent spliceosomal components are analogous and the reaction occurs in a similar manner. For this reason, I will focus on the U2-dependent spliceosome in this text.

1.8.6 The spliceosome and catalysis of splicing

The U2-dependent spliceosome is assembled from five uridine-rich small nuclear ribonucleoproteins (snRNPs) known as U1, U2, U4, U5 and U6, along with a large number of non-snRNP proteins. The assembly is a multi-stage process with several remodelling and conformational changes throughout, leading from a

recognition stage through two consecutive transesterification reactions to the final spliced mRNA (Figure 1.4).

Spliceosome assembly begins with formation of the E complex, via recruitment of the U1 snRNP to the 5' SS and the interaction of the non-snRNP factors SF1, U2AF65 and U2AF35 with the branch point (BP), polypyrimidine tract (PPT) and 3' SS respectively[124,125,128]. The U2 snRNP then binds to the BP, producing the A complex (or prespliceosome). The U2AF heterodimer and SF1 then detach and the tri-snRNP (made up of the U5 and U4/U6 snRNPs in a heterotrimer) joins U1 and U2 to form the B complex (or pre-catalytic spliceosome). Subsequent conformation changes and the disengagement of the U1 and U4 snRNPs leads to the active B complex (B^{act} complex), followed by a further activation reaction giving rise to the catalytically active B* complex, in which the U2/U6 structure is responsible for the first catalytic step[129]; cleaving the 5'SS and forming the lariat structure of the intron[124,125].

This reaction generates the C complex, consisting of the U2, U5 and U6 snRNPs bound to the free exon and the exon/lariat intermediate. Further conformational changes occur followed by the second catalytic step, whereby the lariat is cleaved from the 3'SS and the two exons are ligated to form the spliced mRNA molecule[124,125] (Figure 1.4).

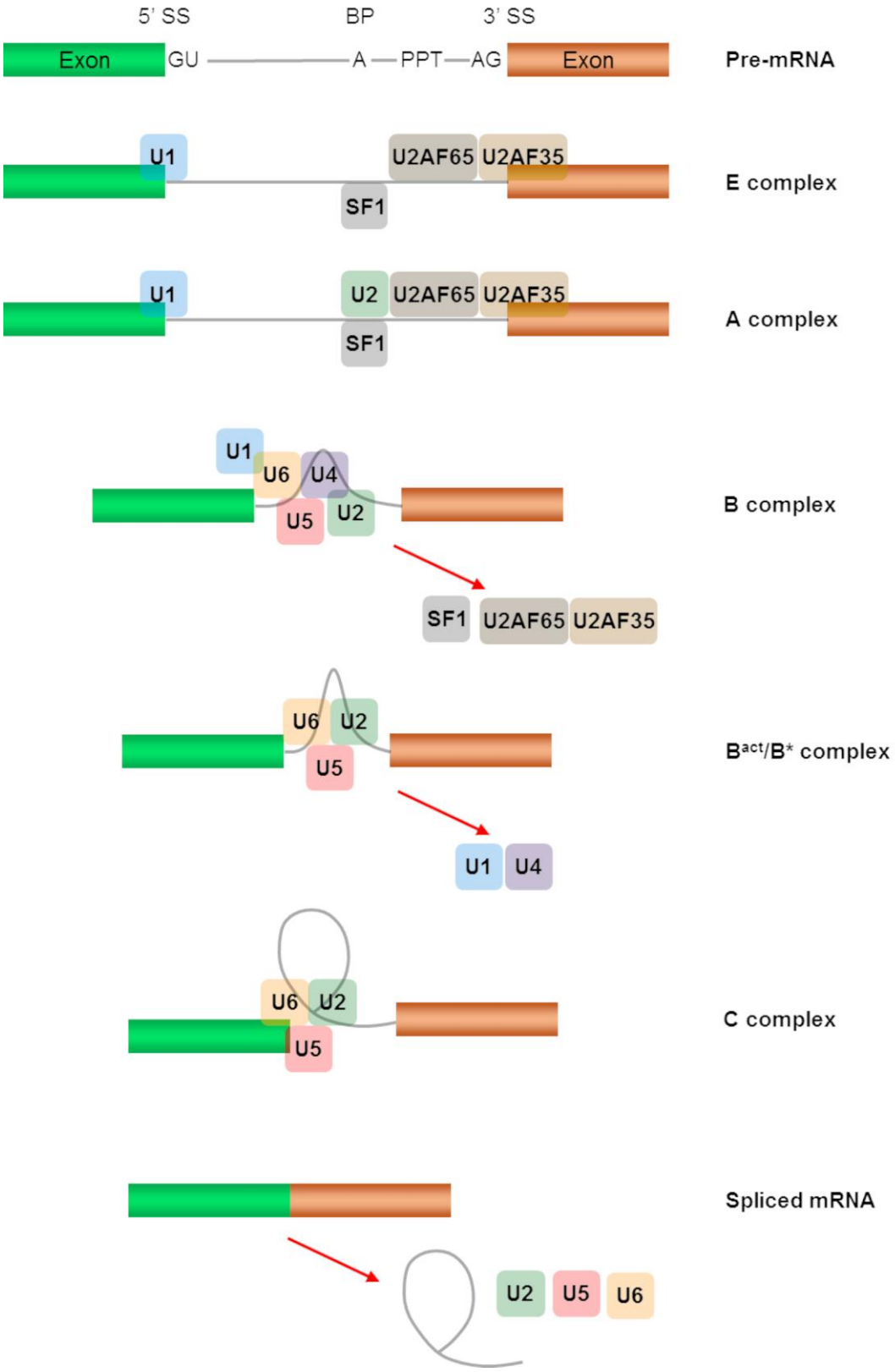

Figure 1.4 Pre-mRNA splicing by the U2-dependent spliceosome

Steps involved in the recruitment of snRNPs, conformational changes and catalysis of intron removal by the U2-dependent spliceosome. Several spatial alterations occur to the spliceosome, along with changes in the milieu of subunits involved, in order to recognise the splice sites and enact the transesterification reactions necessary to produce a fully spliced mRNA. See section 1.8.6 for full details. SS: Splice Site, BP: Branch Point, PPT: Polypyrimidine tract.

1.8.7 Constitutive and alternative splicing

Constitutive splicing is the process by which introns are removed in the same manner every time for a given transcript, whereas alternative splicing is a departure from the canonical splicing pattern, allowing for a single gene to give rise to multiple mature mRNA products and therefore multiple protein isoforms. Over 95% of human genes have been shown to be alternatively spliced[130], and alternative splicing is thought to be the major mechanism behind the discrepancy between the number of genes observed in the human genome (≈19,000), and the number of proteins produced (>90,000)[131].

The most common form of alternative splicing involves cassette-type exons, which are either included or skipped in the final mRNA, however several other types of alternative splicing have been identified, including; alternative 3' and 5' SS, intron retention, mutually exclusive exons, alternative promoters and alternative polyadenylation sites[132]. These different types of alternative splicing are illustrated in Figure 1.5.

Apart from conferring the ability to produce an extended proteome, alternative splicing can also play a regulatory role. For example, alternate isoforms may contain non-coding sequence which can regulate translational efficiency[133], or the inclusion of a 'poison' exon with an in-frame premature stop codon can trigger nonsense-mediated decay pathways, as can several other splicing events[134], leading to degradation of the transcript.

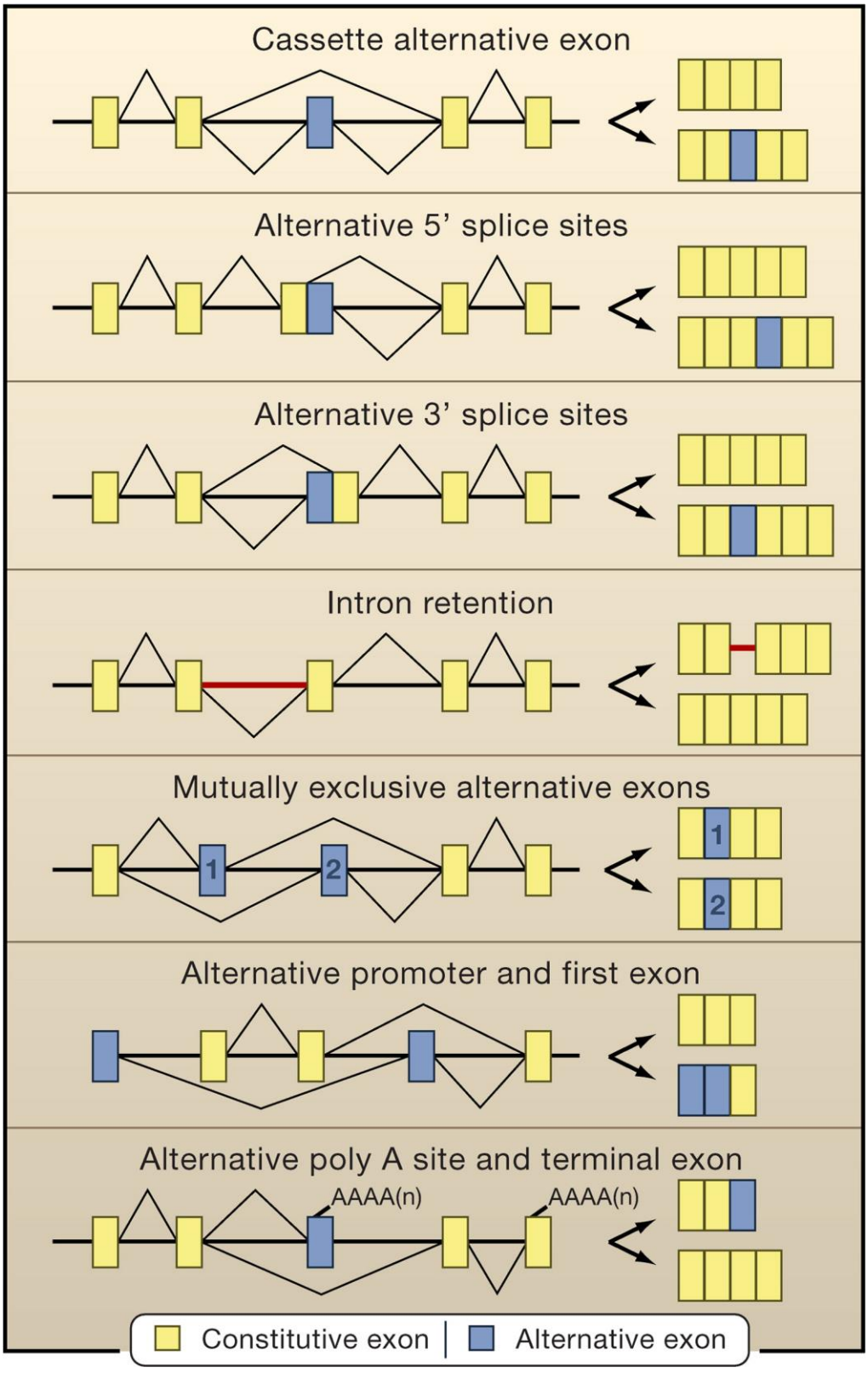

Figure 1.5 Alternative splicing events

Schematic showing the various types of alternative splicing events, and how these can produce many distinct variations of mature mRNA transcripts from a single pre-mRNA (reproduced from Blencowe[132], with permission from Elsevier; © 2006).

1.8.8 Non-coding RNAs

It is known that most transcripts produced from eukaryotic genomes are in fact non-coding[114]. Several classes of non-coding RNA (ncRNA) exist; small interfering RNAs (siRNA), long non-coding RNAs (lncRNA), long intergenic non-coding RNAs (lincRNA), piwi-interacting RNAs (piRNA) and microRNAs (miRNA). All of these classes have been found to affect gene expression at different stages, from transcription to splicing, mRNA degradation and translation[114,135]. ncRNA biogenesis and modes of action have been reviewed extensively elsewhere[135,136], however for the purposes of this thesis I will describe miRNAs in more detail in the following section.

1.8.9 MicroRNA biogenesis and action

MiRNAs are short (usually 21-25 nucleotides) regulatory ncRNA molecules which exert their effect on gene expression largely by targeting mRNA transcripts for translational repression or degradation[137].

MiRNAs are transcribed as long, primary miRNAs (pri-miRNA) by RNA polymerase II (Pol II) or RNA polymerase III (Pol III)[138]. MiRNA genes are often in the form of clusters of individual miRNAs which are expressed in a poly-cistronic manner, and can be found in intergenic regions, introns and in some cases in exons[137]. The pri-mRNA transcript is then cleaved within the nucleus by the Drosha RNase III enzyme into a short stem-loop precursor miRNA (pre-miRNA) structure, which is then exported to the cytoplasm through the action of the Exportin 5-Ran-GTP complex[137-139]. Once in the cytoplasm, the pre-miRNA is further cleaved by another RNAse III enzyme known as Dicer, leaving a linear miRNA duplex which is bound by the Argonaute 2 (Ago2) protein. Ago2 facilitates the unwinding of the miRNA duplex so that the active ‘guide’ strand can be

separated from the 'passenger' strand (which in most cases is subsequently degraded). The Ago2 and guide strand then recruit diverse groups of proteins in order to form various RNA-induced silencing complexes (RISC)[138,139]. The RISC is then guided to target transcripts by virtue of a 6-8 base 'seed sequence' of the bound miRNA. Complementary base pairing of this sequence with the 3' untranslated region (UTR) of the target mRNA leads to its repression or degradation[137,139] (see Figure 1.6 for schematic of this process).

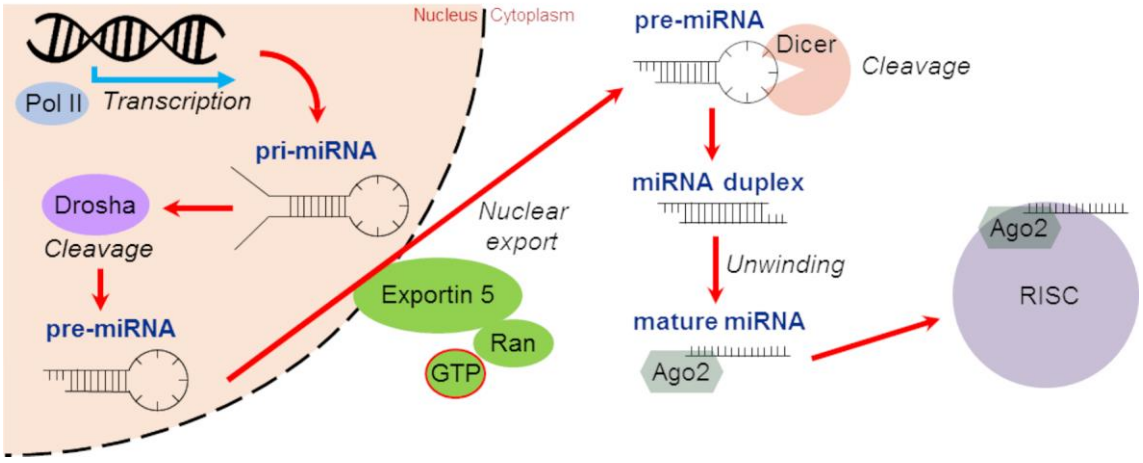

Figure 1.6 MicroRNA biogenesis and processing

Schematic of the steps involved in production of a mature miRNA from primary transcript. Pri-miRNA is transcribed from DNA template, cleaved by Drosha within the nucleus and exported via Exportin 5. Cytoplasmic Dicer then cleaves the stem-loop structure and the mature miRNA is loaded into the RISC via the action of Ago2.

A single miRNA can target multiple mRNAs and many mRNAs have multiple miRNA binding sites in their 3' UTR[140]. In this manner, miRNAs have the capacity to regulate complex networks such as those implicated in ageing and longevity[141].

1.9 Manipulation of ageing processes

The desire to change the way we age is not a new phenomenon, indeed a 'Fountain of Youth' has featured in mythological tales for thousands of years[142].

However as alluded to in section 1.1, considering the current trends in worldwide demographics, there is a clear and growing need to develop means to improve healthy ageing before the socio-economic cost of age-related morbidities becomes an overwhelming pressure on our society and healthcare providers.

1.9.1 Ageing, lifespan and healthspan

Thus far, I have described the theories and mechanisms of ageing according to current observations. It is implied in such a narrative that ageing is heavily involved in the determination of lifespan, however there are two schools of thought on this. The more traditional viewpoint is that longevity is genetically determined and due to antagonistic pleiotropy there is an upper limit on lifespan even in the absence of age-related disease[143-145], while ageing as a process is a product of the random accumulation of damage as described in section 1.4. The second, perhaps more controversial outlook is that lifespan is entirely a function of age-related damage, and therefore effective repair strategies could theoretically lead to extreme longevity[146].

Whichever of these ultimately proves to be true, arguably the more relevant consideration from the current perspective of public health and quality of life is healthspan. Healthspan can be defined as the period of life spent free from chronic age-related disease[147]. While healthspan is difficult to quantify in any meaningful sense[147], conceptually it is self-evident that any treatments which could positively affect healthspan would be highly desirable. It is however almost certainly true that ageing, lifespan and healthspan are all intimately linked, therefore interventions designed to improve healthspan are likely to have effects on the ageing process and/or lifespan[148].

1.9.2 Compression of morbidity

The idea of compression of morbidity as a consequence of both social and scientific progress was introduced by James Fries in 1980[149], and in essence refers to a postponement of the onset of chronic age-related illnesses, i.e. an increase in healthspan. However, when considering the case of an intervention to extend lifespan, this definition must be qualified. Figure 1.7 shows a theoretical situation whereby an intervention has been used which doubles the lifespan of an organism.

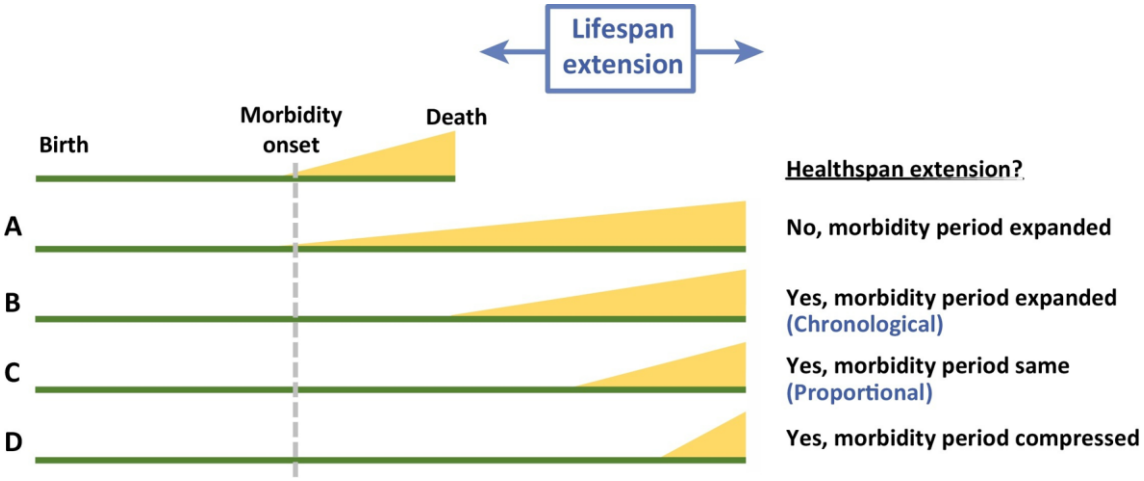

Figure 1.7 Schematic showing different scenarios for lifespan extension

Shown here are potential effects on healthspan in a theoretical example of lifespan extension (reproduced from Hansen & Kennedy[150], with permission from Elsevier; © 2016).

As can be seen, there are a range of possible outcomes of such a lifespan increase;

A. No extension of healthspan; morbidity effectively tripled
B. Healthspan extended; lifespan and morbidity extended by the same amount therefore morbidity doubled
C. Healthspan extended; morbidity remains the same as before intervention
D. Healthspan extended; true compression of morbidity

Logically, the reduction in time spent suffering from any morbidities should be the ultimate goal of any treatment for ageing, whether or not increased lifespan is a factor. Therefore the desirability of the outcome increases from top to bottom of this list, with scenario D being the best result for any treatment designed to increase lifespan[150]. However, it must also be said that a treatment which has no effect on lifespan extension yet confers a compression of morbidity would be just as important from a socio-economic perspective. The arguments for desirability of treatments that may have effects in the B or C categories are less clear-cut.

1.9.3 Potential targets for intervention

It has not been until relatively recently that the idea of treating ageing, rather than the symptoms of ageing (i.e. individual age-related diseases) has gained traction in medical and scientific fields[151]. However, it is now widely accepted that ageing is the process which gives rise to many late-life pathologies[152], and much attention has turned to identifying potential target pathways and interventions to enhance healthy ageing.

Several promising avenues are currently being investigated as therapeutic strategies, as summarised in Table 1.1:

Table 1.1 Therapeutic strategies for ageing interventions

Key targets and pathways with potential for lifespan and/or healthspan extension (Data taken from Trounson & McDonald[153], Martinez & Blasco[154], Campisi *et al*.[155] and Hodgson *et al*.[156]).

Intervention	Pathway	Mechanism/effect
Rapamycin	mTOR	Central to nutrient sensing pathways and shown to affect lifespan and healthspan in model organisms
Metformin	Mitochondria	Targets several ageing pathways, diabetic patients prescribed metformin display increased lifespan and reduced incidence of cancer
Senolytics	Senescent cells	Senescence known to be associated with several age-related pathologies and clearance of senescent cells shown to affect lifespan and healthspan in model organisms
Sirtuin activators	Sirtuins	Modifier of epigenetic marks on histone proteins, shown to be associated with lifespan and healthspan in model organisms
NAD precursors	NAD metabolism	Critical coenzyme for sirtuins and other important enzymes, NAD^+ levels known to decline with age - supplementation shown to be protective during ageing
Telomerase	Shortened telomeres	Well known marker of ageing, transient activation has been shown to improve healthspan in model organisms
Stem cells	Stem cell exhaustion	Key to regenerative capacity of tissues, several stem cell therapies currently in clinical trials with promising outlook
Exercise	Unknown	Known to be essential for healthy ageing, associated with increased lifespan and healthspan in humans
Dietary restriction	Several, including mTOR & sirtuins	Affects nutrient-sensing pathways, most robust method for increasing lifespan and healthspan in model organisms

1.10 Conclusion

As discussed, ageing is a complex and heterogeneous process which is still relatively poorly understood. It is likely that the underlying cause of ageing is a network or combination of many of the aspects described in the preceding sections, therefore much work remains to be done to disentangle the effects of different pathways and mechanisms in the overall phenotype. It is also apparent that ageing, lifespan and healthspan are all intimately linked, so increasing our knowledge of any one of these could be expected to yield insights into other aspects. Previous findings from our research group lead us to postulate a central role for the regulation of gene expression in the ageing process and thus determination of lifespan and healthspan, however to date little is known about how these two complex networks interact with each other. Greater understanding of the role of RNA regulation in the ageing process could provide attractive targets for novel interventions or potential biomarkers of age-related disease.

1.11 Research hypothesis

We believe that regulators of gene expression (specifically mRNA splicing factors and microRNAs) are fundamentally involved in the ageing process and determination of lifespan in mammals, and that therefore these regulators may have potential either as biomarkers of ageing phenotypes or as targets for intervention to improve healthspan.

1.12 Aims and objectives of thesis

The overarching objective of this thesis was to increase our knowledge of the involvement of mRNA splicing factors and miRNAs in ageing and lifespan, from a mechanistic and predictive perspective, both in murine models and in humans.

1.12.1 Chapter 3: Changes in the expression of splicing factor transcripts and variations in alternative splicing are associated with lifespan in mice and humans.

In this chapter, the aim was to characterise transcript expression profiles of splicing factors and alternatively spliced transcripts in mouse strains of varying median lifespan.

To do this, transcript expression levels of a panel of splicing factors were to be measured in spleen and muscle tissues from both young and old mice of six different strains with median lifespan ranging from 623 to 1005 days. Expression levels would then be tested for correlations with age and strain lifespan.

Following this, expression levels of two separate tissue-specific panels of alternatively spliced transcript isoforms would be measured in the same mice, and similarly tested for correlations with age and strain lifespan.

Based on the results from these experiments, bioinformatic analysis of transcriptome-wide expression levels from a human cohort was to be carried out to assess whether any associations seen in the mouse model were also found in humans.

1.12.2 Chapter 4: MicroRNAs miR-203-3p, miR-664-3p and miR-708-5p are associated with median strain lifespan in mice.

The experiments in this chapter were intended to determine whether miRNAs may be associated with median strain lifespan in the spleen tissue taken from the same mouse collection as used in chapter 3.

For this, a high-throughput approach was to be used for discovery; expression levels of 521 miRNAs would be tested in a subset of young animals from the longest- and shortest-lived strains. The top ten miRNAs displaying the most

significant differences in the discovery phase were then to be taken forward into a validation phase. Validation would consist of measuring expression levels of these ten miRNAs in all available spleen samples from young and old mice from all six strains of different median lifespan. Expression levels would then be tested for associations with median strain lifespan.

For any miRNAs showing significant associations, bioinformatic analysis was to be carried out to identify pathways targeted by these miRNAs. Exemplar target genes would then be identified from these pathways in order to measure mRNA expression levels in the same samples to identify whether it was likely that miRNA-mediated regulation was taking place.

1.12.3 Chapter 5: Dietary restriction in ILSXISS mice is associated with widespread changes in splicing regulatory factor expression levels.

For this chapter, the aim was to determine whether splicing factor expression in a mouse model was mechanistically associated with dietary restriction (DR), an established modifier of lifespan.

To achieve this, three strains of ILSXISS mice would be used as they have been shown to have reproducibly variable responses to DR, one displaying lifespan extension, one lifespan reduction and a third showing no change. Brain, heart and kidney tissues were to be collected both from mice fed *ad libitum* (AL) and from mice under 40% DR conditions, for two different lengths of treatment; two months and ten months.

Transcript expression levels of a panel of splicing factors would then be measured in all samples and tested for associations with responder strain and DR regime. Furthermore, the data would be assessed for potential statistical

interactions between these two variables, which could indicate a mechanistic involvement of splicing factors in the different strain responses to DR.

1.12.4 Chapter 6: The transcript expression levels of HNRNPM, HNRNPA0 and AKAP17A splicing factors may be predictively associated with ageing phenotypes in human peripheral blood.

The aim of this chapter was to assess whether splicing factor transcript expression levels were an indicator of future health outcomes and as such could have potential applications as biomarkers

To do this, an existing resource would be used; the InCHIANTI longitudinal study of human ageing. In this cohort, RNA from peripheral blood along with detailed anthropometric data from over 400 individuals is available for multiple follow-up study visits.

Transcript expression levels of a panel of splicing factors would be measured in a set of samples from a baseline time-point and this data would then be used to test for associations with changes over time in age-related health measures.

The health measures to be assessed initially would be the Mini Mental State Exam (MMSE) to evaluate cognitive decline, and mean hand-grip strength as one of the accepted measures of frailty. Any splicing factors found to be significantly associated with change in these outcomes would then be validated within the same cohort, using other measures of cognitive ability and frailty as well as testing for associations in specific subsets of the cohort.

Chapter 2

Experimental Procedures

2.1 Samples

2.1.1 Mouse tissues

Two collections of mouse tissues were used in this thesis, both of which were kindly provided to us by collaborators.

The first of these collections was used to generate the data in chapters 3 & 4 and was supplied by Professor Luanne Peters of the Jackson Laboratory Nathan Shock Center of Excellence in the Basic Biology of Aging, Bar Harbor, ME, USA. The tissues used in the studies described here were collected as part of a much larger cross-sectional and longitudinal study into lifespan and ageing phenotypes across 31 strains of inbred mouse[157-159]. The animal husbandry and sample collection methodologies have been described at length in the 2009 publication reporting the study design and initial findings from the larger study[157]. Abridged versions of these procedures are given in sections 3.7.1, 4.7.1 and Supplementary data S1.

The second collection was used to generate the data for chapter 5 and was supplied by Professor Colin Selman of the Institute of Biodiversity Animal Health & Comparative Medicine, University of Glasgow, UK. These tissues were collected as part of a study into the effects of dietary restriction on metabolic function in mice[160,161]. Again, animal husbandry/sample collection have been covered in detail elsewhere[160,161], with an abridged version given in section 5.5.1.

2.1.2 Human blood samples

Peripheral blood from a human cohort was used to generate the data in chapters 3 & 6. Blood samples were made available through a collaboration with the InCHIANTI study of Aging, a longitudinal study of ageing that has been running

since 1998 in the Tuscany region of Italy. The InCHIANTI study has collected a vast quantity of data on a host of different aspects of ageing – to date over 350 primary research papers have been published based on data from this resource[162]. Full details of participant recruitment, follow-up procedures, assessments and tests performed during the study etc. have all previously been described in many publications deriving from this invaluable resource[163,164]. Excerpts of the procedures used which pertain to this thesis are given in sections 3.7.8, 6.5.1 and 6.5.6.

2.2 RNA extractions

2.2.1 RNA protection strategies

As RNA is a particularly labile molecule and subject to rapid degradation by ubiquitous, naturally occurring RNase enzymes, steps must be taken to preserve the integrity of the transcriptome in any study that concerns gene expression. The most effective method for stabilisation of RNA is to snap-freeze samples in liquid nitrogen (-196°C) on collection, however there are additional reagents and procedures that are designed to enhance and/or replace this rapid freezing. Three different strategies were used in this thesis, one for each of the sample sets described above in section 2.1, as each one was from a different source.

For the mouse tissue samples from the Jackson Laboratory Nathan Shock Center of Excellence in the Basic Biology of Aging, RNA*later*® (a commercial RNA stabilisation solution: Thermo Fisher, Waltham, MA, USA) was used; RNA*later*® is a combination of sodium citrate, EDTA and ammonium sulphate which permeates tissues and cells rapidly in order to protect the cellular RNA while inactivating RNases, and has been shown to be effective for up to one week at

room temperature. In this case, the samples were submerged in the solution at the point of dissection followed by snap-freezing using liquid nitrogen. Samples were then kept in Ultra-Low Temperature (ULT) storage (-80°C) before being shipped to the UK on dry ice. On receipt, the samples were returned to ULT storage until RNA extractions could be performed. As the RNA*later*® protects the RNA at higher temperatures, it is not necessary to work on dry ice with frozen tissue and samples can be allowed to defrost within the solution, therefore handling and preparation of tissue for RNA extractions is greatly simplified.

The tissue samples from the Institute of Biodiversity Animal Health & Comparative Medicine were snap-frozen in liquid nitrogen at the point of dissection and kept in ULT storage until shipping without use of additional RNA stabilisation measures. In order to preserve RNA integrity prior to and during the extraction process, another commercial RNA stabilisation solution, RNA*later*®-ICE Frozen Tissue Transition Solution (Thermo Fisher, Waltham, MA, USA) was used. RNA*later*®-ICE is based on RNA*later*® but is designed specifically to protect RNA during the transition of snap-frozen tissues to a thawed state which facilitates handling during RNA extraction. RNA*later*®-ICE was cooled to -80°C and added to the frozen tissue samples in small batches (to avoid excessive thawing during this step), after which the samples were then allowed to thaw overnight at -20°C. Samples were then returned to ULT storage until RNA extractions were performed, and as with RNA*later*®, the ability to work with the samples at room temperature during extraction without the potential for RNA degradation is highly beneficial.

Finally, the peripheral blood samples from the InCHIANTI cohort were collected into PAXgene Blood RNA Tubes (IVD) (PreAnalytiX GmbH, Hombrechtikon, Switzerland). These are commercially available tubes which form part of a

workflow specifically designed to stabilise RNA from blood samples. The tubes contain a stabilisation reagent, which must be mixed with the blood. After blood samples were collected into PAXgene tubes, the tubes were inverted 8-10 times and then left at room temperature for a minimum of 2 hours and a maximum of 72 hours before transfer to -20°C for 24 hours, and finally into ULT storage. Blood samples were then shipped to the UK on dry ice and returned to ULT storage before RNA extraction using the PAXgene workflow as detailed below in section 2.2.3.

2.2.2 Tissue extractions

RNA was extracted from mouse spleen, skeletal muscle, brain, heart and kidney tissue for subsequent analysis in chapters 3, 4 & 5, using a classical phenol-chloroform methodology. TRI Reagent® Solution was used for all these extractions. TRI Reagent® contains phenol and guanidine thiocyanate which assist with cell lysis, assure immediate inhibition of RNase activity and partition the RNA into the aqueous phase. In the protocol used in this thesis, 10mM $MgCl_2$ was added to the TRI Reagent® before use, as it has previously been reported that when using phenol-chloroform extraction, certain low-GC content microRNAs are selectively lost during extraction (in comparison to other column-based methods). The addition of Mg^{2+} ions stabilises RNA-RNA interactions and allows longer cellular RNAs to act as 'carriers' for microRNAs during precipitation[165].

In all extractions performed, tissue samples and a 5mm stainless steel bead were added to 1ml of TRI Reagent® (with $MgCl_2$) in a round-bottomed Eppendorf tube. Samples were then placed into a Retsch Bead Mill (Retsch Technology GmbH, Haan, Germany) and tissue completely homogenised at a frequency of 30 cycles

per second. 15 minutes was sufficient for all tissues except skeletal muscle, which required 30 minutes to achieve complete homogenisation. Samples were then centrifuged at 13,872 x g at 4°C for 10 minutes to pellet the remaining larger cell debris. The supernatant was transferred to a new Eppendorf tube and 200µl of chloroform was added to assist with phase separation. A further centrifugation at 21,100 x g at 4°C for 20 minutes resulted in full separation of the phases, after which the upper aqueous phase containing the RNA was transferred to another new Eppendorf tube. 1.2µl of GlycoBlue™ Coprecipitant (Thermo Fisher, Waltham, MA, USA) was added (final concentration ≈40µg/ml) along with 500µl of 100% isopropanol, prior to an overnight precipitation step at -20°C. Following precipitation, samples were centrifuged at 21,100 x g at 4°C for 1 hour to pellet the RNA. The pellet was washed twice in 75% ethanol, air-dried for ≈15 minutes and re-suspended in either RNase-free dH_2O or 1X TE Buffer pH8.0 (Thermo Fisher, Waltham, MA, USA).

2.2.3 Blood extractions

RNA was extracted from human blood samples using the PAXgene Blood RNA Kit (Qiagen, Hilden, Germany) and the QIAcube robotic semi-automated extraction protocol. PAXgene Blood RNA Tubes were completely thawed and allowed to stand at room temperature for at least 2 hours before extraction. The tubes were centrifuged at 5000 x g for 10 minutes, the supernatant was removed and 4ml of RNase-free water added to the cell pellet. To wash the cell pellet, it was re-suspended by vortexing and then re-pelleted by a further centrifugation at 5000 x g for 10 minutes. Supernatant was once again discarded and 350µl of lysis buffer was added. At this point, the lysed cells were transferred to the QIAcube robot, which handled the remainder of the protocol. Briefly, the QIAcube performed a proteinase K incubation then passed the resultant treated lysate

through a PAXgene shredder column to further fragment cell debris. Ethanol was added to the flow-through from the shredder column to create conditions which favour RNA binding. This flow-through was then applied to a PAXgene RNA spin column, in which a silica membrane captures the RNA while contaminants can pass through. Several wash steps and a DNase I treatment were then performed before RNA was eluted in a proprietary elution buffer and heat denatured.

2.2.4 RNA quantification

All RNA samples were quantified using a NanoDrop spectrophotometer (NanoDrop, Wilmington, DE, USA), and where appropriate, diluted to a final concentration of ≈500ng/µl (using the appropriate elution buffer) in order to facilitate downstream normalisation of RNA input quantities.

2.3 Reverse transcription

Reverse transcription (RT) is the process whereby single-stranded complementary DNA (cDNA) is synthesised from an RNA template. This process serves two main purposes; firstly, the cDNA is much more stable than RNA therefore after processing, samples are much more robust. Secondly, most downstream workflows such as quantitative real-time polymerase chain reaction (qRT-PCR) etc. rely on enzymes which require a DNA substrate.

RT reactions are catalysed by reverse transcriptases, a class of enzymes most commonly used by retroviruses to replicate their genomes but also found in some non-retroviruses as well as eukaryotes. Commercially available kits generally contain recombinant versions of Avian Myeloblastosis Virus (AMV) Reverse Transcriptase or Moloney Murine Leukemia Virus (M-MuLV or MMLV) Reverse

Transcriptase, engineered for specific desirable qualities such as greater temperature stability or higher processivity.

In this thesis, three different RT kits were used: for the gene expression analyses, Invitrogen™ SuperScript™ VILO™ cDNA Synthesis Kit (Thermo Fisher, Waltham, MA, USA) was used in chapters 3, 4 & 6 while EvoScript Universal cDNA Master kit (Roche LifeScience, Burgess Hill, West Sussex, UK) was used in chapter 5. Applied Biosystems™ TaqMan™ MicroRNA Reverse Transcription Kit was used for the microRNA analysis in chapter 4.

2.3.1 SuperScript™ VILO™ reverse transcription

Invitrogen™ SuperScript™ VILO™ cDNA Synthesis Kit is a two-tube format kit, with an “Enzyme mix” tube containing SuperScript™ III reverse transcriptase (a genetically engineered MMLV-derived enzyme with reduced RNase H activity and improved thermostability), RNaseOUT™ Recombinant Ribonuclease Inhibitor, and a proprietary helper protein. A second “Reaction mix” tube contains random primers, $MgCl_2$, and dNTPs in a proprietary buffer.

Different input quantities of RNA were used in each chapter of this thesis, dependant on the availability of starting material and the planned usage of the cDNA, however as a general rule all RNA samples were normalised to a specified concentration before being added to an RT reaction containing 1X “Enzyme mix”, 1X “Reaction mix” and RNase-free dH_2O to a final volume of 20µl. Reactions were placed onto a thermal cycler where the following incubations were carried out: 25°C for 10 minutes, 42°C for 60 minutes, 85°C for 5 minutes and a final hold at 4°C.

Full details of RNA input quantities and any subsequent cDNA dilutions for the different approaches used in each chapter are given in sections 3.7.5, 4.7.9 and 6.5.4.

2.3.2 EvoScript Universal cDNA reverse transcription

EvoScript Universal cDNA Master kit is also a two-tube format kit, with an "Enzyme mix" tube containing a proprietary enzyme blend and Protector RNase Inhibitor. A second "Reaction buffer" tube contains random primers, anchored oligo$(dT)_{18}$, dNTP, and $Mg(OAc)_2$. Unlike the SuperScript™ III reverse transcriptase, EvoScript reverse transcriptase retains RNase H activity which removes the RNA template after cDNA synthesis, allowing PCR primers to more easily bind the cDNA. As this is the case, extra care must be taken to add the "Enzyme mix" just before incubation to avoid digestion of the sample.

RNA samples were normalised to 500ng/µl, and 1µl of this was added to an RT reaction containing 1X "Reaction buffer" and RNase-free dH_2O to a final volume of 18µl, samples were then placed on ice for 5 minutes to allow primers to anneal to the RNA, after which 2µl of "Enzyme mix" was added to give a 1X concentration in a final volume of 20µl. Reactions were placed onto a thermal cycler where the following incubations were carried out: 42°C for 30 minutes, 85°C for 5 minutes, 65°C for 15 minutes and a final hold at 4°C. cDNA samples were then diluted to ensure sufficient material for further analysis; details are given in section 5.5.4.

2.3.3 TaqMan™ MicroRNA reverse transcription

Applied Biosystems™ TaqMan™ MicroRNA Reverse Transcription Kit is a multi-component kit including MultiScribe™ reverse transcriptase (a recombinant MMLV-derived enzyme with reduced RNase H activity), and other requisite

reagents in separate tubes such that the kit can be used for different applications, depending on the priming strategy used. In chapter 4, this kit was used for two different RT approaches, one for high-throughput microRNA screening and another for targeted microRNA expression measurement.

For the high-throughput screening, Megaplex™ RT Primers, Rodent Pool Set v3.0 (Thermo Fisher, Waltham, MA, USA) were used. The Megaplex™ RT Primer pool set is supplied as separate A and B pools, which between them contain all the primers necessary to reverse transcribe 521 unique microRNAs. Due to this, the following procedure was carried out twice, once for pool A and once for pool B: RNA samples were normalised to 400ng/µl, and 1µl of this was added to an RT reaction containing 1X Megaplex™ RT Primers, 20mM dNTPs with dTTP, 75U MultiScribe™ Reverse Transcriptase, 1X RT Buffer, 3mM $MgCl_2$, 2U RNase Inhibitor and RNase-free dH_2O to a final volume of 7.5µl. Reactions were incubated on ice for 5 minutes, after which they were placed onto a thermal cycler where the following steps were carried out: 40 cycles of 16°C for 2 minutes, 42°C for 1 minute and 50°C for 1 second, followed by a single step of 85°C for 5 minutes and a final hold at 4°C.

For the targeted expression measurement, specific RT primers were used. These are provided when purchasing individual TaqMan™ microRNA qRT-PCR assays and can be multiplexed into an RT pool which can then be used in a similar manner to the Megaplex™ pools described in the previous paragraph. For the experiments described here, equal volumes of 13 microRNA RT primers (listed in Supplementary table S19) were combined into a multiplex pool for use in the RT. RNA samples were normalised to 60ng/µl, and 1µl of this was added to an RT reaction containing 13µl of the RT primer multiplex (as described above), 10 mM dNTPs (with dTTP), 100 U MultiScribe™ Reverse Transcriptase, 1X RT

Buffer, 7.6U RNase Inhibitor and RNase-free dH_2O to a final volume of 30µl. Reactions were placed onto a thermal cycler where the following incubations were carried out: 16 °C for 30 minutes, 42 °C for 30 minutes, 85 °C for 5 minutes and a final hold at 4 °C.

2.4 Quantitative Real-Time Polymerase Chain Reaction

Quantitative Real-Time Polymerase Chain Reaction (qRT-PCR) is a method by which gene expression levels can be directly quantified in cDNA which has been reverse transcribed from cellular RNA samples. The basis of qRT-PCR is the polymerase chain reaction (PCR), a technique first devised in the early 1980s to amplify specific short regions of DNA through thermal cycling with a DNA polymerase enzyme. PCR requires a template DNA molecule to amplify and uses; **1)** a pair of oligonucleotide primers (each one designed to opposite strands of the DNA molecule and specific to the target region in question), **2)** a thermostable DNA polymerase enzyme (most commonly *Taq* polymerase, so called due to its origin in the thermophilic *Thermus aquaticus* bacteria), **3)** deoxynucleoside triphosphates (dNTPs, which will form the base-pairs of the new DNA strand), **4)** magnesium ions (usually in the form of $MgCl_2$, a required cofactor for *Taq* polymerase) and **5)** an aqueous buffer to provide optimum stability and activity of the *Taq* polymerase. With all these components present in a reaction, repeated cycles of heating and cooling to predefined temperatures (thermal cycling) serve to sequentially denature the template DNA, anneal the primers and extend new DNA strands complementary to the target region of the template, resulting in an exponential amplification of said target until a plateau is reached due to accumulation of amplification products (amplicons)[166] (Figure 2.1a & 2.1b).

While this technique is extremely useful for the amplification of DNA, the fact that all reactions using a given set of primers will reach a similar plateau level, as an end-point assay it is not suitable for measurement of the input quantity of template DNA. However, in the early 1990s researchers realised that the kinetics of accumulation of amplicons during a PCR reaction is directly related to the starting number of copies of the template DNA molecule and thus the dynamics of the amplification curve differ with template input concentration. Given this knowledge, it was discovered that by tracking a reaction in real-time using a fluorescent DNA marker it was indeed possible to determine the input quantity of DNA, based on the number of cycles at which the fluorescence produced crosses a pre-defined threshold[167] (Figure 2.1c). Subsequent refinements to this technique led to the development of several chemistries for detection and measurement of amplification, collectively known as quantitative Real-Time PCR or qRT-PCR.

There are two relatively broad categories of qRT-PCR chemistry:

2.4.1 Intercalating dyes

Intercalating dyes, such as SYBR Green I and similar DNA-binding dyes, fluoresce preferentially when bound to double-stranded DNA (ds-DNA), therefore giving an increase in fluorescence proportional to the increasing numbers of ds-DNA amplicons produced during each round of amplification. While these dyes benefit from simplicity and only require the design of a single pair of sequence-specific primers, they have a major drawback in their lack of specificity. Any ds-DNA present in the reaction will fluoresce, thus non-specific amplicons or primer-dimers will cause an increase in fluorescence, reducing the accuracy of the quantification.

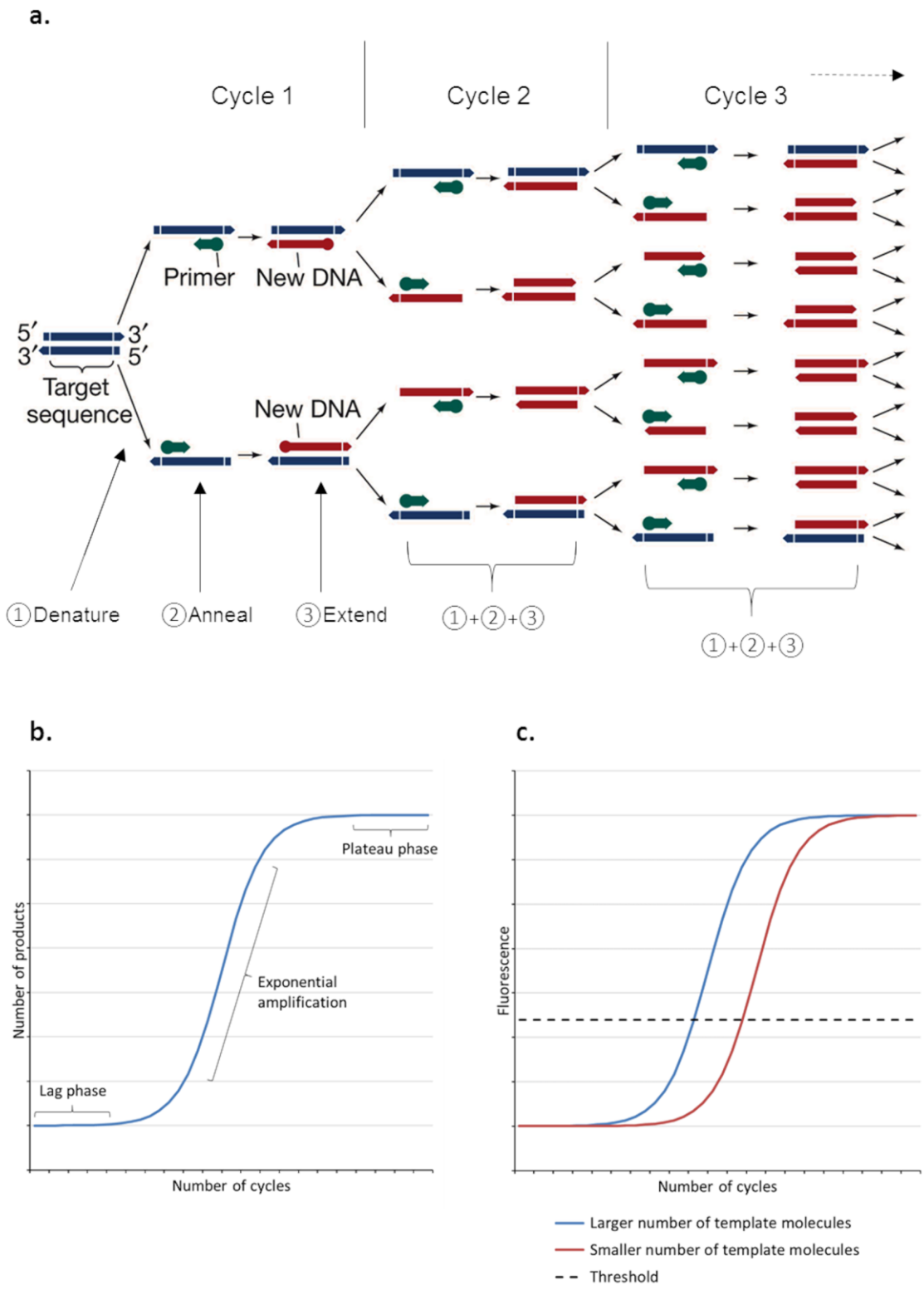

Figure 2.1: Schematic representation of PCR/qRT-PCR kinetics

Shown here are depictions of a theoretical PCR reaction. Panel a. shows the process by which a target region of DNA is amplified in successive cycles of a reaction, panel b. shows the overall reaction kinetics indicating the three phases of an amplification reaction and panel c. shows the kinetics of two theoretical qRT-PCR reactions with differing input quantities of template DNA. (Panel a. adapted from royalty-free online resource: https://slideplayer.com/slide/13784204/)

2.4.2 Oligonucleotide probes

Oligonucleotide probes are short oligonucleotides, complementary to a specific target sequence within the PCR amplicon which are added to the reaction along with standard PCR primers. These usually utilise both a fluorescent reporter and some means of quenching the reporter, which serve to ensure that fluorescence is detected only when the amplicon of interest is present. Detection is normally achieved through some type of conformational or spatial change in the reporter/quencher relationship, allowing the reporter to fluoresce. By virtue of the specific design of the probe and the fact that they will only produce fluorescence when the target amplicon is detected, they benefit from hugely increased accuracy in comparison to intercalating dye chemistries. There are many probe-based chemistries available, but probably the most commonly used is a combination of forward and reverse PCR primer along with a fluorescent hydrolysis probe, which together are more widely known as TaqMan™ assays (a brand name of Roche Diagnostics and Applied Biosystems which has become synonymous with the chemistry itself). The hydrolysis probes employed in TaqMan™ assays carry a reporter fluorophore covalently attached to the 5' end, a non-fluorescent quencher (NFQ) at the 3' end and a Minor Groove Binding (MGB) domain attached via a flexible linker. The MGB acts to stabilise probe binding to its complementary sequence and raises the melting temperature (T_m) of the probe by up to 10°C, allowing for shorter oligonucleotides to be designed which in turn gives both higher specificity and lower background fluorescence. In their native conformation, the fluorophore and quencher are in close proximity therefore very little fluorescence is detectable. During the annealing step of thermal cycling, these probes will bind to the target along with the PCR primers. During the extension step of PCR, the probe is cleaved by the 5' to 3' exonuclease

activity of *Taq* polymerase, leading to the fluorophore and quencher being decoupled. As these are no longer close enough together to allow quenching to occur, the result is a fluorescent signal proportional to the number of cleaved probes and also therefore the number of amplicons in the reaction (Figure 2.2).

In this thesis, qRT-PCR has been carried out exclusively using Taqman™ assays.

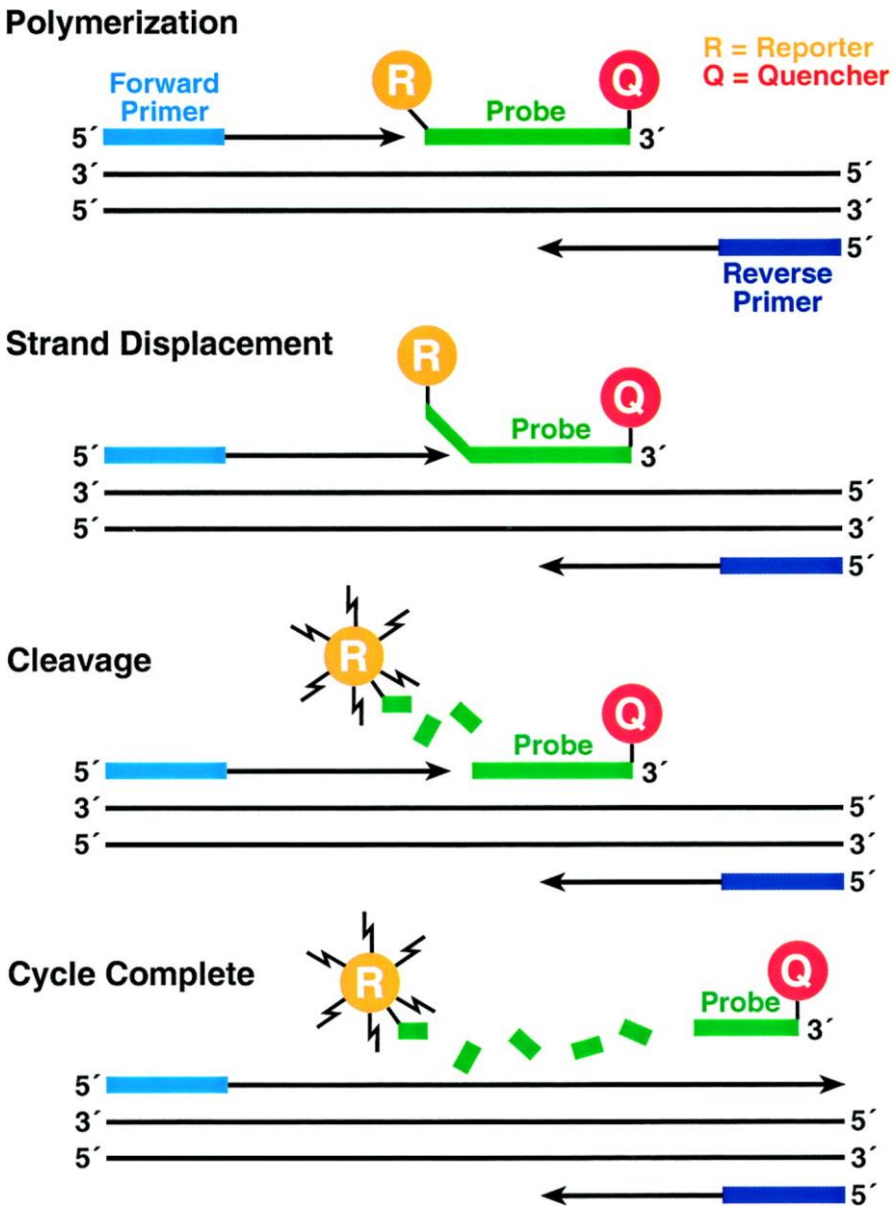

Figure 2.2: Schematic of hydrolysis probe qRT-PCR chemistry

Shown here is the principle by which Taqman™ assays detect a specific amplicon during a qPCR reaction. Taqman™ probes have a Minor Groove Binding domain attached at the 3' end (not shown). Fluorescence is denoted by the lightning bolt icons (reproduced from Yuan *et al*.[168], with permission from American Association for Clinical Chemistry, Inc; © 2000).

2.4.3 Measurement of gene expression

Perhaps one the most important recent developments in the field of gene expression was the marriage of reverse transcription with qRT-PCR in the mid-1990s, which for the first time allowed true quantitative analysis of expression levels of mRNA transcripts. By quantifying the amount of cDNA reverse-transcribed from a cellular RNA sample, this technique allows researchers to determine the amount of transcription taking place (gene expression), at a specific time-point, for any given gene or genes.

As alluded to in section 2.4, quantification is achieved through the capture of fluorescence data, specifically the point at which the fluorescence produced by a given sample crosses a pre-defined threshold (Figure 2.1c). This point is termed the cycle threshold or C_T value, and forms the basic unit of measurement of all qRT-PCR analyses. The threshold is arbitrarily defined independently for each gene in a particular study, however two rules must be obeyed when placing a threshold; 1) it must be sufficiently far above the baseline fluorescence so as not to be affected by background noise, and 2) it must be within the linear portion of the exponential phase of the amplification curve. Assuming these rules are adhered to, the exact positioning of the threshold is irrelevant, as the relative difference between C_T values will remain equal. For most analyses, proprietary software provided by qRT-PCR instrument manufacturers will set the baseline and threshold parameters automatically, with baseline measurements usually being averaged across all samples between cycles 3 and 15, and the threshold being set in the linear phase a minimum of ten standard deviations above the baseline value. In certain cases in this thesis, it was necessary to alter these default settings, however descriptions of any alterations are provided in the supplementary data wherever this has been done.

There are two methods for measuring gene expression using qRT-PCR; absolute and relative quantification.

Absolute quantification relies on use of a standard curve prepared via a serial dilution from a stock containing a known number of template molecules. C_T values from this standard curve are plotted on a log-scale graph in order to produce a straight-line plot against which C_T values of unknown samples are compared, giving a measurement of number of copies per sample[169]. The absolute quantification approach is useful in certain cases where exact number of copies is required (for example in the calculation of viral load[170]), but more often relative quantification of expression will suffice.

Relative quantification compares C_T values of one set of samples relative to C_T values of a second set (for example treated vs control samples or similar) and gives a measurement in fold-change in expression between the two sample sets. This approach dispenses with the time-consuming step of preparing a highly accurate, precisely quantified standard curve for each set of reactions as is required in absolute quantification.

In both of these methodologies, some means of normalising potential discrepancies in input quantity of total RNA is required. Such variance can arise from inherent technical variability in the accuracy of RNA measurement, or from (human) pipetting error during the RT and/or qRT-PCR set-up steps and, if not accounted for, could potentially result in gross over- or under-estimation of gene expression changes. Such correction is achieved through the inclusion of endogenous control genes in the experimental design. These are also known as housekeeping genes as they are usually involved in pathways or structural elements that are fundamental to cellular processes and/or survival and therefore

likely to be expressed at stable levels across different experimental conditions. C_T values for endogenous control genes are collected from the samples in the experiment (along with the C_T values for the genes of interest), and these are used for downstream normalisation. This normalisation is discussed in more detail in section 2.4.6.

In this thesis, relative quantification has been the method of choice for quantification of gene expression.

2.4.4 Taqman™ Array qRT-PCR

Taqman™ Array microfluidics cards (Thermo Fisher, Waltham, MA, USA) were used to generate data for chapters 3, 4 & 6. The Taqman™ Array system consists of a foil-backed card overlaid with an arrangement of plastic microfluidic channels connecting 384 reaction chambers of 1µl volume, each of which contains a lyophilised Taqman™ assay. The cards can be purchased in several pre-configured layouts or alternatively can be custom designed to contain any required selection of Taqman™ assays. Up to eight samples can be loaded onto a card, with differing numbers of assays per sample according to the chosen layout.

The Taqman™ MicroRNA Arrays used in this thesis contain a single reaction per assay for each sample, whereas the Taqman™ Low Density Arrays custom gene expression cards contain duplicate reactions per assay for each sample.

RNA samples were first reverse transcribed using the SuperScript™ VILO™ cDNA Synthesis Kit as described in section 2.3.1. The resulting 20µl of cDNA was mixed with 50µl of TaqMan™ Universal Master Mix II, no UNG (Thermo Fisher, Waltham, MA, USA) and 30µl RNase-free dH_2O. The resulting reaction

mixture was then loaded onto the array through a loading port at one end of the card. Once loaded, the Taqman™ Array cards were centrifuged twice for 1 minute at 216 x g in order to distribute the mixture through the microfluidics channels and into each of the reaction chambers. The chambers were then sealed using a proprietary tool and the card loaded onto a qRT-PCR machine with correct capability to run this format of array. In this thesis, Taqman™ Array cards were all run on an Applied Biosystems™ 7900HT Fast Real-Time PCR System (Thermo Fisher, Waltham, MA, USA). Cycling conditions were a single cycle of 50°C for 2 minutes followed by a single cycle of 94.5°C for 10 minutes then 40-50 cycles of 97°C for 30 seconds and 59.7°C for 1 minute. Details of array types used, specific assay configurations, cycling conditions and endogenous controls for the arrays run in each chapter are given in sections 3.7.6, 4.7.4, 6.5.4, Supplementary Data S2 and Supplementary tables S18 & S27.

NB. Taqman™ Arrays are referred to in this thesis as both Taqman™ MicroRNA Arrays and Taqman™ Low Density Arrays (TLDA) depending on the format in use (pre-designed microRNA cards or custom gene expression cards), however all array cards have recently been renamed by Thermo Fisher as Taqman™ Array Cards (TAC).

2.4.5 Manual 384-well qRT-PCR

Single-tube Taqman™ Assays (Thermo Fisher, Waltham, MA, USA) were used to generate data for chapters 4 & 5. Experiments using these assays were performed in manually loaded 384-well plates and run on either an Applied Biosystems™ 7900HT Fast Real-Time PCR System, Applied Biosystems™ QuantStudio 12K Flex Real-Time PCR System or Applied Biosystems™ QuantStudio 6 Flex Real-Time PCR System. Minor variations in the exact

contents of each reaction exist between the experiments in different chapters, dependent on the RNA availability and the type of assay being used for each experiment. Full details of reaction mixes for each experiment are given in sections 4.7.5, 4.7.9 and 5.5.5. In general, cDNA, Taqman™ Assay, TaqMan™ Universal Master Mix II, no UNG and RNase-free dH_2O were mixed in appropriate volumes to give a 5µl final reaction volume per well. Individual cDNA samples were run using three technical replicates, with these replicates mixed as a single large volume before being loaded onto the 384-well plate to minimise pipetting error. Cycling conditions were a single cycle of 95°C for 10 minutes, followed by 40-50 cycles of 95°C for 15 seconds and 60°C for 1 minute. Details of Taqman™ Assays and endogenous controls used in each chapter are given in Supplementary tables S19, S20 & S21.

2.4.6 Relative quantification

There are three approaches for calculating relative gene expression levels from qRT-PCR data; the $2^{-\Delta\Delta C_T}$ method, the Pfaffl method[171] and sigmoidal curve-fitting.

The $2^{-\Delta\Delta C_T}$ method is the simplest and most commonly used form of relative quantification calculation. As mentioned in section 2.4.3, C_T values are collected from each sample for the genes of interest (GOI) and endogenous control (EC) gene(s). It is worth noting that more than one EC is often included in the experimental design and an average (or geometric mean) of the C_T values of these genes may be used. The first part of the $2^{-\Delta\Delta C_T}$ calculation is within-sample normalisation using the EC gene(s) to account for any variation in RNA/cDNA input. This is achieved by subtracting the EC C_T value from the GOI C_T value, resulting in a ΔC_T value. The next step is to calculate the change in ΔC_T value

relative to a calibrator sample or samples; the calibrator(s) are not a fixed entity and will be different depending on the experimental design and aim. For example, a set of control samples, zero time-point samples, or even a population median are all potentially valid calibrators for particular data sets. Subtracting each sample's ΔC_T value from the chosen calibrator(s) ΔC_T value gives the $\Delta\Delta C_T$ value for each sample (and effectively sets the calibrator(s) to zero). The $\Delta\Delta C_T$ value represents the change in expression of each sample relative to the calibrator, but in its current state is a function of the number of cycles difference, so requires transformation to give a more understandable fold-change measurement. Assuming a doubling of PCR product in every cycle, the formula $2^{-\Delta\Delta C_T}$ converts this cycle difference value into a fold-change value, which can then be used for statistical analysis. The main disadvantage of the $2^{-\Delta\Delta C_T}$ method is that it relies on the assumption that all assay efficiencies are approximately equivalent, and preferably in the region of 100%.

The Pfaffl method is based on the same equations as the $2^{-\Delta\Delta C_T}$ method but also incorporates the PCR efficiency of each assay into the fold-change calculations, which is particularly useful when measurements have been carried out with assays with variable efficiencies. However, this approach does require construction of standard curves to test assay efficiencies, although unlike absolute quantification it does not require the standards to be present alongside every set of reactions[171].

Sigmoidal curve-fitting dispenses with the need for any standard curves by fitting the fluorescence data to a non-linear regression model, resulting in a quantitative measure of target quantity in arbitrary units. The disadvantage of sigmoidal curve-fitting is the complexity of calculation and that each reaction must be fitted to the model individually, so analysis of this type requires specialist software. Some

examples of this type of software are now available but are generally targeted at more high-throughput applications[172].

Throughout this thesis, the $2^{-\Delta\Delta C_T}$ method was the analysis type employed for relative quantification of gene expression. This method was used since all qRT-PCR was performed using either inventoried Taqman™ Assays from Thermo Fisher (Waltham, MA, USA) which are validated to perform at an efficiency between 95% and 105%, or if custom assays were used, these were experimentally validated to be within the same range.

In the case of the manual 384-well qRT-PCR analyses, prior to the $2^{-\Delta\Delta CT}$ step standard deviations of the three technical replicate C_T values were manually checked and any samples showing a deviation >0.5 cycles had outlying C_T values removed. However, this step was not possible for either type of Taqman™ Array used in this thesis as they contained a maximum of two technical replicates per sample.

2.5 Statistical approaches

2.5.1 Transformations

qRT-PCR data was subject to transformations appropriate to the dataset in each chapter. In chapters 3 & 4, a $\log_{10}$ transformation was used, whereas a natural log was used in chapters 5 & 6. Transformations were chosen based on visual inspection of the data in each case as empirical tests of normality such as Kolmogorov-Smirnov or Shapiro-Wilk tests tend to overestimate non-normality on larger datasets, such as those in this thesis[173].

2.5.2 Outlier detection

In chapters 3 & 4, due to the smaller relative size of the datasets involved, no formal outlier detection strategy was applied beyond the removal of any samples missing >50% of data points across all genes measured. For chapters 5 & 6 (which correspondingly have larger datasets), a combination of univariate and multivariate outlier detection was used. Univariate detection was carried out first using standardised z-scores followed by multivariate detection by means of a Mahalanobis distance calculation. Full details of outlier detection approaches are given in sections 5.5.6 and 6.5.5.

2.5.3 Student's t-test

The Student's t-test was used in chapter 3 to compare mean gene expression values. Details are given in section 4.7.10.

2.5.4 Linear regressions

Data analyses in chapters 3, 4, 5 and 6 were carried out using linear regression models including varying numbers of covariates. In all cases, gene expression was entered into the model as the dependent variable and all other relevant covariates added as independent variables. Exact details of the regression parameters and the software used to run the models are given in sections 3.7.6, 3.7.8, 4.7.11, 5.5.7 and 6.5.8.

2.5.5 Binary logistic regressions

Binary logistic regression was used as a secondary analysis in chapter 3 in order to assess the potential effects of non-linearity on the results of the linear regressions. Details are given in section 3.7.6.

2.5.6 Interaction terms

Interaction terms were included between two categorical variables in certain regression models to determine whether one variable could potentially be mediating the effect of the other variable on gene expression levels (see Figure 5.5). Full details of interaction analyses used in this thesis are given in sections 3.7.6, 4.7.6 and 5.5.7.

2.5.7 ANCOVA

Analyses of covariance (ANCOVA) were used in chapter 5 to test for differences in mean gene expression across different groups with the inclusion of a single covariate. Details are given in section 5.5.7.

2.5.8 Multiple testing

Different strategies were employed in order to account for increased potential for Type I errors due to multiple testing.

No *p*-value correction was used in chapter 3, as the genes in question were chosen *a priori* based on previous work and only one phenotype was tested.

In chapter 4, Bonferroni correction[174] was used for the two microRNA analyses carried out: n=279 tests, p=0.000179 for the discovery set, and n=10 tests, p=0.005 for the validation set. However, no correction was made for the mRNA target follow-up analyses as the genes tested were chosen *a priori* based on the microRNA target predictions.

A false discovery rate (FDR) control method proposed by Benjamini, Krieger and Yekutieli[175] was used for the data in chapter 5. As the potential for correlations within and between the results was particularly high in the inbred recombinant

mouse strains used in this chapter, Bonferroni correction was not appropriate due to the fact that a lack of inter-dependence between findings is assumed for correct implementation of this procedure.

Chapter 6 also used Bonferroni correction, although in this case the correction was limited to the number of phenotypes tested (n=6, p=0.00833), as the genes tested were once again chosen *a priori* based on previous findings. Although the human cohort in this chapter would most likely present fewer correlations than the inbred mice from chapter 5, the phenotypes tested had potential to show a degree of correlation, so proper handling of multiple testing in this case was not straight-forward. Both full Bonferroni or FDR-type correction may well have been too stringent, so the approach taken was deemed to be a satisfactory compromise.

Chapter 3

Data Chapter.

Changes in the expression of splicing factor transcripts and variations in alternative splicing are associated with lifespan in mice and humans.

Published in: Aging Cell. October 2016. doi: 10.1111/acel.12499.

3.1 Author List

Ben P. Lee[1], Luke C. Pilling[2], Florence Emond[1], Kevin Flurkey[3], David E. Harrison[3], Rong Yuan[3,6], Luanne L. Peters[3], George A. Kuchel[4], Luigi Ferrucci[5], David Melzer*[2&4] and Lorna W. Harries*[1].

1 - RNA-mediated mechanisms of Disease, Institute of Biomedical and Clinical Sciences, University of Exeter Medical School, University of Exeter, Devon, UK.
2 - Epidemiology and Public Health, Institute of Biomedical and Clinical Sciences, University of Exeter Medical School, University of Exeter, Devon, UK.
3 - The Jackson Laboratory Nathan Shock Center of Excellence in the Basic Biology of Aging, Bar Harbor, Maine, USA.
4 - UConn Centre on Aging, University of Connecticut Health Centre, Farmington, Connecticut, USA.
5 - National Institute on Aging, Baltimore, Maryland, USA.
6 - Current address: Geriatric Research Division, Department of Internal Medicine, Southern Illinois University School of Medicine, Springfield, IL, USA.

3.2 Author Contributions

BL carried out laboratory work, analysis and contributed to the manuscript, LCP contributed the statistical assessment of parental longevity in the human samples. FE contributed technical assistance and analysis. KF advised on selection and mouse strains and analytical approaches. RY and LP designed and managed the initial mouse lifespan study, identified genetic differences in *Hnrnpa2b1* and *Hnrnpa1* discordant between strains and contributed to the manuscript. DEH codirected the Jackson laboratory Nathan Shock Centre of Excellence in the Basic Biology of Aging at the time this work was performed, and was instrumental in facilitating the mouse collection and animal husbandry facilities used in this study. GAK contributed to and reviewed the manuscript. LF provided access to the InCHIANTI study data. DM comanaged the study and reviewed the manuscript. LWH managed the study, interpreted the data and wrote the manuscript.

3.3 Abstract

Dysregulation of splicing factor expression and altered alternative splicing are associated with ageing in humans and other species, and also with replicative senescence in cultured cells. Here, we assess whether expression changes of key splicing regulator genes and consequent effects on alternative splicing are also associated with strain longevity in old and young mice, across 6 different mouse strains with varying lifespan (A/J, NOD.B10Sn-H2^{b}/J, PWD.Phj, 129S1/SvlmJ, C57BL/6J and WSB/EiJ). Splicing factor expression and changes to alternative splicing were associated with strain lifespan in spleen and to a lesser extent in muscle. These changes mainly involved hnRNP splicing inhibitor transcripts with most changes more marked in spleens of young animals from long-lived strains. Changes in spleen isoform expression were suggestive of reduced cellular senescence and retained cellular proliferative capacity in long-lived strains. Changes in muscle isoform expression were consistent with reduced pro-inflammatory signalling in longer-lived strains. Two splicing regulators, *HNRNPA1* and *HNRNPA2B1*, were also associated with parental longevity in humans, in the InCHIANTI ageing study. Splicing factors may represent a driver, mediator or early marker of lifespan in mouse, as expression differences were present in the young animals of long-lived strains. Changes to alternative splicing patterns of key senescence genes in spleen and key remodelling genes in muscle suggest that correct regulation of alternative splicing may enhance lifespan in mice. Expression of some splicing factors in humans was also associated with parental longevity, suggesting that splicing regulation may also influence lifespan in humans.

3.4 Introduction

Ageing is a dynamic, multisystem process, which is highly heterogeneous in humans with some people surviving disease-free until advanced age whilst others succumb to age-related conditions in mid-life. The factors underlying individual lifespan are currently unclear, but increasing our understanding of determinants of longevity and 'healthspan' are key aims for the future.

Correct expression and regulation of genes is critical for maintenance of cellular and organismal function. Alternative splicing, the process by which single genes can make multiple gene products in an adaptive and reactive fashion is a key part of this process[176]. Indeed, breakdown in the regulation of mRNA splicing is a prominent feature in many age-related diseases such as Alzheimer's disease, Parkinson's disease and several tumour types[177-180]. This may indicate that defects in the splicing machinery may cause the cellular response to stress to be less specific, with effects on cellular resiliency and accumulation of DNA damage. We have previously identified deregulation of splicing factor expression and alternative splicing as a key factor in normal human and cellular ageing[101,103]. Alternatively expressed isoforms also demonstrate tissue-specific differences in ageing, as they do for many other phenomena[103]. Splicing factors themselves demonstrate high species conservation[181], whereas patterns of alternative splicing are partially determined by genetic differences and may be species specific. Splicing patterns show drastically more interspecies variability than gene expression with only 50% of alternatively expressed isoforms being conserved between species[182]. Alternatively regulated splice sites demonstrating temporal, spatial or reactive expression are less likely to show species conservation[183].

Several splicing factors have been suggested to be involved in organismal lifespan. The pre-mRNA processing factor 19 homologue (SNEV) protein, important for spliceosome assembly and mRNA processing, has been shown to suppress cellular senescence and suppress apoptosis when phosphorylated by the ataxia-telangiectasia (ATM) kinase in endothelial cells[184]. The DNA damage protein ATM also appears to be an important regulator of splicing factor expression in our previous work, since targeted gene knockdown of the ATM gene resulted in increased levels of splicing factor expression in fibroblasts[103]. There is also evidence from systemic models. A network-based model of genes altered by calorific restriction across 17 tissues in mice revealed that the largest and most responsive gene regulatory module was associated with mRNA processing, with a disproportionally large number of genes being involved in splicing, metabolism, processing and biosynthesis of mRNA[185]. Finally, a study of the relationship between copy number variation (CNV) and longevity in humans revealed that lifespan-associated CNVs were preferentially located in or near genes encoding proteins involved in splicing control. This led them to conclude that genetic variation that disrupts the processes of alternative splicing may have long-term effects on lifespan[186].

The study of inbred strains of mice has proven fruitful in uncovering factors associated with lifespan, as for other phenotypes. The Jackson Laboratory has characterized 30 strains of mice, for ageing and longevity-related traits[157,158]. Initial work with this resource identified that plasma IGF1 levels were related to lifespan in rodents[157]. This collection, together with the associated repository of mouse phenome data, represents a rich resource[187]. Here, we have harnessed this resource to assess the contribution of regulation of alternative splicing to longevity in mice.

We have systematically assessed the expression of splicing factors previously demonstrated to be altered in human ageing in relation to lifespan in six mouse strains of different longevities. Our study design is illustrated in Figure 3.1. Splicing factor expression and alternative splicing of key genes are associated with lifespan in mouse spleen tissue and to a lesser extent in mouse muscle, suggesting that ageing effects may be driven by immune tissues. Some strain differences in expression are most marked in the young mice, suggesting that they may represent determinants or early markers of longevity rather than representing secondary effects of ageing. We also identified differences in expression levels of alternatively expressed isoforms of key ageing genes indicative of reduced cellular senescence, maintained cellular proliferative capacity (spleen) and reduced pro-inflammatory signalling (muscle) in long-lived mouse strains. Two splicing factors, *HNRNPA2B1* and *HNRNPA1*, were also associated with parental longevity in a large population study of ageing, suggesting that regulation of splicing may also be involved in lifespan in human populations.

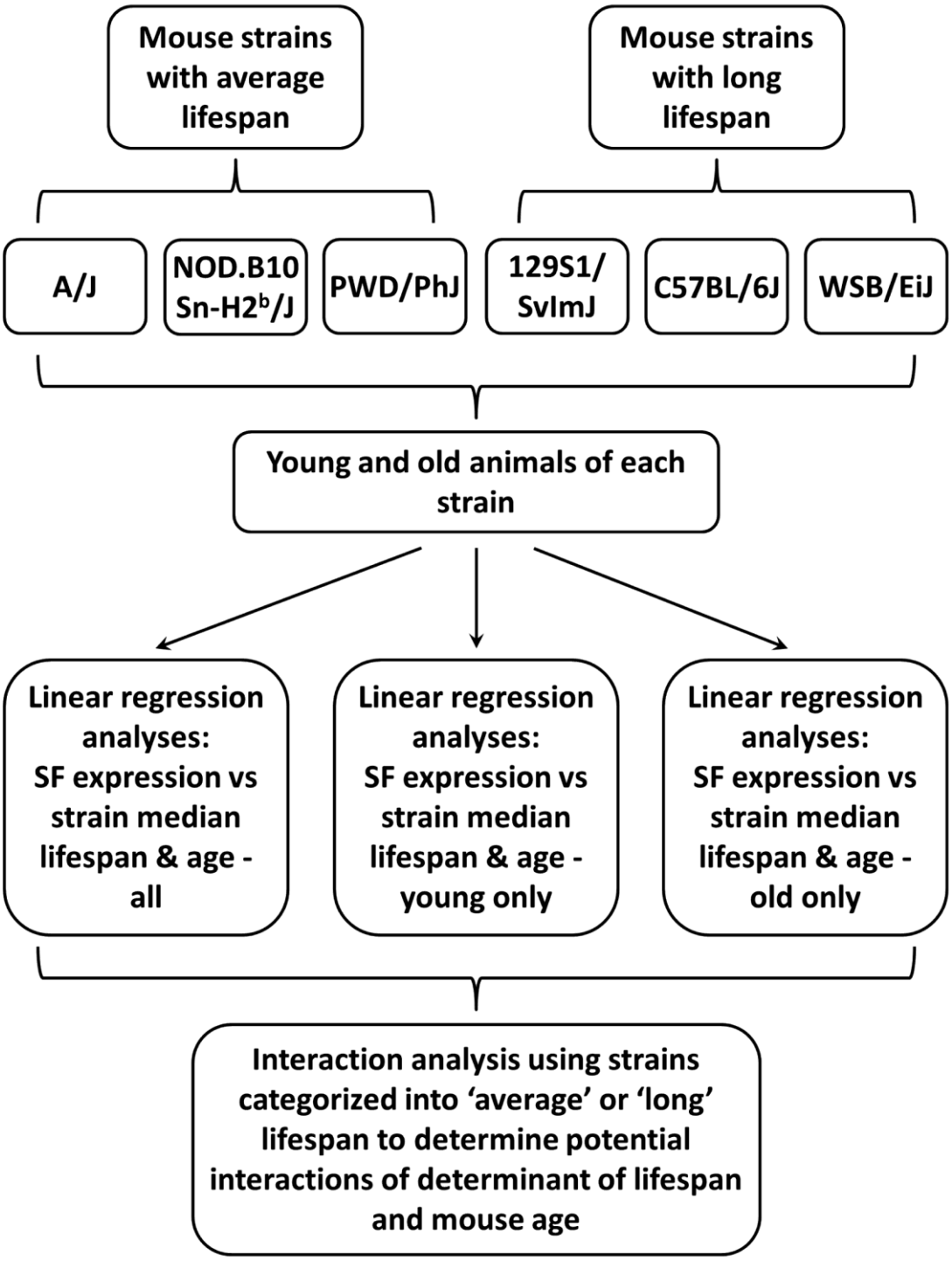

Figure 3.1: Schematic of study design

This figure shows the experimental strategy employed to assess the effects of strain longevity and mouse age on the expression of an a priori panel of splicing factors (SFs).

3.5 Results

3.5.1 Splicing factor transcript expression is associated with lifespan in mouse spleen and to a lesser extent in muscle tissues

We assessed splicing factors that we have previously demonstrated to be altered in human ageing in relation to lifespan in 6 mouse strains of different longevities and in samples from both old and young mice as in Figure 3.1. The expression of 8/15 and 3/15 splicing factors was associated with strain lifespan in mouse spleen and muscle tissue, respectively.

In spleen, we found associations between strain lifespan and the expression of the *Hnrnpa1*, *Hnrnpa2b1*, *Hnrnpk*, *Hnrnpm*, *Hnrnpul2*, *Sf3b1*, *Srsf3* and *Tra2b* genes (beta coefficients -0.40, -0.26, -0.32, -0.31, -0.22, -0.13 and -0.36; P = 0.01, 0.02, 0.003, 0.003, 0.04, 0.05, 0.02 and 0.02, respectively; Figure 3.2A, Supplementary table S1). When an analysis was carried out to assess interactions between strain lifespan and mouse age, we found effects in both young and old mice of long-lived strains for all associated genes except *Hnrnpul2*. In the case of *Hnrnpa1* and *Hnrnpa2b1* genes, these differences were more marked in the young mice of long-lived strains (beta coefficients -0.14 and -0.19, P = 0.001 and <0.0001 in the young long-lived mice compared with -0.09 and -0.12; P = 0.01 and 0.02 for the old long-lived mice for *Hnrnpa1* and *Hnrnpa2b1*, respectively; Supplementary table S9). For *Srsf3*, the associations between splicing factor expression/age and splicing factor expression/strain median lifespan appear to be comparable, whereas for *Tra2b*, our data suggest that the effects of age are stronger than those of lifespan (Supplementary table S9). The majority (5/8) of the splicing factors demonstrating association of expression differences with lifespan belonged to the hnRNP class of splicing inhibitors, with

only 2 splicing activators (*Srsf3* and *Tra2b*) showing expression changes with lifespan. The remaining associated splicing factor, *Sf3b1*, encodes a component of the U2 snRNP in the core spliceosome complex, rather than a splicing regulator. When data were assessed by binary logistic regression to allow for nonlinearity of response, all but one (*Hnrnpul2*) of the splicing regulators associated with lifespan in spleen remained associated with median strain lifespan (Supplementary table S10).

Fewer splicing factors were associated with strain lifespan in muscle tissue (Figure 3.2B, Supplementary table S2). *Hnrnpa0* expression was found to be positively correlated with long life (beta coefficient 0.36; P = 0.01), whereas *Hnrnpd* and *Srsf3* transcripts both demonstrated reduced expression (beta coefficients -0.24 and -0.40; P = 0.03 and 0.02, respectively). Interaction analysis revealed that the *Srsf3* effect was again driven by effects in the young animals of the long-lived strains (beta coefficient -0.14, P = 0.01 in the young long-lived mice compared with beta coefficient -0.05, P = 0.28 in the old long-lived mice; Supplementary table S9). Again 2/3 lifespan-associated splicing factors represented hnRNP splicing inhibitors rather than SRSF splicing activators. When data were assessed by binary logistic regression to allow for nonlinearity of response, all of the splicing regulators associated with lifespan in muscle remained associated with median strain lifespan (Supplementary table S11). Effects were tissue specific, with little overlap between lifespan-associated splicing factors in spleen and those in muscle, with only *Srsf3* common to both data sets.

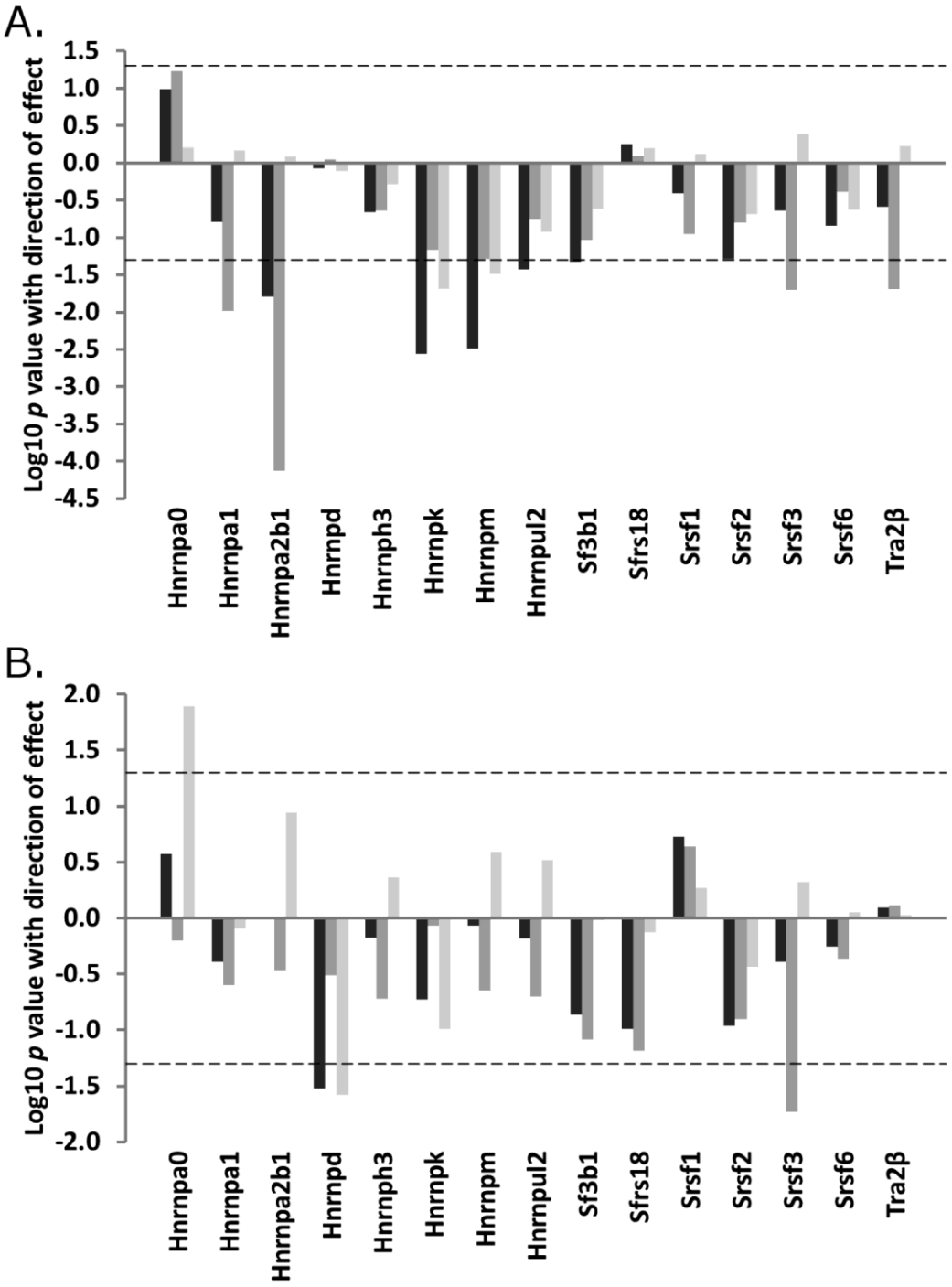

Figure 3.2: Splicing factor expression according to mouse lifespan

This plot illustrates association between median lifespan and splicing factor expression in total RNA from spleen (A) or muscle (B) tissues in mice of 6 strains of different longevities, as assessed by linear regression against median strain lifespan. The identity of specific splicing factors is given on the *x-axis*. The $\log_{10}$ *P*-values for associations between lifespan and splicing factor expression from mice of strains with different lifespans and of different ages are given on the *y-axis*. Direction of effect is also indicated; data appearing above the zero line on the *y-axis* represent positive associations, whilst data appearing below the zero line represent negative associations. Analysis including all animals in the sample is given by dark grey bars, in young animals only by medium grey bars and in old animals only by light grey bars. The dotted line refers to a *P*-value cut-off for statistical significance of $P = 0.05$.

3.5.2 Alternatively spliced genes demonstrate longevity-associated isoform changes in mouse spleen and muscle tissue

In spleen, we found splicing differences in association with lifespan for 4/8 genes tested (Figure 3.3A; Supplementary table S3). Both uc008toi.1 and uc008toh.1 transcripts encoding p16INK4A and p14ARF isoforms of the *Cdkn2a* gene were expressed at lower levels in the long-lived strains (beta coefficients -0.43 and -0.59; P = 0.002 and <0.0001 for uc008toi.1 [p16INK4A] and uc008toh.1 [p14ARF], respectively). Analysis of the interaction of strain longevity and mouse age revealed that although the effects on *Cdkn2a* isoform expression increased with age as expected in both average-lived and long-lived mice, the increase in expression was much less marked in the old long-lived mice than in old mice of average lifespan (beta coefficients 0.44 and 0.50, P = <0.0001 and <0.0001 for the old average-lived mice compared with beta coefficients 0.22 and 0.27, P = 0.01 and 0.001 for the old long-lived mice; Supplementary table S9).

We also found expression of the uc007bju.2 isoform only of the *Fn1* gene to be increased in the long-lived strains (beta coefficient 0.25, P = 0.02). There is increased expression of the long isoform of the *Trp53* gene encoding full-length p53 (uc007jql.2/uc007jqn.2), but reduced expression of the truncated *p53AS* isoforms (uc011xww.1/uc007jqm.2; beta coefficients 0.41 and -0.35, P = 0.009 and 0.03 for full-length *Trp53* and truncated *p53AS* isoforms, respectively). Assessment of the interaction between strain longevity and mouse age revealed that expression of the full-length p53 isoform is only significantly increased in the young animals of long-lived strains (in comparison with young animals of short-lived strains P = 0.004; the older animals were not significantly different to young short-lived strains P > 0.05) and that diminished expression of *p53AS* was only significantly decreased in the old animals of long-lived strains (P = 0.009, in

comparison with young animals of short-lived strains; other groups were $P > 0.05$, Supplementary table S9). Finally, expression of the full-length uc007rjg.1 isoform of the *Vcan* gene is upregulated (beta coefficient 0.34, $P = 0.001$).

In mouse muscle, expression of isoforms of all five genes tested in relation to lifespan was altered (Figure 3.3B, Supplementary table S4). First, expression of the full-length uc008mht.1 isoform of the *Il1b* gene was reduced in the long-lived strains (beta coefficient -0.46, $P = 0.007$), whilst the intron-retained uc008mhu.1 *Il1b* isoform was unaffected. Interaction analysis revealed that this difference was limited to the young mice of the long-lived strains ($P = 0.004$ for young long-lived mice compared with $P = 0.34$ for the old long-lived mice). Expression levels of the intron-retained uc008wuv.1 and full-length uc008wuw.1 isoforms of the *Il6* gene were also reduced (beta coefficient -0.48, $P = 0.006$ and -0.28, $P = 0.01$, respectively). Interaction analyses revealed that the effects on the intron-retained isoform were significant in the young long-lived mice only ($P = 0.04$ for young long-lived mice compared with $P = 0.72$ for old long-lived mice; Supplementary table S9).

Expression of the uc012cyg.1/uc008rlx.1 isoforms which encode the long full-length forms of the *Nfkb1* gene was greater in long-lived strains (beta coefficient 0.31, $P = 0.005$). No difference was seen in the expression of the noncoding truncated uc012cyf.1 *Nfkb1* isoform. Isoform usage for the *Stat1* gene in long-lived strains differed; the uc007axz.1 and uc007aya.2 isoforms of *Stat1* that both encode ‘variant 2’ of the STAT1 protein demonstrated diminished expression in the long-lived strains (beta coefficients -0.63, $P = <0.0001$), whereas the *Stat1* uc007ayc.2 isoform encoding ‘variant 1’ demonstrated increased expression in the long-lived strains (beta coefficient 0.46, $P = 0.007$). Interaction analysis revealed that the decrease in *Stat1* variant 2 expression was present only in the

old long-lived mice (*P* = 0.01 in old long-lived mice compared with *P* = 0.28 in the young long-lived mice; Supplementary table S9). The greater *Stat1* variant 1 expression was driven by effects in the young long-lived mice (*P* = 0.03 in young long-lived mice compared with *P* = 0.95 in old long-lived mice). Transcript uc007ayb.2, encoding *Stat1* 'variant 3', was also upregulated (beta coefficient 0.33, *P* = 0.005) although this was seen in both young and old animals of long-lived strains. Finally, expression of both the uc012arb.2 and uc008cgs.2 isoforms of the *Tnf* gene which encode TNF variants 1 and 2 were reduced in muscle (beta coefficients -0.27 and -0.18, *P* = 0.02 and 0.04 for uc012arb.2 and uc008cgs.2, respectively). Interaction analyses revealed that the effect for *Tnf* variant 1 is most marked in the old long-lived animals (*P* = 0.008 in the old long-lived animals compared with *P* = 0.05 in the young long-lived animals, Supplementary table S9).

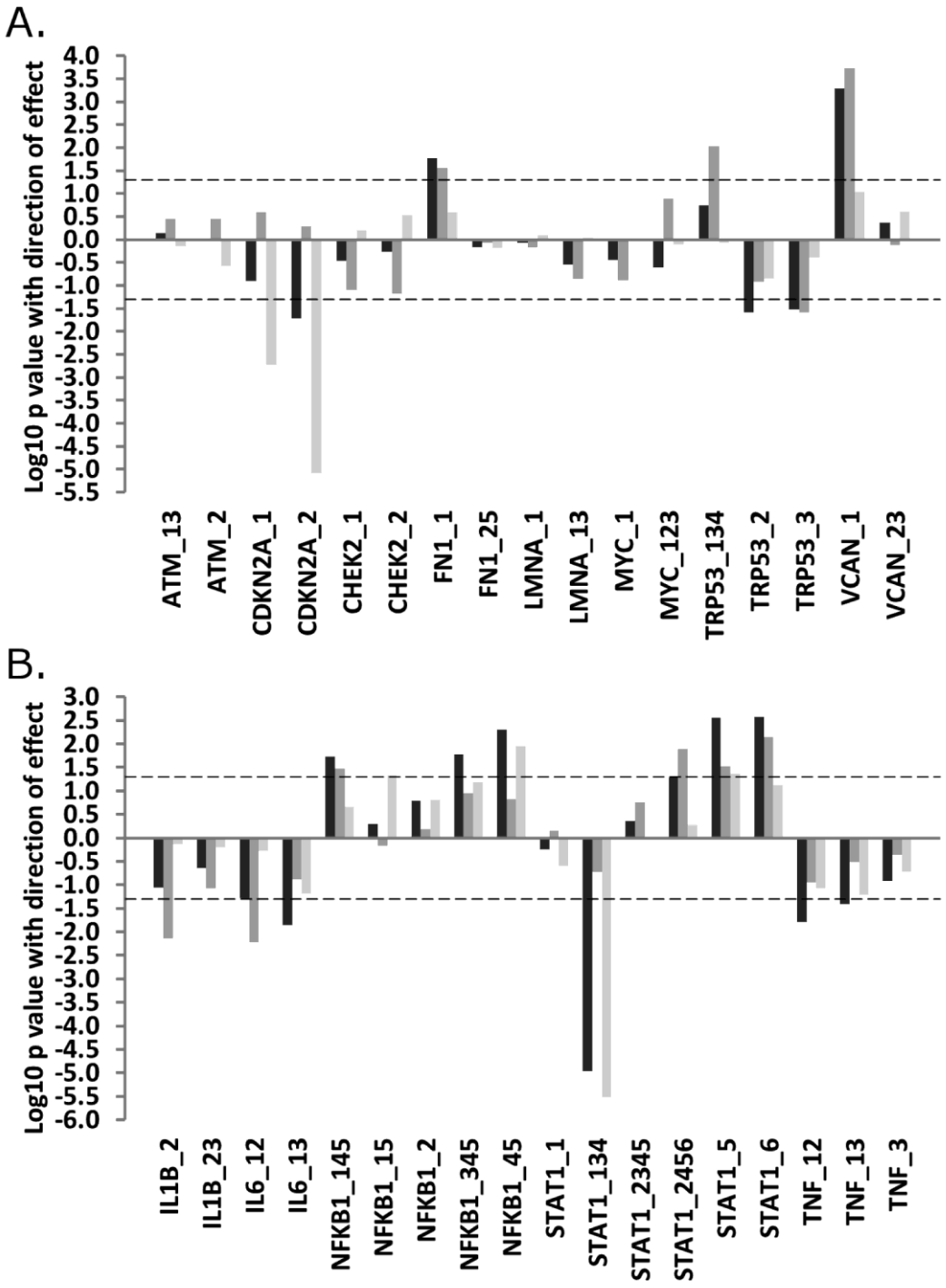

Figure 3.3: The expression of alternative isoforms of key genes according to mouse lifespan

This plot illustrates association between median lifespan and the expression of alternatively expressed isoforms of key genes in total RNA from spleen (A) or muscle (B) tissues in mice of 6 strains of different longevities as assessed by linear regression against median strain lifespan. The identity of specific splicing factors is given on the *x-axis*. The $\log_{10}$ *P*-values for associations between lifespan and splicing factor expression from mice of strains with different lifespans and of different ages are given on the *y-axis*. Direction of effect is also indicated; data appearing above the zero line on the *y-axis* represent positive associations, whilst data appearing below the zero line represent negative associations. Analysis including all animals in the sample is given by dark grey bars, in young animals only by medium grey bars and in old animals only by light grey bars. The dotted line refers to a *P*-value cut-off for statistical significance of $P = 0.05$.

3.5.3 Few splicing factors are associated with age in mouse spleen and muscle tissues

Associations between mouse age and splicing factor expression were less marked than those seen for strain longevity (Figure 3.4A, 3.4B, Supplementary tables S5 and S6). In spleen, we found reduced expression of the *Hnrnpa2b1*, *Srsf1*, *Srsf3* and *Tra2b* transcripts in old mice (beta coefficients -0.46, -0.34, -0.45 and -0.53; P = 0.005, 0.05, 0.007 and 0.008, respectively). Effects on *Srsf1*, *Srsf3* and *Tra2b* expression were evident in old animals of both average-lived and long-lived strains, but interaction analysis revealed that the age-associated difference in *Hnrnpa2b1* expression was most marked in the old animals of strains of average lifespan (beta coefficients -0.11, P = 0.02 in the old long-lived animals compared to beta coefficient -0.13 P = <0.0001 in the old average-lived animals). Age-associated changes to splicing factor expression were much less evident in muscle tissue, with only *Hnrnpa1* demonstrating increased expression (beta coefficient 0.22, P = 0.05). Analysis of cluster patterns for age revealed considerable inter- and intrastrain heterogeneity in splicing factor expression (Supplementary figure S1).

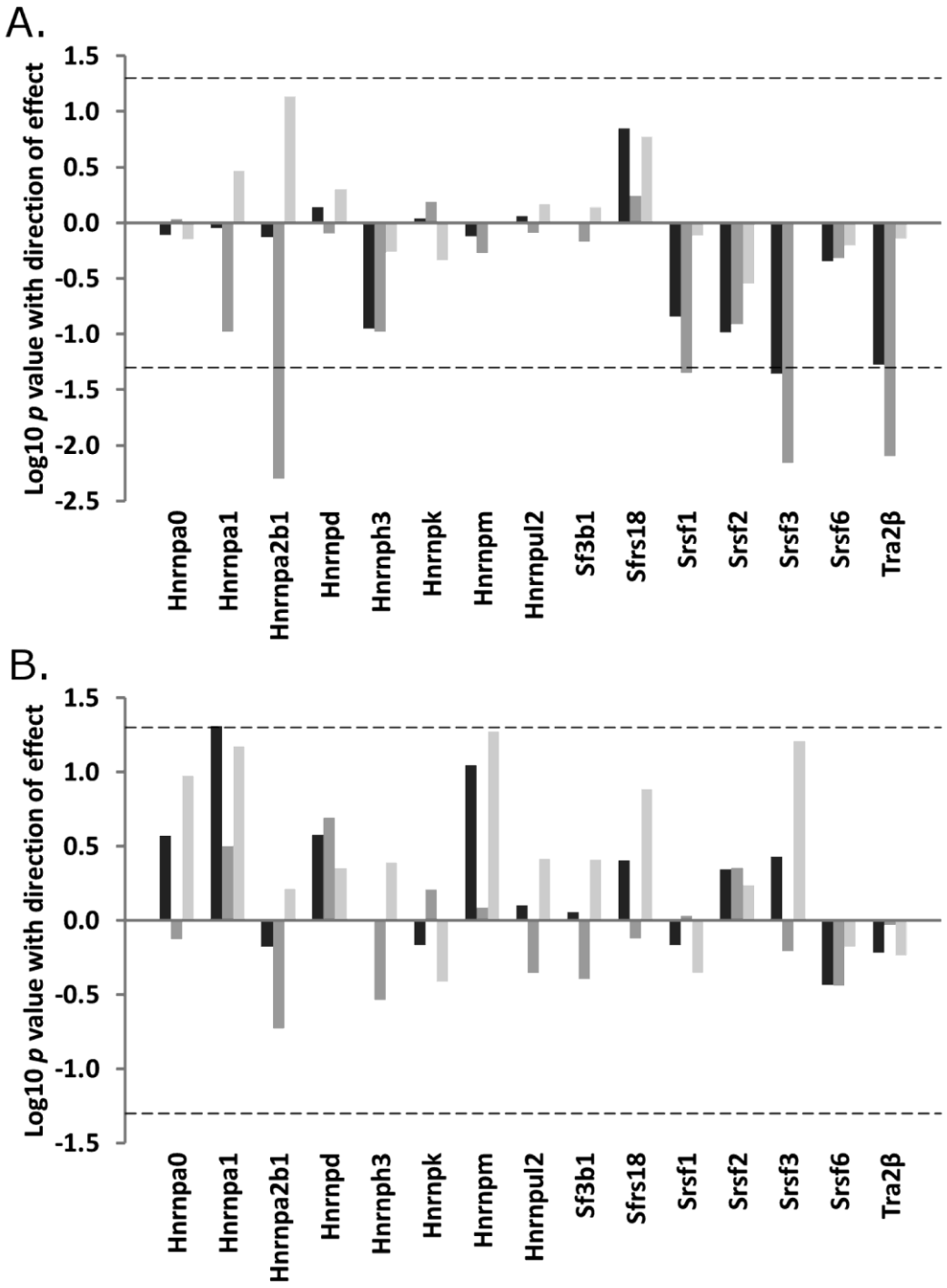

Figure 3.4: Splicing factor expression according to mouse age

This plot illustrates association between age and splicing factor expression in total RNA from spleen (A) or muscle (B) tissues in young (6 months) vs. old (20–22 months) mice. The identity of specific splicing factors is given on the *x-axis*. The $\log_{10}$ P-values for associations between age and splicing factor expression from mice of different ages and of different strains are given on the *y-axis*. Direction of effect is also indicated; data appearing above the zero line on the *y-axis* represent positive associations, whilst data appearing below the zero line represent negative associations. Analysis including all animals in the sample is given by dark grey bars, in animals of average-lived strains only by medium grey bars and in long-lived animals only by light grey bars. The dotted line refers to a *P*-value cut-off for statistical significance of $P = 0.05$.

3.5.4 Alternatively expressed isoforms demonstrate differential expression with age in mouse spleen and muscle tissue

Despite the small numbers of splicing factors demonstrating age-associated differences in splicing factor expression, we noted differences in alternative splicing in both spleen and muscle from aged mice (Figure 3.5A, 3.5B, Supplementary tables S7 and S8).

In mouse spleen, we identified increased expression of both uc008toi.1 and uc008toh.1 transcripts encoding p16INK4A and p14ARF isoforms of the *Cdkn2a* gene in the old animals as expected (beta coefficients 0.40 and 0.53, *P* = <0.0001 and <0.0001, respectively). Interaction analyses revealed the age-associated increase in both *Cdkn2a* isoforms to be significantly reduced in old animals of long-lived strains as described above. We also identified decreased expression of both uc008yrw.1 (full length) and uc008yrx.1 (exon skipped) isoforms of the *Chek2* gene with increasing age (beta coefficients -0.33 and -0.35, *P* = 0.02 and 0.01, respectively). Interaction analyses between mouse age and strain longevity revealed that reduced expression of the full-length *Chek2* isoform was more marked in the old animals of the long-lived strains (beta coefficient -0.26, *P* = <0.0001 in the old long-lived animals compared with beta coefficient -0.24, *P* = 0.003 in the old average-lived animals; Supplementary table S9). *Trp53* isoforms also demonstrated effects with age in mouse spleen. With age, there was a reduction in levels of transcripts encoding both full-length p53 (uc007jql.2/uc007jqn.2) and also those encoding the truncated alternatively spliced p53AS (uc007jqm.2) isoform (beta coefficients -0.24 and -0.24, *P* = 0.02 and 0.03, respectively).

In mouse muscle, we found increased expression of both the full-length (uc008mht.1) and the intron-inclusion (uc008mhu.1) *Il1b* transcripts with age (beta coefficients 0.37 and 0.39, P = 0.001 and <0.0001). The old animals also demonstrated elevated expression of the uc008wuv.1 isoform of the *Il6* gene, which contains a retention of intron 4 relative to the consensus transcript (beta coefficient 0.44, *P* = 0.003). Old animals also demonstrated reduction of uc007ayd.2, uc007aya.2, uc007ayb.2 and uc007ayc.2 isoforms of the *Stat1* gene, with the effects on uc007aya.2 being revealed by interaction analysis between mouse age and strain lifespan to be present exclusively in the old animals of long-lived strains (beta coefficient -0.17, *P* = 0.01; Supplementary table S9).

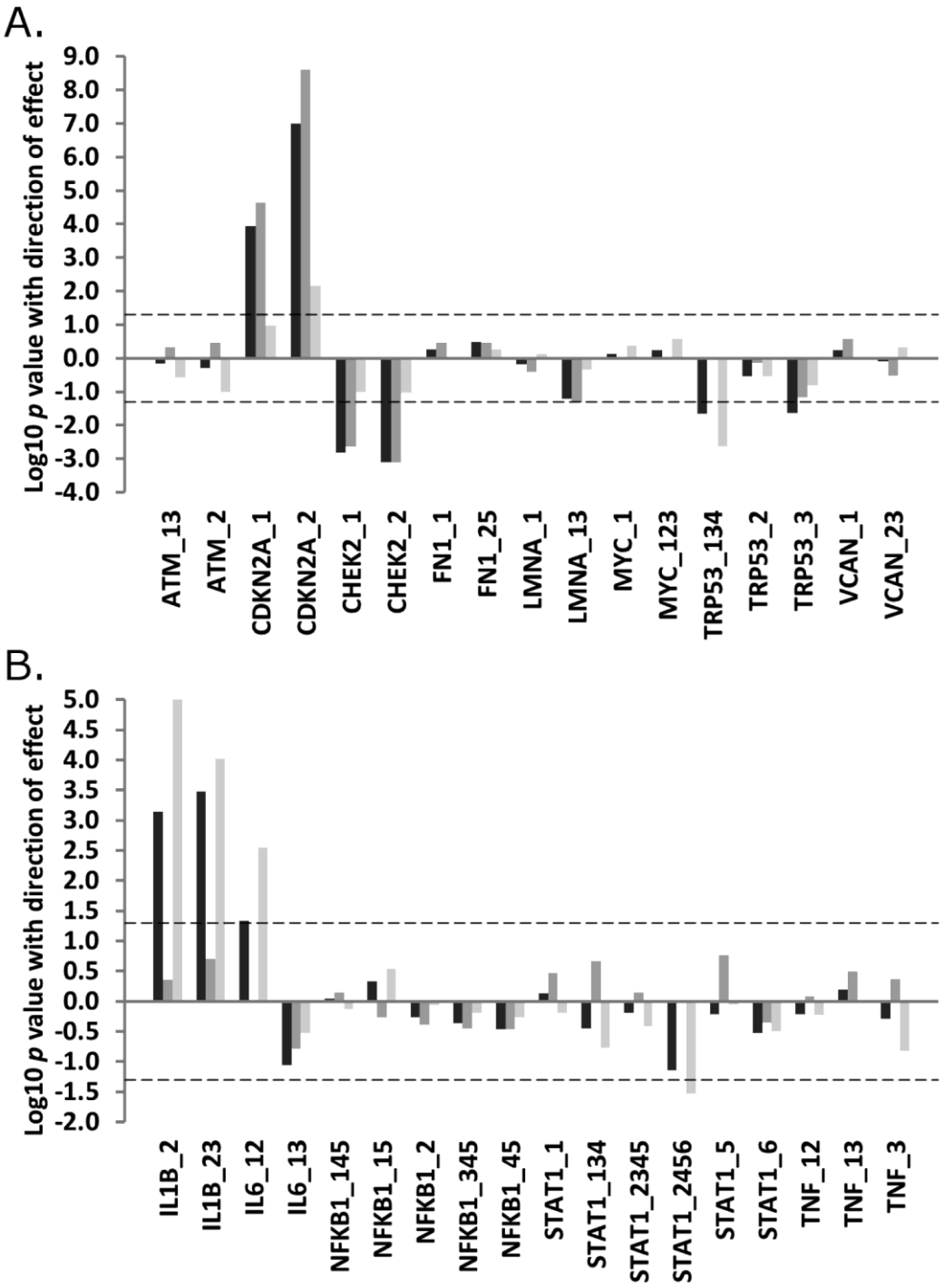

Figure 3.5: The expression of alternative isoforms of key genes according to mouse age

This plot illustrates association between the expression of age and the expression of alternatively expressed isoforms of key genes in total RNA from spleen (A) or muscle (B) tissues in young (6 months) vs. old (20–22 months) mice. The identity of isoforms is given on the *x-axis*. The $\log_{10}$ *P*-values for associations between age and the expression of alternative isoforms from mice of different ages and of different strains are given on the *y-axis*. Direction of effect is also indicated; data appearing above the zero line on the *y-axis* represent positive associations, whilst data appearing below the zero line represent negative associations. Analysis including all animals in the sample is given by dark grey bars, in animals of average-lived strains only by medium grey bars and in long-lived animals only by light grey bars. The dotted line refers to a *P*-value cut-off for statistical significance of $P = 0.05$.

3.5.5 The expression of some splicing factors is associated with parental longevity in a large human population

We examined the expression of 15 splicing factors identified through the mouse work described in this study and previous analyses[103] and determined that 2 genes, *HNRNPA2B1* and *HNRNPA1*, demonstrated associations of their expression with parental longevity, as defined in Dutta *et al*.[188] in the human InCHIANTI population study as well as in mice (Table 3.1). *HNRNPA2B1* transcripts demonstrated increased expression in the offspring of long-lived parents (beta coefficient 0.12, P = 0.017), whereas *HNRNPA1* demonstrated reduced expression in the offspring of long-lived parents (beta coefficient -0.09; P = 0.035, respectively; Table 3.1). *Hnrnpa1* demonstrates reduced expression in association with longevity in both man and mouse, whereas *Hnrnpa2b1* shows elevated expression with longevity in people, but reduced expression with longevity in mice.

Table 3.1: Associations between splicing factor expression and parental longevity in humans (the InCHIANTI population)

The relationship of parental longevity with expression of 15 unique splicing factors in 405 individuals by multivariate linear regression. Genes demonstrating significant associations at *P* = <0.05 are indicated in bold underlined text.

Gene name	Probe ID	Beta coefficient	95% Confidence intervals		*P*-value
HNRNPA2B1	ILMN_1886493	0.116	0.020	0.212	**0.017**
HNRNPA1	ILMN_1676091	-0.091	-0.176	-0.006	**0.035**
HNRNPA2B1	ILMN_2369682	0.088	0.002	0.175	**0.044**
TRA2B	ILMN_1742798	0.092	-0.001	0.186	0.051
HNRNPA1	ILMN_1661346	0.069	-0.004	0.143	0.065
SRSF1	ILMN_1795341	0.082	-0.008	0.171	0.073
HNRNPD	ILMN_2321451	0.088	-0.010	0.186	0.078
HNRNPK	ILMN_1701753	-0.066	-0.176	0.043	0.232
HNRNPUL2	ILMN_2072091	0.076	-0.053	0.205	0.246
HNRNPK	ILMN_2378048	0.060	-0.058	0.178	0.319
SRSF18	ILMN_2161357	0.068	-0.072	0.209	0.341
HNRNPUL2	ILMN_1810327	0.055	-0.066	0.176	0.374
HNRNPA1	ILMN_2220283	0.034	-0.051	0.119	0.432
SRSF2	ILMN_1696407	0.047	-0.074	0.167	0.446
HNRNPD	ILMN_1751368	-0.034	-0.137	0.068	0.511
SRSF6	ILMN_1697469	0.033	-0.077	0.143	0.552
SRSF6	ILMN_1754304	0.030	-0.078	0.138	0.585
HNRNPA0	ILMN_1753279	-0.035	-0.164	0.095	0.598
HNRNPA1	ILMN_1663447	-0.034	-0.168	0.101	0.624
HNRNPA1	ILMN_1720745	0.025	-0.080	0.131	0.637
HNRNPM	ILMN_2385173	-0.029	-0.161	0.103	0.668
SRSF6	ILMN_1805371	-0.026	-0.149	0.096	0.673
SF3B1	ILMN_1712347	-0.022	-0.151	0.107	0.738
SF3B1	ILMN_1705151	0.017	-0.091	0.125	0.754
HNRNPM	ILMN_1745385	-0.016	-0.119	0.086	0.756
HNRNPA1	ILMN_2175075	-0.012	-0.126	0.102	0.838
SRSF3	ILMN_2389582	0.004	-0.118	0.125	0.951

3.5.6 Genetic variation within Hnrnpa2b1 and Hnrnpa1 that is discrepant between strains is unlikely to contribute to differences in gene expression

We have carried out a bioinformatic analysis of the potential for genetic variation that is discrepant between strains of mice to affect the regulation of the *Hnrnpa2b1* and *Hnrnpa1* genes. These genes were selected because their expression is associated with longevity in both mouse and man. The *Hnrnpa2b1* gene harbours 14 genetic variants that are discordant between strains. Two of these variants, rs51031918 and rs252413833, are associated with changes to the binding efficiencies of *SRSF2* and *SRSF5* splicing enhancers (see Supplementary table S12). These changes are, however, very subtle and may not adversely affect *SRSF2* or *SRSF5* binding. Similarly, two *Hnrnpa1* variants (rs32398879 and rs50030666) are discordant between the strains. One of these, rs50030666, lies in a cassette exon which is intronic in some *Hnrnpa1* isoforms, but coding in others (see Supplementary table S12). The coding change causes the substitution of glycine residue for a similarly sized serine residue with equivalent charge. No other predicted effects of genetic variation on transcription factor binding, RNA regulatory elements (A-rich elements, C to U RNA editing sites or microRNA binding sites) were identified for any variant studied.

3.6 Discussion

Splicing factor expression has been shown to be conclusively associated with chronological age in humans[101] and also with cellular senescence in multiple human primary cell lines in culture[103], indicating that these factors may be linked with cellular plasticity and adaptability during the ageing process. Here, we have assessed the potential relationships between splicing factor expression and alternative splicing with strain longevity across 6 mouse strains of variable medium to long lifespans, in both young and old animals. We also assessed associations between splicing factor expression and parental longevity in the offspring of long-lived parents in humans.

We have found that over half of the splicing factors tested are associated with longevity in mouse spleen, and to a lesser extent in mouse muscle and that these changes are accompanied by alterations to the profile of selected alternatively expressed isoforms in both tissues. Two splicing factors, *HNRNPA1* and *HNRNPA2B1*, also showed evidence of an association with parental longevity in humans. These results, to our knowledge, represent the first link between the regulation of alternative splicing and inherited longevity traits in mammals.

In spleen, 7/15 splicing factors tested demonstrated associations with strain longevity in both young and old animals, with effects being predominant in the young animals of longer-lived strains suggesting that these differences in splicing factor expression are not the end result of ageing processes as such, but rather may represent fundamental differences in factor expression that drive or contribute to the ageing process. It is possible that changes happening early on in life may set the scene for future longevity, which is an interesting concept given that several genes such as *Foxo1*, known to be associated with extended

lifespan, are developmental genes[189]. It is very difficult to predict what the consequence of these changes will be to the overall level or pattern of splicing in long-lived mice or humans, since splice site choice at any given exon: intron junction is determined by the balance of activators and repressors, and that this balance is individually determined for each splice site in each gene[176]. However, diminished splicing factor expression may be beneficial in younger animals, since both SRSF and hnRNP splicing factors are known to have oncogenic features[190-192]. Lower splicing factor expression in younger animals may thus protect against an earlier death from malignancy.

We also found clear evidence to suggest tissue specificity of effect which is very common in studies of splicing with 8/15 (53%) splicing factors showing associations with strain longevity in spleen, but only 3/15 (20%) in muscle. It would be interesting to determine whether the splicing events targeted by these sets of splicing factors also show associations between median strain lifespan and splice site usage, but such analysis would be very difficult due to degeneracy of splicing factor binding sites, potential for compensation by other splicing factors and the fact that splice site usage is dependent on the balance of enhancers and silencers rather than on the binding of a specific splicing factor *per se*. The pattern of longevity-associated splicing regulator transcripts showed little overlap between the spleen and muscle data sets, with only changes to *Srsf3* expression being common to both tissues. This is in line with our previous findings, as we have previously shown that although fibroblasts and endothelial cells that have undergone *in vitro* senescence both show deregulation of splicing factors, the patterns of precisely which regulators are altered show quite marked differences between cell types[103]. Spleen is a lymphoid organ, consisting of large numbers of white blood cells. Most of the transcripts extracted from spleen will arise from

B cells, T cells and mononuclear phagocytes. Our findings may thus reflect the hypothesis that ageing of the immune system is one of the drivers of development of ageing phenotypes[193]. It should also be considered that the preponderance of splicing factor expression changes in spleen compared with muscle could also reflect an accelerated rate of ageing and more extensive tissue modification in spleen compared to muscle. White blood cells are also highly heterogeneous, reactive and proliferative but relatively unspecialized compared to the highly differentiated non-proliferative muscle cells. It may be that muscle requires less adaptive response than spleen cells, since it has a defined and tightly regulated function with less need to respond to environmental challenge.

Previous work from our group has identified that offspring of long-lived parents may have better health[188,194]. In the current study, two of the associations between splicing factor expression and longevity were also seen in RNA samples derived from the peripheral blood of participants in the InCHIANTI study[163], where we found relationships between expression of the *HNRNPA2B1* and *HNRNPA1* transcripts and parental longevity. *HNRNPA2B1* demonstrated increased expression in blood RNA from people with at least one long-lived parent, whereas parental longevity (as a continuous trait reflecting the combined age at death of both parents) was associated with lower *HNRNPA1* expression (Table 3.1). *Hnrnpa1* is also downregulated with greater lifespan in mouse splenocytes, but the *HNRNPA2B1* effect in humans is reversed compared to what we observe in the mice. This may be because the association between *Hnrnpa2b1* expression and longevity is most marked in the young animals of the long-lived strains, and our human subjects are mostly elderly, with a mean age of approximately 75 years[101]. Interestingly, both *Hnrnpa2b1* and *Hnrnpa1* are known to be determinants of lifespan in Drosophila species, by virtue of their regulation of the

TDP-43 protein[195]. TDP-43 is crucial in fruit flies for correct splicing and regulation of mRNA stability and is associated with amyotrophic lobar sclerosis and frontotemporal lobar degeneration in humans[196,197]. Mutations have also been described in age-related diseases such as Alzheimer's, Parkinson's and Huntington's diseases[198]. Recent studies have shown that the action of TDP-43 relies on its ability to tether hnRNPA2B1 and hnRNPA1 proteins, and disruption or abolition of this association dramatically reduces lifespan in Drosophila[195].

The consequences of altered splicing in spleen give a broad picture of altered expression and processing of genes involved in reduced cell senescence, superior DNA repair and retained cellular proliferative capacity in the long-lived strains. Old animals of long-lived strains of mice expressed reduced amounts of *Cdkn2a* isoforms compared with old animals of average-lived strains. *Cdkn2a* is an important marker of cellular senescence[199] and ablation of *Cdkn2a* expression reverses ageing phenotypes in klotho mice[200], indicating that old animals of long-lived strains may have lower levels of senescent cells. Young animals of longer-lived strains also expressed profiles of *Trp53* isoforms consistent with enhanced transcription and cell growth properties compared to young animals of average-lived strains, since they express higher levels of full-length p53 and lower levels of truncated p53AS which is thought to have antagonistic function[201-203]. Altered splicing of inflammatory genes involved in muscle remodelling produces a picture consistent with lower levels of pro-inflammatory signalling by virtue of lower levels of *Il1b* and *Il6* expression in young animals and reduced *Tnf* signalling in the older animals of long-lived strains.

We saw fewer associations of splicing factor expression with chronological age than we expected based on our previous human data. Our previous work suggests that splicing factor expression is strongly associated with age in humans

and with cellular senescence in human cell models[101,103]. In our human work, the per-year age-related changes in splicing factor expression were also relatively small (beta coefficients ranging from -0.01 to 0.005)[103], which may explain why strong effects were not seen in the current mouse study where our sample numbers were much smaller. There is also considerable interstrain heterogeneity for most splicing factors; the young animals of one strain may express lower basal levels of splicing factors than the older animals of another and effects of ageing may thus be difficult to detect in small numbers of samples (Supplementary figure S1). These data suggest that the associations of splicing factor expression with longevity across strains may actually be considerably larger than effects of age alone on splicing factor expression within strains. Again, most changes seen in this study were seen in spleen, which is consistent with a key role in senescence for immune-mediated drivers of ageing and ageing phenotypes.

The limitations of our study include the relatively small sample sizes, restriction of our analyses to a small number of tissues, and the fact that we have assessed splicing patterns only at the mRNA level. Gene expression is a highly variable parameter in biological systems, so future experiments are likely to need larger sample sizes and assessment of potential effects in other tissue types, as well as assessment of effects on protein levels. Although the genes tested were selected *a priori* and therefore do not require adjustment for multiple testing, one must recognize that this does not entirely remove the possibility of false positives. It must also be considered that differences in splicing factor and isoform expression may arise not only from changes in the amount of transcription, but also from differences in the relative stabilities of different isoforms. These changes may form part of the mechanistic basis for our associations, as we would not expect stability changes unrelated to longevity to associate statistically with strain

median lifespan. Finally, in the human follow up work described here, we were also restricted by the availability of expression data for all interesting splicing factors on the array and the likelihood that any effects were likely to be moderate on a per-year basis as they were in our previous human age data. This is likely to have reduced our power in the human study, and thus further work in larger populations is now required to definitively explore this possibility in human subjects.

Another potential caveat is that the splicing factor expression differences we have discovered in this study reflect other strain differences that are unrelated to longevity. Whilst this is a possibility, the links between splicing factor expression and ageing in humans and other animals are well documented from our previous work[101,103] and that of other groups[204]. Our observation that the lifespan-associated expression changes relating to *Hnnrpa2b1* and *Hnrnpa1* we observe in mice are also translatable to humans is also supportive of our conclusions. More broadly, the importance of splicing factors in determination of lifespan is also suggested by studies of the effects of calorific restriction in mice[185] and studies of the relationship between copy number variant (CNV) polymorphisms and longevity in humans[186].

Some of the genetic differences between strains may actually contribute mechanistically to the differences in strain median lifespan. To that effect, we carried out a bioinformatic analysis on the potential for genetic variation discordant between strains to lead to gene regulation differences for *Hnrnpa2b1* and *Hnrnpa1*, where we also found effects in man. We discovered some minor changes to the bioinformatically predicted strength of SRSF2 and SRSF5 binding within *Hnrnpa2b1* and a potential amino acid change for an alternatively expressed isoform of *Hnrnpa1*. Although these predictions are interesting, the

predicted effects of the changes on *Hnrnpa2b1* or *Hnrnpa1* expression or activity are likely to be slight. The splicing effects cause only a slight alteration to predicted binding efficiency of SRSF2 or SRSF5, and the coding change involves the substitution of a serine for a glycine in an alternatively spliced cassette exon of *Hnrnpa1*, which may not comprise the major isoform at this locus. These amino acids are in any case of similar size and charge and may not cause much change to protein functionality. It is likely the effects on median strain longevity arise from multiple changes in many genes.

To be able to assign definitive causality for a role for splicing factors as determinants of longevity, it would be necessary to carry out detailed functional experiments *in vivo* and *in vitro*, which could form the basis for future studies. Such studies could comprise constitutive or conditional knockout or overexpression studies in animal models followed by assessment of effects on lifespan, or *in vitro* manipulation of splicing factor levels followed by investigation of effects on cellular senescence. Such an approach has previously been employed for the *Hnrnpa1* and *Hnrnpa2b1* genes where upregulation of the *Hnrnpa1* gene or the *Hnrnpa2* isoform of the *Hnrnpa2b1* gene in mouse hepatocarcinoma cells was shown to cause activation of the RAS-MAPK-ERK pathway[205]. This is potentially important since a recent study has shown that activation of the RAS-ERK-ETS pathway is a key determinant of lifespan in Drosophila species[206].

Both *in vivo* and *in vitro* studies to moderate the levels or activity of splicing factors in relation to longevity would not be without caveat. Splice site choice is a complex phenomenon and relies upon the balance of splicing activators or silencers, rather than the activity of a single splicing factor *per se*[176]. This finding, together with observations that exon and intron splicing enhancers and silencers

often cluster near splice sites, raises the possibility of compensation between splicing regulatory factors. Selective modulation of a single splicing factor may not then show direct effects on longevity, effects would most probably only be noted after knockdown or overexpression of multiple splicing factors which would have technical challenges both *in vitro* and *in vivo*.

This study reports the first evidence of a link between expression of splicing regulator genes and strain lifespan in mice, together with data in support of potential roles for *HNRNPA1* and *HNRNPA2B1* in parental longevity in humans. We hypothesize that an influence of splicing factor expression on longevity may be mediated by slower immune ageing and a protection from malignancy in the young mice of long-lived strains by virtue of restricting expression of SR and hnRNP proteins which have oncogenic potential in young animals. Both of the splicing factor transcripts demonstrating reduced expression in the old long-lived mice belonged to the hnRNP class of splicing regulators, indicating that these mice may have less inhibition of splice site usage and be better able to maintain splicing, and therefore cellular plasticity into older age. The changes in splicing factor expression in the spleen are accompanied by changes in alternatively spliced genes indicative of reduced cell senescence, superior DNA repair and retained cellular proliferative capacity, and changes in splicing factor expression in muscle are indicative of lower pro-inflammatory signalling. Our data highlight the importance of regulation of mRNA processing in determination of lifespan and suggest that splicing factors may provide novel points of intervention for future therapies to reduce disease burden in old age. Moreover, since some of these strains (e.g. C57BL/6J, A/J) are commonly used for the creation and cross-breeding of genetically modified mice, strain-specific alterations in alternative

splicing could account for unexpected contributions to the final phenotype arising from the genetic background.

3.7 Experimental Procedures

3.7.1 Mouse strains used for analysis

Strains were chosen on the basis of differential lifespan (A/J, NOD.B10Sn-H2^{b}/J, PWD.Phj, 129S1/SvlmJ, C57BL/6J and WSB/EiJ; see Table 3.2 for lifespan details) that were measured in a longitudinal study[157-159] at Jackson Laboratory Nathan Shock Center of Excellence in the Basic Biology of Aging. Strains with extremely short lifespans (median lifespan less than 600 days) were excluded on the basis that a short lifespan may be associated with significant comorbidities. Characteristics of the mice and the numbers of animals used in each category are given in Table 3.2. All mice used in this study were male. All tissues were obtained from the mice of a cross-sectional study that was conducted at the same period of time and in the same mouse room with the longitudinal study. Animal housing conditions have been fully described previously[157,159]. Briefly, mice were fed *ad libitum* an autoclaved pellet diet with 6% fat and acidified water (pH 2.8–3.1). Animals were kept on a 12:12-h light/dark cycle at 50% relative humidity at 21–23 °C, in a restricted access specific pathogen-free barrier facility. Mice were housed four animals per pen in individually ventilated polycarbonate cages supplied with HEPA-filtered air and were tested quarterly for (and were free of) common viral, bacterial and mycoplasmal species. Mice were inspected daily and excluded if ill. At 6 or 20/22 months of age, mice were euthanized by CO_2 asphyxiation, followed by blood collection via cardiac puncture and cervical dislocation. A detailed description of the tissue collection procedure is given in Supplementary table S1. Immediately after death, spleen and quadriceps muscle

tissues were excised and snap-frozen in vapour-phase liquid nitrogen for storage within 5 min of collection. Tissues were stored at -80 °C.

3.7.2 Splicing factor candidate genes for analysis

An *a priori* list of splicing factor candidate genes were chosen on the basis that they were associated with human ageing in populations and in primary human cell lines that had undergone *in vitro* senescence in our previous work[101,103]. The list of genes included the positive regulatory splicing factors *Srsf1*, *Srsf2*, *Srsf3*, *Srsf6*, *Srsf18* and *Tra2b*, the negative regulatory splicing inhibitors *Hnrnpa0*, *Hnrnpa1*, *Hnrnpa2b1*, *Hnrnpd*, *Hnrnph3*, *Hnrnpk*, *Hnrnpm*, *Hnrnpul2* and the *Sf3b1* subunit of the U2 spliceosome snRNP, which we have previously shown to be associated with age-related altered DNA methylation[207]. Assays were obtained in custom TaqMan low-density array (TLDA) format from Life Technologies (Foster City, CA, USA). Assay Identifiers are given in Supplementary table S2.

3.7.3 Alternatively spliced target genes in spleen

Genes were chosen for assessment of alternative splicing in spleen on the basis of potential roles in cellular senescence (*Cdkn2a*), cell cycle regulation (*Trp53*, *Myc*), extracellular matrix (*Fn1*, *Vcan*) or DNA damage response (*Atm*, *Chek2*), since these genes may also be important in determination of lifespan. We designed TaqMan quantitative real-time PCR assays to identify specific isoforms or groups of isoforms (if large numbers of common regions rendered the design of specific probes impossible). Assays were obtained in custom TaqMan low-density array (TLDA) format from Life Technologies. Assay Identifiers are given in Supplementary data S2. A list of transcripts captured by each assay are given in Supplementary data S3.

Table 3.2: Characteristics of mouse strains

The mean lifespan and the maximum lifespan (20% longest lived) are given for each strain used in this study. All mice used in this study were male. Young mice were 6 months old, and old mice were 20–22 months old. Muscle tissue was taken from the quadriceps.

*Strain Max Age = the mean of the longest lived 20% within each strain. Data for median and maximum lifespans are given in Yuan et al. (2011) from a longitudinal study that was performed in conjunction with the cross-sectional study described in the present paper.

Strain	Strain Median lifespan (days)	Strain Max Age (days)*	Longevity class	N Young	N Old
A/J	623	785	Average lifespan	Spleen - 7 Muscle - 8	Spleen - 7 Muscle - 7
NOD.B10Sn-H2^{b}/J	696	954	Average lifespan	Spleen - 4 Muscle - 4	Spleen - 6 Muscle - 6
PWD/PhJ	813	956	Average lifespan	Spleen - 5 Muscle - 4	Spleen - 6 Muscle - 6
129S1/SvlmJ	882	1044	Long-lived	Spleen - 10 Muscle - 4	Spleen - 10 Muscle - 10
C57BL/6J	901	1061	Long-lived	Spleen - 10 Muscle - 10	Spleen - 8 Muscle - 9
WSB/EiJ	1005	1213	Long-lived	Spleen - 5 Muscle - 5	Spleen - 10 Muscle - 10

3.7.4 Alternatively spliced target genes in muscle

Genes were selected for analysis of alternative splicing in muscle on the basis of potential roles in inflammatory processes relating to muscle remodelling since we have shown in our previous work that these processes are key determinants of muscle strength in older humans[208,209]. Our gene list included isoforms of the *Il1b*, *Il6*, *Nfkb1*, *Stat1* and *Tnf* genes. As above, TaqMan quantitative real-time PCR assays were designed to identify specific isoforms or groups of isoforms (if large numbers of common regions rendered the design of specific probes impossible). Assays were obtained in custom TaqMan low-density array (TLDA) format from Life Technologies. Assay Identifiers are given in Supplementary data S2.

3.7.5 RNA extraction and reverse transcription

Tissue samples were removed from storage and placed in 1 mL TRI Reagent® solution supplemented with the addition of 10 mM $MgCl_2$ to aid recovery of microRNAs for future analysis[165]. Samples were then completely homogenized (15mins for spleen samples, 30mins for muscle samples) using a bead mill (Retsch Technology GmbH, Haan, Germany). Phase separation was carried out using chloroform. Total RNA was precipitated from the aqueous phase by means of an overnight incubation at -20 °C with isopropanol. RNA pellets were then ethanol-washed twice and resuspended in RNase-free dH_2O. RNA quality and concentration was assessed by Nanodrop spectrophotometry (Wilmington, DE, USA). Complementary DNA (cDNA) was then reverse transcribed from 100 ng total RNA using the Invitrogen VILO cDNA synthesis kit (Life Technologies) in 20 µL reactions according to manufacturer's instructions.

3.7.6 Quantitative real-time PCR and data analysis

Quantitative RT–PCRs were performed on the ABI 7900HT platform (Life Technologies) on the TaqMan low-density array (TLDA) platform. Cycling conditions were 50 °C for 2 min, 94.5 °C for 10 min and 50 cycles of 97 °C for 30 s and 57.9 °C for 1 min. The reaction mixes included 50 µL TaqMan® Universal PCR Mastermix II (no AmpErase® UNG) (Life Technologies), 30 µL dH2O and 20 µL cDNA template. 100 µL reaction solution was dispensed into the TLDA card chamber and centrifuged twice for 1 min at 216 × g to ensure distribution of solution to each well. The expression of transcripts in each sample was measured in duplicate replicates. The comparative C_T technique was used to calculate the expression of each test transcript[210]. Expression was assessed relative to the global mean of expression and normalized to the median level of expression for each individual transcript. Data were log-transformed to ensure normal distribution of data. Associations of transcript expression were assessed by linear regression against age, or lifespan as appropriate. Associations of transcript expression with mouse age were assessed in all animals and in animals of average-lived or long-lived strains individually, and associations of transcript expression with strain lifespan were assessed in all animals and in young and old groups individually. We also assessed the effect of potential nonlinearity of response for the splicing factor genes in spleen and muscle by a secondary analysis using binary logistic regression on data split by the median lifespan of all the strains. These statistical analyses were carried out using SPSS v.22 (IBM, North Castle, NY, USA). Interaction between strain longevity and mouse age was assessed using data categorized into average-lived or long-lived on the basis of interstrain median lifespan and was carried out in STATA v.14 (StataCorp, College Station, TX, USA).

3.7.7 Gene expression cluster analysis for heterogeneity of splicing factor expression with age

The expression of each gene was z-transformed to be on the scale of standard deviations from the mean, and then the expression values for each gene were plotted against the corresponding sample to generate a heat map. Hierarchical clustering methods were used to group similar expression profiles together. This analysis was done using the 'HEATMAP.2' package in R statistical software package v3.1.1 (Vienna, Austria).

3.7.8 Association between splicing factor expression and parental longevity in the InCHIANTI population

The participants in the InCHIANTI study aged 65+ years were categorized based on the age at death of their parents, the parental longevity score (PLS). Participants (total *n* = 405) were classified as either 'two short-lived parents' (*n* = 17), 'one short- and one intermediate-lived parent' (*n* = 140), 'two intermediate-lived parents' (*n* = 190) or 'any long-lived parents' (*n* = 58). Short-, intermediate- and long-lived cut-offs were calculated separately for mothers and fathers based on the normal distribution of age at death in the cohort, as described in Dutta et al.[188]. The cut-offs for mothers were as follows: short-lived (49–72 years), intermediate-lived (72–95 years) and long-lived (> 95 years); mothers aged < 49 years at death were classed as premature and excluded. The cut-offs for fathers were: short-lived (52–67 years), intermediate-lived (68–89 years) and long-lived (> 89 years); fathers aged < 52 years at death were classed as premature and excluded.

To assess the association between the gene expression levels of the 15 splicing factor genes in whole blood as defined in our previous work[103] and parental

longevity score, linear regression models were carried out using R statistical software package v3.1.1 (Vienna, Austria), with gene expression as the dependent variable. Models were adjusted for age, sex, waist circumference, highest education level attained, smoking (pack-years), study site, batches and cell counts (neutrophils, monocytes, basophils, eosinophils and whole white blood cell count). Gene expression data were rank-normalized prior to analysis to remove any skew.

3.7.9 Bioinformatic assessment of potential regulatory effects of genetic variation within Hnrnpa2b1 and Hnrnpa1 genes

To assess the potential for genetic variation to contribute to splicing factor expression differences that we observe between strains, we have carried out a detailed examination of the strain-discordant genetic differences in the splicing factor genes *Hnrnpa2b1* and *Hnrnpa1*, which demonstrate links with longevity in both mouse and man. Complete genome sequence data were available for 4 of the strains we have used in our analysis (C57BL/6J, 129S1/SvImJ, A/J and WSB/EiJ). SNPs discordant between strains were examined for evidence of effects on gene regulation by a variety of bioinformatic approaches. Firstly, SNPs located in the 5' UTR of the *Hnrnpa2b1* or *Hnrnpa1* genes were assessed for position relative to known transcription factor binding sites using REGRNA2.0 (http://regrna2.mbc.nctu.edu.tw/), an integrated web server tool that allows screening for potential regulatory elements. Secondly, intronic SNPs were assessed for their ability to interrupt exon and intron splicing enhancer and silencer loci using REGRNA2.0 and ESEFINDER (http://rulai.cshl.edu/cgi-bin/tools/ESE3/esefinder.cgi?process=home), a specific tool for the identification of splicing regulatory elements. Finally, sequences in the 3' untranslated region

were screened for ability to disrupt elements with potential to disrupt elements important for mRNA stability (A-rich elements, C to U RNA editing sites and miRNA binding sites) using REGRNA2.0.

3.8 Acknowledgements

The authors would like to acknowledge the Wellcome Trust (grant number WT097835MF LWH, DM), and NIH-NIA grant number AG038070 to The Jackson Laboratory for providing the funding for this study. We would also like to acknowledge the contributions of Federica Bighi and John Watt for technical assistance. The authors have no conflict of interest to disclose.

Chapter 4

Data Chapter.

MicroRNAs miR-203-3p, miR-664-3p and miR-708-5p are associated with median strain lifespan in mice.

Published in: Scientific Reports. March 2017. doi: 10.1038/srep44620.

4.1 Author List

Benjamin P. Lee[1], Ivana Burić[1], Anupriya George-Pandeth[1], Kevin Flurkey[2], David E. Harrison[2], Rong Yuan[2],[5] Luanne L. Peters[2], George A. Kuchel[3], David Melzer[3,4], and Lorna W. Harries[1]

1 - RNA-mediated mechanisms of Disease, Institute of Biomedical and Clinical Sciences, University of Exeter Medical School, University of Exeter, Devon, UK.

2 - The Jackson Laboratory Nathan Shock Center of Excellence in the Basic Biology of Aging, Bar Harbor, Maine, USA.

3 - UConn Centre on Aging, University of Connecticut Health Centre, Farmington, Connecticut, USA.

4 - Epidemiology and Public Health, Institute of Biomedical and Clinical Sciences, University of Exeter Medical School, University of Exeter, Devon, UK.

5 - Present Address: Geriatric Research Division, Department of Internal Medicine, Southern Illinois University School of Medicine, Springfield, IL, USA.

4.2 Author Contributions

BPL, IB and AGP carried out and interpreted the experiments. KF contributed to collection and characterization of samples. DHE co-directs the Jackson laboratory Nathan Shock Centre of Excellence in the Basic Biology of Aging, and was instrumental in facilitating the mouse collection and animal husbandry facilities used in this study. RY and LP designed and managed the initial mouse lifespan study and contributed to the manuscript. BPL also co-wrote the manuscript. GAK and DM contributed to and reviewed the manuscript. LWH managed the study, interpreted the data, and co-wrote the manuscript.

4.3 Abstract

MicroRNAs (miRNAs) are small non-coding RNA species that have been shown to have roles in multiple processes that occur in higher eukaryotes. They act by binding to specific sequences in the 3' untranslated region of their target genes and causing the transcripts to be degraded by the RNA-induced silencing complex (RISC). MicroRNAs have previously been reported to demonstrate altered expression in several ageing phenotypes such as cellular senescence and age itself. Here, we have measured the expression levels of 521 small regulatory microRNAs (miRNAs) in spleen tissue from young and old animals of 6 mouse strains with different median strain lifespans by quantitative real-time PCR. Expression levels of 3 microRNAs were robustly associated with strain lifespan, after correction for multiple statistical testing (miR-203-3p [β-coefficient = −0.6447, $p = 4.8 \times 10^{-11}$], miR-664-3p [β-coefficient = 0.5552, $p = 5.1 \times 10^{-8}$] and miR-708-5p [β-coefficient = 0.4986, $p = 1.6 \times 10^{-6}$]). Pathway analysis of binding sites for these three microRNAs revealed enrichment of target genes involved in key ageing and longevity pathways including mTOR, FOXO and MAPK, most of which also demonstrated associations with longevity. Our results suggest that miR-203-3p, miR-664-3p and miR-708-5p may be implicated in pathways determining lifespan in mammals.

4.4 Introduction

Although lifestyle and environmental factors are the major influences on lifespan, inherited factors remain important, with approximately 25% of the variation in lifespan attributable to genetics[211,212]. This is reflected in the observation that children of longer-lived parents have lower levels of age-related disease, lower all-cause mortality and greater life expectancy than those with shorter-lived parents[188,194]. In addition to the contribution of 'conventional' genetics, there is increasing evidence that epigenetic factors such as DNA methylation, histone modifications, and fine tuning of gene expression by small non-coding RNA regulators such as microRNAs (miRNAs) may also contribute significantly to ageing and longevity[213,214].

MicroRNAs (miRNAs) are short, non-coding RNAs that regulate mRNA expression[215]. Targets are recognized by virtue of sequence complementarity between specific sequences in the 3' untranslated region (3' UTR) of mRNA transcripts. Once bound, miRNAs act to either repress translation of the mRNA or target it for degradation. A single miRNA can target multiple mRNAs and many mRNAs have multiple miRNA binding sites in their 3' UTR[140]. In this manner, miRNAs have the capacity to regulate complex networks such as those implicated in ageing and longevity[141]. Several of the 'hallmarks' of ageing[94] including cellular senescence and genomic instability have been shown to be associated with multiple miRNAs[216]. Moreover, in several cases, individual miRNAs (or families of miRNAs) are associated with more than one of these processes[216]. Nevertheless, while several studies have implicated miRNAs in prediction of lifespan in C. elegans[217-219], less is known about their potential role

in mammalian lifespan. Identification of determinants of longevity is a key aim in identifying biomarkers of healthy ageing.

Inbred strains of mice, with very well defined phenotypic characteristics and fully characterized genetics have proved a useful tool in understanding complex phenotypes such as ageing[104,157,158]. In the present study, we assessed the potential role of miRNAs in longevity using spleen tissue from 6 inbred strains of mice of different median strain lifespans[104,157,158]. These mice have median strain lifespans ranging from 623 days to 1005 days and as a result we have previously used them for our studies of the factors influencing lifespan[104,187]. We carried out a high-throughput screen of 521 miRNAs in the young animals of the 2 strains at the extremes of the lifespan range, to identify candidate miRNAs associated with longer lifespan. We then tested for associations between median strain lifespan and the expression of the emerging miRNAs in young and old mice of all 6 strains, to determine whether these were robust associations. We found that 3 miRNAs, miR-203-3p, miR-664-3p and miR-708-5p, were all associated with lifespan in these mice. Subsequent bioinformatic analyses of pathways predicted to be targeted by these miRNAs included several that are known to be involved in determining lifespan e.g. FoxO[220], mTOR[221] and stem cell pluripotency pathways. Furthermore, genes predicted to be targeted by these miRNAs also show evidence of associations with median strain longevity. Our results suggest that differential regulation of key ageing and longevity pathways by miRNAs may underpin some of the phenotypic variation in lifespan in mammals.

4.5 Results

4.5.1 High-throughput MicroRNA Arrays

We carried out a near-global, high throughput screen of expression of 521 miRNAs in spleen samples of young animals culled at 6 months of age from the 2 mouse strains from our collection showing the most marked divergence in lifespan (A/J; 623 days and WSB/EiJ; 1005 days) by qRT-PCR using TaqMan® MicroRNA Array cards. 279 miRNAs were found to be expressed above the limit of detection and of these, 5 (miR-297b-5p, miR-708-5p, miR-224-5p, miR-203-3p and miR-327) were shown to be differentially expressed between average-lived and long-lived strains after correction for multiple testing (significance cutoff: $p < 0.0002$). Five additional miRNAs (miR-664-3p, miR-592-5p, miR-484, miR-687 and miR-192-5p) showed expression differences which were close to significance (significance cut-off: $p < 0.002$). The results for these 10 miRNAs are summarized in Table 4.1. See Supplementary table S13 for results of the full analysis.

Table 4.1: MicroRNAs with strongest association between expression and lifespan in spleen tissue from young mice of shortest-lived and longest-lived strains (A/J and WSB/EiJ respectively)

MicroRNAs significantly associated below the Bonferroni-corrected significance threshold (p <0.0002) are shown in bold italics. The ten most strongly associated microRNAs followed up in the targeted analysis are shown in italics. *P*-values were determined using independent sample t-tests on log-transformed relative expression data from TaqMan® MicroRNA Array cards.

MicroRNA Assay ID	Mean Difference	95% CI of the difference		*p*-value
		Upper	Lower	
mmu-miR-297b-5p	***4.29***	***4.53***	***4.05***	***$1.64x10^{-11}$***
mmu-miR-708	***0.47***	***0.59***	***0.36***	***$5.80x10^{-6}$***
mmu-miR-224	***-0.97***	***-0.63***	***-1.30***	***0.0001***
mmu-miR-203	***-0.55***	***-0.35***	***-0.75***	***0.0002***
rno-miR-327	***-3.70***	***-2.33***	***-5.07***	***0.0002***
mmu-miR-664	*0.46*	*0.66*	*0.27*	*0.0005*
mmu-miR-592	*0.50*	*0.73*	*0.27*	*0.0008*
mmu-miR-484	*0.33*	*0.49*	*0.17*	*0.001*
mmu-miR-687	*5.02*	*7.58*	*2.46*	*0.002*
mmu-miR-192	*0.31*	*0.47*	*0.15*	*0.002*

4.5.2 Targeted microRNA Expression

We then measured the expression levels of the 10 miRNAs demonstrating significant or near significant associations with median strain lifespan in spleen samples from both young and old animals of all 6 mouse strains. We found that 3 miRNAs; miR-203-3p, miR-664-3p and miR-708-5p were associated with median strain lifespan (Supplementary table S14). These 3 miRNAs were also associated with strain median lifespan in a replication sub analysis excluding all animals included in the discovery analysis (Supplementary table S15). Analysis of expression in relation to age of the animals revealed that miR-203-3p was not significantly associated with age whereas both miR664-3p and miR-708-5p were positively associated (see Supplementary table S16). This finding led us to

perform an analysis to detect interactions between miRNA expression, age, and median strain lifespan, results of which are given in Supplementary table S17.

MicroRNA miR-203-3p showed significantly reduced expression in both young and old animals of strains of longer lifespan when considered separately, as well as in the analysis of old and young animals of different median strain lifespans combined, after correction for multiple testing (β-coefficients = −0.64, −0.67 and −0.67; $p = 4.78 \times 10^{-11}$, 3.60×10^{-6} and 4.74×10^{-7} for all, young and old analyses respectively, see Supplementary table S14 and Figure 4.1a-c). Interaction analysis revealed no significant difference between young and old animals of average-lifespan strains (β-coefficient = −0.05; SE = 0.08; $p = 0.55$, see Supplementary table S17 and Figure 4.2). However, significant expression differences were seen between strains of average lifespan and long lifespan, with the most marked differences occurring in the young animals of long-lived strains (β-coefficient = −0.29; SE = 0.08; $p = 0.004$ compared with β-coefficient = −0.17; SE = 0.08; $p = 0.03$ in the old animals of long-lived strains, see Supplementary table S17 and Figure 4.2).

Conversely, miR-664-3p demonstrated increased expression in strains of longer lifespan in both old and young animals, after correction for multiple testing (β-coefficient = 0.56, $p = 5.12 \times 10^{-8}$, see Supplementary table S14 and Figure 4.1d). When expression was analyzed in young animals only, a trend was observed but this did not meet multiple testing criteria (β-coefficient = 0.42, $p = 0.008$, see Supplementary table S14 and Figure 4.1e) while in the analysis of old animals only, a significant association with lifespan was seen (β-coefficient = 0.75, $p = 3.93 \times 10^{-9}$, see Supplementary table S14 and Figure 4.1f). Analysis of strain lifespan and age interactions for miR-664-3p showed significant differences in

expression between young and old animals of average lifespan (β-coefficient = 0.15; $p = 0.04$, see Supplementary table S17 and Figure 4.2). Significant differences were also apparent when comparing expression of miR-664-3p between strains of average lifespan and long lifespan, although the effect was much more marked in the old animals of long-lived strains (β-coefficient = 0.18; $p = 0.01$ in young long-lived animals compared with β-coefficient = 0.46; $p = 6.59 \times 10^{-10}$, see Supplementary table S17 and Figure 4.2).

MicroRNA miR-708-5p also showed increased expression in strains of longer lifespan in the combined analysis of old and young animals, after correction for multiple testing (β-coefficient = 0.50; $p = 1.61 \times 10^{-6}$, see Supplementary table S14 and Figure 4.1g). Again, when expression was analyzed in young animals only, a trend was observed that did not meet multiple testing criteria (β-coefficient = 0.36; $p = 0.02$, see Supplementary table S14 and Figure 4.1h) while the analysis of old animals only showed a significant association with lifespan (β-coefficient = 0.64, $p = 2.70 \times 10-6$, see Supplementary table S14 and Figure 4.1i). Interaction analysis for miR-708-5p showed no significant difference in expression between young and old animals of average lifespan (β-coefficient = 0.12; $p = 0.33$, see Supplementary table S17 and Figure 4.2). Significant differences were observed between average-lived and long-lived strains, but these were only present in the old animals (β-coefficient = 0.08; $p = 0.49$ in young long-lived animals compared with β-coefficient = 0.31; $p = 0.007$ in the old animals of long-lived strains, see Supplementary table S17 and Figure 4.2).

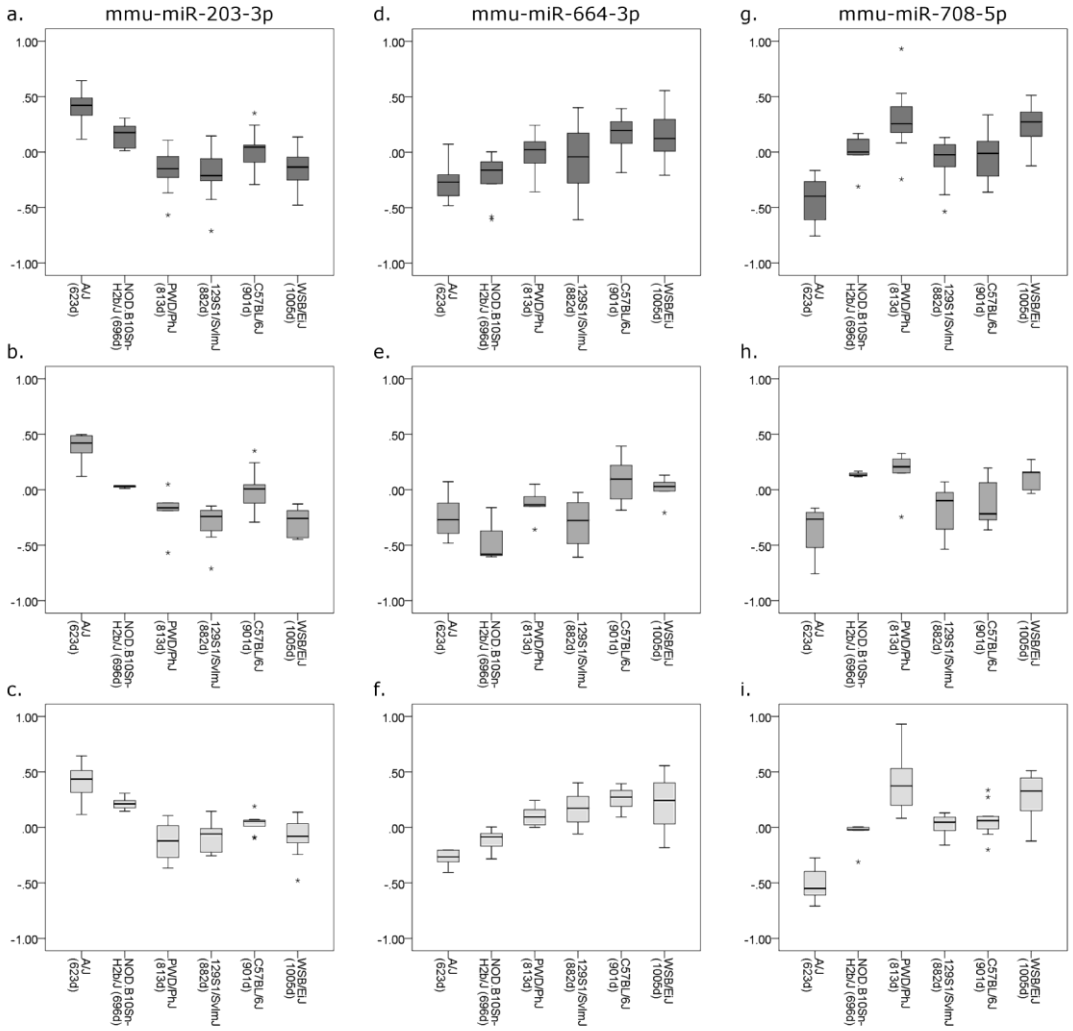

Figure 4.1: MicroRNA expression against lifespan as measured in targeted assessment of all available mouse strains

Box-and-whisker plots of relative microRNA expression for the 3 microRNAs found to be significantly associated with strain lifespan in the targeted assessment. Strains and median lifespan in days are given on the *x-axis*, while the *y-axis* shows mean log-transformed relative expression. Dark grey boxes show data for all mice analyzed, mid-grey boxes show data for young mice only and light grey boxes show data for old mice only. (**a**,**b** and **c**) expression data for miR-203-3p; (**d**,**e** and **f**) miR-664-3p; (**g**,**h** and **i**) miR-708-5p.

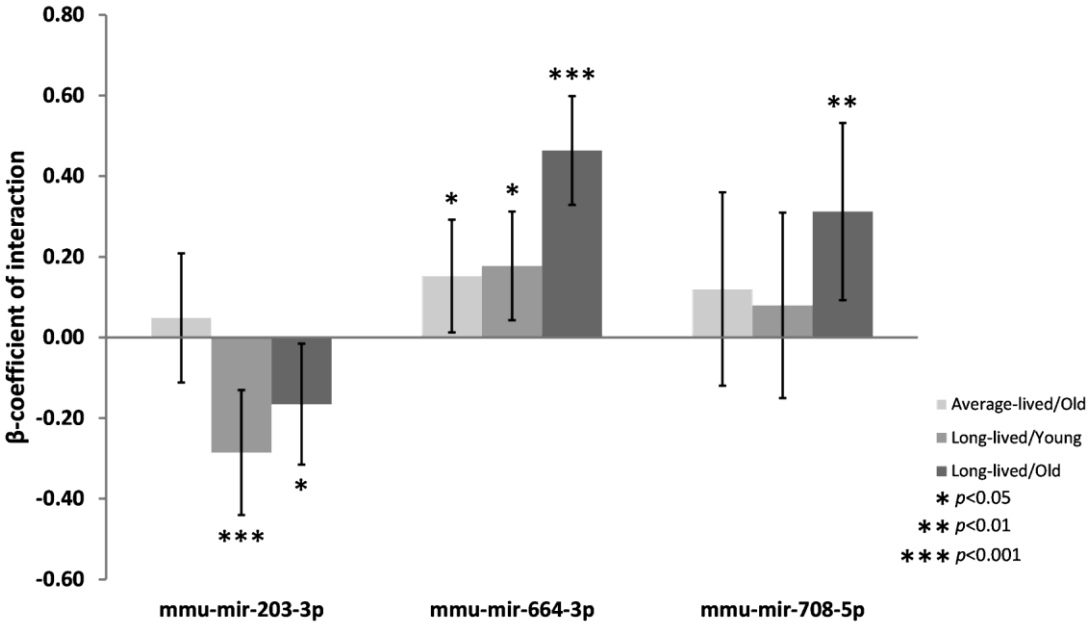

Figure 4.2: Longevity:Age interactions for microRNAs significantly associated with strain lifespan

This graph shows the relative expression changes in all mouse strains, categorized based on whether the median individual strain lifespan was above or below the median lifespan calculated across all strains, with 'Average-lived' being <847.5 days and 'Long-lived' >847.5 days. Young mice are 6 months and old mice are 20–22 months old. All changes are shown in relation to the young animals of the average-lived strains. Average-lived/old mice are shown in light grey, long-lived/young in mid-grey and long-lived/old animals in dark grey. Error bars denote the 95% confidence intervals and statistical significance is indicated by stars, where: *$p < 0.05$, **$p < 0.01$ and ***$p < 0.001$.

4.5.3 Pathways Analysis

The lifespan effects of miR-203-3p, miR-664-3p and miR-708-5p are probably mediated by altered regulation of their target genes. We therefore used a gene set enrichment bioinformatic prediction approach specialized for miRNA targets[222] to determine the biochemical and functional pathways that are enriched for genes targeted by the 3 microRNAs significantly associated with strain lifespan. We identified 15 pathways that were predicted to be enriched in miR-203-3p, miR-664-3p or miR-708-5p target genes, many of which are known to be associated with ageing or longevity (see Table 4.2). Prominent pathways targeted

by all 3 miRNAs include the ‘FoxO signalling pathway (mmu04068)’ and ‘mTOR signalling pathway (mmu04150)’, which contain 16 and 11 genes with predicted miR-203-3p, miR-664-3p and miR-708-5p binding sites (FDR-adjusted *p*-values = 0.02 and 0.01 respectively). Also predicted to be enriched for miR-203-3p, miR-664-3p and miR-708-5p binding sites are the ‘Pathways in cancer (mmu05200)’ pathway, the ‘MAPK signalling pathway (mmu04010), the ‘signalling pathways regulating pluripotency of stem cells (mmu04550)’ pathway and the ‘TGF-beta signalling pathway (mmu04350)’, with 33, 26, 14 and 10 genes targeted respectively (FDR-adjusted *p*-values = 0.03, 0.005, 0.05 and 0.0001 respectively). To provide empirical evidence that the genes identified to lie within these pathways also showed associations with longevity, we characterized the expression of selected target genes in relation to median strain lifespan. We identified that the 7/9 of these target genes were indeed associated with longevity in the mouse spleen samples (Table 4.3).

Table 4.2: Pathways affected by longevity-associated microRNAs

DIANA-mirPath v3.0 software[222] was used to determine pathways targeted by the microRNAs associated with strain lifespan, using predicted targets from the DIANA-microT-CDS v5.0 algorithm. Pathways are listed in order of the number of genes which are predicted to interact with these microRNAs.

KEGG Pathway	*p*-value	Number of genes	Number of miRNAs
Pathways in cancer (mmu05200)	0.03	33	3
MAPK signalling pathway (mmu04010)	0.005	26	3
FoxO signalling pathway (mmu04068)	0.016	16	3
Transcriptional misregulation in cancer (mmu05202)	0.03	15	3
Signalling pathways regulating pluripotency of stem cells (mmu04550)	0.05	14	3
Thyroid hormone signalling pathway (mmu04919)	0.002	12	2
mTOR signalling pathway (mmu04150)	0.01	11	3
Long-term potentiation (mmu04720)	0.01	11	3
TGF-beta signalling pathway (mmu04350)	0.0001	10	3
Long-term depression (mmu04730)	0.002	10	2
Chronic myeloid leukaemia (mmu05220)	0.02	9	3
Amphetamine addiction (mmu05031)	0.02	8	2
Thyroid hormone synthesis (mmu04918)	0.0004	6	3
ECM-receptor interaction (mmu04512)	0.023	6	2
Glycosphingolipid biosynthesis - lacto and neolacto series (mmu00601)	1.46×10^{-9}	4	2

Table 4.3: Association of predicted target mRNA expression and lifespan in mouse spleen tissue across 6 strains of different longevities

Data from mice of all ages, young mice only (6 months) and old mice only (20–22 months) are given separately. For each gene, the associated pathway is given, along with the microRNA predicted to target the transcript. mRNAs significantly associated below the significance threshold ($p < 0.05$) are shown in bold italics. *P*-values were determined from linear regression of log-transformed relative expression data.

			ALL MICE			YOUNG MICE ONLY			OLD MICE ONLY		
Predicted Target Gene	**KEGG Pathway**	**MicroRNA**	**Beta coefficient**	**Std. Error**	***P*-value**	**Beta coefficient**	**Std. Error**	***P*-value**	**Beta coefficient**	**Std. Error**	***P*-value**
Acvr2a	Signalling pathways regulating pluripotency of stem cells (mmu04550)	mmu-miR-664-3p	-0.12	0.00	0.26	-0.38	0.00	***0.01***	0.19	0.00	0.19
Dusp5	MAPK signalling pathway (mmu04010)	mmu-miR-203-3p	-0.17	0.00	0.11	-0.37	0.00	***0.02***	0.03	0.00	0.84
Fgf7	Pathways in cancer (mmu05200) MAPK signalling pathway (mmu04010)	mmu-miR-664-3p	-0.08	0.00	0.48	-0.24	0.00	0.14	0.11	0.00	0.45
Gabarapl1	FoxO signalling pathway (mmu04068)	mmu-miR-203-3p	-0.12	0.00	0.26	-0.48	0.00	***0.001***	0.29	0.00	***0.05***
Mmp9	Pathways in cancer (mmu05200)	mmu-miR-664-3p	0.45	0.00	***<0.001***	0.35	0.00	***0.02***	0.59	0.00	***<0.001***
Pten	FoxO signalling pathway (mmu04068) mTOR signalling pathway (mmu04150) Pathways in cancer (mmu05200)	mmu-miR-664-3p	0.18	0.00	0.09	-0.17	0.00	0.29	0.40	0.00	***0.004***
Rps6ka3	mTOR signalling pathway (mmu04150) MAPK signalling pathway (mmu04010)	mmu-miR-664-3p	0.07	0.00	0.54	-0.16	0.00	0.31	0.31	0.00	***0.03***
Smad4	Pathways in cancer (mmu05200) FoxO signalling pathway (mmu04068) Signalling pathways regulating pluripotency of stem cells (mmu04550)	mmu-miR-664-3p	-0.36	0.00	***<0.001***	-0.38	0.00	***0.02***	-0.41	0.00	***0.004***
Zfhx3	Signalling pathways regulating pluripotency of stem cells (mmu04550)	mmu-miR-664-3p mmu-miR-203-3p	0.03	0.00	0.80	-0.02	0.00	0.90	0.03	0.00	0.82

4.6 Discussion

Even once the effects of lifestyle and environment are considered, conventional genetics cannot account for all of the variation in mammalian lifespan and other factors, such as epigenetic regulation of key genes, have also been suggested to play a role. Here we show that three miRNAs; miR-203-3p, miR-664-3p and miR-708-5p, are significantly associated with strain lifespan in mouse spleen.

The expression of miR-203-3p was negatively correlated with longer lifespan. Although effects were seen in both young and old animals of long-lived strains, the most marked effects were noted in the young animals, suggesting that modulated expression of this miRNA may be a determining factor in longevity rather than simply a consequence of advancing age. Elevated levels of miR-203-3p have previously been shown to suppress “stemness” in mouse keratinocytes with several studies finding that higher levels of miR-203-3p expression promote terminal differentiation, repress proliferation and induce senescence in human melanoma cells[223-225]. This microRNA has also been shown to be up-regulated in senescence in human in vitro models using WI-38 human diploid fibroblast cells[226] and human melanoma cells[227]. The p63 and caveolin genes are known to be targets of miR-203-3p[228]. p63 is a member of the p53 family of transcription factors and the absence of expression of one of its isoforms, TAp63, has been shown to lead to senescence and premature ageing of epidermal and dermal precursors[229]. Caveolin is thought to have a tumor-suppressor function at early stages of malignant transformation[230], to contribute to immune senescence[231] and the ability of aged cells to respond to oxidative stress[232]. Our finding of reduced miR-203-3p expression in long-lived mouse strains may be indicative of a phenotype in which cells have greater proliferative and adaptive capacity

alongside a reduced propensity to become senescent, all of which could create favorable conditions for increased longevity. miR-203 was also one of the miRNAs demonstrated to be inversely associated with lifespan in a longitudinal study of human serum samples from the Baltimore Longitudinal Study of Aging (BLSA)[233].

Conversely, expression of miR-664-3p showed a positive correlation with longer lifespan in our data. In contrast to miR-203-3p, the changes we noted were most evident in the old animals of the long-lived strains, suggesting that increased expression of miR-664-3p may be a later life effect on longevity. In comparison with miR-203-3p, miR-664-3p has not been extensively studied, with conflicting conclusions having been drawn by different research groups. It has been linked to both pro- and anti-proliferative action in different tumor types[234,235], which complicates any attempts at prediction of putative function in terms of longevity. However, elevated hsa-miR-664 expression has been noted in human blood samples from nonagenarians and centenarians compared with samples from younger individuals[236], indicating that in human populations, the expression of this miRNA also correlates with longevity.

MicroRNA miR-708-5p was also positively correlated with longer lifespan. Again, the changes we noted were most evident in the old animals of the long-lived strains, suggesting that increased expression of miR-708-5p may also be a later life effect on longevity. In human cells, hsa-miR-708 has been shown to have a tumor-suppressor function in several human cancer types[237-239]. Reduced expression of hsa-miR-708 expression has also been seen in blood taken from old individuals in comparison to young individuals[240]. In our data, elevated, rather than decreased miR-708-5p expression was found to be associated with longer

lifespan. This may be partially explained if the effects on miR-708-5p expression reflect a balance between protection from malignancy and maintained proliferative capacity.

The effects of altered miRNA expression on median strain lifespan will be mediated by altered regulation of their target genes. Gene set enrichment analysis using the DIANA miRPath webtool[222] reveals 15 pathways that are enriched for miR-203-3p, miR-664-3p and miR-708-5p target genes. The expression of the majority of the genes enriched for longevity-associated miRNA binding sites also demonstrated associations with longevity (Table 4.3). Although not all of these relationships were entirely straightforward in terms of the direction of effect one would predict based on expression differences of the specific miRNAs, this is to be expected, since transcripts will be targeted by many miRNAs in addition to the one tested, and several of our candidates are targeted by multiple miRNAs, often with antagonistic relationships with longevity. For example, *Zfhx3*, in the 'pluripotency of stem cells' pathway is targeted by both mmu-miR-203-3p and mmu-664-3p, one of which is negatively associated with lifespan and the other positively. MicroRNAs have also been previously reported to be associated with both positive and negative associations with the expression of their target genes[241].

Most notable amongst the pathways we found were FoxO signalling, mTOR, MAPK signaling, pathways regulating pluripotency of stem cells, TGF-beta signaling and pathways involved in cancer. FoxO is well known to be involved in the regulation of lifespan, with strong evidence that alterations in proteins in this pathway can radically increase lifespan in several model organisms as well as humans, while mTOR inhibition has also been shown to increase lifespan in

several species, from yeast to mice[242]. The observation that many of the pathways implicated contain genes that are known to control shared outcomes such as apoptosis, cell cycle regulation, differentiation, proliferation, cell survival, autophagy and DNA repair adds strength to the hypothesis that miR-203-3p, miR-664-3p and miR-708-5p may have functionality in terms of longevity. Our group has previously shown that other aspects of RNA processing and regulation are important in ageing and longevity in humans, in animal models and *in vitro*[101,103,104]. The results of the present study provide further evidence that post-transcriptional control of mRNA expression is a key factor in the ageing process and determination of lifespan.

The use of mouse tissues from very well characterized inbred strains is a strength of our study and allows us to be precise about the genetics and phenotypes associated with each strain, and allows assessment of median strain lifespan with some confidence. Spleen is an appropriate tissue for analysis, given the known role of the immune system and inflammation as drivers of ageing[193]. However, our study cannot comment on the potential tissue-specificity of the effects we have seen and may not be representative of mechanism elsewhere in the organism. We also recognize that there are both strain-specific and age-related differences in the cellular composition of the spleen. While strain differences in the cell types found in mouse spleen are apparent, the kinetics of change of cell composition with age are similar at different stages of life in separate mouse strains where this has been measured[243]. It must also be mentioned that there is a relatively large amount of inter-individual cell-type variation, in some cases more pronounced than the inter-strain variability[243,244]. Unfortunately, data on splenic cellular composition for the strains used in this paper are not available, however while we cannot definitively state that all of our findings are not linked to

age-related cell-type changes in the splenic make-up, the associations that are present only in the young mice are far less likely to be influenced by such changes. Our use of a wide-spectrum discovery phase in a limited sample set, followed by targeted validation and replication of results in a larger inclusive cohort ensures robust results, but we recognize that for some of the mouse strains analyzed, low numbers of samples may have affected the statistical power to detect more subtle changes. The use of pathways analysis also allows a larger 'systems'-based assessment of the effects of deregulation of modules of miRNAs in determination of longevity. Of course, it must be recognized that these results are from an *in silico* predictive algorithm and are not necessarily indicative of actual interactions *in vivo* or *in vitro*. Finally, it is possible that the effects we see may derive from differences between the strains unrelated to longevity. However, evidence suggests that there are links between both miR-664-3p and miR-203-3p and lifespan in human studies[233,236], suggesting that unrelated strain differences alone probably do not account for our observations, at least for these microRNAs.

In conclusion, we present evidence that three miRNAs, miR-203-3p, miR-664-3p and miR-708-5p are robustly associated with median strain lifespan in 6 well-characterized inbred strains of mice, and that both early life (miR-203-3p) and later life (miR-664-3p and miR-708-5p) changes in their expression may modulate the expression of target genes in several very well-known ageing and longevity pathways. These studies demonstrate the importance of miRNAs in determination of mammalian longevity and raise the possibility that they may have utility as biomarkers of healthy ageing in the future.

4.7 Methods

4.7.1 Mouse tissue used in the study

Samples of spleen tissue were obtained from mice of six strains (A/J, NOD.B10Sn-H2^{b}/J, PWD/PhJ, 129S1/SvImJ, C57BL/6J and WSB/EiJ), selected for having variable life expectancy (see Table 4.4 for details of lifespan, numbers of animals used in each category and their respective characteristics). Median lifespan was measured in a longitudinal study[157,159] at Jackson Laboratory Nathan Shock Center of Excellence in the Basic Biology of Aging. All tissues used in the present study were taken from male animals which were part of a cross sectional study being run at the same time, in the same mouse room as the longitudinal study mentioned above. All experiments were carried out in accordance with National Institutes of Health Laboratory Animal Care Guidelines and was approved by the Animal Care and Use Committee (ACUC) of The Jackson Laboratory. Details of mouse strains used and animal husbandry have been previously published[104]. Spleen tissue was excised immediately after death, placed into RNA-later storage solution (Sigma-Aldrich, St. Louis, MO, USA) and snap-frozen in vapor phase liquid nitrogen for storage within 5 minutes of collection.

Table 4.4: Mouse strains and characteristics

Median lifespan and maximum age (average of longest-surviving 20% of animals) are given for each strain in the present study. All mice used were male.

Strain	Strain Median Lifespan (days)	Strain Maximum Age (days)	Longevity Category	n Young (6 months)	n Old (20/22 months)
A/J	623	785	Average lifespan	7	6
NOD.B10Sn-H2^{b}/J	696	954	Average lifespan	3	6
PWD/PhJ	813	956	Average lifespan	5	6
129S1/SvImJ	882	1044	Long-lived	8	8
C57BL/6J	901	1061	Long-lived	10	9
WSB/EiJ	1005	1213	Long-lived	5	10

4.7.2 MicroRNA candidate transcripts for analysis

To determine which microRNA transcripts to assess for association with longevity, an initial high-throughput array analysis was performed to measure the expression of a wide spectrum of microRNAs. In an attempt to ensure the best possible chance of detecting differences with lifespan, the arrays were run using all available samples from young animals (sacrificed at 6 months old) of A/J and WSB/EiJ, the two strains at either extreme of lifespan (623 days for A/J and 1005 days for WSB/EiJ). The top 10 most significantly associated microRNAs from this analysis were followed up with targeted microRNA expression experiments in old and young animals from all 6 strains.

4.7.3 RNA Extraction

Tissue samples were removed from RNA-later storage solution and placed in 1 mL TRI Reagent® Solution (Thermo Fisher, Waltham, MA, USA) supplemented with the addition of 10 mM $MgCl_2$ to aid recovery of microRNAs[165]. Samples were then completely homogenized for 15 mins in a bead mill (Retsch Technology GmbH, Haan, Germany). Phase separation was carried out using chloroform. Total RNA was precipitated from the aqueous phase by means of an overnight incubation at −20 °C with isopropanol. RNA pellets were then ethanol-washed twice and re-suspended in RNase-free dH_2O. RNA quality and concentration was assessed by NanoDrop spectrophotometry (NanoDrop, Wilmington, DE, USA).

4.7.4 High-throughput MicroRNA Arrays

MegaPlex Reverse Transcription 400ng of RNA per reaction was reverse transcribed using the TaqMan® MicroRNA Reverse Transcription Kit and Megaplex™ RT Primers, Rodent Pool Set v3.0 (Thermo Fisher, Waltham, MA, USA) in separate reactions for Pool A and Pool B, according to the manufacturer's instructions.

MicroRNA Array qRT-PCR Expression of a wide spectrum of microRNAs was measured using Quantitative RT-PCR, performed on the ABI 7900HT platform (Thermo Fisher, Waltham, MA, USA), using both TaqMan® Rodent MicroRNA A Array v2.0 and TaqMan® Rodent MicroRNA Array B cards (Thermo Fisher, Waltham, MA, USA). Supplementary table S18 lists the 521 unique microRNAs tested using this approach. Reaction mixes included 415 µl Taqman® Universal PCR Master Mix II (no AmpErase® UNG) (Thermo Fisher, Waltham, MA, USA), 407.5 µl dH2O and 7.5 µl cDNA template from Pool A or Pool B Megaplex™ reverse transcriptions as appropriate. 100 µl of reaction solution for each sample

was dispensed into all chambers of an array card (again, A or B accordingly), then centrifuged twice for 1 minute at 1000 rpm to ensure distribution of solution to each well. Amplification conditions were 50 °C for 2 minutes, 94.5 °C for 10 minutes, followed by 50 cycles of 97 °C for 30 seconds and 57.9 °C for 1 minute.

4.7.5 Targeted MicroRNA Expression

Multiplex Reverse Transcription 60 ng of RNA per reaction was reverse transcribed using the TaqMan® MicroRNA Reverse Transcription Kit and RT primers provided with the TaqMan® MicroRNA Assays detailed in Supplementary table S19 (Thermo Fisher, Waltham, MA, USA). Each reaction contained 1 µl each of all the RT primers of the microRNAs to be analyzed, 10 mM dNTPs (with dTTP), 100 U MultiScribe™ Reverse Transcriptase, 1X Reverse Transcription Buffer, 7.6U RNase Inhibitor and dH2O to a final volume of 30 µl. The thermal profile for the reactions was 16 °C for 30 minutes, 42 °C for 30 minutes, 85 °C for 5 minutes and a final hold at 4 °C.

Individual microRNA qRT-PCR MicroRNA expression was measured using Quantitative RT-PCR, performed on the ABI 7900HT platform (Thermo Fisher, Waltham, MA, USA), using the TaqMan® MicroRNA Assays detailed in Supplementary table S19 (Thermo Fisher, Waltham, MA, USA). Reactions were run in triplicate on 384-well plates, using one assay per plate containing all samples. Each reaction included 2.5 µl TaqMan® Universal Master Mix II (no AmpErase® UNG) and 0.25 µl TaqMan® MicroRNA Assay (Thermo Fisher, Waltham, MA, USA), 0.5 µl cDNA (multiplex reverse transcribed as indicated above) and dH2O to a final volume of 5 µl. Amplification conditions were a single

cycle of 95 °C for 10 minutes, followed by 50 cycles of 95 °C for 15 seconds and 60 °C for 1 minute.

4.7.6 Interaction analysis

Analyses of interactions between mouse age and strain longevity were carried out for the three significantly associated microRNAs using data categorized based on whether the median individual strain lifespan was above or below the median lifespan calculated across all strains, with 'average-lived' being <847.5 days and 'long-lived' >847.5 days (see Table 4.4 for details). Interaction terms for the relationship between age and median strain longevity were included. Analyses were carried out in STATA 14 (StataCorp, College Station, TX, USA).

4.7.7 Pathway analysis

Pathway analysis was carried out with DIANA-miRPath v3.0[222], using predicted microRNA targets from the DIANA-microT-CDS v5.0 algorithm[245] and Gene Ontology genesets derived from KEGG. The *p*-value threshold was set to 0.05 and MicroT threshold to 0.8.

4.7.8 Predicted target mRNA candidates for analysis

Target genes for validation were selected based on the MiTG scores taken from the DIANA-microT-CDS v5.0 algorithm[245]. We elected to assess the two genes with the highest MiTG score from each of the three pathways with the highest numbers of genes predicted to be targeted by the microRNAs in question; 'Pathways in cancer' (mmu05200), 'MAPK signalling pathway' (mmu04010) and 'FoxO signalling pathway' (mmu04068). We also decided to assess the two genes with the highest MiTG score from the 'mTOR signalling pathway' (mmu04150) and 'Signalling pathways regulating pluripotency of stem cells'

(mmu04550), as these were likely to be of interest in relation to lifespan. One other gene was picked (*Smad4*), as it is the only one to be present in 3 of the 5 pathways we had elected to pursue and is also present in 5 of the 15 pathways identified from DIANA-miRPath[222].

4.7.9 Predicted Target mRNA Expression

Reverse Transcription 200 ng of RNA per reaction was reverse transcribed using the SuperScript® VILO™ cDNA Synthesis Kit (Thermo Fisher, Waltham, MA, USA) in 20 µl reactions, according to the manufacturer's instructions. Each cDNA was then diluted with 10 µl of water to give sufficient volume to carry out the necessary qPCR reactions.

Predicted target mRNA qRT-PCR Predicted target mRNA expression was measured using Quantitative RT-PCR, performed on the QuantStudio 12 K Flex platform (Thermo Fisher, Waltham, MA, USA), using the TaqMan® Gene Expression Assays detailed in Supplementary table S20 (Thermo Fisher, Waltham, MA, USA). Reactions were run in triplicate on 384-well plates, using one assay per plate containing all samples. Each reaction included 2.5 µl TaqMan® Universal Master Mix II (no AmpErase® UNG) and 0.25 µl TaqMan® Gene Expression Assay (Thermo Fisher, Waltham, MA, USA), 0.5 µl cDNA (reverse transcribed as indicated above) and dH_2O to a final volume of 5 µl. Amplification conditions were a single cycle of 95 °C for 10 minutes, followed by 40 cycles of 95 °C for 15 seconds and 60 °C for 1 minute.

4.7.10 Relative quantification

In all experiments described here, the $\Delta\Delta C_t$ method was used to calculate relative expression levels of the microRNAs tested[210]. Expression was assessed relative

to the global mean of the 279 expressed microRNAs and normalized to the mean level of expression of each individual transcript in the shorter lifespan animals (A/J) for the high-throughput microRNA arrays. Data were log transformed to ensure normal distribution and differences in expression were tested with independent t-tests, using SPSS v22 (IBM, North Castle, NY, USA). For the targeted microRNA experiments, expression was assessed relative to the mean expression of three endogenous control small RNA species (snoRNA202, U6 snRNA and U87 snRNA) and normalized to the median level of expression for each individual transcript across all samples. Data were $\log_{10}$ transformed to ensure normal distribution. For the predicted target mRNA experiments, expression was assessed relative to the mean expression of two endogenous control genes (*Gusb* and *Idh3b*) and normalized to the median level of expression for each individual transcript across all samples. Data were $\log_{10}$ transformed to ensure normal distribution.

4.7.11 Statistical approach

Associations between both miRNA and mRNA target expression and median strain lifespan were assessed using linear regression. The relationships between these parameters were assessed in both young and old animals of all 6 strains. We also assessed the relationship between median strain lifespan and miRNA expression in the animals not originally tested in the global analysis, to comprise an independent replication. Regressions were carried out using SPSS v22 (IBM, North Castle, NY, USA).

4.8 Acknowledgements

This work was funded by the Wellcome Trust (grant number WT097835MF to D. Melzer and L.W. Harries), and the NIH-NIA (grant number AG038070 to The Jackson Laboratory). The authors would like to thank Miss Florence Emond for technical assistance. The authors declare no competing financial interests.

Chapter 5

Data Chapter.

Dietary restriction in ILSXISS mice is associated with widespread changes in splicing regulatory factor expression levels.

Published in: Experimental Gerontology. September 2019. doi: 10.1016/j.exger.2019.110736.

5.1 Author List

Benjamin P. Lee[1], Lorna Mulvey[2], Gregory Barr[1], Jemma Garratt[1], Emily Goodman[1], Colin Selman[2], Lorna W. Harries[1].

1 - Institute of Biomedical and Clinical Sciences, University of Exeter Medical School, UK, EX2 5DW.
2 - Institute of Biodiversity Animal Health & Comparative Medicine, University of Glasgow, UK, G12 8QQ.

5.2 Author contributions

LWH managed the project, designed the study and reviewed the manuscript. BPL coordinated experiments, performed the data analysis and wrote the manuscript. LM handled animal husbandry. GB, JG and EG all performed parts of the gene expression experiments. CS assisted with study design, provided the tissue samples and reviewed the manuscript.

5.3 Abstract

Dietary restriction (DR) represents one of the most reproducible interventions to extend lifespan and improve health outcomes in a wide range of species, but substantial variability in DR response has been observed, both between and within species. The mechanisms underlying this variation in effect are still not well characterised. Splicing regulatory factors have been implicated in the pathways linked with DR-induced longevity in *C. elegans* and are associated with lifespan itself in mice and humans.

We used qRT-PCR to measure the expression levels of a panel of 16 age- and lifespan-associated splicing regulatory factors in brain, heart and kidney derived from three recombinant inbred strains of mice with variable lifespan responses to short-term (2 months) or long-term (10 months) 40% DR to determine their relationship to DR-induced longevity.

We identified 3 patterns of association; i) splicing factors associated with DR alone, ii) splicing factors associated with strain alone or iii) splicing factors associated with both DR and strain. Tissue specific variation was noted in response to short-term or long-term DR, with the majority of effects noted in brain following long-term DR in the positive responder strain TejJ89. Association in heart and kidney were less evident, and occurred following short-term DR.

Splicing factors associated with both DR and strain may be mechanistically involved in strain-specific differences in response to DR. We provide here evidence concordant with a role for some splicing factors in the lifespan modulatory effects of DR across different mouse strains and in different tissues.

5.4 Introduction

Since the lifespan extension effects of dietary restriction (DR) were first reported in the early 1900s[246,247], intensive effort has focused on characterisation of the underlying mechanism(s) in model organisms[248-250]. Several studies have shown the beneficial effects of DR in terms of extended lifespan to be conserved across many species ranging from single-celled organisms to non-human primates[251-254]. To date no lifespan data are available in humans, although there are many opinions as to the potential for DR to affect human lifespan[250,255-258]. Notwithstanding the reported effects on lifespan, there remains clear evidence that DR results in multiple health benefits in many organisms including humans[258-261]. These benefits could contribute to extended 'health span' (the period of life spent free from age-related chronic diseases) in ageing human populations, which is arguably far more relevant from a public health perspective than increasing lifespan alone. However, the exact nature of the mechanism(s) which lead to such benefits remains the subject of discussion. There is therefore a need to elucidate the pathways underlying the actions of DR in order to better understand how it could potentially be used to extend 'health span' in human populations.

When discussing DR as a potential intervention, it must be recognised that the universality of the beneficial effects is far from clear cut. In animal models, lifespan extension results vary with the experimental methodology used; animal husbandry conditions, level of DR imposed, age at initiation of DR and method of introduction of DR may all influence the amount of extension reported[262-264]. Genetics is clearly also an important factor to be considered, especially given that studies conducted across different species show highly variable effects, with

several reports showing dietary restriction to have no effect, or even a negative effect on lifespan[250,262,265]. However, such disparity is not limited to cross-species differences; two studies from 2010[266,267] tested a large number of ILSXISS recombinant inbred mouse strains and reported wide variability in lifespan response to 40% DR, both lifespan extension and lifespan reduction were observed in similar numbers of strains in each of these experiments. It is currently unclear as to what caused the variation in response to DR, although a number of reasons have been suggested[262]. However, the simple fact that such variation exists presents valuable opportunities to study the molecular mechanisms involved in differential lifespan response to dietary restriction.

One molecular mechanism with potential to play a role in the DR response is alternative mRNA splicing; components of the machinery that regulates this process have previously been implicated in DR in *C.elegans*[67] . Alternative splicing is known to be a contributor to cellular plasticity and is a key element of the homeostatic stress response, both of which are important factors in the ageing process[110,268]. Dysregulated splicing is also a major feature of age-related diseases including Alzheimer's disease, Parkinson's disease and several tumour types[177-179]. Regulation of alternative splicing events is complex and multifactorial, however trans-acting splicing factors are necessary to determine the outcome of any particular splicing event[126]. The Serine Arginine-rich (SR) family of splicing factors and the heterogeneous nuclear ribonucleoprotein (HNRNP) family of splicing factors usually, but not exclusively, have stimulatory and inhibitory roles respectively in the determination of splice site usage[176]. We have previously shown that alternative splicing and splicing factor expression are deregulated during normal human ageing[101] and that splicing factor expression levels are associated with lifespan in mice and humans[104]. We have also

demonstrated changes in splicing factor expression in senescent cells from multiple human tissue types *in vitro*[103,108] and recently we reported the reversal of several senescent cell phenotypes through moderation of splicing factor expression levels using resveratrol analogues, hydrogen sulfide donors or inhibition of the ERK or AKT signalling pathways in cultured human cells[107,269,270].

Given the emerging importance of splicing factors in the ageing phenotype and links to longevity, we hypothesised that their expression may be altered under DR conditions, and may present some insight into the role of alternative splicing in the effects of DR. To explore this, we measured splicing factor transcript expression levels in three recombinant ILSXISS mouse strains with differential responses to short-term or long-term 40% DR. We identified striking tissue specificity in expression profiles. The expression of some splicing factors was associated with exposure to either short-term or long-term DR, or both, but demonstrated no associations with strain. Others demonstrated strain specific responses but were unrelated to DR status. Some splicing factors however demonstrated interactions between both strain and DR, and may underlie the observed strain specificity in DR response.

5.5 Materials and Methods

5.5.1 ILSXISS Mice

The mouse strains used in the present study have been extensively described elsewhere[161,266,267,271,272]. In brief, the ILSXISS recombinant inbred (RI) mouse strains were originally derived from a cross between inbred long sleep (ILS) and inbred short sleep (ISS) mice. These two strains were developed from an original eight-way cross using heterogeneous stock; A, AKR, BALB/c, C3H/2, C57BL,

DBA/2, IsBi and RIII, the offspring of which were subsequently bred for differential ethanol sensitivity, giving the long and short sleep models. Over 20 successive generations of inbreeding of these progenitor strains (ILS X ISS) resulted in >75 ILSXISS RI lines, each genetically distinct from each other[266]. These lines have previously been shown to have variable lifespan responses to DR, making them ideal for exploration of the mechanisms underlying DR-induced lifespan extension[266,267].

Mice from three of these strains were chosen for use in the present study, on the basis of replicable responses to 40% DR across two previous independent studies with no significant strain-specific differences in median lifespan under AL conditions[266,267]. Only female mice were used in the present study for consistency since one previous study[267] did not include male mice. Lifespan measurements from the Liao study[266] therefore could not be corroborated for both sexes. Mice were maintained in groups of 4 post-weaning in shoebox cages (48 cm × 15 cm × 13 cm), with AL access to water and standard chow (CRM(P), Research Diets Services, LBS Biotech, UK; Atwater Fuel Energy-protein 22%, carbohydrate 69%, fat 9%) and maintained on a 12L/12D cycle (lights on 0700–1900h) at 22 ± 2 °C.

One of the strains chosen showed an extension of lifespan under life-long 40% DR (TejJ89), one showed a lifespan reduction response to 40% DR (TejJ114) and one exhibited no response to 40% DR (TejJ48) relative to strain-specific *ad libitum* fed controls. There is some debate as to whether these strain responses truly reflect each strain's true potential for lifespan extension or simply that a 40% DR regime is sub-optimal in the cases of TejJ48 and TejJ114[262]. However for purposes of clarity, the strains will be referred to as positive-, negative- and non-

responder strains since these are the responses that have previously been reported under 40% DR[161,266,267]. Mice were introduced to DR in a graded fashion; at 10 weeks of age mice were exposed to 10% DR (90% of AL feeding), at 11 weeks this was increased to 20% DR, and from 12 weeks of age until the termination of the experiment mice were exposed to 40% DR, relative to their appropriate strain-specific AL controls. Mice were given either *ad libitum* (AL) feed or short- (2 months) or long-term (10 months) 40% DR, as previously published[161]. Brain, heart and kidney tissue samples were collected as part of a previous study, therefore full details of animal husbandry conditions, DR protocols and treatment of dissected tissues have all been previously described in Mulvey *et al*[161]. All experiments were carried out under a licence from the UK Home Office (Project Licence 60/4504) and followed the "principles of laboratory animal care" (NIH Publication No.86-23, revised 1985).

5.5.2 Splicing factor candidate genes for analysis

An *a priori* list of splicing factor candidate genes were chosen based on associations previously seen in multiple human ageing cohorts and in senescent primary human cell lines[101,103,107,108]. Some of the splicing factors in this list have also been shown to associate with lifespan in both mice and humans[104]. The list of genes included the negative regulatory splicing factors *Hnrnpa0*, *Hnrnpa1*, *Hnrnpa2b1*, *Hnrnpd*, *Hnrnph3*, *Hnrnpk*, *Hnrnpm*, *Hnrnpul2*, the positive regulatory splicing enhancers *Pnisr*, *Srsf1*, *Srsf2*, *Srsf3*, *Srsf6*, *Tra2b* and the core components of the spliceosome *Sf1* and *Sf3b1*. Expression assays were obtained in single-tube TaqMan® Assays-on-Demand™ format (ThermoFisher, Waltham, MA, USA). Assay Identifiers are given in Supplementary table S21.

5.5.3 RNA extraction

Snap-frozen tissues were first treated with RNA*later*™-ICE Frozen Tissue Transition Solution (ThermoFisher, Waltham, MA, USA) according to the manufacturer's instructions, in order to allow handling of the tissue without RNA degradation occurring due to thawing of sample. Tissue sections were then placed in 1 ml TRI Reagent® Solution (ThermoFisher, Waltham, MA, USA) supplemented with the addition of 10mM MgCl2 to aid recovery of microRNAs[165]. Samples were then completely homogenised in a bead mill (Retsch Technology GmbH, Haan, Germany) at a frequency of 30 cycles per second for 15 mins. Phase separation was carried out using chloroform. Total RNA was precipitated from the aqueous phase by means of an overnight incubation at -20°C with isopropanol. 1.2µl Invitrogen™ GlycoBlue™ Coprecipitant (ThermoFisher, Waltham, MA, USA) was added prior to incubation to aid pellet recovery. RNA pellets were then ethanol-washed twice and re-suspended in 1 x TE buffer, pH8.0. RNA quality and concentration were assessed by NanoDrop spectrophotometry (NanoDrop, Wilmington, DE, USA).

5.5.4 Reverse transcription

500ng of total RNA was reverse transcribed using EvoScript Universal cDNA Master kit (Roche LifeScience, Burgess Hill, West Sussex, UK) in 20µl reactions, according to the manufacturer's instructions except for a change to the extension phase of the reaction: a step of 30 min at 65°C was used instead of 15 min at 65°C. Resulting cDNA was then diluted to a final volume of 80µl with dH_2O to ensure sufficient volume for all subsequent qRT-PCR reactions.

5.5.5 Quantitative real-time PCR

1.0µl cDNA (reverse transcribed as indicated above) was added to a 5µl qRT-PCR reaction including 2.5µl TaqMan® Universal Master Mix II, no UNG (ThermoFisher, Waltham, MA, USA) and 0.125µl TaqMan® Assays-on-Demand™ probe and primer mix (corresponding to 450nM each primer and 125nM probe). Reactions were run in triplicate on 384-well plates using the QuantStudio 6 Flex Real-Time PCR System (ThermoFisher, Waltham, MA, USA). Amplification conditions were a single cycle of 95°C for 10 min followed by 40 cycles of 95°C for 15 s and 60°C for 1 min. As this study consisted of a collection of 288 samples, three separate plates were required to run all samples with each Taqman® assay. To mitigate the effects of plate-to-plate variation, two approaches were used. Firstly, samples were randomised before being assigned to a plate such that any given plate did not contain all the samples from one strain, tissue or DR condition. Secondly, internal calibrator samples were used: 6 samples were chosen at random from the collection and separate to the main workflow, each sample was reverse-transcribed 3 times and diluted as described above. The 3 resulting cDNA samples were then pooled for each sample, mixed thoroughly and added as extra samples to each plate. These internal calibrator samples were used in the downstream analysis to normalise across plates.

5.5.6 Data preparation

EDS files were uploaded to the ThermoFisher Cloud (ThermoFisher, Waltham, MA, USA) and analysed using the Relative Quantification qPCR App within the software (https://www.thermofisher.com/uk/en/home/cloud.html). This platform was used to manually set Baseline and Threshold for each assay (see Supplementary table S21 for values) and to ensure there were no apparent outliers before further

analysis. One sample was excluded from the TejJ89 dataset at this stage as expression data was missing for >50% of all genes measured. Output was imported into Excel (Microsoft, Redmond, WA, USA) and the C_T values used for analysis using the comparative C_T method. First, raw C_T values were corrected using the internal calibrator samples from each of the three plates. Corrected C_T data from all genes measured, endogenous controls, calculated averages and geometric means of these controls along with calculated 'global' averages and geometric means across all genes measured were then uploaded to the RefFinder webtool[273] to establish the most stable gene(s). This returned the 'global' geometric mean value across all genes measured as the most stable and thus the most appropriate for the ΔC_T normalisation step. At this point, $\Delta\Delta C_T$ expression calculations were performed for each strain separately; expression for each transcript was calculated relative to the average expression in the *ad-libitum* fed animals, for each tissue individually and separately for long-term and short-term treatments. Following the $\Delta\Delta C_T$ normalisation, the fold-changes were calculated using the $2^{-\Delta\Delta C_T}$ method, followed by an additional normalisation using the geometric mean expression of the non-responder strain (TejJ48) as a baseline.

This final normalisation step was intended to account for any minor changes in splicing factor expression caused by DR, but presumably unrelated to the lifespan-alteration response seen in the positive (TejJ89) and negative (TejJ114) responder strains. The expression profiles of splicing factors in the non-responder strain (TejJ48) under DR conditions are shown in Supplementary figure S2 and Supplementary table S22. As can be seen, there are very few significant alterations in expression levels (and none that meet multiple testing criteria), although a certain amount of deviation from zero can be seen. These

deviations in expression are likely to be brought about through the imposition of a DR regime, however owing to the lack of response in this strain it is reasonable to assume that they are highly unlikely to be contributory to the responses seen in the other strains. As such, normalisation using these minor deviations should merely remove a certain amount of 'background' from the positive- and negative-responder strain data. As a consequence of this normalisation, the data from TejJ48 were effectively set as a zero point against which TejJ89 and TejJ114 were compared, so results for TejJ48 are presented only in supplementary data.

Data were log transformed to ensure normal distribution and outlier detection was then performed in SPSS (IBM, Armonk, NY, USA). Univariate outliers were identified using standardised z-scores, with any individual measures for each gene falling outside the cut-off (set at 3 standard deviations from the mean) being discarded. Multivariate outliers were identified using a regression model with Mahalanobis distance as an output, followed by comparison of the calculated Mahalanobis distances with the critical χ^2 value for the dataset[274]. One sample from the TejJ89 dataset for which the Mahalanobis distance exceeded the critical χ^2 was discarded, leaving a total of n = 286 samples to take forward for statistical testing. The characteristics of this final set of samples are summarised in Table 5.1.

5.5.7 Statistical analysis

Differences in gene expression were tested using ANCOVA between 1) DR and AL feeding regimes and 2) TejJ89 and TejJ114 positive and negative responder strains under DR conditions. qRT-PCR plate was included as a co-variate in order to control for any batch effects across the 3 plates used for each gene expression assay. Linear regression models were then performed using DR status and

responder strain as independent variables and including an interaction term to determine the presence of moderating effects between the two variables. ANCOVAs and regressions were carried out in STATA v15.1 (StataCorp, College Station, TX, USA). Benjamini, Krieger and Yekutieli false discovery rate (FDR) calculations[175] were performed using GraphPad Prism 8.1.1 (GraphPad Software, San Diego, CA, USA), with the q-value set at 5%.

Table 5.1: Details of mice used in the study

Shown here are the numbers of animals included in each feeding regime and diet for each tissue in each strain of mouse used in the current study.

Strain	Tissue	Diet	Regime	n
TejJ48	Brain	AL	2 month	8
			10 month	8
		DR	2 month	8
			10 month	8
	Heart	AL	2 month	8
			10 month	7
		DR	2 month	8
			10 month	8
	Kidney	AL	2 month	7
			10 month	8
		DR	2 month	7
			10 month	8
TejJ89	Brain	AL	2 month	8
			10 month	8
		DR	2 month	8
			10 month	8
	Heart	AL	2 month	8
			10 month	8
		DR	2 month	9
			10 month	8
	Kidney	AL	2 month	8
			10 month	10
		DR	2 month	8
			10 month	6
TejJ114	Brain	AL	2 month	8
			10 month	8
		DR	2 month	8
			10 month	8
	Heart	AL	2 month	8
			10 month	8
		DR	2 month	8
			10 month	8
	Kidney	AL	2 month	8
			10 month	7
		DR	2 month	9
			10 month	8

5.6 Results

5.6.1 Splicing factors demonstrate altered expression levels under DR conditions ('DR associated factors')

We identified that several splicing factors displayed differential expression levels with short-term or long-term DR, and that these differences displayed striking tissue specificity (Figure 5.1, Supplementary tables S22, S23 and S24). In brain, most of the expression changes we observed were associated with long-term 40% DR, mainly in the positive responder strain TejJ89 and largely belonging to the *Hnrnp* class of splicing inhibitors. Expression levels of over half (9/16) of the splicing factors tested were significantly altered with DR at a nominal level, with 4 of these (*Hnrnpa0*, *Hnrnpa1*, *Hnrnph3* and *Hnrnpk*) remaining statistically significant after correction for multiple testing. Conversely, following short-term 40% DR in brain, differences were seen equally frequently in positively and negatively responding strains and mainly involved *Srsf* splicing activators or core spliceosome components, although only one (*Srsf6*) met multiple testing criteria (Figure 5.2a & 5.2b). In heart, we identified most alterations in conjunction with short-term DR, with almost all differences being found in the negative responder strain TejJ114, involving both *Srsf* and *Hnrnp* splicing factors, the majority of which (*Hnrnpa1*, *Hnrnpa2b1*, *Hnrnpd*, *Srsf6* and *Sf1*) were significant after correcting for multiple testing (Figure 5.3a & 5.3b). Finally, in kidney, as we saw in the heart, most of the changes we identified were in conjunction with short-term DR but occurred in both positively and negatively responsive strains. Differences found involved mainly *Srsf* splicing activators or core components of the spliceosome, and 5 out of 14 of these (*Hnrnpa1*, *Srsf1*, *Srsf6*, *Tra2b* and *Sf1*) remained significant after correction for multiple testing. (Figure 5.4a & 5.4b).

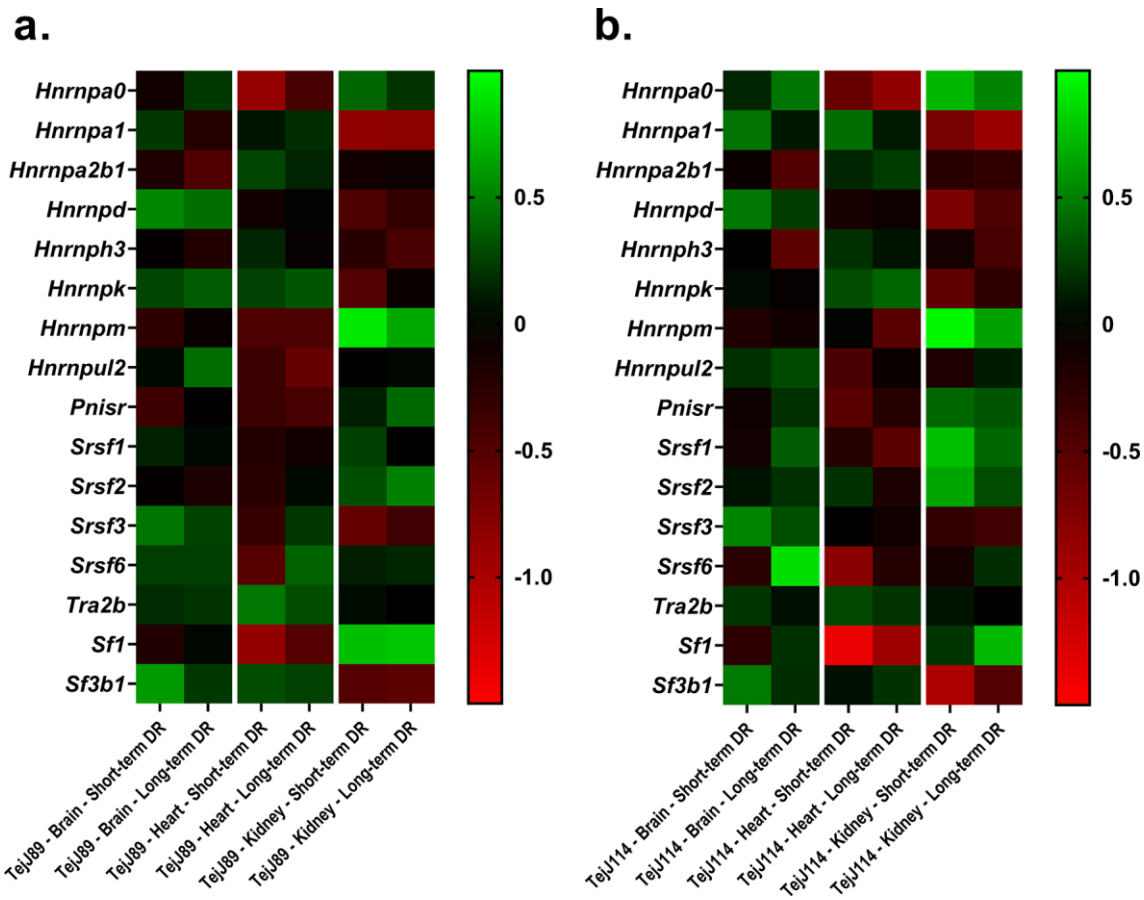

Figure 5.1 Tissue-specificity of splicing factor expression under 40% DR conditions

Heatmaps depicting post-ANCOVA marginal effects for log fold-change in 40% DR expression levels of each transcript (when compared to AL). Data from short-term and long-term 40% DR regimes are shown for each tissue separately. Panel a shows data for the positive responder (TejJ89) and panel b for the negative responder (TejJ114). Transcripts up-regulated in 40% DR are shown in green while those that are down-regulated are shown in red.

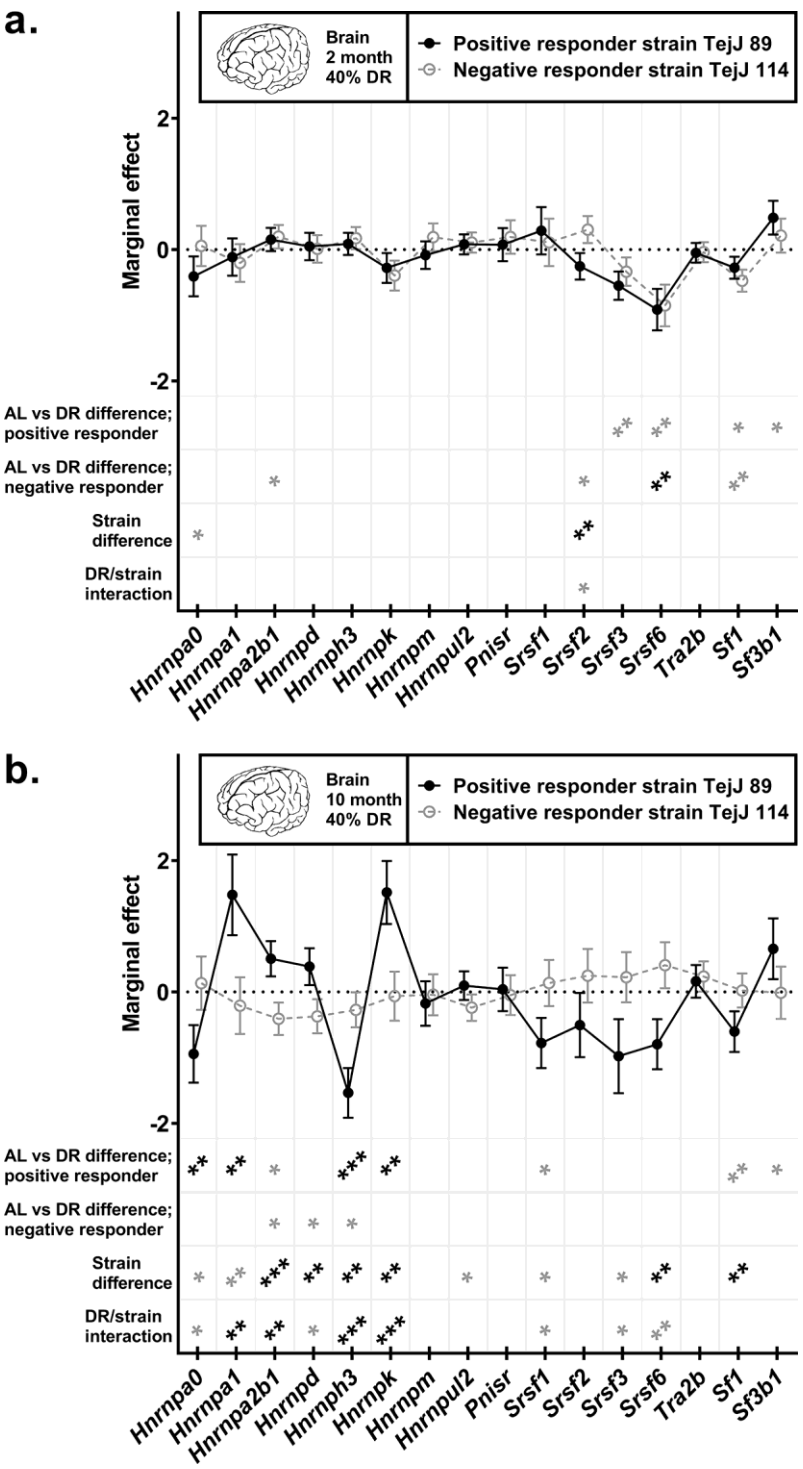

Figure 5.2: Effects of 40% DR on splicing factor expression in brain tissue

Shown here are transcript expression levels in ILSXISS mouse brain tissue under short-term and long-term DR conditions. Panel a shows expression under short-term 40% DR, panel b shows expression under long-term 40% DR. Plots show post-estimation marginal effects from the linear regressions used for interaction analysis. Data points represent log fold-change in DR expression levels of each transcript (when compared to AL), separately for the two mouse strains. Significant differences are denoted with stars: ∗ = p<0.05, ∗∗ = p<0.01, ∗∗∗ = p<0.001. Stars indicated in black denote associations which meet the multiple testing threshold, while those in grey represent nominal associations. Data for the positive responder strain (TejJ89) is shown as solid points and line in black, while the negative responder strain (TejJ114) is shown as open points and dashed line in grey. The null point is indicated by a dotted line. Error bars represent 95% confidence intervals.

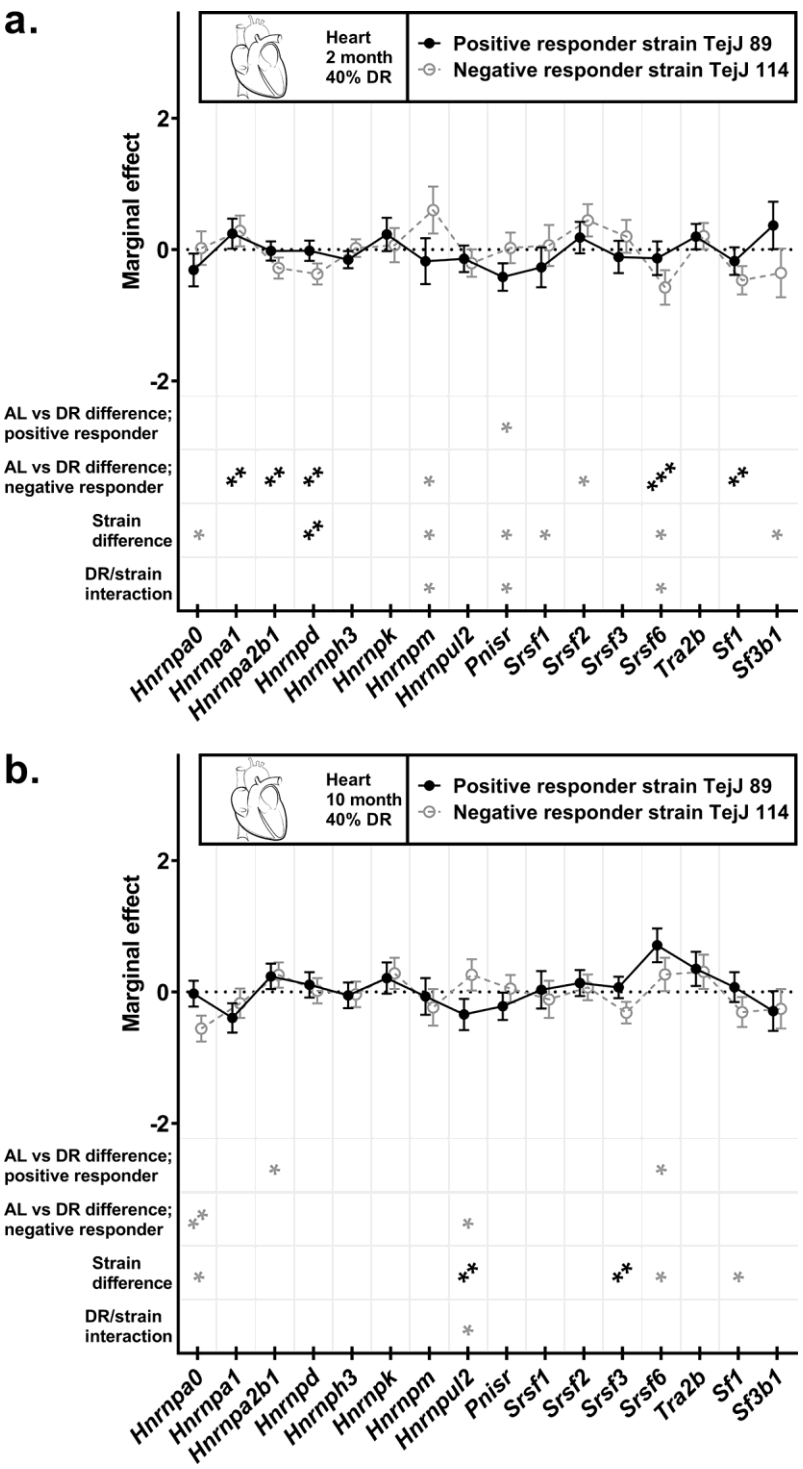

Figure 5.3: Effects of 40% DR on splicing factor expression in heart tissue

Shown here are transcript expression levels in ILSXISS mouse heart tissue under short-term and long-term DR conditions. Panel **a** shows expression under short-term 40% DR, panel **b** shows expression under long-term 40% DR. Plots show post-estimation marginal effects from the linear regressions used for interaction analysis. Data points represent log fold-change in DR expression levels of each transcript (when compared to AL), separately for the two mouse strains. Significant differences are denoted with stars: ∗ = p<0.05, ∗∗ = p<0.01, ∗∗∗ = p<0.001. Stars indicated in black denote associations which meet the multiple testing threshold, while those in grey represent nominal associations Data for the positive responder strain (TejJ89) is shown as solid points and line in black, while the negative responder strain (TejJ114) is shown as open points and dashed line in grey. The null point is indicated by a dotted line. Error bars represent 95% confidence intervals.

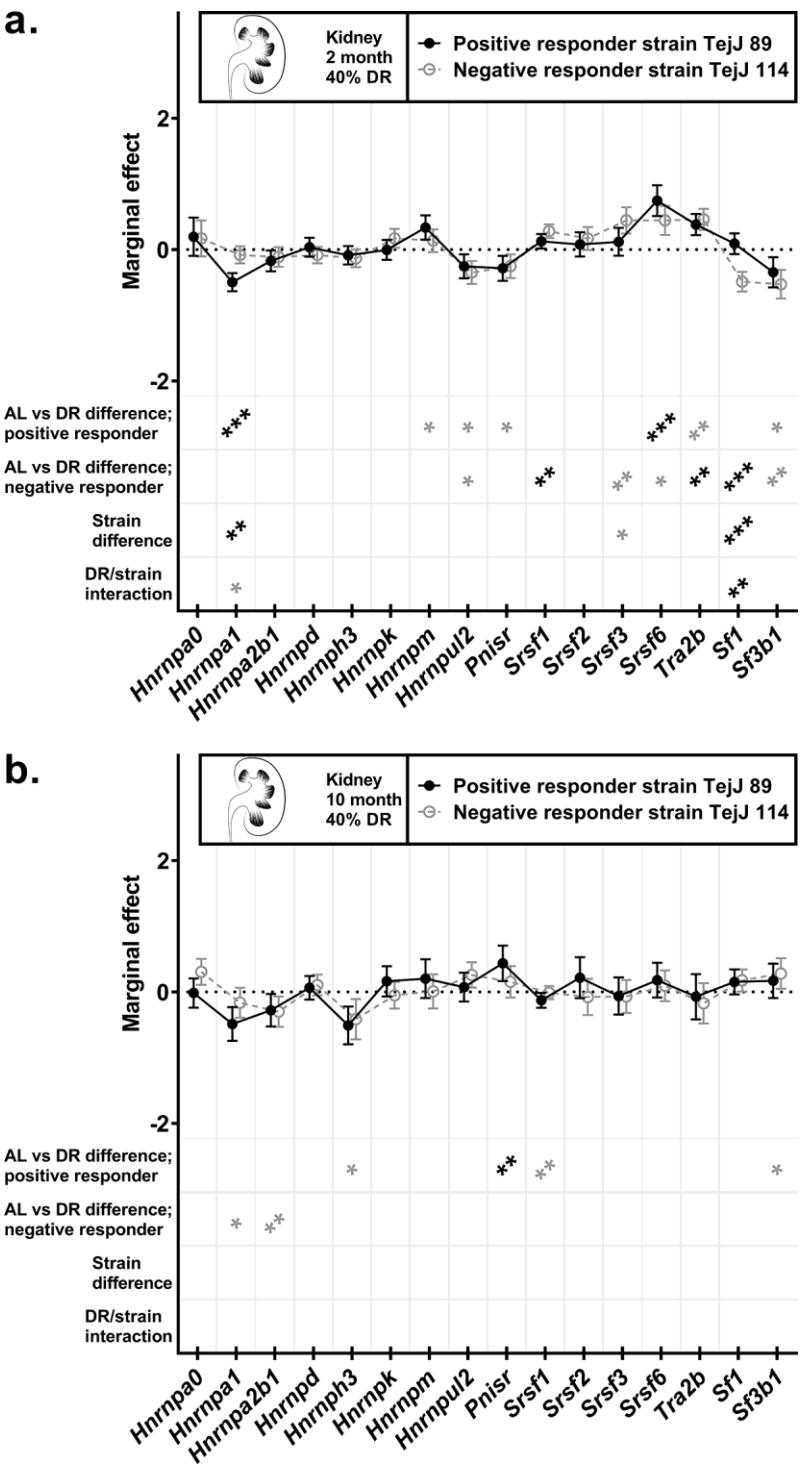

Figure 5.4: Effects of 40% DR on splicing factor expression in kidney tissue

Shown here are transcript expression levels in ILSXISS mouse kidney tissue under short-term and long-term DR conditions. Panel **a** shows expression under short-term 40% DR, panel **b** shows expression under long-term 40% DR. Plots show post-estimation marginal effects from the linear regressions used for interaction analysis. Data points represent log fold-change in DR expression levels of each transcript (when compared to AL), separately for the two mouse strains.

Significant differences are denoted with stars: ∗ = p<0.05, ∗∗ = p<0.01, ∗∗∗ = p<0.001. Stars indicated in black denote associations which meet the multiple testing threshold, while those in grey represent nominal associations. Data for the positive responder strain (TejJ89) is shown as solid points and line in black, while the negative responder strain (TejJ114) is shown as open points and dashed line in grey. The null point is indicated by a dotted line. Error bars represent 95% confidence intervals.

5.6.2 Splicing factors demonstrate different patterns of expression with DR in positive and negative responder strains ('strain-associated factors')

We next identified splicing factors that demonstrated differences in expression patterns between the positive and negative responder strains under short-term or long-term 40% DR. With the exception of brain, most of the differential expression levels in the two strains were present under short-term DR conditions (Supplementary table S25). In brain, only expression of *Hnrnpa0* and *Srsf2* differed between strains under short-term DR, and only *Srsf2* remained significant after correction for multiple testing (Figure 5.2a). Many more incidences where the positive and negative responder strains demonstrated differences in splicing factor expression were evident in brain in response to long-term DR; 11/16 genes exhibited differential expression between strains under these conditions, with 6 of these (*Hnrnpa2b1*, *Hnrnpd*, *Hnrnph3*, *Hnrnpk*, *Srsf6* and *Sf1*) meeting the multiple testing threshold (Figure 5.2b). Several differences between strains were apparent in heart under conditions of short-term DR, which involved both *Srsf* and *Hnrnp* transcripts (Figure 5.3a), although only one of these (*Hnrnpd*) was significant when corrected for multiple testing. Fewer expression differences were apparent overall under long-term DR in heart (Figure 5.3b), however 2 of these (*Hnrnpul2* and *Srsf3*) met multiple testing criteria. Kidney demonstrated fewer alterations than either brain or heart, with differences seen only in response to short-term DR, although 2 of these (*Hnrnpa1* and *Sf1*) met the multiple testing threshold (Figure 5.4a & 5.4b).

5.6.3 Expression levels of some splicing factors are associated with both lifespan effects and DR ('interacting factors')

Some of the most interesting associations are those in which splicing factor expression is associated with both DR and strain. In such cases it is reasonable to postulate that those transcripts may be involved in pathways which contribute to the observed responses to 40% DR within each strain, but are also playing some part in the differences seen in strain-specific lifespan response, and so these splicing factors may comprise part of the molecular mechanism behind the response to DR. We therefore sought to identify situations where a statistical interaction was apparent between DR, strain and splicing factor expression (Supplementary table S26). In brain, only *Srsf2* displayed a nominal interaction under short-term DR conditions (Figure 5.2a), whereas under long-term DR, 9 of 16 splicing factors tested showed at least nominal interactions, with 4 of these (*Hnrnpa1*, *Hnrnpa2b1*, *Hnrnph3* and *Hnrnpk*) significant after correction for multiple testing (Figure 5.2b). In heart, far fewer interactions were apparent overall, with 3 of the 16 splicing factors having nominally significant interactions under short-term DR (Figure 5.3a) and only 1 nominal interaction was detected under long-term DR conditions (Figure 5.3b), however none of these were significant after correction for multiple testing. Finally, in kidney tissue only 2 transcripts were found to show interactions, and only under conditions of short-term DR, with one of these (*Sf1*) meeting the criteria for multiple testing (Figure 5.4a & 5.4b).

5.7 Discussion

Lifespan extension as a result of dietary restriction (DR) has been recognised for over a century[246,247] and has since been the subject of intensive research. The relationship between DR and lifespan is however sometimes unclear, with variation in the lifespan effect reported both across and within species[250,262,265-267]. It is apparent therefore that our understanding of the mechanistic basis underpinning responses to DR is not complete, and that other influences exist which may explain some of the observed strain heterogeneity. One such influence may be the interface between the environmental stimulus (DR) and factors moderating the expression or activity of gene expression. While many such factors exist, one that is highly likely to play a part is alternative splicing, as it is a fundamental component of the response of cells to external and internal stimuli[121], and components of the splicing machinery have previously been implicated in response to DR[67,185]. Here, we have measured transcript expression levels of an *a priori* panel of age- or senescence-related splicing regulatory factors in brain, heart and kidney tissue taken from three ILSXISS recombinant inbred mouse strains with previously reported different lifespan responses to 40% DR. Animals were exposed to both short-term and long-term 40% DR and subsequent analyses were performed to characterise expression differences related to DR alone, differences only related to strain, and effects attributable to both. Our results show that expression levels of several splicing factor transcripts are significantly affected by either short-term or long-term DR, that there are significant differences in expression levels of some transcripts between positive and negative responder strains, and that there are strong tissue specific influences on both effects. Furthermore, some splicing factors demonstrate statistical interactions between their expression, DR and strain lifespan response,

which may indicate mechanistic involvement in the divergent lifespan response to DR observed in these mouse strains under DR conditions.

Dietary restriction has been shown to be linked to lifespan, with multiple pathways involved including those involved in genomic stability, proteostasis, inflammation, autophagy, mitochondrial function, oxidative damage and nutrient signalling pathways (IIS, IGF-1, SIRT, AMPK and mTOR)[242,275]. It is known that the ability to respond to internal and external sources of cellular stress is an important factor in successful ageing[110], and that transcriptomic responsiveness plays a large part in this, including the plasticity of response that is achieved through alternative splicing[268]. A recent study has shown that the splicing factor SF1 is necessary for lifespan extension by DR in *C. elegans*, specifically through the modulation of TORC1 pathway components[67]. Our previous work has shown that both alternative splicing and more specifically the expression levels of splicing regulatory factors that control it, are associated with ageing in humans[101], cellular senescence *in vitro*[103,108] and lifespan in animal models[104]. Recently we also showed that alteration of splicing factor levels using small molecules such as resveratrol analogues, hydrogen sulfide donors or inhibitors of ERK or AKT signalling can reverse senescence phenotypes *in vitro*[107,269,270]. Given this evidence, it is reasonable to hypothesise that regulation of alternative splicing may play a role in the lifespan modification response following DR.

The results presented here are consistent with a hypothesis that altered splicing regulation may form part of the mechanistic response to DR in mice. We propose that the splicing factors we tested can be classified into three broad classes: *1) DR-associated factors.* Expression of these splicing factors is significantly affected by DR, but no differences are apparent between strains, suggesting that although they may have some association to DR, they are unlikely to contribute

to any strain-specific differences seen in the DR response. *2) Strain-associated factors.* Expression of these splicing factors is significantly different between strains but do not differ between AL and DR. *3) Interacting factors***.** Splicing factors showing statistically significant interactions between DR and strain lifespan response in terms of their expression. Where such interactions exist, the associations between splicing factor expression and either DR or responder strain (or both), coupled with a statistically significant mediation effect between the two variables (Figure 5.5), suggests that these splicing factors may be mechanistically involved in defining the divergent lifespan response observed in these mouse strains under 40% DR.

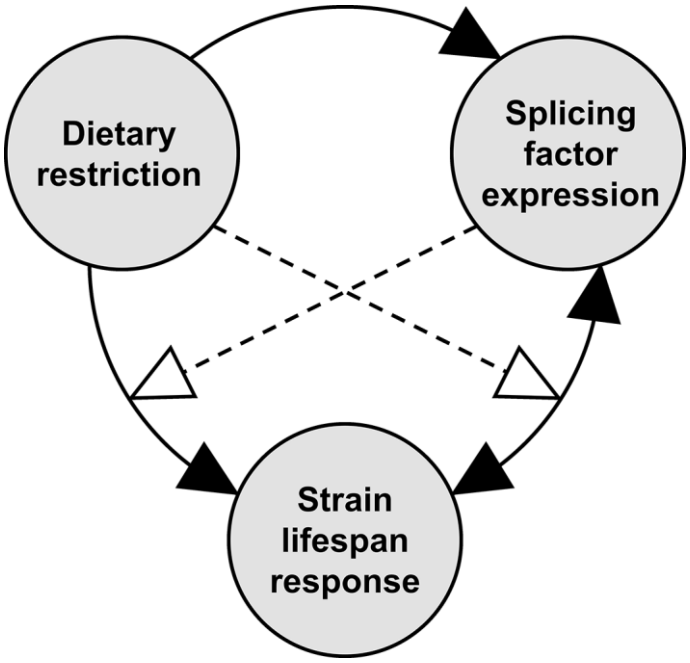

Figure 5.5: Directionality of effects and potential moderating interactions

This figure shows the likely interplay between the variables measured in the present study. Direct effects are shown as solid black arrows, while interactions where one variable could be moderating the effect exerted between other variables are shown as dashed arrows.

Splicing factors showing statistical interactions between strain and DR were very common in brain, particularly in response to long-term DR. This may reflect a more pressing need for the brain to moderate gene output to maintain

homeostatic control than is necessary in the other tissues. It is interesting to note that within the splicing factors affected in the brain, a preponderance of the differences noted between AL and DR (7 out of 8) are observed in the positive responder strain while only 3 of 8 are altered in the negative responder. Few associations were shared between tissues, with only *Srsf6* and *Hnrnpa1* showing patterns that were shared between brain and heart (*Srsf6*) or brain and kidney (*Hnrnpa1*).

Our study has several strengths, including a comprehensive assessment of strain-, tissue- and duration effects. There are of course also limitations to this work; it would have been advantageous to measure alternative isoform expression of target genes of these splicing factors to determine whether they could actively be affecting alternative splicing. Another caveat to the work is that optimally, protein levels of splicing factors would be informative. Unfortunately this was not possible due to limits on starting material. We have used an FDR approach to account for multiple testing, following the two-stage linear step-up procedure of Benjamini, Krieger and Yekutieli[175]. However, it must be recognised that although relatively modest, correlations do exist between expression levels of many splicing factors (Figure 5.6) and that further correlations are likely to exist between different DR treatments and indeed to an extent between the different mouse strains. All of this suggests that the tests performed here are not completely independent, which in turn greatly complicates any sensible application of multiple testing criteria. In addition, while groups of 8 animals per condition is reasonable for a study of this type, there may be an impact on statistical power which could result in Type II errors. Therefore, we recognise that the multiple testing threshold applied here may be overly severe, and as such

have presented nominal findings alongside those which are FDR-corrected, although we recognise that careful interpretation must be applied to such results.

In summary, this study has shown that the expression of splicing factor transcripts shows widespread alterations in response to dietary restriction, and that these are highly tissue specific. It is also apparent that certain transcripts show interactions between the effects of DR, expression levels and strain lifespan response, which could therefore be involved in the mechanisms driving lifespan modulation via DR.

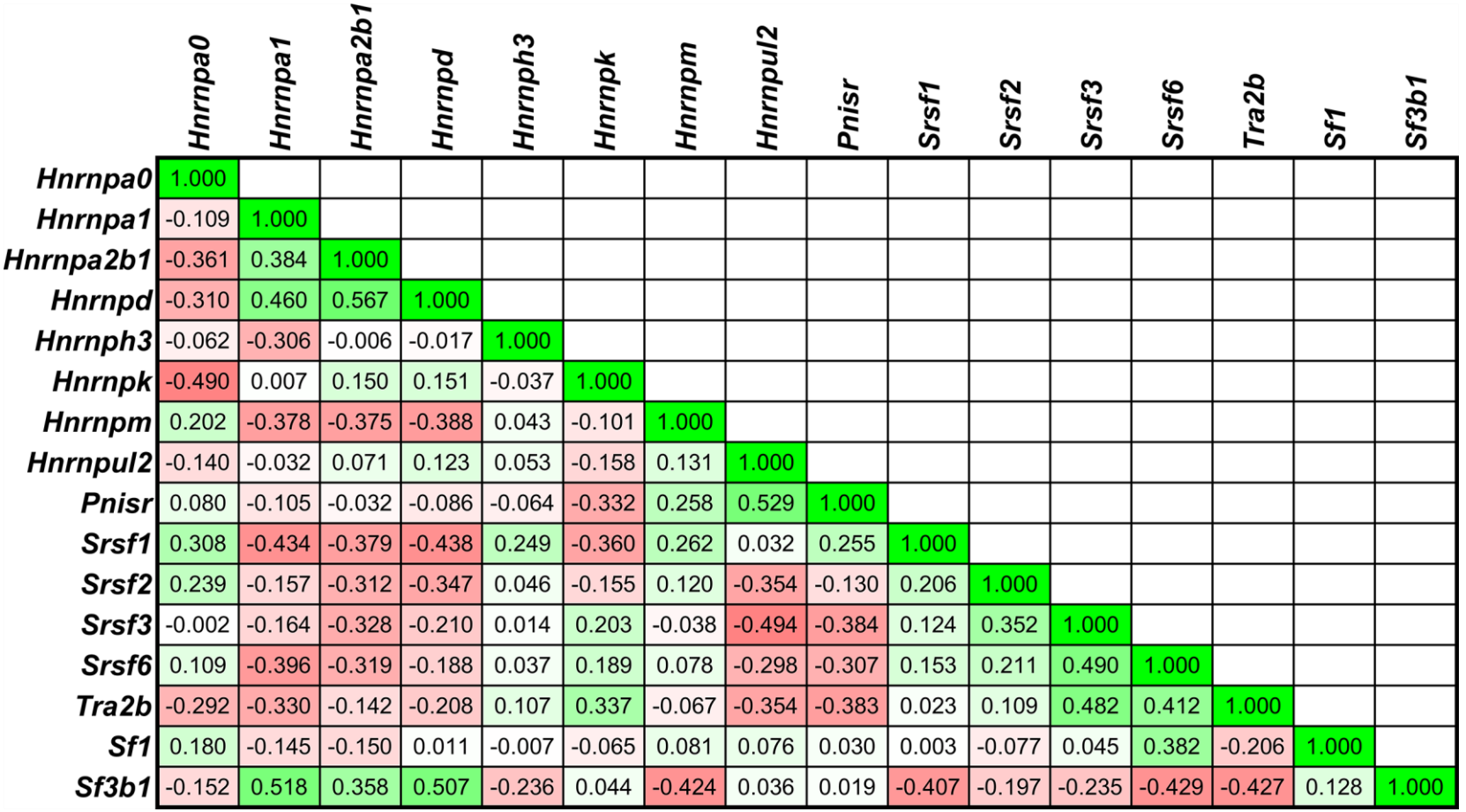

	Hnrnpa0	*Hnrnpa1*	*Hnrnpa2b1*	*Hnrnpd*	*Hnrnph3*	*Hnrnpk*	*Hnrnpm*	*Hnrnpul2*	*Pnisr*	*Srsf1*	*Srsf2*	*Srsf3*	*Srsf6*	*Tra2b*	*Sf1*	*Sf3b1*
Hnrnpa0	1.000															
Hnrnpa1	-0.109	1.000														
Hnrnpa2b1	-0.361	0.384	1.000													
Hnrnpd	-0.310	0.460	0.567	1.000												
Hnrnph3	-0.062	-0.306	-0.006	-0.017	1.000											
Hnrnpk	-0.490	0.007	0.150	0.151	-0.037	1.000										
Hnrnpm	0.202	-0.378	-0.375	-0.388	0.043	-0.101	1.000									
Hnrnpul2	-0.140	-0.032	0.071	0.123	0.053	-0.158	0.131	1.000								
Pnisr	0.080	-0.105	-0.032	-0.086	-0.064	-0.332	0.258	0.529	1.000							
Srsf1	0.308	-0.434	-0.379	-0.438	0.249	-0.360	0.262	0.032	0.255	1.000						
Srsf2	0.239	-0.157	-0.312	-0.347	0.046	-0.155	0.120	-0.354	-0.130	0.206	1.000					
Srsf3	-0.002	-0.164	-0.328	-0.210	0.014	0.203	-0.038	-0.494	-0.384	0.124	0.352	1.000				
Srsf6	0.109	-0.396	-0.319	-0.188	0.037	0.189	0.078	-0.298	-0.307	0.153	0.211	0.490	1.000			
Tra2b	-0.292	-0.330	-0.142	-0.208	0.107	0.337	-0.067	-0.354	-0.383	0.023	0.109	0.482	0.412	1.000		
Sf1	0.180	-0.145	-0.150	0.011	-0.007	-0.065	0.081	0.076	0.030	0.003	-0.077	0.045	0.382	-0.206	1.000	
Sf3b1	-0.152	0.518	0.358	0.507	-0.236	0.044	-0.424	0.036	0.019	-0.407	-0.197	-0.235	-0.429	-0.427	0.128	1.000

Figure 5.6 Correlations between splicing factor expression levels

Pearson correlations of relationships between expression levels of all splicing factors measured. Positive correlations are shown in green and negative correlations in red.

5.8 Acknowledgements

This research did not receive any specific grant from funding agencies in the public, commercial, or not-for-profit sectors. LM was supported through start-up funds from the University of Glasgow (College of Medical, Veterinary and Life Sciences) to CS.

Chapter 6

Data Chapter.

The transcript expression levels of *HNRNPM*, *HNRNPA0* and *AKAP17A* splicing factors may be predictively associated with ageing phenotypes in human peripheral blood.

Published in: Biogerontology. October 2019. doi: 10.1007/s10522-019-09819-0.

6.1 Author List

Benjamin P. Lee[1], Luke C. Pilling[2], Stefania Bandinelli[3], Luigi Ferrucci[4], David Melzer[2] and Lorna W. Harries[1]

1 - Institute of Biomedical and Clinical Sciences, University of College of Medicine and Health, UK, EX2 5DW.
2 - Epidemiology and Public Health, University of College of Medicine and Health, UK, EX2 5DW.
3 - Geriatric Unit, USL Toscana Centro, Florence, 50122 Italy.
4 - National Institute on Aging, Clinical Research Branch, Harbor Hospital, Baltimore, MD 21225.

6.2 Author contributions

LH managed the project, designed the experiments and co-wrote the manuscript. BL coordinated and performed experiments, performed the data analysis and co-wrote the manuscript. LP carried out cross-checks during cohort selection, advised on statistical techniques and reviewed the manuscript. SB oversaw participant interviews and sample collection. LF provided access to the InCHIANTI cohort and NIA resources. DM contributed to data analysis and reviewed the manuscript.

6.3 Abstract

Dysregulation of splicing factor expression is emerging as a driver of human ageing; levels of transcripts encoding splicing regulators have previously been implicated in ageing and cellular senescence both *in vitro* and *in vivo*. We measured the expression levels of an *a priori* panel of 20 age- or senescence-associated splicing factors by qRT-PCR in peripheral blood samples from the InCHIANTI Study of Aging, and assessed longitudinal relationships with human ageing phenotypes (cognitive decline and physical ability) using multivariate linear regression. *AKAP17A, HNRNPA0* and *HNRNPM* transcript levels were all predictively associated with severe decline in MMSE score (p = 0.007, 0.001 and 0.008 respectively). Further analyses also found expression of these genes was associated with a performance decline in two other cognitive measures; the Trail Making Test and the Purdue Pegboard Test. *AKAP17A* was nominally associated with a decline in mean hand-grip strength (p = 0.023), and further analyses found nominal associations with two other physical ability measures; the Epidemiologic Studies of the Elderly – Short Physical Performance Battery and calculated speed (m/s) during a timed 400m fast walking test. These data add weight to the hypothesis that splicing dysregulation may contribute to the development of some ageing phenotypes in the human population.

6.4 Introduction

There is an intimate relationship between stress responses and successful ageing[110] yet the ability to respond appropriately to stressful environments and to maintain systemic homeostasis declines with age in multiple species[276-278]. Cellular responses to external and internal stressors are mediated at the level of genomic plasticity, in particular at the level of the transcriptome. Several mechanisms are known to play a part in the diversity of response, including transcriptional regulation at the level of polymerase activity[117], post-transcriptional regulation[120], epigenetics[279] and genomic landscape[119]. Alternative splicing comprises a key part of the homeostatic response to stress[121,280,281], and dysregulation of this process is now emerging as a new and important driver of cellular ageing[101,103,282]. Over 95% of genes are capable of producing more than one mRNA product under different conditions and alternatively-expressed mRNAs can have profoundly different temporal or spatial expression patterns, or demonstrate major differences in functionality[283-285].

Alternative splicing decisions are made by a series of trans-acting splicing regulatory proteins termed splicing factors. These are the Serine Arginine-rich (SR) family of splicing factors which usually, but not exclusively, promote splice site usage, and the heterogeneous nuclear ribonucleoprotein (HNRNP) family of splicing factors which are usually, but not exclusively, associated with inhibition of splice site usage[176]. SR proteins and HNRNPs bind to exon/intron splicing enhancer (ESE/ISE) or silencer (ESS/ISS) elements in the vicinity of the splice sites and the balance of activators and inhibitors at any given splice site regulates splice site usage[126]. The expression levels of splicing regulators is known to be associated with ageing; of 7 gene ontology pathways robustly associated with

age in a large cross-sectional population study of human ageing, 6 were directly involved in mRNA splicing processes[101]. Splicing factor expression is also associated with lifespan in mice and humans[104]. Alterations in splicing factor expression have also been reported in senescent human cells of multiple tissue types[103,108] and restoration of splicing factor expression to levels consistent with a younger profile was sufficient to reverse multiple senescent cell phenotypes in senescent human fibroblasts *in vitro*[107].

We have previously observed disruption of splicing factor expression in human senescent cells[103,108], and demonstrated that experimental manipulation of splicing factor expression is capable of inducing rescue from the senescent cell phenotype[107,269,270]. Although we have demonstrated epidemiological links with ageing itself, and reversal of cellular senescence *in vitro*, evidence that the phenomena we observe *in vitro* is linked with downstream ageing phenotypes is lacking. In this study, we addressed this question by measurement of the expression of an *a priori* panel of age- and senescence-related splicing factor genes in human peripheral blood mRNA from the InCHIANTI study of Aging. We used samples from two follow-up visits (FU3; 2007 – 2010 and FU4; 2012 - 2014) of the InCHIANTI study of Aging, and related their expression to changes in recorded measures of two important human ageing phenotypes; cognitive and physical function. We initially used the Mini Mental State Exam (MMSE) score and mean hand-grip strength to identify putative associations between splicing factor expression and changes in cognitive or physical ability respectively. We then assessed expression of these transcripts against other cognitive and physical measures available in the dataset. In each case, a set of sub-analyses were also performed to test the robustness of the findings.

We found that the expression of three splicing factor genes, *HNRNPM*, *HNRNPA0* and *AKAP17A* may be predictive for change in this population; all three genes were associated with cognitive decline as measured by the Mini-Mental State Examination (MMSE), Trail-Making Tests part A and B (TMT A/B), and the Purdue Pegboard Test (PPT). *AKAP17A* was also associated with a decline in physical ability as measured by hand-grip strength, the Epidemiologic Studies of the Elderly – Short Physical Performance Battery (EPESE-SPPB) and calculated speed during a timed 400m fast walking test. Our data suggest that age-associated dysregulation of splicing factor expression in ageing humans may contribute to the development of downstream ageing outcomes.

6.5 Methods

6.5.1 InCHIANTI cohort and selection of participants

The InCHIANTI study of Aging is a population study of ageing[163]. Participants undertook detailed assessment of health and lifestyle parameters at baseline, and again at 3 subsequent follow-ups (FU2; 2004 – 2006, FU3; 2007 – 2010 and FU4; 2012 - 2014). The present study used participants from the third and fourth follow-up visits (FU3 and FU4). RNA samples and clinical/phenotypic data were already available for 698 participants at FU3. The collection of the FU4 samples and data comprise part of this study. During the FU4 interviews in 2012/13, blood and clinical/phenotypic data were collected from 455 study participants. These data were cross-checked against RNA samples and clinical/phenotypic data already held from FU3, to ensure that sample and phenotypic data was available from both collections. 393 individuals fitted these criteria, of which 9 died shortly after the FU4 visit and so were excluded from the analysis. From the remaining

384 eligible samples, 300 were randomly selected from the cohort to be analysed for expression of splicing factor genes. Anthropometric parameters and blood cell subtypes in FU4 were measured as previously[163].

6.5.2 Splicing factor candidate genes for analysis

An *a priori* list of splicing factor candidate genes were chosen based on associations we had documented with human ageing in multiple populations and in senescent primary human cell lines in our previous work[101,103,107]. We have also found associations of components of this gene set with lifespan in both mice and humans[104]. The list of genes included the positive regulatory splicing factors *AKAP17A*, *SRSF1*, *SRSF2*, *SRSF3*, *SRSF6*, *SRSF7*, *PNISR* and *TRA2B*, the negative regulatory splicing inhibitors *HNRNPA0*, *HNRNPA1*, *HNRNPA2B1*, *HNRNPD*, *HNRNPH3*, *HNRNPK*, *HNRNPM*, *HNRNPUL2* and the *IMP3*, *LSM14A*, *LSM2* and *SF3B1* core components of the spliceosome. Expression assays were obtained in custom TaqMan® low-density array (TLDA) format (ThermoFisher, Waltham, MA, USA). Assay Identifiers are given in Supplementary table S27.

6.5.3 RNA Collection and Extraction

2.5ml of peripheral blood was collected from each participant into PAXgene Blood RNA Tubes (IVD) (PreAnalytiX GmbH, Hombrechtikon, Switzerland). Blood tubes were then treated according to the manufacturer's instructions and subsequently cold-chain shipped to the UK. RNA extractions were then carried out using the PAXgene Blood mRNA Kit (Qiagen, Hilden, Germany), according to manufacturer's instructions. Samples were assessed for RNA quality and quantity by Nanodrop spectrophotometry (NanoDrop, Wilmington, DE, USA).

6.5.4 Reverse Transcription and quantitative RT-PCR

100ng of total RNA was reverse transcribed using SuperScript® VILO™ cDNA Synthesis Kit (ThermoFisher, Waltham, MA, USA) in 20µl reactions, according to the manufacturer's instructions. 20µl cDNA (reverse transcribed as indicated above) was added to 50µl TaqMan® Universal Master Mix II, no UNG (ThermoFisher, Waltham, MA, USA) and 30µl RNase-free dH_2O, then loaded onto TaqMan® Low-Density Array 384-Well Microfluidic cards. 100µL reaction solution was dispensed into each TLDA card chamber and the card centrifuged twice for 1 min at 216 x g to ensure distribution of solution to each well. The expression of transcripts in each sample was measured in duplicate replicates. Cards were run on the 7900HT Fast Real-Time PCR System (ThermoFisher, Waltham, MA, USA). Amplification conditions were as follows: a single cycle of 50°C for 2 minutes, a single cycle of 94.5°C for 10 minutes followed by 40 cycles of 97°C for 30 seconds and 59.7°C for 1 minute.

6.5.5 Data preparation

SDS files were uploaded to the ThermoFisher Cloud (ThermoFisher, Waltham, MA, USA) and analysed using the Relative Quantification qPCR App encompassed within the software (https://www.thermofisher.com/uk/en/home/cloud.html). This platform was used to manually set Baseline and Threshold for each assay (see Supplementary table S27 for values) and to ensure there were no apparent outliers before further analysis. One sample was excluded at this stage as expression data was missing for all genes measured. Output was imported into Excel (Microsoft, Redmond, WA, USA) and the C_T values used for analysis using the comparative C_T method. The most stable genes for use as endogenous controls were determined from the raw data using the RefFinder webtool[273],

which returned the geometric mean value across all genes measured as the most stable control, and thus the most appropriate for the ΔC_T normalisation step. Expression was then calculated relative to the median expression for each individual transcript. Data were log transformed to ensure normal distribution. Outlier detection was performed in SPSS (IBM, Armonk, NY, USA). Univariate outliers were identified using standardised z-scores, with any individual measures for each gene falling outside the cut-off (set at 3 standard deviations from the mean) being discarded. Multivariate outliers were identified using a regression model with Mahalanobis distance as an output, followed by comparison of the calculated Mahalanobis distances with the critical $\chi 2$ value for the dataset[274]. One sample for which the Mahalanobis distance exceeded the critical $\chi 2$ was discarded, leaving a total of n=298 samples to take forward for statistical testing. The characteristics of this final subset of participants are summarised in Table 6.1.

Table 6.1: Participant details

Characteristics of the InCHIANTI participants used in the present study. Panel A shows summary of non-clinical details, panel B shows summary results of clinical/laboratory tests and panel C shows summary results of phenotypic measures used for analysis.

A.

		Follow-up 3		Follow-up 4	
		n	%	n	%
Participants		298	100	298	100
Age (years)	**30-39**	21	7.05	11	3.69
	40-49	31	10.40	28	9.40
	50-59	31	10.40	28	9.40
	60-69	35	11.74	34	11.41
	70-79	111	37.25	38	12.75
	80-89	67	22.48	142	47.65
	90-100	2	0.67	17	5.70
Gender	**Male**	136	45.64	136	45.64
	Female	162	54.36	162	54.36
Pack years smoked (lifetime)	**None**	159	53.36	NO	DATA
	<20	79	26.51	NO	DATA
	20-39	44	14.76	NO	DATA
	40+	16	5.37	NO	DATA
Site	**Greve**	140	46.98	140	46.98
	Bagno a Ripoli	158	53.02	158	53.02
Education level attained	**Nothing**	28	9.4	24	8.05
	Elementary	121	40.6	125	41.95
	Secondary	51	17.11	59	19.80
	High School	46	15.44	58	19.46
	Professional school	33	11.07	11	3.69
	University or equivalent	19	6.38	21	7.05

B.

	Follow-up 3				Follow-up 4			
	Mean	**Std. Dev.**	**Min**	**Max**	**Mean**	**Std. Dev.**	**Min**	**Max**
Age (years)	67.69	15.68	30.00	94.00	72.92	15.68	35.00	100.00
BMI	26.97	4.27	15.01	42.99	26.86	4.42	13.39	41.19
White blood cell count (n, K/ul)	6.39	1.60	2.10	13.00	6.16	1.72	2.30	16.59
Neutrophils (%)	56.61	8.61	26.20	81.20	56.50	9.23	22.20	88.40
Lymphocytes (%)	31.56	8.04	9.80	59.90	32.47	8.70	8.30	63.30
Monocytes (%)	8.08	2.22	3.70	21.30	7.36	2.28	1.60	24.40
Eosinophils (%)	3.19	2.20	0.00	21.50	3.21	2.02	0.00	13.00
Basophils (%)	0.55	0.20	0.10	1.30	0.47	0.29	0.00	2.10

Table 6.1 (cont.)

C.

	Follow-up 3					Follow-up 4			
	n	**Mean**	**Std. Dev.**	**Min**	**Max**	**Mean**	**Std. Dev.**	**Min**	**Max**
Corrected MMSE score	296	27.22	3.18	14.00	30.00	25.71	5.11	0.00	30.00
Trail-Making Test Part A (mins)	268	0.91	0.62	0.23	5.00	1.13	0.83	0.25	5.00
Trail-Making Test Part B (mins)	179	1.56	1.02	0.47	5.00	1.91	1.19	0.52	5.00
Mean hand-grip strength (Kg)	285	29.67	12.28	10.00	70.75	28.11	12.14	5.00	65.50

6.5.6 Phenotypic outcomes for analysis

The current study analysed the associations of splicing factor gene expression at FU3 with the following cognitive phenotypic outcomes; MMSE score, Trail-Making-Test (TMT A&B) and Purdue Pegboard Test (as measures of cognitive function), along with hand-grip strength, EPESE-SPPB composite score and calculated speed during a 400m fast walk (as measures of physical ability).

MMSE score was measured at both FU3 and FU4 using the standard test, after which the data was corrected to adjust for incomplete tests. This was calculated using the score attained as a proportion of the maximum possible points for the parts of the test that were completed. Decline in MMSE score was calculated by subtracting the score at FU4 from the score at FU3. Time taken to complete the Trail-Making-Tests part A and B were measured in seconds at both FU3 and FU4 using the standard tests. Decline in performance on the tests was calculated by subtracting the score at FU4 from the score at FU3. Decline in seconds was then converted to a decline in fractions of a minute prior to analysis. The Purdue Pegboard Test was administered as standard (although data for the assembly portion of the test was not available), and scores for number of pegs placed in the board for right-hand, left-hand and both-hands were summed to give a total

number of pegs placed during the test. Decline in performance on the test was calculated by subtracting the total number of pegs placed at FU4 from the total number of pegs placed at FU3.

Hand-grip strength was measured in kilograms at both FU3 and FU4 using a dynamometer, with two separate measurements taken for each hand. Mean hand-grip strength was used for the analyses in this study, and was calculated as the mean of all 4 hand-grip strength measurements across both hands. Decline in mean hand-grip strength was calculated by subtracting the measurement at FU4 from the measurement at FU3. The EPESE-SPPB was administered and scored as described elsewhere[286], and a composite score generated from the sub-scores of the 3 activities performed: repeated chair-stand, standing balance and 4m normal pace walk. Decline in performance was calculated by subtracting the composite score at FU4 from the composite score at FU3. The 400m fast walk was performed by completing 20 laps of a 20m circuit with a maximum of 2 stops if the subject required. Speed in m/s was calculated over the entire distance (any individuals who did not complete the test were excluded from further analysis), and decline in performance was calculated by subtracting the speed at FU4 from the speed at FU3.

6.5.7 Sub-analyses for robustness testing

For all phenotypes, any associations found in the full cohort were then tested for robustness through four sub-analyses on different subsets of the data.

First, individuals with the lowest initial scores (at FU3) were excluded from the analysis, to avoid confounding due to the inclusion of participants already on a trajectory to decline. For MMSE score, the cut-off was set at >=28, as a score above 28 is clearly indicative of a lack of cognitive impairment. In the case of

mean hand-grip strength, the cut-offs used were those previously reported as a consensus definition of sarcopenia by The European Working Group on Sarcopenia in Older People (EWGSOP)[287], i.e. <20kg for females and <30kg for males. For all the other phenotypes analysed, the dataset at FU3 was divided into quintiles, with the lowest scoring quintile being excluded from this sub-analysis.

Second, an analysis was carried out using only the eldest participants aged >= 70 years at FU3 to exclude any potential confounding effects from younger participants. Declining cognitive and physical ability are predominantly features of ageing, and measures such as mean hand-grip strength and MMSE are likely to perform poorly in measuring change of function in young, non-compromised individuals.

Third, some individuals measured showed an apparent improvement in performance over time between FU3 and FU4, which may reflect a degree of measurement error. To test this, we first calculated an allowed error of 5% (as a fraction of the total range of change measured), then removed any individuals with scores showing an increase greater than the allowed error between the follow-ups, for each phenotype.

Finally, participants were categorised into mild or severe decline classes, to assess whether the associations seen were specific to either group of individuals. Decline in MMSE score was categorised for sub-analysis as follows; ‘No decline’ (score change of -1 to +7, based on a 5% allowable error calculated as described above), ‘Mild decline’ (-2 to -8), and ‘Severe decline’ (-9 to -22). While opinion differs as to what amounts to a significant rate of change in MMSE during cognitive decline, we chose to classify a severe decline as a drop in MMSE score

of >3 per annum on average, based on information from several previous studies [288-290]. Analysis of categorised MMSE decline was carried out using the 'No decline' class as the comparator.

Decline in mean hand-grip strength was categorised as follows; quintiles of change in mean hand-grip were calculated separately for males and females, after which the respective 20% of males and females displaying the largest decline in mean hand-grip strength were together designated as the 'Severe decline' class (mean hand-grip change of -3.75kg to -22kg). The remainder of the cohort was divided into 'No decline' (-1kg to +15.5kg, based on a 5% allowable error calculated as described above) and 'Mild decline' (-1.25kg to -6kg) categories. Analysis of categorised mean hand-grip strength decline was carried out using the 'No decline' class as the comparator.

For all other measures used for analysis, categorisation was carried out by dividing using the cohort into quintiles based on the change in score, and the quintile with the greatest decline in performance designated as the 'Severe decline' class. The remainder of the cohort was divided into 'No decline' and 'Mild decline' classes using the same method as described above for MMSE and mean hand-grip strength. Analysis of categorised variables was carried out using the 'No decline' class as the comparator in all cases.

6.5.8 Statistical Analysis

Associations of gene expression with cognitive and physical phenotype measures were assessed using multivariate linear regression models. All models were adjusted for age, sex, BMI, smoking (lifetime pack-years), highest education level attained, study site, TLDA batch and cell counts (neutrophils, lymphocytes, monocytes, eosinophils and overall white blood cell count). Regressions were

carried out in STATA SE v15.1 (StataCorp, College Station, TX, USA). Pearson correlation tests were carried out in SPSS (IBM, Armonk, NY, USA) to assess relationships between splicing factor expression levels, phenotypic measures and established biomarkers of ageing.

6.6 Results

6.6.1 AKAP17A, HNRNPA0 and HNRNPM transcript levels are associated with change in MMSE score

MMSE is a commonly used measure of cognitive decline[288-290]. *HNRNPM* expression showed a significant association with decline in MMSE score in the entire cohort (β-coefficient -0.005, p = 0.006), with *HNRNPA0* also showing a nominal association (β-coefficient -0.003, p = 0.019). In both cases individuals with lower expression levels at the early time-point (FU3) had subsequently experienced a greater drop in MMSE score (Figure 6.1, Supplementary table S28). The remaining splicing factor genes did not demonstrate associations between MMSE and expression.

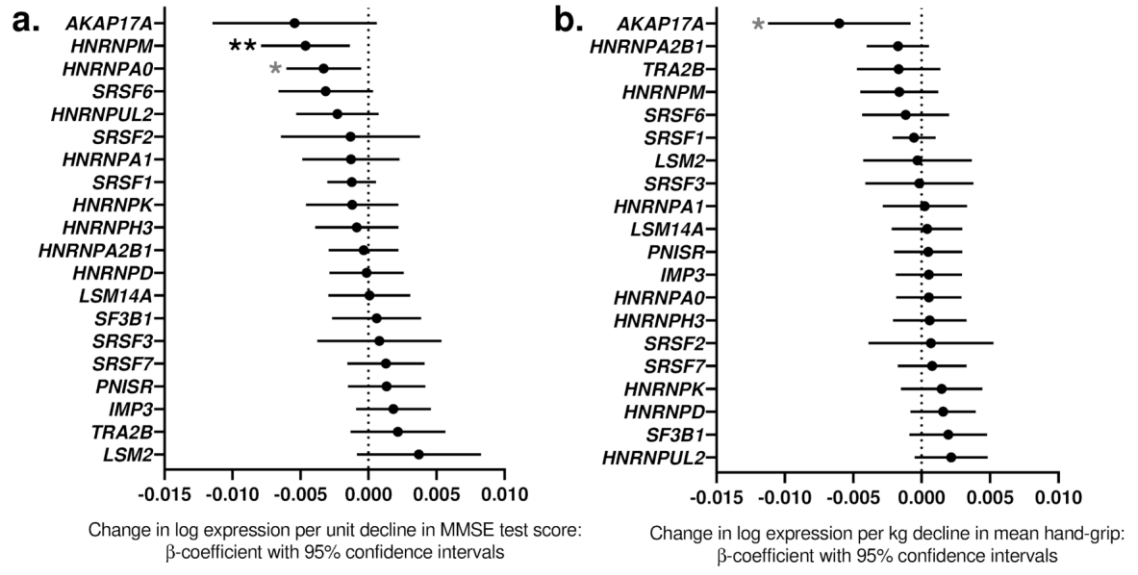

Figure 6.1: Associations of splicing factor expression with MMSE score and mean hand-grip strength

Forest plots showing splicing factor expression in relation to (a.) decline in corrected MMSE scores and (b.) mean hand-grip strength in the InCHIANTI human ageing cohort. Individual splicing factors are indicated on the *y-axis* while β-coefficients of change in log expression per unit change in measurements are given on the *x-axis*. Positive values denote an increase in expression with larger decline in score while negative values denote a decrease in expression with larger decline in score. Error bars denote 95% confidence intervals, significance is shown using stars as follows: * = $p<0.05$, ** = $p<0.01$. Stars indicated in black denote associations which meet multiple testing thresholds, while those in grey represent nominal associations

To test the robustness of our findings we carried out four sub-analyses. Similar sub-analyses were also used on all other associations found in the present study and full details can be found in the Methods. In brief, regression models were repeated on the following subsets of data: firstly we removed individuals with low starting scores, secondly only individuals over 70 years of age were included, thirdly any individuals showing an increase in performance over time were excluded, and finally participants were categorised into ‘mild’ or ‘severe’ decline classes.

Although *AKAP17A* showed only a trend with MMSE decline in the initial analysis, the observation that it had the largest β-coefficient, coupled with a suggestive *p*-value of 0.077 merited its inclusion in these further analyses. As can be seen in Figure 6.2a, 6.3a and 6.4a (Supplementary table S29), both *HNRNPA0* and

HNRNPM remained at least nominally associated with decline in MMSE score across all sub-analyses, and significantly associated with severe decline in the categorised analysis. *AKAP17A* on the other hand was only nominally associated with decline in MMSE in the sub-analysis excluding the individuals displaying an apparent improvement over time, but in the categorised analysis a significant association was also seen between *AKAP17A* expression and severe decline.

To assess whether these findings represent independent effects or could be driven by co-ordinate expression of the three genes, we carried out correlation analysis. Correlations between the 3 genes in question were only moderate (R values: *HNRNPA0* & *HNRNPM*: 0.282, *HNRNPA0* & *AKAP17A*: 0.239, *HNRNPM* & *AKAP17A*: 0.440 (Supplementary table S30).

6.6.2 Expression of HNRNPA0, HNRNPM and AKAP17A transcripts are also associated with two other measures of cognitive ability

The Trail Making Test (TMT) is another widely used test for cognitive assessment which addresses visual scanning, graphomotor speed and executive function[291]. Figure 6.2b&c, 6.3b&c and 6.4b&c (Supplementary table S31) show *AKAP17A* and *HNRNPA0* transcript levels were at least nominally associated with increased time to complete TMT-A, both in the full cohort (β-coefficients 0.057 and 0.028, p = 0.009 and 0.004 for *AKAP17A* and *HNRNPA0* respectively) and in all sub-analyses with the exception of the categorised analysis for *AKAP17A*. *HNRNPM* expression was nominally associated with increased time to complete TMT-B, but only in the full cohort (β-coefficient 0.026, p = 0.036) and categorised analyses. In all cases, lower expression levels were associated with an increase in the time taken to complete the test (i.e. a decline in performance).

The Purdue Pegboard Test (PPT) was originally developed as a tool to evaluate fine manual dexterity but has since been used for assessments of cognitive function[292,293]. As shown in Figure 6.2d, 6.3d and 6.4d (Supplementary table S31), all three transcripts were nominally associated with a performance decline in the full cohort (β-coefficients -0.005, -0.002 and -0.002, p = 0.012, 0.047 and 0.044 for *AKAP17A*, *HNRNPA0* and *HNRNPM* respectively). While *AKAP17A* and *HNRNPA0* transcript levels were found to be significantly associated with performance decline in some of the sub-analyses, *HNRNPM* showed no such further associations.

Pearson correlations were also carried out to assess relationships between the aspects of cognition being measured by MMSE, TMT and PPT. Correlations between the measures were relatively weak (R values range from -0.381 to 0.322, see Supplementary table S32a).

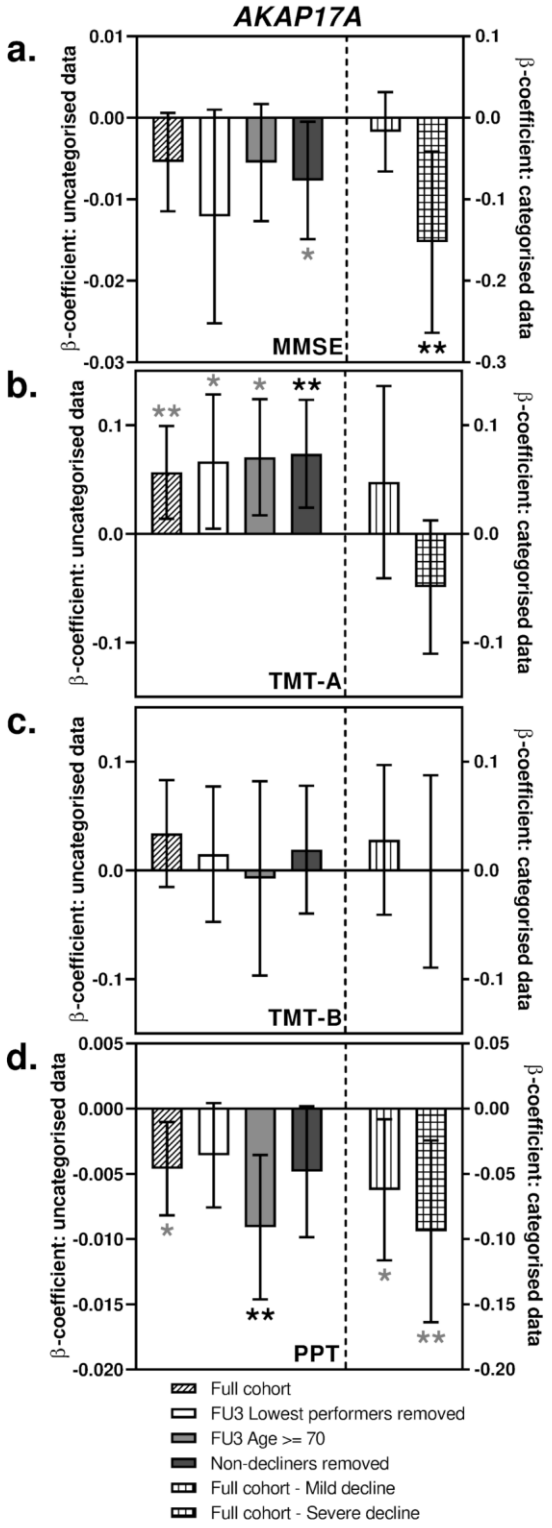

Figure 6.2: Sub-analyses of *AKAP17A* associations with measures of cognitive function

Bar charts showing the associations between expression of *AKAP17A* and change in performance in tests of cognitive function. Panel (a.) shows associations with MMSE score, panel (b.) shows associations with TMT-A, panel (c.) shows associations with TMT-B and panel (d.) shows associations with PPT. Different sub-analyses are plotted separately as indicated in the figure legend. Error bars denote 95% confidence intervals, significance is shown using stars as follows: * = p<0.05, ** = p<0.01. Stars indicated in black denote associations which meet multiple testing thresholds, while those in grey represent nominal associations

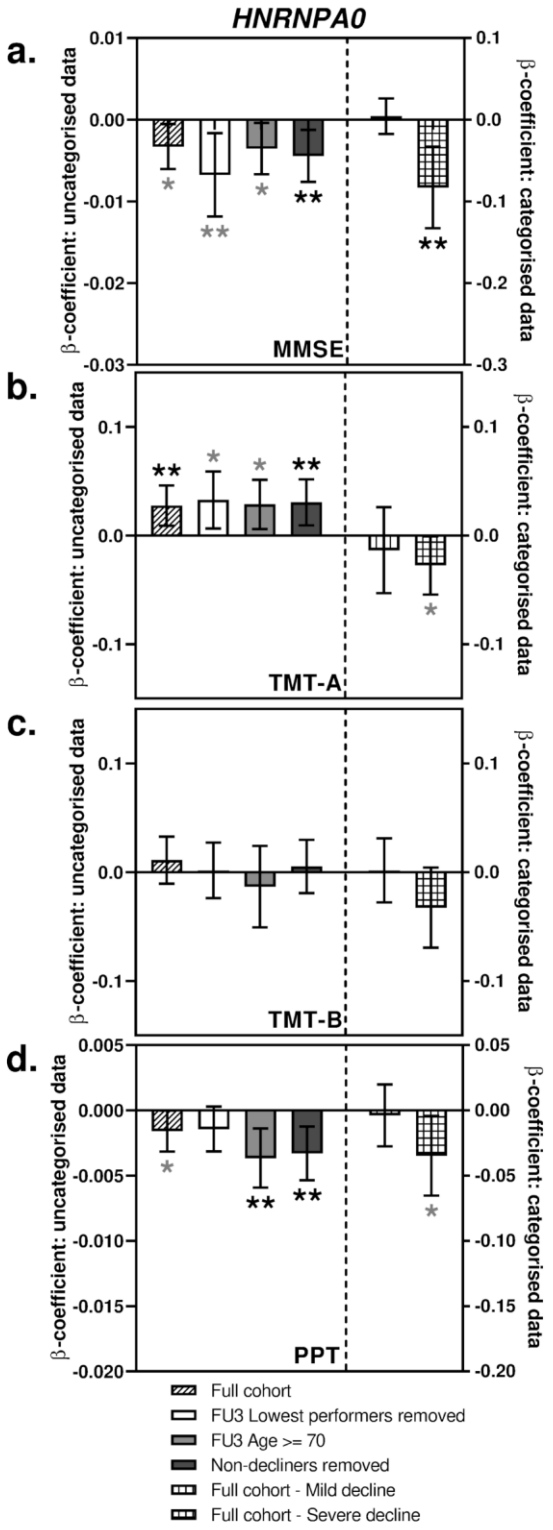

Figure 6.3: Sub-analyses of *HNRNPA0* associations with measures of cognitive function

Bar charts showing the associations between expression of *HNRNPA0* and change in performance in tests of cognitive function. Panel (a.) shows associations with MMSE score, panel (b.) shows associations with TMT-A, panel (c.) shows associations with TMT-B and panel (d.) shows associations with PPT. Different sub-analyses are plotted separately as indicated in the figure legend. Error bars denote 95% confidence intervals, significance is shown using stars as follows: * = p<0.05, ** = p<0.01. Stars indicated in black denote associations which meet multiple testing thresholds, while those in grey represent nominal associations

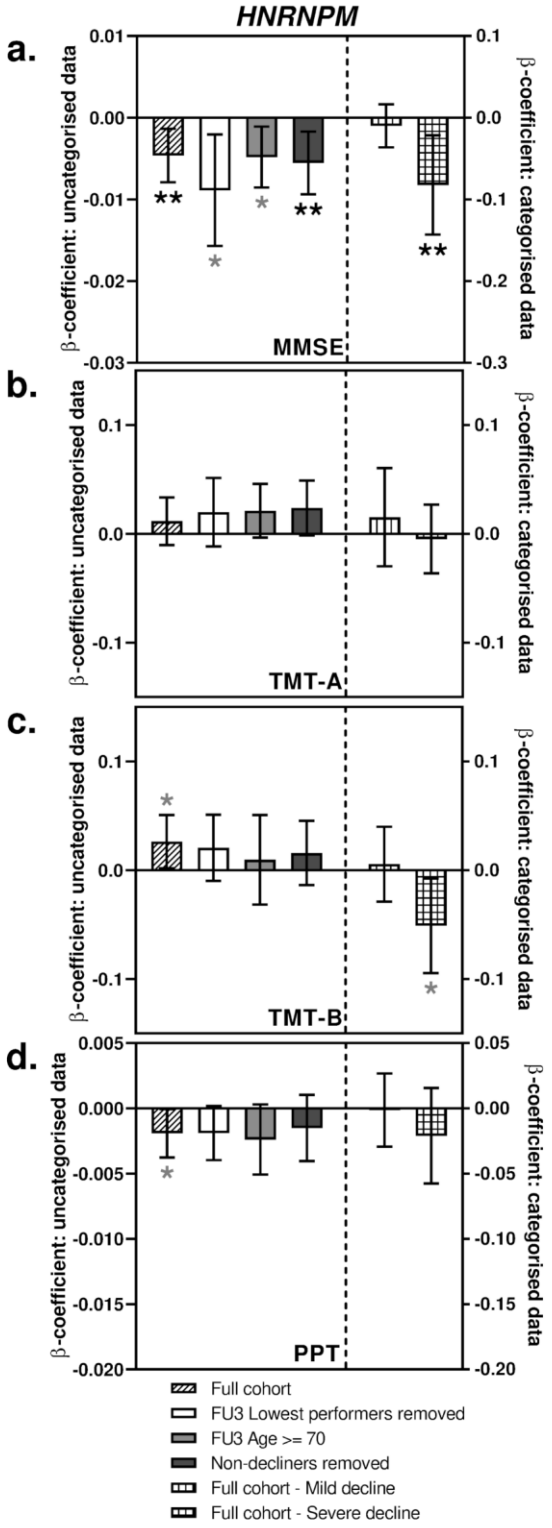

Figure 6.4: Sub-analyses of *HNRNPM* associations with measures of cognitive function

Bar charts showing the associations between expression of *HNRNPM* and change in performance in tests of cognitive function. Panel (a.) shows associations with MMSE score, panel (b.) shows associations with TMT-A, panel (c.) shows associations with TMT-B and panel (d.) shows associations with PPT. Different sub-analyses are plotted separately as indicated in the figure legend. Error bars denote 95% confidence intervals, significance is shown using stars as follows: * = $p<0.05$, ** = $p<0.01$. Stars indicated in black denote associations which meet multiple testing thresholds, while those in grey represent nominal associations

6.6.3 Expression of AKAP17A transcript is associated with mean hand-grip strength

Hand-grip strength, a measure of muscle weakness, is a useful indicator of physical functioning and health-related quality of life in the elderly[294]. Of the transcripts tested, only *AKAP17A* transcript levels were nominally associated with decline in hand-grip strength between FU3 and FU4 (β-coefficient -0.006, p = 0.023) (Figure 6.1, Supplementary table S33). As shown in Figure 6.5a (Supplementary table S34), robustness testing of this finding revealed one nominal and one significant association in the sub-analyses, and no associations with the categorised data.

6.6.4 Expression of AKAP17A transcript is also associated with two other measures of physical ability

The Epidemiologic Studies of the Elderly – Short Physical Performance Battery (EPESE-SPPB) is a validated measure of lower body function and is predictive of several important health outcomes, including mortality[295]. *AKAP17A* expression was found to be nominally associated with decline in the EPESE-SPPB composite score (β-coefficient -0.011, p = 0.048), and as can be seen in Figure 6.5b (Supplementary table S35), subsequent testing showed it also to be nominally associated in two of the sub-analyses.

Another measure of physical ability that was available in the data set was the calculated speed (m/s) during a timed 400m fast walking test. Once again, *AKAP17A* expression was found to be nominally associated with decline in walking speed (β-coefficient -0.252, p = 0.013). Figure 6.5c (Supplementary table S35) shows that this nominal association only held true in one sub-analysis.

Finally, Pearson correlations were carried out to assess relationships between the aspects of physical ability being measured. Again, correlations between the measures were relatively weak (R values range from 0.217 to 0.357, see Supplementary table S32b).

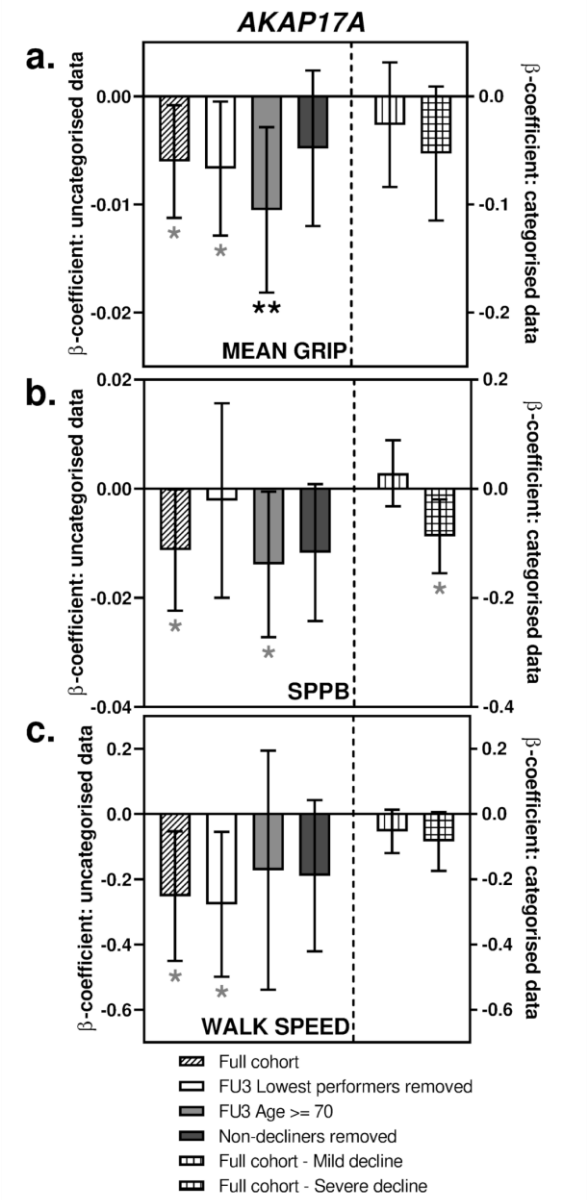

Figure 6.5: Sub-analyses of *AKAP17A* associations with measures of physical ability

Bar charts showing the associations between expression of *AKAP17A* and change in performance in tests of physical ability. Panel (a.) shows associations with mean hand-grip strength, panel (b.) shows associations with the EPESE-SPPB composite score and panel (c.) shows associations with calculated speed (m/s) during a 400m fast walking test. Different sub-analyses are plotted separately as indicated in the figure legend. Error bars denote 95% confidence intervals, significance is shown using stars as follows: * = p<0.05, ** = p<0.01. Stars indicated in black denote associations which meet multiple testing thresholds, while those in grey represent nominal associations

6.6.5 HNRNPA0, HNRNPM and AKAP17A transcripts show correlations with known biomarkers of ageing

To test whether these transcripts might share expression patterns with levels of recognised biomarkers of ageing[296], where such measures were available in our dataset, we carried out Pearson correlations between transcript expression levels and measurements of interleukin-6 (IL-6), albumin and total erythrocyte numbers. Significant correlations were found between: *AKAP17A* expression and IL-6 levels (R value = 0.144, p = 0.013); *HNRNPA0* expression and both IL-6 and erythrocyte number (R values = -0.200 and 0.115, p = 0.001 and 0.048 respectively); *HNRNPM* expression and albumin levels (R value = -0.137, p = 0.018).

6.7 Discussion

The human genome is equipped with mechanisms to generate transcriptomic diversity from a relatively small DNA complement[130]. This transcriptomic diversity underpins our ability to respond appropriately to internal and external environmental challenges, while the failure of such cellular stress responses contributes to ageing itself and to age-related diseases[110]. Alternative splicing is one of the major mechanisms for generation of such diversity[268], and is regulated by the combinatorial binding of a set of trans-acting activating and inhibitory proteins termed splicing factors to *cis*- sequence control elements[126]. Dysregulation of splicing factor expression occurs with human ageing at the epidemiological and cellular levels [101,103], and is also associated with longevity in animal models [104]. These changes are drivers of cellular ageing, since restoration of splicing factor levels is able to reverse multiple senescence phenotypes in aged human cells *in vitro* [107,269,270]. In the work described here, we provide

evidence that changes in splicing factor expression are not only present in *in vitro* data, but may also contribute to the development of downstream ageing phenotypes in older people. We report predictive associations between the transcript expression levels of three splicing factor genes, *HNRNPM*, *HNRNPA0* and *AKAP17A* with ageing phenotypes in a human population study, the InCHIANTI study of Aging[163].

HNRNPM, *HNRNPA0* and *AKAP17A* transcript levels were predictively associated with a decline in MMSE score as well as a decline in performance on the Trail-Making Test parts A & B and the Purdue Pegboard Test. Associations between transcript expression of all 3 genes and ageing phenotypes were strongest in the individuals with severe cognitive decline as measured by MMSE. It is possible that these three splicing factors are not independently associated with the traits in question, but correlations between them are only moderate. *HNRNPM* and *HNRNPA0* encode splicing inhibitor proteins that have roles in determining the splicing patterns of several genes with relevance to brain physiology. TDP-43 is one of the major proteins involved with Amyotrophic lateral sclerosis (ALS) and Frontotemporal Dementia (FTD) in humans[297]. HNRNPM and HNRNPA0 are both known to interact with TDP-43[298], and mutations in other HNRNPs have been described in patients with ALS[299]. In *Drosophila* species, depletion of the fly homologue of *HNRNPM* (*Rump*) is associated with loss of neuronal dendritic terminal branches; a phenotype that could be partially restored by the addition of a Rump transgene[300]. HNRNPM has also been demonstrated to directly regulate alternative splicing of the dopamine receptor 2 (*DRD2*) gene, whereby it inhibits the inclusion of exon 6[301]. *DRD2* splice variants have previously been implicated with schizophrenia and impaired cognitive function in humans[302,303]. Similarly, increased protein expression of Hnrnpa0 in

hippocampus has been shown to be associated with memory formation and consolidation in mice[304]. *AKAP17A*, otherwise known as *SFSR17A*, is an X-linked gene encoding a splicing regulatory factor that also has roles in targeting protein kinase A anchoring protein to splicing factor compartments[305]. It is a poorly characterised gene, but has been previously associated with the development of Alzheimer's disease; sequences deriving from this gene appear twice amongst probes that best differentiate Alzheimer's disease brain samples from controls[306].

AKAP17A was also found to be associated with decline over time in measures of physical function, although the sporadic nature of replication of this association in the sub-analyses suggests that either this finding is less robust, or the measurements themselves are more subject to variation. No functional role for *AKAP17A* has previously been reported in relation to muscle function.

Although the changes reported here represent changes in peripheral blood, similar changes to splicing regulation have been reported in senescent cell lines from other, less accessible tissues[107,108]. Splicing factor expression is ubiquitous, although changes in the exact composition of the splicing factor milieu will occur from tissue to tissue. We postulate that the expression patterns of splicing factors in peripheral blood may at least partly reflect changes in less accessible tissues. We previously demonstrated that senescence-related changes in splicing factor expression in endothelial cells and cardiomyocytes are preserved in human peripheral blood, and resultant changes in the alternative splicing of the *VEGFA* gene are associated with incident and prevalent coronary artery disease[108]. Both cognitive decline and deterioration in muscle strength also have a significant inflammatory component[208,307].

Our study has several strengths; the use of a longitudinal population study has allowed some assessment of causality of effect. Placed in the context of the known dysregulation of splicing factor expression in human and animal ageing, their associations with longevity in both animals and humans[67,104] and the observation that correction of splicing factor levels is sufficient to reverse senescence phenotypes *in vitro*[107] suggests that these changes may be a driver of ageing rather than an effect. The data presented here suggest that the presence of dysregulated splicing factor transcripts before the emergence of overt disease in peripheral blood may contribute to the development of age-related phenotypes such as cognitive decline. Our finding that expression of these transcripts correlate with established biomarkers of ageing is also suggestive that they may be indicative of future outcomes. Our study is not without limitations however; we have only assessed splicing factor expression at the level of the mRNA transcript for reasons of practicality. It is possible that processes such as post-transcriptional regulation of mRNA transcripts or altered protein kinetics may also contribute and would not be identified in our study. However, the observation of phenotypic changes in senescent cells *in vitro* strongly suggests that these changes may also occur at the protein level. Our study cohort is also relatively small in comparison to some resources. It is however exquisitely well characterised and features longitudinal waves of samples which many other studies do not. These observations require replication in an additional dataset in the future. However, we have measures from two waves of the study, which although they comprise the same people, represent completely separate sample collection, sample handling and analytical subsets.

We recognise that although an adjustment for multiple testing has been applied at the level of phenotype (i.e. accounting for 6 measurements) throughout this

study, there remains a risk of Type I error in the results presented by using a significance level of p=0.0083 as the corrected threshold. However, the genes tested represented an *a priori* list on the basis of known associations with age or cellular senescence[101,103], and we show here that although moderate, correlations do exist between splicing factor expression levels as well as between the measured phenotypic outcomes (Supplementary tables S30 & S32), all of which complicate a sensible implementation of multiple testing criteria. It is also possible that the statistical power of this study may be limited given the number of samples and the observed effect sizes, leading to potential inflation of Type II error. Therefore, either Bonferroni or Benjamini-Hochberg correction for both the number of genes and phenotypes seem likely to be overly stringent for this dataset, however the issue of multiple testing persists, so without independent validation of the findings presented here, we must be conservative with any interpretation of these results.

We present here evidence to suggest that expression levels of *HNRNPM*, *HNRNPA0* and *AKAP17A* genes may be associated with cognitive decline, whilst *AKAP17A* levels may be associated with decline in physical performance in a human population. These findings suggest that the age-related splicing factor changes we have previously reported *in vitro* and *in vivo* may contribute to the development of downstream ageing phenotypes in older humans. Given validation of these findings in an independent data set, splicing factor expression could comprise a relatively non-invasive biomarker of cognitive decline or physical ability in the future, which could be assessed from samples collected from routine screening of the vulnerable people in the population.

6.8 Acknowledgements

The authors acknowledge the technical assistance of Federica Bighi and Robert Morse for help with the RNA extractions. We are also grateful to Eleonora Talluri for collection of RNA samples and anthropometric/clinical data. This work was funded by the Velux Stiftung Foundation (grant number 822) and supported in part by the Intramural Research Program of the NIH, National institute on Aging. The authors declare no competing interests.

6.9 Ethical approval and informed consent

Ethical approval was granted by the Instituto Nazionale Riposo e Cura Anziani institutional review board in Italy. Methods were carried out in accordance with the relevant guidelines and regulations. Informed consent was obtained from all participants.

Chapter 7

Discussion

7.1 Summary of thesis

Current demographic trends predict that the elderly will make up an ever-increasing proportion of the world's population, and that dependency ratios will increase because of this. Advancing age is known to be the largest risk factor for most chronic diseases, therefore the progressive ageing of the population will bring increased incidence of morbidities and the associated socio-economic impact.

Ageing is a complex and heterogeneous process with a host of potential pathways contributing to the process. Understanding the interplay between these mechanisms and their regulation will be essential to the development of strategies aimed at increasing healthspan and alleviating the negative effects of age-related disease.

I have investigated the role of RNA regulatory processes in ageing and lifespan, both in model organisms and in humans, to provide some insight into the ways in which this regulation could be involved in the development of the ageing phenotype and determination of lifespan/healthspan.

7.2 Summary of data chapters

7.2.1 Chapter 3: Changes in the expression of splicing factor transcripts and variations in alternative splicing are associated with lifespan in mice and humans.

Summary

In chapter 3, I investigated the relationship of splicing factor transcript expression and alternatively expressed isoforms with age and strain lifespan in mice. The mouse husbandry and determination of median strain lifespan were carried out

by collaborators at the Jackson laboratory Nathan Shock Centre of Excellence in the Basic Biology of Aging, who provided flash-frozen tissue for RNA extractions. We were supplied with spleen and quadriceps muscle samples from both young (6 month old) and old (20-22 month old) animals from six strains with varying median lifespan (range: 623 days to 1005 days). I measured expression levels of splicing factors and alternative isoforms using qRT-PCR on custom Taqman™ Low Density Arrays (TLDA) and tested this data for associations with age and median strain lifespan.

It was found that several splicing factors were associated with both age and strain lifespan, in a highly tissue-specific manner. Importantly, these expression differences were apparent in young animals of the long-lived strains, suggesting that splicing factors may represent a determinant of lifespan. It was also shown that shifts in isoform expression seemed to be indicative of reduced cellular senescence and pro-inflammatory signalling in long-lived strains, potentially contributing to the longevity phenotype.

The splicing factors that had shown significant results in the mouse work were then tested in pre-existing microarray-based gene expression data from a human cohort, to assess whether they were associated with parental longevity score (as a proxy measure for longevity[188]). Two of the splicing factors also showed associations in humans, strengthening the case that splicing factors are central to the pathways involved in mammalian ageing.

Limitations to this chapter were the relatively small number of animals available for testing from each strain, and the fact that splicing patterns were only assessed at the level of mRNA expression.

Importance of findings

To my knowledge, this work represented the first reported indication that regulation of alternative splicing may be involved in determination of longevity in mammals. Shortly after publication of this work, Will Mair's lab at Harvard published a study showing that the splicing factor SF1 modulates longevity in *C. elegans*[67], further strengthening our argument.

Future work

To address the limitations of this study, it would be advantageous to extend the current experiments to include a larger sample size, a greater number of tissues, as well as analysis of splicing patterns at the level of protein synthesis.

Further *in vitro* and *in vivo* experiments could also be performed to establish causality and mechanism in terms of the role of splicing factors in determining lifespan. These could take the form of manipulation of splicing factor expression in cell culture and/or conditional knockout studies in model organisms.

7.2.2 Chapter 4: MicroRNAs miR-203-3p, miR-664-3p and miR-708-5p are associated with median strain lifespan in mice.

Summary

In chapter 4, I examined the relationship between miRNA expression levels and median strain lifespan in mice. The spleen tissue used was from the same collection of six strains (and two ages) as used in chapter 3 (see section 7.2.1). I measured near-global miRNA expression in a subset of samples using a high-throughput qRT-PCR approach, followed by a targeted validation step in all

available samples. Expression levels of three miRNAs were found to be robustly associated with strain lifespan by this method.

Pathway analysis was carried out for these three miRNAs and target genes from several of the predicted target pathways were chosen for further analysis. I then measured expression levels of the mRNAs of the chosen genes and tested for associations of these with lifespan. Almost all of the genes in question also proved to show expression levels associated with lifespan, suggesting that these miRNAs are having some functional effect in the determination of lifespan.

Limitations to this chapter were the relatively small number of animals available for testing from each strain, the use of a single tissue for analysis and the potential for cell-type variations due to the plastic nature of splenic tissue.

Importance of findings

While miRNAs had already been implicated in lifespan regulation of *C. elegans* and *Drosophila* prior to this work, only a very small number of miRNAs were known to have roles in longevity in mice, and these had usually been discovered in a single strain. This study represents a screen of six independent strains and has found associations of miRNAs with lifespan that had not previously been described. These findings add to the evidence suggesting that RNA regulation of gene expression is important in determining lifespan.

Future work

Similar to chapter 3, to address the limitations of this study it would be advantageous to extend the current experiments to include a larger sample size and a greater number of tissues.

To assess the importance of these miRNAs in the ageing process, further experiments using miRNA mimics or antagomirs could be carried out, either *in vitro* using primary cells - measuring cellular senescence as an output, or in model organisms to determine whether any effects on lifespan could be detected *in vivo*.

7.2.3 Chapter 5: Dietary restriction in ILSXISS mice is associated with widespread changes in splicing regulatory factor expression levels.

Summary

In chapter 5, I investigated the relationship between splicing factor expression and strain lifespan response to dietary restriction (DR) in mice. The mouse husbandry was carried out by collaborators at the Institute of Biodiversity Animal Health & Comparative Medicine at the University of Glasgow, who provided flash-frozen tissue for RNA extractions. We were supplied with brain, heart and kidney tissues from three strains of mice known to show differing lifespan responses to DR treatment. Tissues were taken from a set of animals allowed *ad libitum* (AL) feeding and a second set kept under 40% DR conditions, for two separate lengths of treatment; two months and ten months. I measured splicing factor transcript expression levels in all of these samples and tested for associations with DR in short- and long-term treatments, as well as associations with strain response.

Three distinct groups of associations were found:

1. Splicing factors associated with DR only
2. Splicing factors associated with strain only
3. Splicing factors associated with both DR and strain

The third group represent splicing factors which could be involved in the mechanisms determining strain-specific lifespan response to DR. The associations found were both tissue- and duration-specific.

Limitations to this chapter were the fact that only levels of splicing factors were measured, and not alternatively spliced isoforms or protein.

Importance of findings

At the time of publication of this chapter, post-transcriptional RNA processing and alternative splicing had previously been linked to ageing and lifespan in model organisms[308], and the aforementioned publication from the Mair lab[67] (see section 7.2.1) had shown that a splicing factor was directly involved in the lifespan extension seen under DR in *C. elegans*. However, to my knowledge this is the first study to examine the role of splicing factors during DR in multiple tissues from mice displaying variable lifespan response to the treatment and therefore able to offer mechanistic insights into the role of splicing in determination of lifespan in a mammalian system.

Future work

To address the limitations of this study, it would be useful to assess splicing factor expression at the protein level, and to test expression levels of alternatively spliced isoform transcripts. Considering the shifts seen in splicing factors, it is likely that changes would be apparent in isoform expression of alternatively spliced genes. It would therefore be highly informative to obtain transcriptome-wide isoform level data from these samples to determine which transcripts are showing isoform ratio shifts in the different responder strains. If candidate genes were revealed by such work, it would also be interesting to deliver splice-

switching oligos into model organisms, in a tissue-specific manner, to assess potential non-autonomous effects on longevity from isoform shifts of key genes in different tissues.

7.2.4 Chapter 6: The transcript expression levels of HNRNPM, HNRNPA0 and AKAP17A splicing factors may be predictively associated with ageing phenotypes in human peripheral blood.

Summary

In chapter 6, I examined the relationship between splicing factor expression and a set of measures of two human ageing phenotypes; cognitive decline and reduced physical ability. Peripheral blood samples and detailed anthropometric data were collected from participants by collaborators involved in the InCHIANTI study of Aging, a longitudinal population study of human ageing in the Chianti region of Italy[163] which has been running since 1998. We were supplied with blood samples and data from two of the follow-up visits in the study. I measured splicing factor transcript expression levels in the blood samples from the earlier time-point and tested for associations with decline in measures of cognitive function and physical ability.

Expression levels of three splicing factors were found to predict change in cognitive performance, and one of these also predicted change in physical performance. Correlations were also found between expression levels of these three splicing factors and established biomarkers of ageing. These findings further reinforce the idea that splicing factors are central to the ageing process and also provide evidence that altered regulation of alternative splicing may be a driver in the development of ageing phenotypes.

Limitations to this chapter were that our findings were based on a single human cohort, also that measurements were only carried out for splicing factors at the mRNA level, and not alternatively spliced isoforms or protein.

Importance of findings

To my knowledge, this is the first report of a link between the expression of splicing regulatory factors and future health outcomes in a human population. The fact that these splicing factors display altered expression levels before overt changes in phenotype suggests that they may be mechanistically involved in the development of age-related phenotypes, and opens the possibility that they could serve as non-invasive biomarkers of declining health.

Future work

To address the limitations of this chapter, it would be desirable to find a separate longitudinal cohort study of ageing with RNA samples and similarly detailed anthropometric data available at multiple time-points in order to validate these findings. It would also be useful to assess splicing factor expression at the protein level. Measurements of isoform expression levels of alternatively spliced genes in these samples could add further valuable insights into mechanisms underlying development of age-related phenotypes.

7.3 Discussion of thesis

This thesis investigates the ways in which aspects of RNA regulation contribute to the ageing process and determination of lifespan in mammals. To achieve this, I have used two different murine models and a human cohort to identify associations and patterns of change in expression levels of splicing factor transcripts, miRNAs and alternatively expressed mRNAs. In the first mouse

model, I assessed the role of splicing factors, alternative splicing and miRNAs in normal ageing and with strain lifespan. In the second mouse model, I considered splicing factors under DR conditions, a well-known modifier of lifespan. In the human cohort, I validated findings from the first mouse model as well as assessing splicing factors as predictive markers of future health outcomes.

Through this work I have shown that splicing factors are associated with lifespan in mice, and with parental longevity score in human peripheral blood. I then showed that alternatively spliced isoforms of key age-related genes are expressed differently according to mouse strain lifespan. Given that some of these associations were found in the young mice, further investigation into potential age/lifespan interactions suggested that these expression patterns could be determinants of longevity. Following on from this, I showed that three specific miRNAs are robustly longevity-associated in these mice. *In silico* pathway analysis of the predicted gene targets of these microRNAs implicated signalling cascades known to be involved in ageing, and expression levels of selected mRNA transcripts from these pathways were also shown to associate with strain lifespan, suggesting that the three miRNAs are affecting the determination of lifespan through modulation of gene expression levels in important age-related pathways. Once again, the presence of these associations in young mice and subsequent interaction analyses suggested that these effects could be determining lifespan.

I then showed that splicing factor transcripts are associated with variable lifespan response in tissues taken from mice housed under 40% DR conditions. Expression patterns were highly tissue-specific and showed distinct differences with short- and long-term DR exposure. Interaction analyses between strain

response and DR status revealed that splicing factor expression may have a mechanistic involvement in determining lifespan response and perhaps suggests a splicing-driven homeostatic adaptation to DR conditions.

Finally, I showed that expression levels of three splicing factor transcripts were predictively associated with future declines in several different measures of cognitive and physical ability in a human cohort, indicating that patterns of mRNA splicing regulation may create conditions which determine healthspan and/or lifespan.

Disrupted splicing is a feature of many human diseases[309-311], and several age-related disorders are known to be directly caused by altered splicing patterns[312,313], for example:

- Mutations in the *ABCR* gene have been shown to disrupt splice sites, resulting in age-related macular degeneration[314-316].
- Retention of intronic sequences in the *ENG* and *ANKRD1* genes cause vascular disease[317] and heart disease[318] respectively.
- Alternative splicing of exon 10 in the *MAPT* gene disturbs the 3R-tau:4R-tau protein ratio which in turn causes a set of neurodegenerative diseases collectively known as ‘tauopathies’ including frontotemporal dementia and Alzheimer’s disease[319].
- A panel of genes known to be involved in alternative splicing are also implicated in the onset of amyotrophic lateral sclerosis[320,321].

It is also the case that many of the progeroid syndromes can be caused by splicing defects in key genes. Hutchinson-Gilford Progeria is caused by a mutation in the *LMNA* gene which creates a cryptic splice site in exon 11 and thus produces ‘progerin’, a pathogenic form of the lamin A nuclear envelope protein[322].

Around half of the pathogenic mutations in the *WRN* helicase gene responsible for Werner syndrome are either truncations due to exon skipping or splicing mutations[323]. Branch-point site mutations in the *XPC* gene cause skipping of exon 4, reduced protein levels, and have been associated with pathogenesis of xeroderma pigmentosum[324]. All known Cockayne syndrome subtypes are associated with mutations in either the *ERCC6* or *ERCC8* gene, which include splicing alterations[325]. Finally, ataxia telangiectasia is caused by mutations in the *ATM* gene, which in ≈90% of cases either truncate the transcript or affect splicing[326].

Added to this, many key genes in the age-related signalling pathways are alternatively spliced. In the IIS pathway, the insulin receptor gene (*IR*) is known to produce two alternative splice isoforms; IR-A and IR-B[327], while *IGF-1* produces at least three isoforms, IGF-1Ea, IGF-1Eb and IGF-1Ec, each of which activates IIS in a different manner[328]. The mTOR pathway is known to feature at least 20 alternatively spliced genes, including *mTOR* itself[312]. The tumour suppressor transcription factor p53 is involved in several age-related processes[91] and is also a regulator of the IIS and mTOR pathways[329]. Alternative splicing of p53 produces a truncated isoform (p44 in mice, p47 in humans), increased expression of which shortens healthspan and lifespan in mice[330].

All the above evidence points to a central role for alternative splicing in ageing, lifespan and healthspan. The work that I have presented in this thesis goes a step further and suggests not only that alternative splicing and its regulation are associated with ageing and longevity, but also that there is a strong likelihood that they play a causal role in the determination of lifespan in mammals.

Very large numbers of miRNAs are known to be both correlated with and/or causative of progression of many diseases, both age-related and otherwise[331-335]. A smaller number have also been shown to affect expression of the genes causing the premature ageing phenotypes seen in Hutchinson-Gilford progeria[336] and Werner syndrome[337].

It is also recognised that many miRNAs interact with genes in the signalling pathways involved in ageing and lifespan. A number of miRNAs have been shown to modulate ageing and/or lifespan by targeting genes in the IIS pathway[99], and others are known to target elements of the mTOR pathway[338]. Several of these miRNAs and their functions are also well conserved from invertebrates through to mammals[99], implying a key role in the regulation of these pathways.

A review by Lorna Harries[216] describes 85 miRNAs currently known to be involved in the ageing process, and how these relate to López-Otin's hallmarks of ageing[94]. Interestingly, over 20% of the miRNAs described potentially target genes involved in more than one of the hallmarks, raising the possibility that networks of miRNAs may act in a coordinate fashion to allow fine control over several different aspects of the ageing process at once.

Once again, existing evidence strongly suggests miRNAs play an important role in ageing longevity. The work presented in this thesis strengthens this hypothesis, implicates miRNAs that had not previously been associated with lifespan and indicates that they could be a causal factor in determination of lifespan.

7.4 Conclusion

Regulation of gene expression at the RNA level is clearly an important factor in ageing and determination of lifespan/healthspan. This thesis reinforces the

current knowledge and builds upon it, providing novel insights into the roles of splicing factors, alternative splicing and miRNAs in these processes.

The finding that aspects of the RNA regulatory network show differential patterns of expression in young mice of different strain lifespan, coupled with the discovery that levels of specific splicing factors are predictive of human ageing phenotypes, raises the exciting possibility that direct modulation of RNA regulatory processes could potentially be harnessed to improve human healthspan. Alternatively, elements of the RNA regulatory machinery may have use as biomarkers of future health outcomes, allowing for application of health maintenance interventions at an earlier stage.

This work, along with existing and currently unpublished data, constitute a growing body of evidence underlining the importance of RNA regulation in ageing. Taken together with the fact that López-Otin's criteria have largely been met in terms of defining core mechanisms of ageing, I feel that there may be a case for 'Altered control of gene expression' to be added as a 10th hallmark of ageing.

References

1 United Nations World Population Prospects: The 2017 Revision, DVD Edition. *Department of Economic and Social Affairs, Population Division* (2017).

2 Office of Budget Responsibility. Fiscal Sustainability Report - July 2018. *Available: https://obr.uk/fsr/fiscal-sustainability-report-july-2018/* (2018).

3 Niccoli, T. & Partridge, L. Ageing as a risk factor for disease. *Curr Biol* **22**, R741-752 (2012).

4 Flatt, T. A New Definition of Aging? *Frontiers in Genetics* **3** (2012).

5 Tacutu, R. *et al.* Human Ageing Genomic Resources: new and updated databases. *Nucleic acids research* **46**, D1083-d1090 (2018).

6 Williams, G. C. Pleiotropy, Natural Selection, and the Evolution of Senescence. *Evolution* **11**, 398-411 (1957).

7 Gavrilov, L. A. & Gavrilova, N. S. Evolutionary theories of aging and longevity. *TheScientificWorldJournal* **2**, 339-356 (2002).

8 Darwin, C. *On the origin of species by means of natural selection, or preservation of favoured races in the struggle for life*. (London : John Murray, 1859, 1859).

9 Kirkwood, T. B. & Cremer, T. Cytogerontology since 1881: a reappraisal of August Weismann and a review of modern progress. *Human genetics* **60**, 101-121 (1982).

10 Reichard, M. Evolutionary perspectives on ageing. *Seminars in cell & developmental biology* **70**, 99-107 (2017).

11 Medawar, P. B. *An unsolved problem of biology*. (Published for the College by H.K. Lewis, 1952).

12 Carter, A. J. & Nguyen, A. Q. Antagonistic pleiotropy as a widespread mechanism for the maintenance of polymorphic disease alleles. *BMC medical genetics* **12**, 160 (2011).

13 Kirkwood, T. B. Evolution of ageing. *Nature* **270**, 301-304 (1977).

14 Kirkwood, T. B. & Holliday, R. The evolution of ageing and longevity. *Proceedings of the Royal Society of London. Series B, Biological sciences* **205**, 531-546 (1979).

15 Hulbert, A. J., Pamplona, R., Buffenstein, R. & Buttemer, W. A. Life and death: metabolic rate, membrane composition, and life span of animals. *Physiological reviews* **87**, 1175-1213 (2007).

16 Pearl, R. *The Rate of Living*. (Alfred A. Knopf, 1928).

17 Lints, F. A. The rate of living theory revisited. *Gerontology* **35**, 36-57 (1989).

18 Harman, D. Aging: a theory based on free radical and radiation chemistry. *Journal of gerontology* **11**, 298-300 (1956).

19 Beckman, K. B. & Ames, B. N. The free radical theory of aging matures. *Physiological reviews* **78**, 547-581 (1998).

20 Gabriela Jimenez, A. "The Same Thing That Makes You Live Can Kill You in the End": Exploring the Effects of Growth Rates and Longevity on Cellular Metabolic Rates and Oxidative Stress in Mammals and Birds. *Integrative and comparative biology* **58**, 544-558 (2018).

21 Bjorksten, J. The crosslinkage theory of aging. *Journal of the American Geriatrics Society* **16**, 408-427 (1968).

22 Bjorksten, J. & Tenhu, H. The crosslinking theory of aging--added evidence. *Experimental gerontology* **25**, 91-95 (1990).

23 Orgel, L. E. The maintenance of the accuracy of protein synthesis and its relevance to ageing. *Proceedings of the National Academy of Sciences of the United States of America* **49**, 517-521 (1963).

24 Orgel, L. E. Ageing of clones of mammalian cells. *Nature* **243**, 441-445 (1973).

25 Krisko, A. & Radman, M. Protein damage, ageing and age-related diseases. *Open biology* **9**, 180249 (2019).

26 Labbadia, J. & Morimoto, R. I. The biology of proteostasis in aging and disease. *Annual review of biochemistry* **84**, 435-464 (2015).

27 Filfan, M. *et al.* Autophagy in aging and disease. *Romanian journal of morphology and embryology = Revue roumaine de morphologie et embryologie* **58**, 27-31 (2017).

28 Bareja, A., Lee, D. E. & White, J. P. Maximizing Longevity and Healthspan: Multiple Approaches All Converging on Autophagy. *Frontiers in cell and developmental biology* **7**, 183 (2019).

29 Failla, G. The aging process and cancerogenesis. *Ann N Y Acad Sci* **71**, 1124-1140 (1958).

30 Szilard, L. ON THE NATURE OF THE AGING PROCESS. *Proceedings of the National Academy of Sciences of the United States of America* **45**, 30-45 (1959).

31 Gensler, H. L. & Bernstein, H. DNA damage as the primary cause of aging. *The Quarterly review of biology* **56**, 279-303 (1981).

32 Vijg, J. & Dolle, M. E. Large genome rearrangements as a primary cause of aging. *Mechanisms of ageing and development* **123**, 907-915 (2002).

33 Hoeijmakers, J. H. DNA damage, aging, and cancer. *The New England journal of medicine* **361**, 1475-1485 (2009).

34 Freitas, A. A. & de Magalhaes, J. P. A review and appraisal of the DNA damage theory of ageing. *Mutation research* **728**, 12-22 (2011).

35 Ou, H. L. & Schumacher, B. DNA damage responses and p53 in the aging process. *Blood* **131**, 488-495 (2018).

36 De Bont, R. & van Larebeke, N. Endogenous DNA damage in humans: a review of quantitative data. *Mutagenesis* **19**, 169-185 (2004).

37 Dolle, M. E. & Vijg, J. Genome dynamics in aging mice. *Genome research* **12**, 1732-1738 (2002).

38 Lu, T. *et al.* Gene regulation and DNA damage in the ageing human brain. *Nature* **429**, 883-891 (2004).

39 Moskalev, A. A. *et al.* The role of DNA damage and repair in aging through the prism of Koch-like criteria. *Ageing research reviews* **12**, 661-684 (2013).

40 Moro, L. Mitochondrial Dysfunction in Aging and Cancer. *Journal of clinical medicine* **8** (2019).

41 Kirkwood, T. B. & Melov, S. On the programmed/non-programmed nature of ageing within the life history. *Curr Biol* **21**, R701-707 (2011).

42 Kowald, A. & Kirkwood, T. B. L. Can aging be programmed? A critical literature review. *Aging cell* **15**, 986-998 (2016).

43 Smith, J. M. Group Selection. *The Quarterly review of biology* **51**, 277-283 (1976).

44 Blagosklonny, M. V. Aging is not programmed: genetic pseudo-program is a shadow of developmental growth. *Cell Cycle* **12**, 3736-3742 (2013).

45 Austad, S. N. Is aging programed? *Aging cell* **3**, 249-251 (2004).

46 Skulachev, V. P. Aging as a particular case of phenoptosis, the programmed death of an organism (a response to Kirkwood and Melov "On the programmed/non-programmed nature of ageing within the life history"). *Aging* **3**, 1120-1123 (2011).

47 Goldsmith, T. C. On the programmed/non-programmed aging controversy. *Biochemistry. Biokhimiia* **77**, 729-732 (2012).

48 de Grey, A. D. Do we have genes that exist to hasten aging? New data, new arguments, but the answer is still no. *Current aging science* **8**, 24-33 (2015).

49 Skulachev, M. V. & Skulachev, V. P. Programmed Aging of Mammals: Proof of Concept and Prospects of Biochemical Approaches for Anti-aging Therapy. *Biochemistry. Biokhimiia* **82**, 1403-1422 (2017).

50 Weinert, B. T. & Timiras, P. S. Invited review: Theories of aging. *Journal of applied physiology (Bethesda, Md. : 1985)* **95**, 1706-1716 (2003).

51 Chahal, H. S. & Drake, W. M. The endocrine system and ageing. *The Journal of pathology* **211**, 173-180 (2007).

52 Chen, T. T., Maevsky, E. I. & Uchitel, M. L. Maintenance of homeostasis in the aging hypothalamus: the central and peripheral roles of succinate. *Frontiers in endocrinology* **6**, 7 (2015).

53 Cutler, R. R. The Law of Deviation of Homeostasis and Diseases of Aging: Vladimir M. Dilman John Wright, PSG Inc., Boston, 1981 380 pp., $39.50 per vol., ISBN 0-88416-250-8. *Archives of Gerontology and Geriatrics* **4**, 187-189 (1985).

54 Meites, J. The neuroendocrine theory of aging and degenerative disease: by Vladimir M. Dilman and Ward Dean, Center for Bio-Gerontology, Pensacola, FL, 1992, ISBN 0-937777-02-1, $65.00 (case); ISBN 0937777-03-X, $50.00 (paper), 138 pp. *Experimental gerontology* **28**, 205-206 (1993).

55 Armbrecht, H. J. The biology of aging. *The Journal of Laboratory and Clinical Medicine* **138**, 220-225 (2001).

56 Jones, C. M. & Boelaert, K. The Endocrinology of Ageing: A Mini-Review. *Gerontology* **61**, 291-300 (2015).

57 van Heemst, D. Insulin, IGF-1 and longevity. *Aging and disease* **1**, 147-157 (2010).

58 Pan, H. & Finkel, T. Key proteins and pathways that regulate lifespan. *The Journal of biological chemistry* **292**, 6452-6460 (2017).

59 Kenyon, C., Chang, J., Gensch, E., Rudner, A. & Tabtiang, R. A C. elegans mutant that lives twice as long as wild type. *Nature* **366**, 461-464 (1993).

60 Tatar, M. *et al.* A mutant Drosophila insulin receptor homolog that extends life-span and impairs neuroendocrine function. *Science* **292**, 107-110 (2001).

61 Bluher, M., Kahn, B. B. & Kahn, C. R. Extended longevity in mice lacking the insulin receptor in adipose tissue. *Science* **299**, 572-574 (2003).

62 Holzenberger, M. *et al.* IGF-1 receptor regulates lifespan and resistance to oxidative stress in mice. *Nature* **421**, 182-187 (2003).

63 Brown-Borg, H. M., Borg, K. E., Meliska, C. J. & Bartke, A. Dwarf mice and the ageing process. *Nature* **384**, 33 (1996).

64 Johnson, S. C., Rabinovitch, P. S. & Kaeberlein, M. mTOR is a key modulator of ageing and age-related disease. *Nature* **493**, 338-345 (2013).

65 Saxton, R. A. & Sabatini, D. M. mTOR Signaling in Growth, Metabolism, and Disease. *Cell* **168**, 960-976 (2017).

66 Vellai, T. *et al.* Genetics: influence of TOR kinase on lifespan in C. elegans. *Nature* **426**, 620 (2003).

67 Heintz, C. *et al.* Splicing factor 1 modulates dietary restriction and TORC1 pathway longevity in C. elegans. *Nature* **541**, 102-106 (2017).

68 Papadopoli, D. *et al.* mTOR as a central regulator of lifespan and aging. *F1000Res* **8** (2019).

69 Montecino-Rodriguez, E., Berent-Maoz, B. & Dorshkind, K. Causes, consequences, and reversal of immune system aging. *The Journal of clinical investigation* **123**, 958-965 (2013).

70 Weyand, C. M. & Goronzy, J. J. Aging of the Immune System. Mechanisms and Therapeutic Targets. *Annals of the American Thoracic Society* **13 Suppl 5**, S422-s428 (2016).

71 Fulop, T. *et al.* Immunosenescence and Inflamm-Aging As Two Sides of the Same Coin: Friends or Foes? *Frontiers in immunology* **8**, 1960 (2017).

72 Franceschi, C. *et al.* Inflamm-aging. An evolutionary perspective on immunosenescence. *Ann N Y Acad Sci* **908**, 244-254 (2000).

73 Fulop, T., Dupuis, G., Witkowski, J. M. & Larbi, A. The Role of Immunosenescence in the Development of Age-Related Diseases. *Revista de investigacion clinica; organo del Hospital de Enfermedades de la Nutricion* **68**, 84-91 (2016).

74 van Deursen, J. M. The role of senescent cells in ageing. *Nature* **509**, 439-446 (2014).

75 Munoz-Espin, D. & Serrano, M. Cellular senescence: from physiology to pathology. *Nature reviews. Molecular cell biology* **15**, 482-496 (2014).

76 Hayflick, L. & Moorhead, P. S. The serial cultivation of human diploid cell strains. *Experimental cell research* **25**, 585-621 (1961).

77 de Magalhaes, J. P. & Passos, J. F. Stress, cell senescence and organismal ageing. *Mechanisms of ageing and development* **170**, 2-9 (2018).

78 Coppe, J. P. *et al.* Senescence-associated secretory phenotypes reveal cell-nonautonomous functions of oncogenic RAS and the p53 tumor suppressor. *PLoS biology* **6**, 2853-2868 (2008).

79 Acosta, J. C. *et al.* A complex secretory program orchestrated by the inflammasome controls paracrine senescence. *Nature cell biology* **15**, 978-990 (2013).

80 Sikora, E., Bielak-Zmijewska, A. & Mosieniak, G. Cellular senescence in ageing, age-related disease and longevity. *Current vascular pharmacology* **12**, 698-706 (2014).

81 Baker, D. J. *et al.* Clearance of p16Ink4a-positive senescent cells delays ageing-associated disorders. *Nature* **479**, 232-236 (2011).

82 Baker, D. J. *et al.* Naturally occurring p16(Ink4a)-positive cells shorten healthy lifespan. *Nature* **530**, 184-189 (2016).

83 Campisi, J. Aging, cellular senescence, and cancer. *Annual review of physiology* **75**, 685-705 (2013).

84 Schafer, M. J. *et al.* Cellular senescence mediates fibrotic pulmonary disease. *Nat Commun* **8**, 14532 (2017).

85 Hayflick, L. THE LIMITED IN VITRO LIFETIME OF HUMAN DIPLOID CELL STRAINS. *Experimental cell research* **37**, 614-636 (1965).

86 Harley, C. B., Futcher, A. B. & Greider, C. W. Telomeres shorten during ageing of human fibroblasts. *Nature* **345**, 458-460 (1990).

87 d'Adda di Fagagna, F. *et al.* A DNA damage checkpoint response in telomere-initiated senescence. *Nature* **426**, 194-198 (2003).

88 Blackburn, E. H. Structure and function of telomeres. *Nature* **350**, 569-573 (1991).

89 Wright, W. E., Piatyszek, M. A., Rainey, W. E., Byrd, W. & Shay, J. W. Telomerase activity in human germline and embryonic tissues and cells. *Developmental genetics* **18**, 173-179 (1996).

90 Pawlikowski, J. S., Adams, P. D. & Nelson, D. M. Senescence at a glance. *Journal of cell science* **126**, 4061 (2013).

91 Rufini, A., Tucci, P., Celardo, I. & Melino, G. Senescence and aging: the critical roles of p53. *Oncogene* **32**, 5129-5143 (2013).

92 Xu, Y., Li, N., Xiang, R. & Sun, P. Emerging roles of the p38 MAPK and PI3K/AKT/mTOR pathways in oncogene-induced senescence. *Trends in biochemical sciences* **39**, 268-276 (2014).

93 Aravinthan, A. Cellular senescence: a hitchhiker's guide. *Human cell* **28**, 51-64 (2015).

94 Lopez-Otin, C., Blasco, M. A., Partridge, L., Serrano, M. & Kroemer, G. The hallmarks of aging. *Cell* **153**, 1194-1217 (2013).

95 Jin, C. *et al.* Histone demethylase UTX-1 regulates C. elegans life span by targeting the insulin/IGF-1 signaling pathway. *Cell Metab* **14**, 161-172 (2011).

96 Horvath, S. DNA methylation age of human tissues and cell types. *Genome biology* **14**, R115 (2013).

97 Horvath, S. & Raj, K. DNA methylation-based biomarkers and the epigenetic clock theory of ageing. *Nature reviews. Genetics* **19**, 371-384 (2018).

98 Yang, Z. *et al.* Correlation of an epigenetic mitotic clock with cancer risk. *Genome biology* **17**, 205 (2016).

99 Kinser, H. E. & Pincus, Z. MicroRNAs as modulators of longevity and the aging process. *Human genetics* (2019).

100 Lee, B. P. *et al.* MicroRNAs miR-203-3p, miR-664-3p and miR-708-5p are associated with median strain lifespan in mice. *Scientific reports* **7**, 44620 (2017).

101 Harries, L. W. *et al.* Human aging is characterized by focused changes in gene expression and deregulation of alternative splicing. *Aging cell* **10**, 868-878 (2011).

102 Harries, L. W. *et al.* Advancing age is associated with gene expression changes resembling mTOR inhibition: evidence from two human populations. *Mechanisms of ageing and development* **133**, 556-562 (2012).

103 Holly, A. C. *et al.* Changes in splicing factor expression are associated with advancing age in man. *Mechanisms of ageing and development* **134**, 356-366 (2013).

104 Lee, B. P. *et al.* Changes in the expression of splicing factor transcripts and variations in alternative splicing are associated with lifespan in mice and humans. *Aging cell* **15**, 903-913 (2016).

105 Lee, B. P. *et al.* Dietary restriction in ILSXISS mice is associated with widespread changes in splicing regulatory factor expression levels. *Experimental gerontology*, 110736 (2019).

106 Lee, B. P. *et al.* The transcript expression levels of HNRNPM, HNRNPA0 and AKAP17A splicing factors may be predictively associated with ageing phenotypes in human peripheral blood. *Biogerontology* (2019).

107 Latorre, E. *et al.* Small molecule modulation of splicing factor expression is associated with rescue from cellular senescence. *BMC Cell Biol* **18**, 31 (2017).

108 Latorre, E. *et al.* The VEGFA156b isoform is dysregulated in senescent endothelial cells and may be associated with prevalent and incident coronary heart disease. *Clinical science (London, England : 1979)* **132**, 313-325 (2018).

109 de Nadal, E., Ammerer, G. & Posas, F. Controlling gene expression in response to stress. *Nature reviews. Genetics* **12**, 833-845 (2011).

110 Kourtis, N. & Tavernarakis, N. Cellular stress response pathways and ageing: intricate molecular relationships. *The EMBO journal* **30**, 2520-2531 (2011).

111 Lai, R. W. *et al.* Multi-level remodeling of transcriptional landscapes in aging and longevity. *BMB reports* **52**, 86-108 (2019).

112 Lawrence, M., Daujat, S. & Schneider, R. Lateral Thinking: How Histone Modifications Regulate Gene Expression. *Trends in genetics : TIG* **32**, 42-56 (2016).

113 Jiang, C. & Pugh, B. F. Nucleosome positioning and gene regulation: advances through genomics. *Nature reviews. Genetics* **10**, 161-172 (2009).

114 Inbar-Feigenberg, M., Choufani, S., Butcher, D. T., Roifman, M. & Weksberg, R. Basic concepts of epigenetics. *Fertility and sterility* **99**, 607-615 (2013).

115 Arechederra, M. *et al.* Hypermethylation of gene body CpG islands predicts high dosage of functional oncogenes in liver cancer. *Nat Commun* **9**, 3164 (2018).

116 Thomas, M. C. & Chiang, C. M. The general transcription machinery and general cofactors. *Critical reviews in biochemistry and molecular biology* **41**, 105-178 (2006).

117 Chen, F. X., Smith, E. R. & Shilatifard, A. Born to run: control of transcription elongation by RNA polymerase II. *Nature reviews. Molecular cell biology* **19**, 464-478 (2018).

118 Levine, M. Transcriptional enhancers in animal development and evolution. *Curr Biol* **20**, R754-763 (2010).

119 Winick-Ng, W. & Rylett, R. J. Into the Fourth Dimension: Dysregulation of Genome Architecture in Aging and Alzheimer's Disease. *Frontiers in molecular neuroscience* **11**, 60 (2018).

120 Harvey, R., Dezi, V., Pizzinga, M. & Willis, A. E. Post-transcriptional control of gene expression following stress: the role of RNA-binding proteins. *Biochemical Society transactions* **45**, 1007-1014 (2017).

121 Mastrangelo, A. M., Marone, D., Laido, G., De Leonardis, A. M. & De Vita, P. Alternative splicing: enhancing ability to cope with stress via transcriptome plasticity. *Plant science : an international journal of experimental plant biology* **185-186**, 40-49 (2012).

122 Galloway, A. & Cowling, V. H. mRNA cap regulation in mammalian cell function and fate. *Biochimica et biophysica acta. Gene regulatory mechanisms* **1862**, 270-279 (2019).

123 Turner, R. E., Pattison, A. D. & Beilharz, T. H. Alternative polyadenylation in the regulation and dysregulation of gene expression. *Seminars in cell & developmental biology* **75**, 61-69 (2018).

124 Will, C. L. & Luhrmann, R. Spliceosome structure and function. *Cold Spring Harb Perspect Biol* **3** (2011).

125 Matera, A. G. & Wang, Z. A day in the life of the spliceosome. *Nature reviews. Molecular cell biology* **15**, 108-121 (2014).

126 Smith, C. W. & Valcarcel, J. Alternative pre-mRNA splicing: the logic of combinatorial control. *Trends in biochemical sciences* **25**, 381-388 (2000).

127 Turunen, J. J., Niemela, E. H., Verma, B. & Frilander, M. J. The significant other: splicing by the minor spliceosome. *Wiley interdisciplinary reviews. RNA* **4**, 61-76 (2013).

128 Wu, T. & Fu, X.-D. Genomic functions of U2AF in constitutive and regulated splicing. *RNA biology* **12**, 479-485 (2015).

129 Sun, J. S. & Manley, J. L. A novel U2-U6 snRNA structure is necessary for mammalian mRNA splicing. *Genes & development* **9**, 843-854 (1995).

130 Nilsen, T. W. & Graveley, B. R. Expansion of the eukaryotic proteome by alternative splicing. *Nature* **463**, 457-463 (2010).

131 Wang, Y. *et al.* Mechanism of alternative splicing and its regulation. *Biomedical reports* **3**, 152-158 (2015).

132 Blencowe, B. J. Alternative splicing: new insights from global analyses. *Cell* **126**, 37-47 (2006).

133 Mockenhaupt, S. & Makeyev, E. V. Non-coding functions of alternative pre-mRNA splicing in development. *Seminars in cell & developmental biology* **47-48**, 32-39 (2015).

134 Pervouchine, D. *et al.* Integrative transcriptomic analysis suggests new autoregulatory splicing events coupled with nonsense-mediated mRNA decay. *Nucleic acids research* **47**, 5293-5306 (2019).

135 Wei, J. W., Huang, K., Yang, C. & Kang, C. S. Non-coding RNAs as regulators in epigenetics (Review). *Oncology reports* **37**, 3-9 (2017).

136 Ulitsky, I. & Bartel, D. P. lincRNAs: genomics, evolution, and mechanisms. *Cell* **154**, 26-46 (2013).

137 Wahid, F., Shehzad, A., Khan, T. & Kim, Y. Y. MicroRNAs: synthesis, mechanism, function, and recent clinical trials. *Biochimica et biophysica acta* **1803**, 1231-1243 (2010).

138 Catalanotto, C., Cogoni, C. & Zardo, G. MicroRNA in Control of Gene Expression: An Overview of Nuclear Functions. *International journal of molecular sciences* **17** (2016).

139 Winter, J., Jung, S., Keller, S., Gregory, R. I. & Diederichs, S. Many roads to maturity: microRNA biogenesis pathways and their regulation. *Nature cell biology* **11**, 228-234 (2009).

140 Lim, L. P. *et al.* Microarray analysis shows that some microRNAs downregulate large numbers of target mRNAs. *Nature* **433**, 769-773 (2005).

141 Inukai, S. & Slack, F. MicroRNAs and the genetic network in aging. *Journal of molecular biology* **425**, 3601-3608 (2013).

142 Herodotus. *The history of Herodotus / translated by George Rawlinson ; edited by E. H. Blakeney*. (Dent ; Dutton, 1910).

143 Hamilton, W. D. The moulding of senescence by natural selection. *Journal of theoretical biology* **12**, 12-45 (1966).

144 Rose, M. R., Burke, M. K., Shahrestani, P. & Mueller, L. D. Evolution of ageing since Darwin. *Journal of genetics* **87**, 363-371 (2008).

145 McDonald, R. B. & Ruhe, R. C. Aging and longevity: why knowing the difference is important to nutrition research. *Nutrients* **3**, 274-282 (2011).

146 de Grey, A. D. N. J. Escape Velocity: Why the Prospect of Extreme Human Life Extension Matters Now. *PLoS biology* **2**, e187 (2004).

147 Kaeberlein, M. How healthy is the healthspan concept? *Geroscience* **40**, 361-364 (2018).

148 Crimmins, E. M. Lifespan and Healthspan: Past, Present, and Promise. *The Gerontologist* **55**, 901-911 (2015).

149 Fries, J. F. Aging, natural death, and the compression of morbidity. *The New England journal of medicine* **303**, 130-135 (1980).

150 Hansen, M. & Kennedy, B. K. Does Longer Lifespan Mean Longer Healthspan? *Trends in cell biology* **26**, 565-568 (2016).

151 Butler, R. N. *et al.* New model of health promotion and disease prevention for the 21st century. *BMJ (Clinical research ed.)* **337**, a399 (2008).

152 Gems, D. What is an anti-aging treatment? *Experimental gerontology* **58**, 14-18 (2014).

153 Trounson, A. & McDonald, C. Stem Cell Therapies in Clinical Trials: Progress and Challenges. *Cell stem cell* **17**, 11-22 (2015).

154 Martinez, P. & Blasco, M. A. Telomere-driven diseases and telomere-targeting therapies. *The Journal of cell biology* **216**, 875-887 (2017).

155 Campisi, J. *et al.* From discoveries in ageing research to therapeutics for healthy ageing. *Nature* **571**, 183-192 (2019).

156 Hodgson, R. *et al.* AGING: THERAPEUTICS FOR A HEALTHY FUTURE. *Neuroscience and biobehavioral reviews* (2019).

157 Yuan, R. *et al.* Aging in inbred strains of mice: study design and interim report on median lifespans and circulating IGF1 levels. *Aging cell* **8**, 277-287 (2009).

158 Yuan, R., Peters, L. L. & Paigen, B. Mice as a mammalian model for research on the genetics of aging. *ILAR journal / National Research Council, Institute of Laboratory Animal Resources* **52**, 4-15 (2011).

159 Yuan, R. *et al.* Genetic coregulation of age of female sexual maturation and lifespan through circulating IGF1 among inbred mouse strains. *Proceedings of the National Academy of Sciences of the United States of America* **109**, 8224-8229 (2012).

160 Mulvey, L. *Dissecting out the mechanisms to longevity through eating less.* Doctor of Philosophy thesis, University of Glasgow, (2017).

161 Mulvey, L., Sands, W. A., Salin, K., Carr, A. E. & Selman, C. Disentangling the effect of dietary restriction on mitochondrial function using recombinant inbred mice. *Molecular and cellular endocrinology* **455**, 41-53 (2017).

162 InCHIANTI. *Publications*, <http://inchiantistudy.net/wp/pubblicazioni/> (2014).

163 Ferrucci, L. *et al.* Subsystems contributing to the decline in ability to walk: bridging the gap between epidemiology and geriatric practice in the InCHIANTI study. *Journal of the American Geriatrics Society* **48**, 1618-1625 (2000).

164 InCHIANTI. The Study Design. *Available: www.inchiantistudy.net/wp/lo-studio* (2014).

165 Kim, Y. K., Yeo, J., Kim, B., Ha, M. & Kim, V. N. Short structured RNAs with low GC content are selectively lost during extraction from a small number of cells. *Molecular cell* **46**, 893-895 (2012).

166 Kainz, P. The PCR plateau phase - towards an understanding of its limitations. *Biochimica et biophysica acta* **1494**, 23-27 (2000).

167 Higuchi, R., Fockler, C., Dollinger, G. & Watson, R. Kinetic PCR analysis: real-time monitoring of DNA amplification reactions. *Bio/technology (Nature Publishing Company)* **11**, 1026-1030 (1993).

168 Yuan, C. C., Peterson, R. J., Wang, C. D., Goodsaid, F. & Waters, D. J. 5' Nuclease assays for the loci CCR5-+/Delta32, CCR2-V64I, and SDF1-G801A related to pathogenesis of AIDS. *Clinical chemistry* **46**, 24-30 (2000).

169 Chen, C. *et al.* Real-time quantification of microRNAs by stem-loop RT-PCR. *Nucleic acids research* **33**, e179 (2005).

170 Niesters, H. G. Quantitation of viral load using real-time amplification techniques. *Methods (San Diego, Calif.)* **25**, 419-429 (2001).

171 Pfaffl, M. W. A new mathematical model for relative quantification in real-time RT-PCR. *Nucleic acids research* **29**, e45 (2001).

172 Rutledge, R. G. Sigmoidal curve-fitting redefines quantitative real-time PCR with the prospective of developing automated high-throughput applications. *Nucleic acids research* **32**, e178 (2004).

173 Ghasemi, A. & Zahediasl, S. Normality tests for statistical analysis: a guide for non-statisticians. *International journal of endocrinology and metabolism* **10**, 486-489 (2012).

174 Dunn, O. J. Multiple Comparisons among Means. *Journal of the American Statistical Association* **56**, 52-64 (1961).

175 Benjamini, Y., Krieger, A. M. & Yekutieli, D. Adaptive linear step-up procedures that control the false discovery rate. *Biometrika* **93**, 491-507 (2006).

176 Cartegni, L., Chew, S. L. & Krainer, A. R. Listening to silence and understanding nonsense: exonic mutations that affect splicing. *Nature reviews. Genetics* **3**, 285-298 (2002).

177 Scuderi, S., La Cognata, V., Drago, F., Cavallaro, S. & D'Agata, V. Alternative splicing generates different parkin protein isoforms: evidences in human, rat, and mouse brain. *BioMed research international* **2014**, 690796 (2014).

178 Danan-Gotthold, M. *et al.* Identification of recurrent regulated alternative splicing events across human solid tumors. *Nucleic acids research* **43**, 5130-5144 (2015).

179 Lisowiec, J., Magner, D., Kierzek, E., Lenartowicz, E. & Kierzek, R. Structural determinants for alternative splicing regulation of the MAPT pre-mRNA. *RNA biology* **12**, 330-342 (2015).

180 Lu, Z. X. *et al.* Transcriptome-wide landscape of pre-mRNA alternative splicing associated with metastatic colonization. *Molecular cancer research : MCR* **13**, 305-318 (2015).

181 Barbosa-Morais, N. L., Carmo-Fonseca, M. & Aparicio, S. Systematic genome-wide annotation of spliceosomal proteins reveals differential gene family expansion. *Genome research* **16**, 66-77 (2006).

182 Barbosa-Morais, N. L. *et al.* The evolutionary landscape of alternative splicing in vertebrate species. *Science* **338**, 1587-1593 (2012).

183 Garg, K. & Green, P. Differing patterns of selection in alternative and constitutive splice sites. *Genome research* **17**, 1015-1022 (2007).

184 Dellago, H. *et al.* ATM-dependent phosphorylation of SNEVhPrp19/hPso4 is involved in extending cellular life span and suppression of apoptosis. *Aging* **4**, 290-304 (2012).

185 Swindell, W. R. Genes and gene expression modules associated with caloric restriction and aging in the laboratory mouse. *BMC genomics* **10**, 585 (2009).

186 Glessner, J. T. *et al.* Copy number variations in alternative splicing gene networks impact lifespan. *PloS one* **8**, e53846 (2013).

187 Bogue, M. A. *et al.* Accessing Data Resources in the Mouse Phenome Database for Genetic Analysis of Murine Life Span and Health Span. *The journals of gerontology. Series A, Biological sciences and medical sciences* **71**, 170-177 (2016).

188 Dutta, A. *et al.* Longer lived parents: protective associations with cancer incidence and overall mortality. *The journals of gerontology. Series A, Biological sciences and medical sciences* **68**, 1409-1418 (2013).

189 Lunetta, K. L. *et al.* Genetic correlates of longevity and selected age-related phenotypes: a genome-wide association study in the Framingham Study. *BMC medical genetics* **8 Suppl 1**, S13 (2007).

190 Gautrey, H. *et al.* SRSF3 and hnRNP H1 regulate a splicing hotspot of HER2 in breast cancer cells. *RNA biology* **12**, 1139-1151 (2015).

191 Goncalves, V. & Jordan, P. Posttranscriptional Regulation of Splicing Factor SRSF1 and Its Role in Cancer Cell Biology. *BioMed research international* **2015**, 287048 (2015).

192 Guo, J., Jia, J. & Jia, R. PTBP1 and PTBP2 impaired autoregulation of SRSF3 in cancer cells. *Scientific reports* **5**, 14548 (2015).

193 Franceschi, C. & Campisi, J. Chronic inflammation (inflammaging) and its potential contribution to age-associated diseases. *The journals of gerontology. Series A, Biological sciences and medical sciences* **69 Suppl 1**, S4-9 (2014).

194 Dutta, A. *et al.* Aging children of long-lived parents experience slower cognitive decline. *Alzheimer's & dementia : the journal of the Alzheimer's Association* **10**, S315-322 (2014).

195 Romano, M. *et al.* Evolutionarily conserved heterogeneous nuclear ribonucleoprotein (hnRNP) A/B proteins functionally interact with human and Drosophila TAR DNA-binding protein 43 (TDP-43). *The Journal of biological chemistry* **289**, 7121-7130 (2014).

196 Neumann, M. *et al.* Absence of heterogeneous nuclear ribonucleoproteins and survival motor neuron protein in TDP-43 positive inclusions in frontotemporal lobar degeneration. *Acta neuropathologica* **113**, 543-548 (2007).

197 Kim, H. J. *et al.* Mutations in prion-like domains in hnRNPA2B1 and hnRNPA1 cause multisystem proteinopathy and ALS. *Nature* **495**, 467-473 (2013).

198 Baloh, R. H. TDP-43: the relationship between protein aggregation and neurodegeneration in amyotrophic lateral sclerosis and frontotemporal lobar degeneration. *The FEBS journal* **278**, 3539-3549 (2011).

199 Tominaga, K. The emerging role of senescent cells in tissue homeostasis and pathophysiology. *Pathobiology of aging & age related diseases* **5**, 27743 (2015).

200 Sato, S. *et al.* Ablation of the p16(INK4a) tumour suppressor reverses ageing phenotypes of klotho mice. *Nat Commun* **6**, 7035 (2015).

201 Wu, Y., Huang, H., Miner, Z. & Kulesz-Martin, M. Activities and response to DNA damage of latent and active sequence-specific DNA binding forms of mouse p53. *Proceedings of the National Academy of Sciences of the United States of America* **94**, 8982-8987 (1997).

202 Almog, N., Goldfinger, N. & Rotter, V. p53-dependent apoptosis is regulated by a C-terminally alternatively spliced form of murine p53. *Oncogene* **19**, 3395-3403 (2000).

203 Huang, H. *et al.* Repression of transcription and interference with DNA binding of TATA-binding protein by C-terminal alternatively spliced p53. *Experimental cell research* **279**, 248-259 (2002).

204 Meshorer, E. & Soreq, H. Pre-mRNA splicing modulations in senescence. *Aging cell* **1**, 10-16 (2002).

205 Shilo, A. *et al.* Splicing factor hnRNP A2 activates the Ras-MAPK-ERK pathway by controlling A-Raf splicing in hepatocellular carcinoma development. *Rna* **20**, 505-515 (2014).

206 Slack, C. *et al.* The Ras-Erk-ETS-Signaling Pathway Is a Drug Target for Longevity. *Cell* **162**, 72-83 (2015).

207 Holly, A. C. *et al.* Splicing factor 3B1 hypomethylation is associated with altered SF3B1 transcript expression in older humans. *Mechanisms of ageing and development* **135**, 50-56 (2014).

208 Harries, L. W. *et al.* CCAAT-enhancer-binding protein-beta expression in vivo is associated with muscle strength. *Aging cell* **11**, 262-268 (2012).

209 Blackwell, J. *et al.* Changes in CEBPB expression in circulating leukocytes following eccentric elbow-flexion exercise. *The journal of physiological sciences : JPS* **65**, 145-150 (2015).

210 Livak, K. J. & Schmittgen, T. D. Analysis of relative gene expression data using real-time quantitative PCR and the 2(-Delta Delta C(T)) Method. *Methods (San Diego, Calif.)* **25**, 402-408 (2001).

211 Herskind, A. M. *et al.* The heritability of human longevity: a population-based study of 2872 Danish twin pairs born 1870-1900. *Human genetics* **97**, 319-323 (1996).

212 vB Hjelmborg, J. *et al.* Genetic influence on human lifespan and longevity. *Human genetics* **119**, 312-321 (2006).

213 Ben-Avraham, D. Epigenetics of aging. *Advances in experimental medicine and biology* **847**, 179-191 (2015).

214 Taormina, G. & Mirisola, M. G. Longevity: epigenetic and biomolecular aspects. *Biomolecular concepts* **6**, 105-117 (2015).

215 Gregory, R. I., Chendrimada, T. P., Cooch, N. & Shiekhattar, R. Human RISC couples microRNA biogenesis and posttranscriptional gene silencing. *Cell* **123**, 631-640 (2005).

216 Harries, L. W. MicroRNAs as Mediators of the Ageing Process. *Genes* **5**, 656-670 (2014).

217 Boulias, K. & Horvitz, H. R. The C. elegans microRNA mir-71 acts in neurons to promote germline-mediated longevity through regulation of DAF-16/FOXO. *Cell metabolism* **15**, 439-450 (2012).

218 Pincus, Z., Smith-Vikos, T. & Slack, F. J. MicroRNA Predictors of Longevity in Caenorhabditis elegans. *PLoS genetics* **7**, e1002306 (2011).

219 Vora, M. *et al.* Deletion of microRNA-80 Activates Dietary Restriction to Extend C. elegans Healthspan and Lifespan. *PLoS genetics* **9**, e1003737 (2013).

220 Martins, R., Lithgow, G. J. & Link, W. Long live FOXO: unraveling the role of FOXO proteins in aging and longevity. *Aging cell* **15**, 196-207 (2016).

221 Lamming, D. W. Inhibition of the Mechanistic Target of Rapamycin (mTOR)-Rapamycin and Beyond. *Cold Spring Harbor perspectives in medicine* **6** (2016).

222 Vlachos, I. S. *et al.* DIANA-miRPath v3.0: deciphering microRNA function with experimental support. *Nucleic acids research* **43**, W460-466 (2015).

223 Yi, R., Poy, M. N., Stoffel, M. & Fuchs, E. A skin microRNA promotes differentiation by repressing 'stemness'. *Nature* **452**, 225-229 (2008).

224 Lena, A. M. *et al.* miR-203 represses 'stemness' by repressing DeltaNp63. *Cell death and differentiation* **15**, 1187-1195 (2008).

225 Jackson, S. J. *et al.* Rapid and widespread suppression of self-renewal by microRNA-203 during epidermal differentiation. *Development (Cambridge, England)* **140**, 1882-1891 (2013).

226 Marasa, B. S. *et al.* MicroRNA profiling in human diploid fibroblasts uncovers miR-519 role in replicative senescence. *Aging* **2**, 333-343 (2010).

227 Noguchi, S. *et al.* Anti-oncogenic microRNA-203 induces senescence by targeting E2F3 protein in human melanoma cells. *The Journal of biological chemistry* **287**, 11769-11777 (2012).

228 Ørom, U. A. *et al.* MicroRNA-203 regulates caveolin-1 in breast tissue during caloric restriction. *Cell Cycle* **11**, 1291-1295 (2012).

229 Su, X. *et al.* TAp63 prevents premature aging by promoting adult stem cell maintenance. *Cell stem cell* **5**, 64-75 (2009).

230 Shatz, M. & Liscovitch, M. Caveolin-1: a tumor-promoting role in human cancer. *International journal of radiation biology* **84**, 177-189 (2008).

231 Lim, J. S. *et al.* Flagellin-dependent TLR5/caveolin-1 as a promising immune activator in immunosenescence. *Aging cell* **14**, 907-915 (2015).

232 Volonte, D., Liu, Z., Shiva, S. & Galbiati, F. Caveolin-1 controls mitochondrial function through regulation of m-AAA mitochondrial protease. *Aging* **8**, 2355-2369 (2016).

233 Smith-Vikos, T. *et al.* A serum miRNA profile of human longevity: findings from the Baltimore Longitudinal Study of Aging (BLSA). *Aging* **8**, 2971-2987 (2016).

234 Ding, Z. *et al.* Loss of MiR-664 Expression Enhances Cutaneous Malignant Melanoma Proliferation by Upregulating PLP2. *Medicine (Baltimore)* **94**, e1327 (2015).

235 Zhu, H., Miao, M. H., Ji, X. Q., Xue, J. & Shao, X. J. miR-664 negatively regulates PLP2 and promotes cell proliferation and invasion in T-cell acute lymphoblastic leukaemia. *Biochem Biophys Res Commun* **459**, 340-345 (2015).

236 ElSharawy, A. *et al.* Genome-wide miRNA signatures of human longevity. *Aging cell* **11**, 607-616 (2012).

237 Li, G. *et al.* MicroRNA-708 is downregulated in hepatocellular carcinoma and suppresses tumor invasion and migration. *Biomedicine & pharmacotherapy = Biomedecine & pharmacotherapie* **73**, 154-159 (2015).

238 Yang, J. *et al.* Metformin induces ER stress-dependent apoptosis through miR-708-5p/NNAT pathway in prostate cancer. *Oncogenesis* **4**, e158 (2015).

239 Baer, C. *et al.* Epigenetic silencing of miR-708 enhances NF-kappaB signaling in chronic lymphocytic leukemia. *International journal of cancer. Journal international du cancer* **137**, 1352-1361 (2015).

240 Noren Hooten, N. *et al.* microRNA Expression Patterns Reveal Differential Expression of Target Genes with Age. *PloS one* **5**, e10724 (2010).

241 Song, R., Liu, Q., Liu, T. & Li, J. Connecting rules from paired miRNA and mRNA expression data sets of HCV patients to detect both inverse and positive regulatory relationships. *BMC genomics* **16 Suppl 2**, S11 (2015).

242 Kenyon, C. J. The genetics of ageing. *Nature* **464**, 504-512 (2010).

243 Pinchuk, L. M. & Filipov, N. M. Differential effects of age on circulating and splenic leukocyte populations in C57BL/6 and BALB/c male mice. *Immunity & ageing : I & A* **5**, 1-1 (2008).

244 Connoy, A. C., Trader, M. & High, K. P. Age-related changes in cell surface and senescence markers in the spleen of DBA/2 mice: a flow cytometric analysis. *Experimental gerontology* **41**, 225-229 (2006).

245 Paraskevopoulou, M. D. *et al.* DIANA-microT web server v5.0: service integration into miRNA functional analysis workflows. *Nucleic acids research* **41**, W169-173 (2013).

246 Osborne, T. B., Mendel, L. B. & Ferry, E. L. THE EFFECT OF RETARDATION OF GROWTH UPON THE BREEDING PERIOD AND DURATION OF LIFE OF RATS. *Science* **45**, 294-295 (1917).

247 McCay, C. M., Bing, F. C. & Dilley, W. E. FACTOR H IN THE NUTRITION OF TROUT. *Science* **67**, 249-250 (1928).

248 Gems, D. & Partridge, L. Genetics of longevity in model organisms: debates and paradigm shifts. *Annual review of physiology* **75**, 621-644 (2013).

249 Mair, W. & Dillin, A. Aging and survival: the genetics of life span extension by dietary restriction. *Annual review of biochemistry* **77**, 727-754 (2008).

250 Speakman, J. R. & Mitchell, S. E. Caloric restriction. *Molecular aspects of medicine* **32**, 159-221 (2011).

251 Austad, S. N. Life extension by dietary restriction in the bowl and doily spider, Frontinella pyramitela. *Experimental gerontology* **24**, 83-92 (1989).

252 Kealy, R. D. *et al.* Effects of diet restriction on life span and age-related changes in dogs. *Journal of the American Veterinary Medical Association* **220**, 1315-1320 (2002).

253 Masoro, E. J. Overview of caloric restriction and ageing. *Mechanisms of ageing and development* **126**, 913-922 (2005).

254 Mattison, J. A. *et al.* Caloric restriction improves health and survival of rhesus monkeys. *Nat Commun* **8**, 14063 (2017).

255 Speakman, J. R. & Hambly, C. Starving for life: what animal studies can and cannot tell us about the use of caloric restriction to prolong human lifespan. *The Journal of nutrition* **137**, 1078-1086 (2007).

256 Phelan, J. P. & Rose, M. R. Why dietary restriction substantially increases longevity in animal models but won't in humans. *Ageing research reviews* **4**, 339-350 (2005).

257 Ingram, D. K. *et al.* The potential for dietary restriction to increase longevity in humans: extrapolation from monkey studies. *Biogerontology* **7**, 143-148 (2006).

258 Cava, E. & Fontana, L. Will calorie restriction work in humans? *Aging* **5**, 507-514 (2013).

259 Heilbronn, L. K. *et al.* Effect of 6-month calorie restriction on biomarkers of longevity, metabolic adaptation, and oxidative stress in overweight individuals: a randomized controlled trial. *Jama* **295**, 1539-1548 (2006).

260 Larson-Meyer, D. E. *et al.* Effect of calorie restriction with or without exercise on insulin sensitivity, beta-cell function, fat cell size, and ectopic lipid in overweight subjects. *Diabetes care* **29**, 1337-1344 (2006).

261 Smith, D. L., Jr., Nagy, T. R. & Allison, D. B. Calorie restriction: what recent results suggest for the future of ageing research. *European journal of clinical investigation* **40**, 440-450 (2010).

262 Selman, C. & Swindell, W. R. Putting a strain on diversity. *The EMBO journal* **37** (2018).

263 Ingram, D. K. & de Cabo, R. Calorie restriction in rodents: Caveats to consider. *Ageing research reviews* **39**, 15-28 (2017).

264 Vaughan, K. L. *et al.* Caloric Restriction Study Design Limitations in Rodent and Nonhuman Primate Studies. *The journals of gerontology. Series A, Biological sciences and medical sciences* **73**, 48-53 (2017).

265 Mockett, R. J., Cooper, T. M., Orr, W. C. & Sohal, R. S. Effects of caloric restriction are species-specific. *Biogerontology* **7**, 157-160 (2006).

266 Liao, C. Y., Rikke, B. A., Johnson, T. E., Diaz, V. & Nelson, J. F. Genetic variation in the murine lifespan response to dietary restriction: from life extension to life shortening. *Aging cell* **9**, 92-95 (2010).

267 Rikke, B. A., Liao, C. Y., McQueen, M. B., Nelson, J. F. & Johnson, T. E. Genetic dissection of dietary restriction in mice supports the metabolic efficiency model of life extension. *Experimental gerontology* **45**, 691-701 (2010).

268 Kelemen, O. *et al.* Function of alternative splicing. *Gene* **514**, 1-30 (2013).

269 Latorre, E., Ostler, E. O., Faragher, R. G. A. & Harries, L. W. FOXO1 and ETV6 genes may represent novel regulators of splicing factor expression in cellular senescence *FASEB Journal* **33**, 1086-1097 (2018).

270 Latorre, E., Torregrossa, R., Wood, M. E., Whiteman, M. & Harries, L. W. Mitochondria-targeted hydrogen sulfide attenuates endothelial senescence by selective induction of splicing factors HNRNPD and SRSF2. *Aging* **10**, 1666-1681 (2018).

271 Bennett, B., Beeson, M., Gordon, L. & Johnson, T. E. Reciprocal congenics defining individual quantitative trait Loci for sedative/hypnotic sensitivity to ethanol. *Alcoholism, clinical and experimental research* **26**, 149-157 (2002).

272 Williams, R. W. *et al.* Genetic structure of the LXS panel of recombinant inbred mouse strains: a powerful resource for complex trait analysis. *Mammalian genome : official journal of the International Mammalian Genome Society* **15**, 637-647 (2004).

273 Xie, F., Xiao, P., Chen, D., Xu, L. & Zhang, B. miRDeepFinder: a miRNA analysis tool for deep sequencing of plant small RNAs. *Plant molecular biology* (2012).

274 Rasmussen, J. L. Evaluating Outlier Identification Tests: Mahalanobis D Squared and Comrey Dk. *Multivariate behavioral research* **23**, 189-202 (1988).

275 Picca, A., Pesce, V. & Lezza, A. M. S. Does eating less make you live longer and better? An update on calorie restriction. *Clinical interventions in aging* **12**, 1887-1902 (2017).

276 Schorr, A., Carter, C. & Ladiges, W. The potential use of physical resilience to predict healthy aging. *Pathobiology of aging & age related diseases* **8**, 1403844 (2018).

277 Kirkland, J. L., Stout, M. B. & Sierra, F. Resilience in Aging Mice. *The journals of gerontology. Series A, Biological sciences and medical sciences* **71**, 1407-1414 (2016).

278 Varadhan, R., Seplaki, C. L., Xue, Q. L., Bandeen-Roche, K. & Fried, L. P. Stimulus-response paradigm for characterizing the loss of resilience in homeostatic regulation associated with frailty. *Mechanisms of ageing and development* **129**, 666-670 (2008).

279 Guillaumet-Adkins, A. *et al.* Epigenetics and Oxidative Stress in Aging. *Oxidative medicine and cellular longevity* **2017**, 9175806 (2017).

280 Martinez, N. M. & Lynch, K. W. Control of alternative splicing in immune responses: many regulators, many predictions, much still to learn. *Immunological reviews* **253**, 216-236 (2013).

281 Disher, K. & Skandalis, A. Evidence of the modulation of mRNA splicing fidelity in humans by oxidative stress and p53. *Genome* **50**, 946-953 (2007).

282 Latorre, E. & Harries, L. W. Splicing regulatory factors, ageing and age-related disease. *Ageing research reviews* **36**, 165-170 (2017).

283 Celotto, A. M. & Graveley, B. R. Alternative splicing of the Drosophila Dscam pre-mRNA is both temporally and spatially regulated. *Genetics* **159**, 599-608 (2001).

284 Grumont, R. J. & Gerondakis, S. Alternative splicing of RNA transcripts encoded by the murine p105 NF-kappa B gene generates I kappa B gamma isoforms with different inhibitory activities. *Proceedings of the National Academy of Sciences of the United States of America* **91**, 4367-4371 (1994).

285 Pan, Q., Shai, O., Lee, L. J., Frey, B. J. & Blencowe, B. J. Deep surveying of alternative splicing complexity in the human transcriptome by high-throughput sequencing. *Nat Genet* **40**, 1413-1415 (2008).

286 Guralnik, J. M. *et al.* A short physical performance battery assessing lower extremity function: association with self-reported disability and prediction of mortality and nursing home admission. *Journal of gerontology* **49**, M85-94 (1994).

287 Cruz-Jentoft, A. J. *et al.* Sarcopenia: European consensus on definition and diagnosis: Report of the European Working Group on Sarcopenia in Older People. *Age and Ageing* **39**, 412-423 (2010).

288 Hensel, A., Angermeyer, M. C. & Riedel-Heller, S. G. Measuring cognitive change in older adults: reliable change indices for the Mini-Mental State Examination. *Journal of neurology, neurosurgery, and psychiatry* **78**, 1298-1303 (2007).

289 McCarten, J. R., Rottunda, S. J. & Kuskowski, M. A. Change in the mini-mental state exam in Alzheimer's disease over 2 years: the experience of a dementia clinic. *J Alzheimers Dis* **6**, 11-15 (2004).

290 Clark, C. M. *et al.* Variability in annual Mini-Mental State Examination score in patients with probable Alzheimer disease: a clinical perspective of data from the Consortium to Establish a Registry for Alzheimer's Disease. *Archives of neurology* **56**, 857-862 (1999).

291 Llinas-Regla, J. *et al.* The Trail Making Test. *Assessment* **24**, 183-196 (2017).

292 Brown, R. G., Jahanshahi, M. & Marsden, C. D. The execution of bimanual movements in patients with Parkinson's, Huntington's and cerebellar disease. *Journal of neurology, neurosurgery, and psychiatry* **56**, 295-297 (1993).

293 Zakzanis, K. K., Leach, L. & Freedman, M. Structural and functional meta-analytic evidence for fronto-subcortical system deficit in progressive supranuclear palsy. *Brain and cognition* **38**, 283-296 (1998).

294 Bohannon, R. W. Muscle strength: clinical and prognostic value of hand-grip dynamometry. *Current opinion in clinical nutrition and metabolic care* **18**, 465-470 (2015).

295 Pavasini, R. *et al.* Short Physical Performance Battery and all-cause mortality: systematic review and meta-analysis. *BMC medicine* **14**, 215 (2016).

296 Xia, X., Chen, W., McDermott, J. & Han, J. J. Molecular and phenotypic biomarkers of aging. *F1000Res* **6**, 860 (2017).

297 Orr, H. T. FTD and ALS: genetic ties that bind. *Neuron* **72**, 189-190 (2011).

298 Couthouis, J. *et al.* A yeast functional screen predicts new candidate ALS disease genes. *Proceedings of the National Academy of Sciences of the United States of America* **108**, 20881-20890 (2011).

299 Calini, D. *et al.* Analysis of hnRNPA1, A2/B1, and A3 genes in patients with amyotrophic lateral sclerosis. *Neurobiology of aging* **34**, 2695.e2611-2692 (2013).

300 Xu, X., Brechbiel, J. L. & Gavis, E. R. Dynein-dependent transport of nanos RNA in Drosophila sensory neurons requires Rumpelstiltskin and the germ plasm organizer Oskar. *J Neurosci* **33**, 14791-14800 (2013).

301 Park, E. *et al.* Regulatory roles of heterogeneous nuclear ribonucleoprotein M and Nova-1 protein in alternative splicing of dopamine D2 receptor pre-mRNA. *The Journal of biological chemistry* **286**, 25301-25308 (2011).

302 Kaalund, S. S. *et al.* Contrasting changes in DRD1 and DRD2 splice variant expression in schizophrenia and affective disorders, and associations with SNPs in postmortem brain. *Molecular psychiatry* **19**, 1258-1266 (2014).

303 Cohen, O. S. *et al.* A splicing-regulatory polymorphism in DRD2 disrupts ZRANB2 binding, impairs cognitive functioning and increases risk for schizophrenia in six Han Chinese samples. *Molecular psychiatry* **21**, 975-982 (2016).

304 Ferreira, E., Shaw, D. M. & Oddo, S. Identification of learning-induced changes in protein networks in the hippocampi of a mouse model of Alzheimer's disease. *Translational psychiatry* **6**, e849 (2016).

305 Jarnaess, E. *et al.* Splicing factor arginine/serine-rich 17A (SFRS17A) is an A-kinase anchoring protein that targets protein kinase A to splicing factor compartments. *The Journal of biological chemistry* **284**, 35154-35164 (2009).

306 Lunnon, K. *et al.* A blood gene expression marker of early Alzheimer's disease. *J Alzheimers Dis* **33**, 737-753 (2013).

307 Marottoli, F. M. *et al.* Peripheral Inflammation, Apolipoprotein E4, and Amyloid-beta Interact to Induce Cognitive and Cerebrovascular Dysfunction. *ASN neuro* **9**, 1759091417719201 (2017).

308 Rollins, J. A., Shaffer, D., Snow, S. S., Kapahi, P. & Rogers, A. N. Dietary restriction induces posttranscriptional regulation of longevity genes. *Life science alliance* **2** (2019).

309 Tazi, J., Bakkour, N. & Stamm, S. Alternative splicing and disease. *Biochimica et biophysica acta* **1792**, 14-26 (2009).

310 Suñé-Pou, M. *et al.* Targeting Splicing in the Treatment of Human Disease. *Genes* **8**, 87 (2017).

311 Anna, A. & Monika, G. Splicing mutations in human genetic disorders: examples, detection, and confirmation. *J Appl Genet* **59**, 253-268 (2018).

312 Razquin Navas, P. & Thedieck, K. Differential control of ageing and lifespan by isoforms and splice variants across the mTOR network. *Essays in biochemistry* **61**, 349-368 (2017).

313 Li, H., Wang, Z., Ma, T., Wei, G. & Ni, T. Alternative splicing in aging and age-related diseases. *Translational Medicine of Aging* **1**, 32-40 (2017).

314 Allikmets, R. *et al.* Mutation of the Stargardt disease gene (ABCR) in age-related macular degeneration. *Science* **277**, 1805-1807 (1997).

315 Allikmets, R. *et al.* Organization of the ABCR gene: analysis of promoter and splice junction sequences. *Gene* **215**, 111-122 (1998).

316 Rivera, A. *et al.* A comprehensive survey of sequence variation in the ABCA4 (ABCR) gene in Stargardt disease and age-related macular degeneration. *American journal of human genetics* **67**, 800-813 (2000).

317 Blanco, F. J. *et al.* S-endoglin expression is induced in senescent endothelial cells and contributes to vascular pathology. *Circulation Research* **103**, 1383-1392 (2008).

318 Torrado, M. *et al.* Intron retention generates ANKRD1 splice variants that are co-regulated with the main transcript in normal and failing myocardium. *Gene* **440**, 28-41 (2009).

319 Qian, W. & Liu, F. Regulation of alternative splicing of tau exon 10. *Neuroscience bulletin* **30**, 367-377 (2014).

320 Volk, A. E., Weishaupt, J. H., Andersen, P. M., Ludolph, A. C. & Kubisch, C. Current knowledge and recent insights into the genetic basis of amyotrophic lateral sclerosis. *Medizinische Genetik : Mitteilungsblatt des Berufsverbandes Medizinische Genetik e.V* **30**, 252-258 (2018).

321 Perrone, B. *et al.* Alternative Splicing of ALS Genes: Misregulation and Potential Therapies. *Cellular and molecular neurobiology* (2019).

322 Gonzalo, S., Kreienkamp, R. & Askjaer, P. Hutchinson-Gilford Progeria Syndrome: A premature aging disease caused by LMNA gene mutations. *Ageing research reviews* **33**, 18-29 (2017).

323 Friedrich, K. *et al.* WRN mutations in Werner syndrome patients: genomic rearrangements, unusual intronic mutations and ethnic-specific alterations. *Human genetics* **128**, 103-111 (2010).

324 Khan, S. G. *et al.* XPC branch-point sequence mutations disrupt U2 snRNP binding, resulting in abnormal pre-mRNA splicing in xeroderma pigmentosum patients. *Hum Mutat* **31**, 167-175 (2010).

325 Laugel, V. Cockayne syndrome: The expanding clinical and mutational spectrum. *Mechanisms of ageing and development* **134**, 161-170 (2013).

326 Chun, H. H. & Gatti, R. A. Ataxia–telangiectasia, an evolving phenotype. *DNA Repair* **3**, 1187-1196 (2004).

327 Belfiore, A. *et al.* Insulin Receptor Isoforms in Physiology and Disease: An Updated View. *Endocr Rev* **38**, 379-431 (2017).

328 Deschenes, M. & Chabot, B. The emerging role of alternative splicing in senescence and aging. *Aging cell* **16**, 918-933 (2017).

329 Feng, Z. p53 regulation of the IGF-1/AKT/mTOR pathways and the endosomal compartment. *Cold Spring Harb Perspect Biol* **2**, a001057 (2010).

330 Pehar, M. *et al.* Altered longevity-assurance activity of p53:p44 in the mouse causes memory loss, neurodegeneration and premature death. *Aging cell* **9**, 174-190 (2010).

331 Kalozoumi, G., Yacoub, M. & Sanoudou, D. MicroRNAs in heart failure: Small molecules with major impact. *Global cardiology science & practice* **2014**, 79-102 (2014).

332 Bayoumi, A. S. *et al.* Crosstalk between Long Noncoding RNAs and MicroRNAs in Health and Disease. *International journal of molecular sciences* **17**, 356 (2016).

333 Piletic, K. & Kunej, T. MicroRNA epigenetic signatures in human disease. *Archives of toxicology* **90**, 2405-2419 (2016).

334 Sharma, S. & Lu, H.-C. microRNAs in Neurodegeneration: Current Findings and Potential Impacts. *J Alzheimers Dis Parkinsonism* **8**, 420 (2018).

335 Stolzenburg, L. R. & Harris, A. The role of microRNAs in chronic respiratory disease: recent insights. *Biological chemistry* **399**, 219-234 (2018).

336 Frankel, D. *et al.* MicroRNAs in hereditary and sporadic premature aging syndromes and other laminopathies. *Aging cell* **17**, e12766-e12766 (2018).

337 Dallaire, A. *et al.* Down regulation of miR-124 in both Werner syndrome DNA helicase mutant mice and mutant Caenorhabditis elegans wrn-1 reveals the importance of this microRNA in accelerated aging. *Aging* **4**, 636-647 (2012).

338 Zhang, Y., Huang, B., Wang, H. Y., Chang, A. & Zheng, X. F. S. Emerging Role of MicroRNAs in mTOR Signaling. *Cellular and molecular life sciences : CMLS* **74**, 2613-2625 (2017).

Supplementary Information

Supplementary Figures

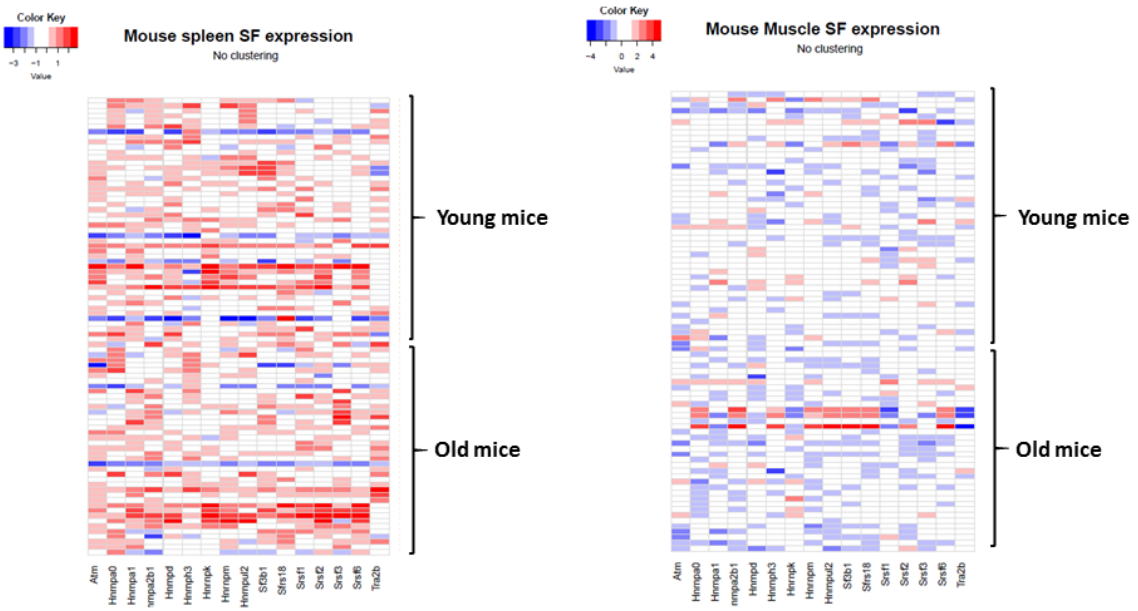

Supplementary Figure S1 (Chapter 3): Heat maps demonstrating inter- and intra-strain heterogeneity in splicing factor expression by age.

Splicing factor expression is given along the bottom of each heat map. Mouse age is given on the Y-axis. No clustering of expression signatures in young or old mice is noted. Data are Z-scored, and each transcript is expressed as standard deviation from the mean.

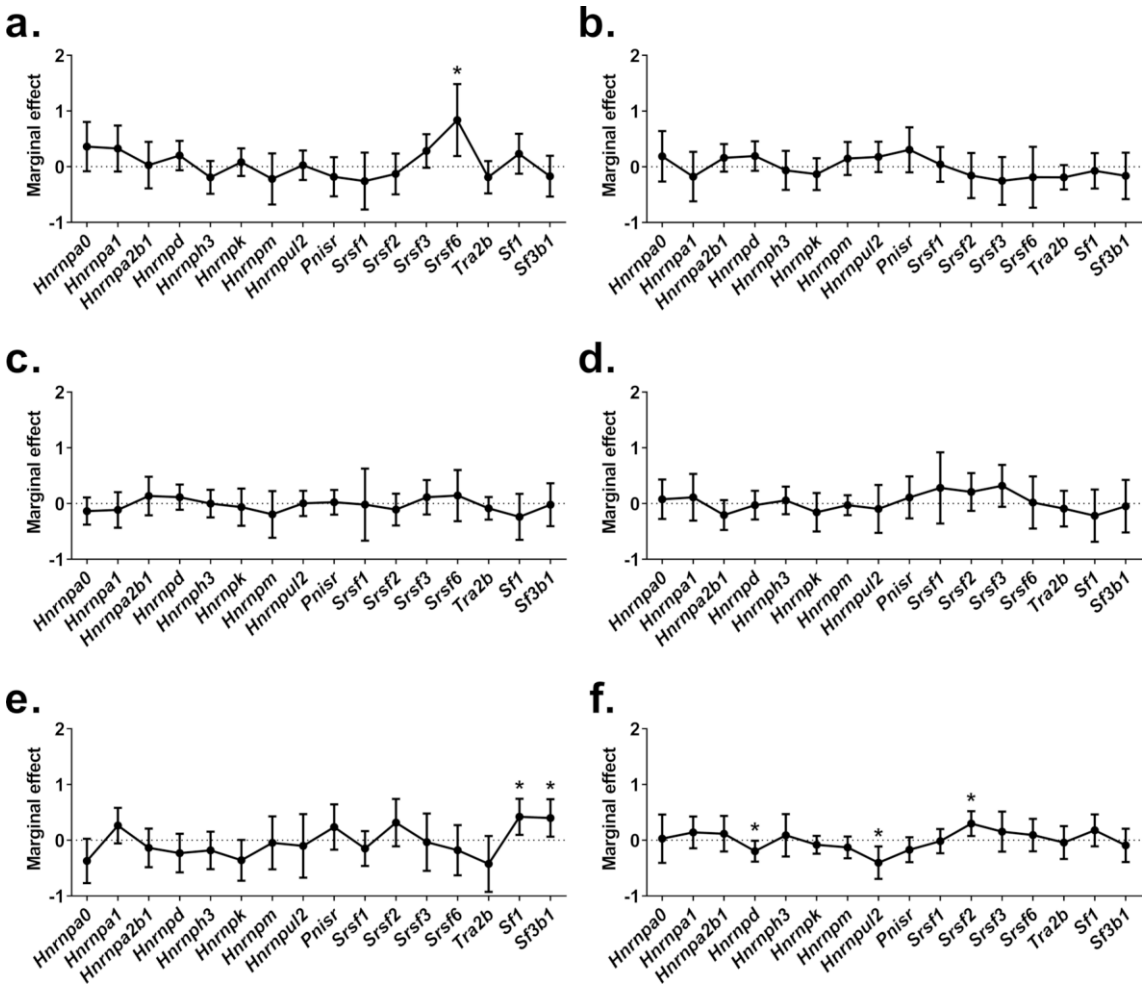

Supplementary Figure S2 (Chapter 5): Changes in splicing factor expression in non-responder strain (TejJ48) under DR conditions

Plots illustrating changes in splicing factor expression with DR in the non-responder strain of ILSXISS mice (TejJ48). Plot **a** shows mean differences between AL and DR in brain tissue under short-term DR, **b** shows mean differences between AL and DR in brain tissue under long-term DR, **c** shows mean differences between AL and DR in heart tissue under short-term DR, **d** shows mean differences between AL and DR in heart tissue under long-term DR, **e** shows mean differences between AL and DR in kidney tissue under short-term DR and **f** shows mean differences between AL and DR in kidney tissue under long-term DR. Error bars represent 95% confidence intervals and significant differences in splicing factor expression are denoted by stars: * = $p<0.05$.

Supplementary Tables

Supplementary Table S1 (Chapter 3): Splicing factor expression in mouse spleen tissue by lifespan, across 6 strains of different longevities

Data from mice of all ages, young mice only (6 months) and old mice only (20-22 months) are given separately. Data with statistically-significant effects at <0.05 are given in bold, underlined italic text. *Tra2ϐ* was not expressed in PWD/Phj mice so this strain was excluded from the analysis for this marker. *P* values were determined from linear regression of logged data.

	All Ages			Young mice only			Old mice only		
Gene	**Beta coefficient**	**Std Error**	***P* value**	**Beta coefficient**	**Std Error**	***P* value**	**Beta coefficient**	**Std Error**	***P* value**
Hnrnpa0	0.175	0.01	0.10	0.297	0.02	0.06	0.075	0.02	0.62
Hnrnpa1	-0.151	0.01	0.16	-0.396	0.01	***0.01***	0.061	0.01	0.69
Hnrnpa2b1	-0.256	0.01	***0.02***	-0.578	0.01	***<0.0001***	0.036	0.01	0.81
Hnrnpd	-0.021	0.01	0.85	0.020	0.12	0.90	-0.045	0.02	0.76
Hnrnph3	-0.133	0.01	0.22	-0.193	0.01	0.23	-0.098	0.02	0.513
Hnrnpk	-0.316	0.01	***0.003***	-0.288	0.02	0.07	-0.337	0.02	***0.02***
Hnrnpm	-0.310	0.01	***0.003***	-0.307	0.01	0.051	-0.312	0.01	***0.03***
Hnrnpul2	-0.223	0.01	***0.04***	-0.214	0.01	0.18	-0.231	0.01	0.12
Sf3b1	-0.212	0.01	***0.05***	-0.267	0.01	0.09	-0.174	0.01	0.24
Srsf18	0.062	0.01	0.57	0.041	0.02	0.80	0.073	0.02	0.63
Srsf1	-0.092	0.01	0.39	-0.253	0.02	0.11	0.047	0.02	0.76
Srsf2	-0.208	0.01	0.052	-0.224	0.02	0.16	-0.189	0.02	0.20
Srsf3	-0.130	0.01	0.23	-0.362	0.02	***0.02***	0.125	0.01	0.40
Srsf6	-0.157	0.01	0.14	-0.132	0.02	0.41	-0.176	0.01	0.24
Tra2ϐ	-0.122	0.01	0.26	-0.361	0.01	***0.02***	0.081	0.01	0.59

Supplementary Table S2 (Chapter 3): Splicing factor expression in mouse muscle tissue by lifespan across 6 strains of different longevities

Data from mice of all ages, young mice only (6 months) and old mice only (20-22 months) are given separately. Data with statistically-significant effects at <0.05 are given in underlined, bold, italic text. *Tra2β* was not expressed in PWD/Phj mice so this strain was excluded from the analysis for this marker. *P* values were determined from linear regression of logged data.

	All Ages			Young mice only			Old mice only		
Gene	**Beta coefficient**	**Std Error**	***P* value**	**Beta coefficient**	**Std Error**	***P* value**	**Beta coefficient**	**Std Error**	***P* value**
Hnrnpa0	0.124	0.02	0.27	-0.086	0.03	0.62	0.357	0.02	***0.01***
Hnrnpa1	-0.093	0.01	0.40	-0.200	0.01	0.25	-0.037	0.01	0.80
Hnrnpa2b1	0.005	0.02	0.96	-0.166	0.03	0.34	0.231	0.02	0.11
Hnrnpd	-0.238	0.01	***0.03***	-0.177	0.01	0.31	-0.321	0.01	***0.03***
Hnrnph3	-0.048	0.02	0.67	-0.227	0.03	0.19	0.115	0.02	0.44
Hnrnpk	-0.146	0.01	0.19	-0.030	0.02	0.86	-0.239	0.02	0.10
Hnrnpm	-0.019	0.01	0.86	-0.211	0.02	0.23	0.168	0.01	0.25
Hnrnpul2	-0.050	0.02	0.66	-0.223	0.03	0.20	0.152	0.02	0.30
Sf3b1	-0.165	0.02	0.14	-0.298	0.03	0.08	-0.008	0.02	0.96
Srsf18	-0.180	0.01	0.10	-0.315	0.03	0.07	-0.047	0.02	0.75
Srsf1	0.147	0.02	0.19	0.209	0.03	0.23	0.092	0.02	0.54
Srsf2	-0.177	0.01	0.11	-0.264	0.01	0.13	-0.134	0.01	0.36
Srsf3	-0.093	0.01	0.40	-0.396	0.01	***0.02***	0.105	0.01	0.48
Srsf6	-0.066	0.02	0.55	-0.136	0.03	0.44	0.023	0.02	0.88
Tra2β	0.030	0.03	0.80	0.054	0.05	0.77	0.013	0.03	0.94

Supplementary Table S3 (Chapter 3): Alternative isoform expression in mouse spleen tissue by lifespan across 6 strains of different longevities

Data from mice of all ages, young (6 months) and old (24 months) are given separately. UCSC transcript Identities identified by each probe set are given under the gene names. Data with statistically-significant effects at <0.05 are given in bold, underlined italic text. *P* values were determined from linear regression on logged data.

	All mice			Young mice only			Old mice only		
Isoform	**Beta coefficient**	**Std Error**	***P* value**	**Beta coefficient**	**Std Error**	***P* value**	**Beta coefficient**	**Std Error**	***P* value**
Atm-1,3 uc009pme.2 uc009pmd.2	0.038	0.01	0.73	0.151	0.05	0.35	-0.054	0.01	0.71
Atm-2 uc012gtj.1	-0.001	0.01	0.99	0.148	0.02	0.36	-0.162	0.01	0.27
Cdkn2a-1 Uc008toi.1	-0.164	0.02	0.13	0.186	0.02	0.26	-0.433	0.03	***0.002***
Cdkn2a-2 uc008toh.1	-0.247	0.02	***0.02***	0.108	0.02	0.51	-0.590	0.02	***<0.0001***
Chek2-1 uc008yrw.1	-0.102	0.02	0.34	-0.281	0.02	0.08	0.070	0.02	0.63
Chek2-2 uc008yrx.1	-0.066	0.01	0.54	-0.292	0.02	0.07	0.154	0.02	0.29
Fn1-1 uc007bju.2	0.253	0.01	***0.02***	0.349	0.02	***0.03***	0.166	0.02	0.25
Fn1-2,5 uc007bjv.2 uc007bjy.2	-0.044	0.02	0.68	-0.030	0.02	0.86	-0.064	0.03	0.66
Lmna-1 uc008pvj.3	-0.022	0.02	0.84	-0.070	0.03	0.67	0.033	0.02	0.82
Lmna-1,3 uc008pvj.3 uc008pvl.3	-0.114	0.02	0.29	-0.237	0.02	0.14	0.017	0.02	0.91

Supplementary Table S3 (cont.)

	All mice			Young mice only			Old mice only		
Isoform	**Beta coefficient**	**Std Error**	***P* value**	**Beta coefficient**	**Std Error**	***P* value**	**Beta coefficient**	**Std Error**	***P* value**
Myc-1 uc007vyh.2	-0.098	0.01	0.36	-0.242	0.01	0.13	0.000	0.01	0.99
Myc-1,2,3 uc007vyh.2 uc007vyg.2 uc007vyi.1	-0.124	0.01	0.25	-0.243	0.02	0.13	-0.037	0.01	0.80
Trp53-1,3,4 uc007jql.2 uc007jqm.2 uc007jqn.2	0.144	0.02	0.18	0.406	0.01	***0.009***	-0.025	0.01	0.86
Trp53-2 uc011xww.1	-0.236	0.01	***0.03***	-0.250	0.01	0.12	-0.214	0.07	0.14
Trp53-3 uc007jqm.2	-0.230	0.01	***0.03***	-0.352	0.01	***0.03***	-0.121	0.01	0.41
Vcan-1 uc007rjg.1	0.365	0.02	***0.001***	0.570	0.03	***<0.0001***	0.243	0.04	0.09
Vcan-2 uc011zck.1	0.109	0.04	0.422	-0.058	0.05	0.77	0.220	0.06	0.24

Supplementary Table S4 (Chapter 3): Alternative isoform expression in mouse muscle tissue by lifespan across 6 strains of different longevities

Data from mice of all ages, young (6 months) and old (20-22 months) are given separately. Data with statistically-significant effects at <0.05 are given in bold, underlined italic text. *P* values were determined from linear regression of logged data.

	All mice			Young mice only			Old mice only		
Isoform	**Beta coefficient**	**Std Error**	***P* value**	**Beta coefficient**	**Std Error**	***P* value**	**Beta coefficient**	**Std Error**	***P* value**
Il1b-2 uc008mht.1	-0.193	0.03	0.09	-0.458	0.04	***0.007***	-0.053	0.04	0.73
Il1b-2,3 uc008mht.1 uc008mhu.1	-0.138	0.03	0.23	-0.306	0.04	0.08	-0.074	0.03	0.63
IL6-1,2 uc008wuu.1 uc008wuv.1	-0.225	0.03	0.052	-0.482	0.04	***0.006***	-0.100	0.04	0.52
Il6-1,3 uc008wuu.1 uc008wuw.1	-0.279	0.03	***0.01***	-0.268	0.05	0.13	-0.281	0.04	0.06
Nfkb1-1,4,5 uc008rly.1 uc012cyg.1 uc008rlx.1	0.264	0.01	***0.02***	0.370	0.01	***0.03***	0.186	0.01	0.22
Nfkb1-1,5 uc008rly.1 uc008rlx.1	0.076	0.02	0.51	-0.071	0.03	0.69	0.294	0.01	***0.05***
Nfkb1-2 uc012cyf.1	0.160	0.02	0.16	0.082	0.02	0.65	0.213	0.02	0.16
Nfkb1-3,4,5 uc008rlw.1 uc012cyg.1 uc008rlx.1	0.268	0.01	***0.02***	0.283	0.01	0.11	0.275	0.01	0.07

Supplementary Table S4 (cont.)

	All mice			Young mice only			Old mice only		
Isoform	**Beta coefficient**	**Std Error**	***P* value**	**Beta coefficient**	**Std Error**	***P* value**	**Beta coefficient**	**Std Error**	***P* value**
Nfkb1-4,5 uc012cyg.1 uc008rlx.1	0.313	0.01	***0.005***	0.257	0.02	0.15	0.371	0.01	***0.01***
Stat1-1 uc007axy.1	-0.066	0.03	0.57	0.069	0.05	0.70	-0.171	0.04	0.26
Stat1-3,4 uc007axz.1 uc007aya.2	-0.472	0.01	***<0.0001***	-0.234	0.02	0.19	-0.625	0.01	***<0.0001***
Stat1-2,3,4,5 uc007ayd.2 uc007axz.1 uc007aya.2 uc007ayb.2	0.088	0.01	0.44	0.241	0.01	0.18	-0.014	0.01	0.92
Stat1-2,4,5,6 uc007ayd.2 uc007aya.2 uc007ayb.2 uc007ayc.2	0.219	0.01	0.052	0.429	0.01	***0.01***	0.096	0.01	0.53
Stat1-5 uc007ayb.2	0.332	0.01	***0.005***	0.378	0.02	***0.03***	0.299	0.02	***0.04***
Stat1-6 uc007ayc.2	0.338	0.03	***0.003***	0.460	0.03	***0.007***	0.271	0.04	0.08
Tnf-1,2 uc008cgr.2 uc012arb.2	-0.269	0.02	***0.02***	-0.282	0.03	0.11	-0.256	0.02	0.09
Tnf-1,3 uc008cgr.2 uc008cgs.2	-0.233	0.02	***0.04***	-0.183	0.03	0.31	-0.280	0.02	0.06
Tnf-3 uc008cgs.2	-0.177	0.02	0.121	-0.139	0.03	0.44	-0.199	0.03	0.19

Supplementary Table S5 (Chapter 3): Splicing factor expression in mouse spleen tissue by age in young (6 months) and old (20-22 months) mice

Data from mice of all strains, average-lived strains (median age <847.5 days) and long-lived (median lifespan >847.5 days) strains are given separately. Data with statistically-significant effects at <0.05 are given in bold, underlined italic text. *Tra2ϐ* was not expressed in PWD/Phj mice so this strain was excluded from the analysis for this marker. *P* values were determined from linear regression analysis of logged data.

	All strains			**Average-lived strains only**			**Long-lived strains only**		
Gene	**Beta coefficient**	**Std Error**	***P* value**	**Beta coefficient**	**Std Error**	***P* value**	**Beta coefficient**	**Std Error**	***P* value**
Hnrnpa0	-0.031	0.04	0.77	0.018	0.05	0.92	-0.053	0.05	0.70
Hnrnpa1	-0.015	0.03	0.89	-0.278	0.04	0.11	0.134	0.03	0.34
Hnrnpa2b1	-0.035	0.04	0.74	-0.460	0.05	***0.005***	0.248	0.04	0.07
Hnrnpd	0.038	0.03	0.73	-0.043	0.06	0.81	0.094	0.04	0.50
Hnrnph3	-0.170	0.03	0.11	-0.278	0.06	0.11	-0.09	0.04	0.54
Hnrnpk	0.012	0.04	0.91	0.081	0.07	0.64	-0.104	0.03	0.46
Hnrnpm	-0.034	0.03	0.75	-0.108	0.05	0.54	-0.001	0.04	0.99
Hnrnpul2	0.018	0.03	0.87	-0.042	0.06	0.81	0.059	0.04	0.68
Sf3B1	0.000	0.03	0.99	-0.073	0.05	0.68	0.05	0.04	0.72
Srsf18	0.158	0.04	0.14	0.098	0.06	0.58	0.193	0.06	0.17
Srsf1	-0.157	0.04	0.14	-0.341	0.06	***0.05***	-0.042	0.05	0.76
Srsf2	-0.178	0.04	0.10	-0.266	0.07	0.12	-0.150	0.04	0.284
Srsf3	-0.215	0.04	***0.04***	-0.449	0.07	***0.007***	-0.007	0.04	0.96
Srsf6	-0.082	0.04	0.45	-0.124	0.06	0.48	-0.068	0.03	0.63
Tra2ϐ	-0.221	0.03	0.053	-0.526	0.06	***0.008***	-0.050	0.04	0.73

Supplementary Table S6 (Chapter 3): Splicing factor expression in mouse muscle tissue by age in young (6 months) and old (20-22 months) mice

Data from mice of all strains, average-lived strains (mean lifespan <847.5 days) and long-lived strains (mean lifespan >847.5 days) are given separately. Data with statistically-significant effects at <0.05 are given in bold, underlined italic text. *Tra2ϐ* was not expressed in PWD/Phj mice so this strain was excluded from the analysis for this marker. *P* values were determined from linear regression of logged data.

	All Ages			Average-lived strains only			Long-lived strains only		
Gene	**Beta coefficient**	**Std Error**	***P* value**	**Beta coefficient**	**Std Error**	***P* value**	**Beta coefficient**	**Std Error**	***P* value**
Hnrnpa0	0.123	0.05	0.27	-0.057	0.08	0.75	0.236	0.07	0.11
Hnrnpa1	0.217	0.03	***0.05***	0.174	0.04	0.32	0.267	0.05	0.07
Hnrnpa2b1	-0.048	0.06	0.67	-0.228	0.08	0.19	0.075	0.07	0.61
Hnrnpd	0.123	0.03	0.27	0.221	0.04	0.20	0.113	0.04	0.44
Hnrnph3	-0.001	0.06	0.99	-0.184	0.08	0.29	0.122	0.08	0.41
Hnrnpk	-0.046	0.04	0.68	0.086	0.07	0.62	-0.128	0.05	0.39
Hnrnpm	0.187	0.04	0.09	0.040	0.05	0.82	0.281	0.05	0.053
Hnrnpul2	0.029	0.05	0.80	-0.134	0.07	0.44	0.128	0.08	0.39
Sf3B1	0.017	0.06	0.88	-0.146	0.08	0.40	0.127	0.08	0.39
Srsf18	0.095	0.05	0.39	-0.055	0.07	0.76	0.222	0.07	0.13
Srsf1	-0.046	0.06	0.68	0.016	0.10	0.93	-0.114	0.07	0.44
Srsf2	0.084	0.03	0.45	0.134	0.04	0.44	0.083	0.05	0.58
Srsf3	0.100	0.04	0.37	-0.086	0.05	0.62	0.272	0.04	0.06
Srsf6	-0.100	0.06	0.37	-0.159	0.08	0.36	-0.063	0.09	0.67
Tra2ϐ	-0.06	0.10	0.61	-0.018	0.18	0.93	-0.082	0.13	0.58

Supplementary Table S7 (Chapter 3): Alternative isoform expression in mouse spleen tissue by age in young (6 months) and old (20 -22 months) mice

Data from mice of all strains, average-lived strains (mean lifespan <847.5 days) and long-lived strains (mean lifespan (>847 days) are given separately. UCSC transcript Identities identified by each probe set are given under the gene names. Data with statistically-significant effects at <0.05 are given in bold, underlined italic text. *P* values were determined from linear regression of logged data.

	All strains			Average-lived strains only			Long-lived strains only		
Isoform	**Beta coefficient**	**Std Error**	***P* value**	**Beta coefficient**	**Std Error**	***P* value**	**Beta coefficient**	**Std Error**	***P* value**
Atm-1,3 uc009pme.2 uc009pmd.2	-0.044	0.04	0.69	0.127	0.06	0.47	-0.156	0.05	0.36
Atm-2 uc012gtj.1	-0.072	0.04	0.50	0.163	0.06	0.35	-0.277	0.05	0.10
Cdkn2a-1 uc008toi.1	0.399	0.06	***<0.0001***	0.659	0.09	***<0.0001***	0.224	0.08	0.10
Cdkn2a-2 uc008toh.1	0.529	0.06	***<0.0001***	0.815	0.06	***<0.0001***	0.346	0.08	***0.007***
Chek2-1 uc008yrw.1	-0.331	0.05	***0.002***	-0.499	0.07	***0.002***	-0.227	0.07	0.10
Chek2-2 uc008yrx.1	-0.349	0.05	***0.001***	-0.542	0.06	***0.001***	-0.232	0.06	0.10
Fn1-1 uc007bju.2	0.065	0.07	0.55	0.164	0.08	0.35	-0.004	0.06	0.98
Fn1-2,5 uc007bjv.2 uc007bjy.2	0.105	0.05	0.33	0.167	0.06	0.34	0.086	0.08	0.54
Lmna-1 uc008pvj.3	-0.047	0.06	0.66	-0.147	0.11	0.40	0.047	0.06	0.73
Lmna-1,3 uc008pvj.3 uc008pvl.3	-0.198	0.05	0.06	-0.335	0.09	***0.05***	-0.101	0.06	0.47
Myc-1 uc007vyh.2	0.03	0.03	0.76	-0.027	0.07	0.88	0.109	0.03	0.43

Supplementary Table S7 (cont.)

	All strains			Average-lived strains only			Long-lived strains only		
Isoform	**Beta coefficient**	**Std Error**	***P* value**	**Beta coefficient**	**Std Error**	***P* value**	**Beta coefficient**	**Std Error**	***P* value**
Myc-1,2,3 uc007vyh.2 uc007vyg.2 uc007vyi.1	0.062	0.04	0.56	0.000	0.08	0.99	0.155	0.03	0.26
Trp53-1,3,4 uc007jql.2 uc007jqm.2 uc007jqn.2	-0.243	0.02	***0.02***	0.007	0.03	0.97	-0.407	0.02	***0.002***
Trp53-2 uc011xww.1	-0.114	0.02	0.29	-0.06	0.03	0.73	-0.147	0.03	0.29
Trp53-3 uc007jqm.2	-0.240	0.03	***0.03***	-0.313	0.05	0.07	-0.194	0.04	0.16
Vcan-1 uc007rjg.1	0.063	0.09	0.56	0.198	0.11	0.26	0.004	0.13	0.98
Vcan-2 uc011zck.1	-0.034	0.13	0.80	-0.217	0.21	0.31	0.129	0.15	0.47

Supplementary Table S8 (Chapter 3): Alternative isoform expression in mouse muscle tissue by age in young (6 months) and old (20 -22 months) mice

Data from mice of all strains, average-lived strains (mean lifespan <847.5 days) and long-lived strains (mean lifespan (>847 days) are given separately. UCSC transcript Identities identified by each probe set are given under the gene names. Data with statistically-significant effects at <0.05 are given in bold, underlined italic text. *P* values were determined from linear regression of logged data.

	All strains			Average-lived mice only			Long-lived mice only		
Isoform	**Beta coefficient**	**Std Error**	***P* value**	**Beta coefficient**	**Std Error**	***P* value**	**Beta coefficient**	**Std Error**	***P* value**
Il1b-2 uc008mht.1	0.373	0.10	***0.001***	0.139	0.17	0.44	0.601	0.10	***<0.0001***
Il1b-2,3 uc008mht.1 uc008mhu.1	0.393	0.10	***<0.0001***	0.231	0.15	0.20	0.544	0.11	***<0.0001***
IL6-1,2 uc008wuu.1 uc008wuv.1	0.230	0.11	***0.05***	-0.008	0.20	0.97	0.435	0.13	***0.003***
Il6-1,3 uc008wuu.1 uc008wuw.1	-0.196	0.12	0.09	-0.247	0.18	0.17	-0.161	0.16	0.30
Nfkb1-1,4,5 uc008rly.1 uc012cyg.1 uc008rlx.1	0.015	0.03	0.90	0.066	0.05	0.71	-0.050	0.04	0.74
Nfkb1-1,5 uc008rly.1 uc008rlx.1	0.083	0.06	0.45	-0.110	0.06	0.54	0.161	0.09	0.29
Nfkb1-2 uc012cyf.1	-0.070	0.06	0.54	-0.149	0.08	0.41	-0.029	0.08	0.85
Nfkb1-3,4,5 uc008rlw.1 uc012cyg.1 uc008rlx.1	-0.088	0.03	0.44	-0.165	0.04	0.36	-0.070	0.05	0.64

Supplementary Table S8 (cont.)

	All strains			Average-lived mice only			Long-lived mice only		
Isoform	**Beta coefficient**	**Std Error**	***P* value**	**Beta coefficient**	**Std Error**	***P* value**	**Beta coefficient**	**Std Error**	***P* value**
Nfkb1-4,5 uc012cyg.1 uc008rlx.1	-0.107	0.04	0.35	-0.170	0.07	0.34	-0.091	0.05	0.55
Stat1-1 uc007axy.1	0.040	0.11	0.73	0.171	0.18	0.34	-0.071	0.14	0.64
Stat1-3,4 uc007axz.1 uc007aya.2	-0.105	0.05	0.36	0.221	0.04	0.22	-0.207	0.07	0.17
Stat1-2,3,4,5 uc007ayd.2 uc007axz.1 uc007aya.2 uc007ayb.2	-0.053	0.04	0.64	0.064	0.05	0.73	-0.130	0.05	0.39
Stat1-2,4,5,6 uc007ayd.2 uc007aya.2 uc007ayb.2 uc007ayc.2	-0.203	0.03	0.07	-0.014	0.04	0.94	-0.321	0.05	***0.03***
Stat1-5 uc007ayb.2	-0.059	0.05	0.61	0.242	0.04	0.17	-0.020	0.07	0.89
Stat1-6 uc007ayc.2	-0.121	0.09	0.30	-0.139	0.15	0.44	-0.155	0.11	0.32
Tnf-1,2 uc008cgr.2 uc012arb.2	-0.058	0.06	0.61	0.040	0.08	0.83	-0.082	0.09	0.59
Tnf-1,3 uc008cgr.2 uc008cgs.2	0.053	0.06	0.64	0.178	0.09	0.32	0.002	0.08	0.99
Tnf-3 uc008cgs.2	-0.076	0.07	0.51	0.145	0.10	0.42	-0.219	0.09	0.15

Supplementary Table S9 (Chapter 3): Analyses of potential interactions between mouse strain longevity and mouse age

Std. Err = standard error, 95% Ci = 95% Confidence intervals. Average lived strains have a lifespan of <847.5 days, long-lived strains have a mean lifespan of >847.5 days. Young mice are 6 months, old mice are 20-22 months old. Statistically significant results are indicated in bold underlined text.

Longevity:age interactions - splicing factors (Spleen)				
Gene	**Beta coefficient**	**Std. Err**	**95% CI**	***P* value**
Hnrnpa1				
Average-lived/old	-0.06	0.04	-0.14 to 0.18	0.13
Long-lived/young	-0.14	0.04	-0.21 to -0.56	**0.001**
Long-lived/old	-0.09	0.04	-0.02 to 0.02	**0.01**
Hnrnpa2b1				
Average-lived/old	-0.15	0.05	-0.26 to -0.05	**0.005**
Long-lived/young	-0.19	0.05	-0.29 to -0.10	**<0.0001**
Long-lived/old	-0.12	0.05	-0.21 to -0.02	**0.02**
Hnrnpk				
Average-lived/old	0.03	0.05	-0.07 to 0.13	0.52
Long-lived/young	-0.18	0.05	-0.27 to -0.08	**<0.0001**
Long-lived/old	-0.20	0.05	-0.29 to -0.10	**<0.0001**
Hnrnpm				
Average-lived/old	-0.03	0.05	-0.12 to 0.06	0.52
Long-lived/young	-0.15	0.05	-0.23 to -0.05	**0.002**
Long-lived/old	-0.14	0.05	-0.23 to -0.08	**0.001**
Sf3b1				
Average-lived/old	-0.02	0.05	-0.12 to 0.07	0.64
Long-lived/young	-0.11	0.05	-0.20 to -0.02	**0.02**
Long-lived/old	-0.09	0.05	-0.19 to -0.01	**0.04**
Srsf3				
Average-lived/old	-0.19	0.05	-0.30 to -0.08	**0.001**
Long-lived/young	-0.17	0.05	-0.28 to -0.07	**0.001**
Long-lived/old	-0.17	0.05	-0.28 to -0.08	**0.001**
Tra2ϐ				
Average-lived/old	-0.18	0.06	-0.30 to -0.07	**0.002**
Long-lived/young	-0.13	0.05	-0.23 to -0.26	**0.02**
Long-lived/old	-0.14	0.05	-0.24 to -0.04	**0.01**

Supplementary Table S9 (cont.)

Longevity:age interactions - splicing factors (Muscle)				
Gene	**Beta coefficient**	**Std. Err**	**95% CI**	***P* value**
Srsf3				
Average-lived/old	-0.03	0.05	-0.13 to 0.07	0.61
Long-lived/young	-0.14	0.05	-0.24 to -0.03	**0.01**
Long-lived/old	-0.05	0.05	-0.14 to 0.04	0.28
Longevity:age interactions - Isoforms (Spleen)				
Gene	**Beta coefficient**	**Std. Err**	**95% CI**	***P* value**
Cdkn2a-1				
Average-lived/old	0.44	0.10	0.25 to 0.63	**<0.0001**
Long-lived/young	0.09	0.09	-0.09 to 0.27	0.34
Long-lived/old	0.22	0.09	0.06 to 0.40	**0.01**
Cdkn2a-2				
Average-lived/old	0.50	0.09	0.32 to 0.67	**<0.0001**
Long-lived/young	0.04	0.08	-0.12 to 0.20	0.66
Long-lived/old	0.27	0.08	0.11 to 0.43	**0.001**
Chek2-1				
Average-lived/old	-0.24	0.08	-0.39 to -0.08	**0.003**
Long-lived/young	-0.15	0.07	-0.30 to 0.001	**0.05**
Long-lived/old	-0.26	0.07	-0.40 to -0.12	**<0.0001**
Trp53-134				
Average-lived/old	0.001	0.03	-0.06 to 0.06	0.97
Long-lived/young	0.08	0.03	0.03 to 0.14	**0.004**
Long-lived/old	0.007	0.03	-0.05 to 0.06	0.79
Trp53-3				
Average-lived/old	-0.09	0.04	-0.18 to 0.01	0.06
Long-lived/young	-0.06	0.04	-0.15 to 0.03	0.18
Long-lived/old	-0.11	0.04	-0.19 to -0.03	**0.01**

Supplementary Table S9 (cont.)

Longevity:age interactions - Isoforms (Muscle)				
Gene	**Beta coefficient**	**Std. Err**	**95% CI**	***P* value**
Il1b-2				
Average-lived/old	0.13	0.14	-0.15 to 0.41	0.36
Long-lived/young	-0.42	0.14	-0.70 to -0.14	**0.004**
Long-lived/old	0.10	0.13	-0.17 to 0.36	0.452
Il6-2				
Average-lived/old	-0.01	0.17	-0.35 to 0.33	0.96
Long-lived/young	-0.36	0.17	-0.70 to -0.02	**0.04**
Long-lived/old	0.05	0.15	-0.25 to 0.36	0.72
Stat1-34				
Average-lived/old	0.05	0.07	-0.08 to 0.18	0.44
Long-lived/young	-0.07	0.07	-0.20 to 0.06	0.28
Long-lived/old	-0.17	0.06	-0.29 to -0.05	**0.01**
Stat1-2456				
Average-lived/old	-0.003	0.05	-0.10 to 0.10	0.95
Long-lived/young	0.11	0.05	0.12 to 0.21	**0.03**
Long-lived/old	0.003	0.05	-0.09 to 0.09	0.951
Tnf-2				
Average-lived/old	0.02	0.09	-0.16 to 0.20	0.85
Long-lived/young	-0.18	0.09	-0.16 to 0.001	0.06
Long-lived/old	-0.23	0.08	-0.39 to -0.06	**0.008**

Supplementary Table S10 (Chapter 3): Splicing factor expression in mouse spleen tissue by lifespan, across 6 strains of different longevities by binary logistic regression

Data from mice of all ages, young mice only (6 months) and old mice only (20-22 months) are given separately. Data with statistically-significant effects at <0.05 are given in bold, underlined italic text. *Tra2ϐ* was not expressed in PWD/Phj mice so this strain was excluded from the analysis for this marker. *P* values were determined from binary logistic regression of logged data. *P* values marked by stars are also significant in linear regression analysis.

	All Ages			Young mice only			Old mice only		
Gene	**Beta coefficient**	**Std Error**	***P* value**	**Beta coefficient**	**Std Error**	***P* value**	**Beta coefficient**	**Std Error**	***P* value**
Hnrnpa0	1.80	1.31	0.17	2.27	1.95	0.24	1.40	1.78	0.43
Hnrnpa1	-5.78	2.05	***0.005***	-10.40	3.63	***0.004****	-2.50	2.53	0.32
Hnrnpa2b1	-2.89	1.47	***0.05****	-10.23	3.36	***0.002****	1.38	1.91	0.47
Hnrnpd	-0.90	1.42	0.54	-3.11	1.28	0.26	-0.06	1.62	0.98
Hnrnph3	1.00	1.43	0.49	-1.19	2.85	0.67	1.83	1.76	0.30
Hnrnpk	-9.50	2.28	***<0.0001****	-9.42	7.05	***0.008***	-9.55	2.99	***0.001****
Hnrnpm	-8.23	2.34	***<0.0001****	-10.67	6.72	***0.01***	-6.70	5.49	***0.02****
Hnrnpul2	-2.88	3.37	0.07*	-4.70	2.95	0.09	-1.84	1.90	0.33
Sf3b1	-4.79	1.81	***0.008****	-8.00	3.44	***0.02***	-3.17	2.11	0.13
Srsf18	-1.96	1.18	0.10	-2.57	1.79	0.15	-1.47	1.62	0.36
Srsf1	-2.45	1.36	0.07	-5.28	2.46	***0.03***	-0.766	1.76	0.66
Srsf2	-5.96	1.63	***<0.0001***	-8.01	3.03	***0.008****	-5.18	2.09	***0.01***
Srsf3	-2.61	1.35	0.054	-6.16	2.35	***0.009***	0.49	2.03	0.81
Srsf6	-6.07	1.98	***0.002***	-6.90	3.11	***0.03***	-5.55	2.63	***0.04***
Tra2ϐ	-1.67	1.72	0.33	-7.48	3.32	***0.02****	1.95	2.29	0.39

Supplementary Table S11 (Chapter 3): Splicing factor expression in mouse muscle tissue by lifespan across 6 strains of different longevities by binary logistic regression analysis

Data from mice of all ages, young mice only (6 months) and old mice only (20-22 months) are given separately. Data with statistically-significant effects at <0.05 are given in underlined, bold, italic text. *Tra2ß* was not expressed in PWD/Phj mice so this strain was excluded from the analysis for this marker. *P* values were determined from binary logistic regression of logged data. *P* values marked by stars are also significant in linear regression analysis.

	All Ages			Young mice only			Old mice only		
Gene	**Beta coefficient**	**Std Error**	***P* value**	**Beta coefficient**	**Std Error**	***P* value**	**Beta coefficient**	**Std Error**	***P* value**
Hnrnpa0	2.20	1.11	***0.05***	0.33	1.21	0.79	6.08	2.30	***0.008****
Hnrnpa1	-2.39	1.60	0.13	-3.70	2.48	0.14	-1.91	2.22	0.39
Hnrnpa2b1	0.66	0.95	0.49	-0.48	1.11	0.62	3.60	2.01	0.07
Hnrnpd	-6.27	2.09	***0.003****	-4.29	2.64	0.10	-9.40	3.45	***0.006****
Hnrnph3	0.16	0.89	0.86	-1.06	1.31	0.42	1.44	1.33	0.23
Hnrnpk	-4.52	1.47	***0.002***	-2.55	1.90	0.18	-6.99	2.49	***0.005***
Hnrnpm	-0.02	1.42	0.99	-1.55	1.90	0.41	2.15	2.50	0.39
Hnrnpul2	0.08	0.94	0.93	-0.79	1.19	0.51	1.67	1.64	0.31
Sf3b1	-0.71	0.89	0.43	-1.34	1.25	0.28	0.34	1.55	0.83
Srsf18	-1.76	1.06	0.10	-2.63	1.68	0.12	-1.05	1.62	0.52
Srsf1	0.94	0.88	0.29	1.16	1.19	0.33	0.72	1.34	0.59
Srsf2	-3.32	1.62	***0.04***	-4.02	2.74	0.14	-3.14	2.03	0.12
Srsf3	-2.99	1.52	***0.05***	-7.90	3.24	***0.02****	-0.95	1.82	0.61
Srsf6	-0.39	0.79	0.63	-0.43	1.03	0.68	-0.22	1.27	0.86
Tra2ß	-0.04	0.58	0.95	0.10	0.69	0.88	-0.28	1.05	0.79

Supplementary Table S12 (Chapter 3): Genetic variation within the mouse Hnrnpa2b1 and Hnrnpa1 genes and its predicted effect on gene regulation

This table gives the SNP identifiers, chromosomal location, gene position and predicted effect on amino acid sequence or parameters of gene regulation for the mouse *Hnrnpa2b1* and *Hnrnpa1* genes. 5' UTR = 5' untranslated region, I = intron, C = coding, SRE = splicing regulatory element, 3' UTR = 3' untranslated region. ARE = A-rich element, C>U = C to U RNA editing site, miR = microRNA binding, TF = transcription factor binding. Where 2 alternative gene position is given, this is due to the possibility that the SNP is located in different genetic regions for different isoforms. '/ '= not applicable.

SNP name	Chromosomal location	Position in gene	TF	Coding change	SRE	ARE	C>U	miR
Hnrnpa2b1								
rs46028062	6:51461052	3'UTR	/	/	/	NO	NO	NO
rs48993060	6:51465149	I 3'UTR	/ /	/ /	NO /	/ NO	/ NO	/ NO
rs224637794	6:51461566	I 3'UTR	/ /	/ /	NO /	/ NO	/ NO	/ NO
rs234970481	6:51465354	I	/	/	NO	/	/	/
rs229198021	6:51465605	I	/	/	NO	/	/	/
rs250280372	6:51465935	I	/	/	NO	/	/	/
rs226722250	6:51466015	I	/	/	NO	/	/	/
rs47522479	6:51466888	I	/	/	NO	/	/	/
rs51031918	6:51467084	I	/	/	**POSSIBLE**	/	/	/
rs252413833	6:51467157	I	/	/	**POSSIBLE**	/	/	/
rs235452001	6:51469308	I	/	/	NO	/	/	/
rs239268432	6:51469567	I	/	/	NO	/	/	/
rs228820180	6:51469765	5'UTR	NO	/	/	/	/	/
rs257262812	6:51470336	Intergenic	NO	/	/	/	/	/
Hnrnpa1								
rs32398879	15:103242334	I	/	/	NO	/	/	/
rs50030666	15:103242939	I C	/ /	/ **Gly257Ser**	NO /	/ /	/ /	/ /

Supplementary Table S13 (Chapter 4): Association of MicroRNA expression and lifespan in spleen tissue from young mice of shortest-lived and longest-lived strains (A/J and WSB/EiJ respectively)

MicroRNAs significantly associated above the Bonferroni-corrected significance threshold (p<0.000179) are shown in bold italics. The ten most strongly associated microRNAs followed up in the targeted analysis are shown in italics. Shown in plain bold are the 6 small RNAs commonly used as endogenous controls. *P*-values were determined using independent sample t-tests on log-transformed relative expression data from TaqMan® MicroRNA Array cards.

		95% CI of the difference		
MicroRNA Assay ID	**Mean Difference**	**Upper**	**Lower**	***P*-value**
mmu-miR-297b-5p	***4.29***	***4.53***	***4.05***	***1.63E-11***
mmu-miR-708	***0.47***	***0.58***	***0.36***	***5.46E-06***
mmu-miR-224	***-0.97***	***-0.64***	***-1.30***	***0.0001***
mmu-miR-203	***-0.55***	***-0.35***	***-0.74***	***0.0001***
rno-miR-327	***-3.70***	***-2.33***	***-5.08***	***0.0002***
rno-miR-664	*0.46*	*0.66*	*0.27*	*0.0005*
mmu-miR-592	*0.50*	*0.73*	*0.27*	*0.0008*
mmu-miR-484	*0.33*	*0.49*	*0.17*	*0.0014*
mmu-miR-687	*5.02*	*7.58*	*2.46*	*0.0016*
mmu-miR-192	*0.31*	*0.47*	*0.15*	*0.0018*
mmu-miR-760	-0.25	-0.11	-0.38	0.003
mmu-miR-186*	0.31	0.49	0.14	0.003
mmu-miR-690	0.39	0.63	0.15	0.005
mmu-miR-31	0.43	0.69	0.16	0.005
mmu-miR-126-5p	0.26	0.42	0.09	0.006
mmu-miR-10a	-0.23	-0.08	-0.38	0.007
mmu-miR-130b*	0.36	0.59	0.12	0.007
mmu-miR-20b	0.17	0.28	0.06	0.008
mmu-miR-455*	0.25	0.42	0.08	0.009
mmu-miR-449a	-0.49	-0.15	-0.84	0.010
mmu-miR-434-3p	-0.28	-0.08	-0.49	0.011
mmu-miR-376c	-0.40	-0.10	-0.69	0.013
mmu-miR-24-2*	0.17	0.29	0.04	0.013
mmu-miR-511	-0.40	-0.09	-0.72	0.018
rno-miR-20b-5p	0.26	0.47	0.05	0.020
mmu-miR-210	0.21	0.37	0.04	0.020
mmu-miR-194	0.18	0.32	0.03	0.021
mmu-miR-411	-0.34	-0.06	-0.63	0.022
mmu-miR-875-5p	1.20	2.19	0.21	0.023
mmu-miR-340-3p	-0.27	-0.05	-0.49	0.023
mmu-miR-365	-0.17	-0.03	-0.32	0.023
mmu-miR-186	0.20	0.36	0.03	0.023
mmu-miR-539	-2.80	-0.48	-5.12	0.023
mmu-miR-140	0.12	0.23	0.01	0.030
mmu-miR-136	-0.42	-0.04	-0.79	0.033
mmu-miR-130b	0.21	0.41	0.02	0.035
mmu-miR-148b	-0.31	-0.02	-0.59	0.036
mmu-miR-31*	2.28	4.39	0.16	0.038
mmu-miR-217	-2.76	-0.15	-5.37	0.040
snoRNA135	**-0.11**	**0.00**	**-0.21**	**0.042**
mmu-miR-193b	0.20	0.39	0.01	0.045
mmu-miR-470*	-1.83	-0.01	-3.66	0.049
mmu-miR-877*	0.19	0.37	0.00	0.051
mmu-miR-674*	0.16	0.31	0.00	0.051
mmu-miR-193*	0.37	0.75	-0.01	0.055
mmu-miR-700	-0.13	0.01	-0.26	0.059

Supplementary Table S13 (cont.)

		95% CI of the difference		
MicroRNA Assay ID	**Mean Difference**	**Upper**	**Lower**	***P*-value**
mmu-miR-15a	-0.23	0.01	-0.46	0.060
mmu-miR-152	-0.19	0.01	-0.40	0.061
rno-miR-743a	-1.29	0.08	-2.66	0.062
mmu-miR-197	2.26	4.68	-0.16	0.064
mmu-miR-34b-3p	-0.22	0.02	-0.45	0.065
mmu-miR-574-3p	0.15	0.31	-0.01	0.067
mmu-miR-297a*	0.17	0.36	-0.02	0.067
mmu-miR-674	2.44	5.12	-0.24	0.070
mmu-miR-682	2.28	4.83	-0.26	0.072
mmu-miR-720	-0.13	0.02	-0.27	0.081
mmu-miR-92a	0.12	0.26	-0.02	0.089
mmu-miR-149	0.10	0.22	-0.02	0.095
mmu-miR-32	-0.24	0.05	-0.54	0.096
mmu-miR-218	-0.14	0.04	-0.32	0.103
mmu-miR-183*	-0.35	0.09	-0.79	0.106
mmu-miR-296-5p	0.22	0.49	-0.06	0.109
mmu-miR-467b*	-0.27	0.08	-0.62	0.119
mmu-miR-345-5p	-1.78	0.56	-4.12	0.119
mmu-miR-335-5p	0.14	0.32	-0.04	0.120
mmu-miR-29b	-0.13	0.04	-0.30	0.129
MammU6	**0.19**	**0.45**	**-0.07**	**0.130**
mmu-miR-322	-0.17	0.06	-0.40	0.132
mmu-miR-547	-1.25	0.48	-2.98	0.138
mmu-miR-467a	0.16	0.37	-0.06	0.138
mmu-miR-503	0.21	0.49	-0.08	0.141
mmu-miR-322*	-0.17	0.07	-0.40	0.142
mmu-miR-184	-0.25	0.10	-0.61	0.143
mmu-miR-195	-0.09	0.04	-0.21	0.145
mmu-miR-685	0.11	0.28	-0.05	0.147
mmu-miR-18a	-0.14	0.06	-0.33	0.152
mmu-miR-132	-0.09	0.04	-0.21	0.154
mmu-miR-135a	1.25	3.08	-0.58	0.156
mmu-miR-125b-5p	-0.09	0.04	-0.21	0.156
mmu-miR-129-3p	1.54	3.80	-0.73	0.159
mmu-miR-25	0.12	0.30	-0.06	0.163
mmu-miR-451	-0.18	0.09	-0.46	0.170
mmu-miR-744*	1.13	2.88	-0.62	0.178
mmu-miR-7a	-1.04	0.57	-2.66	0.178
mmu-miR-29a	0.07	0.18	-0.04	0.186
mmu-miR-15b*	0.14	0.36	-0.08	0.191
mmu-miR-148a	-0.22	0.13	-0.58	0.192
mmu-miR-384-5p	1.12	2.93	-0.69	0.194
mmu-let-7c	-0.15	0.09	-0.38	0.194
mmu-miR-17	0.07	0.18	-0.04	0.197
mmu-miR-211	-0.08	0.05	-0.22	0.204
mmu-miR-188-5p	0.25	0.67	-0.17	0.205
mmu-let-7b	-0.16	0.11	-0.43	0.208
mmu-miR-361	1.12	2.99	-0.76	0.211
mmu-miR-409-3p	1.00	2.69	-0.70	0.217
mmu-miR-9	1.04	2.81	-0.73	0.218
mmu-miR-425*	-0.16	0.11	-0.42	0.222
mmu-miR-494	-0.25	0.19	-0.70	0.229
mmu-miR-130a	0.15	0.40	-0.11	0.230
snoRNA429	**0.46**	**1.28**	**-0.36**	**0.236**

Supplementary Table S13 (cont.)

		95% CI of the difference		
MicroRNA Assay ID	**Mean Difference**	**Upper**	**Lower**	***P*-value**
mmu-miR-103	-0.11	0.09	-0.31	0.236
mmu-miR-29b*	-0.36	0.28	-1.01	0.237
mmu-miR-133a	0.12	0.34	-0.10	0.237
mmu-miR-125a-5p	0.10	0.27	-0.08	0.238
rno-miR-463	-0.10	0.08	-0.27	0.239
mmu-miR-29a*	0.20	0.56	-0.16	0.244
mmu-miR-29c*	-0.11	0.09	-0.30	0.245
mmu-miR-342-3p	0.09	0.26	-0.08	0.247
mmu-miR-467c	1.16	3.28	-0.97	0.249
mmu-miR-326	0.12	0.33	-0.10	0.252
mmu-miR-342-5p	0.16	0.47	-0.14	0.253
mmu-miR-30e*	0.09	0.27	-0.08	0.256
mmu-miR-542-5p	0.89	2.56	-0.78	0.257
mmu-miR-331-3p	-0.08	0.07	-0.23	0.259
mmu-miR-425	0.08	0.22	-0.07	0.268
mmu-miR-467b	0.10	0.28	-0.09	0.268
mmu-miR-30c	-0.08	0.07	-0.23	0.270
mmu-miR-128a	0.94	2.76	-0.88	0.274
mmu-miR-410	-0.80	0.78	-2.38	0.283
mmu-miR-7a*	0.09	0.27	-0.09	0.289
mmu-miR-503*	-0.15	0.16	-0.46	0.295
mmu-miR-181a-1*	0.88	2.68	-0.92	0.299
mmu-miR-335-3p	0.11	0.33	-0.12	0.303
mmu-miR-20a*	0.16	0.49	-0.17	0.306
mmu-miR-100	0.12	0.37	-0.13	0.309
mmu-miR-190b	0.38	1.19	-0.42	0.313
mmu-miR-878-3p	-1.30	1.45	-4.05	0.313
mmu-miR-30b	-0.07	0.08	-0.22	0.313
rno-miR-352	-0.93	1.04	-2.90	0.315
mmu-miR-19b	-0.08	0.09	-0.24	0.316
rno-miR-224	-1.36	1.54	-4.27	0.317
mmu-miR-143	-0.09	0.10	-0.27	0.319
mmu-miR-652	0.11	0.34	-0.12	0.319
mmu-miR-351	0.12	0.39	-0.14	0.322
mmu-miR-804	0.75	2.36	-0.87	0.322
mmu-miR-486	-0.16	0.19	-0.52	0.323
mmu-miR-93*	-0.08	0.09	-0.24	0.324
mmu-miR-125a-3p	0.16	0.51	-0.19	0.326
rno-miR-345-3p	-0.17	0.21	-0.56	0.328
mmu-miR-30a	-0.08	0.10	-0.27	0.328
mmu-miR-101b	0.07	0.22	-0.08	0.329
rno-miR-136*	-1.16	1.42	-3.74	0.337
mmu-miR-28*	-0.06	0.07	-0.19	0.339
mmu-let-7g*	0.76	2.47	-0.96	0.343
mmu-miR-466b-3-3p	0.82	2.69	-1.04	0.344
mmu-miR-21*	-0.17	0.23	-0.58	0.357
mmu-miR-98	-0.14	0.18	-0.45	0.358
rno-miR-351	0.05	0.17	-0.07	0.360
mmu-miR-34a	0.95	3.21	-1.30	0.363
mmu-miR-324-3p	-0.11	0.16	-0.38	0.364
mmu-miR-877	-0.08	0.11	-0.27	0.364
mmu-miR-127	-0.27	0.38	-0.92	0.369
mmu-miR-362-3p	-0.25	0.36	-0.87	0.370
mmu-miR-30e	0.08	0.27	-0.11	0.371

Supplementary Table S13 (cont.)

		95% CI of the difference		
MicroRNA Assay ID	**Mean Difference**	**Upper**	**Lower**	***P*-value**
mmu-miR-30a*	-0.05	0.07	-0.16	0.377
mmu-miR-27b	-0.09	0.12	-0.30	0.377
mmu-miR-324-5p	-0.12	0.18	-0.43	0.384
mmu-miR-680	-0.07	0.10	-0.24	0.388
rno-miR-190b	-0.74	1.11	-2.60	0.390
mmu-miR-669a	0.82	2.87	-1.24	0.393
mmu-miR-133b	0.14	0.49	-0.21	0.394
mmu-miR-126-3p	0.06	0.22	-0.10	0.398
rno-miR-7a*	-0.04	0.07	-0.16	0.412
mmu-miR-497	0.10	0.37	-0.17	0.414
mmu-miR-30d	-0.06	0.09	-0.21	0.420
mmu-let-7a*	-0.11	0.19	-0.42	0.425
mmu-miR-155	-0.06	0.11	-0.24	0.428
mmu-miR-350	0.10	0.36	-0.17	0.432
mmu-miR-218-1*	-0.77	1.36	-2.91	0.432
mmu-miR-15a*	0.08	0.31	-0.15	0.438
mmu-miR-187	-0.04	0.08	-0.16	0.441
rno-miR-30d*	-0.11	0.20	-0.42	0.441
mmu-miR-146a	-0.06	0.12	-0.24	0.446
Y1	**0.06**	**0.23**	**-0.11**	**0.447**
mmu-miR-135a*	-0.08	0.15	-0.31	0.448
mmu-miR-135b	0.19	0.72	-0.35	0.455
rno-miR-148b-5p	0.12	0.49	-0.24	0.455
mmu-miR-28	-0.12	0.23	-0.46	0.457
rno-miR-1	0.64	2.50	-1.22	0.457
mmu-miR-672	-0.11	0.21	-0.43	0.462
mmu-miR-532-5p	0.09	0.34	-0.17	0.462
mmu-miR-151-3p	-0.05	0.10	-0.21	0.464
mmu-miR-221	0.70	2.82	-1.43	0.478
mmu-miR-181a	0.08	0.31	-0.16	0.483
mmu-miR-532-3p	0.06	0.25	-0.13	0.486
mmu-miR-676*	0.50	2.06	-1.07	0.491
mmu-miR-378	0.11	0.47	-0.25	0.492
mmu-miR-331-5p	-0.09	0.19	-0.37	0.493
mmu-miR-27a*	-0.08	0.18	-0.35	0.497
mmu-miR-106b*	0.09	0.37	-0.20	0.504
mmu-miR-320	-0.06	0.14	-0.26	0.508
mmu-miR-339-5p	-0.06	0.15	-0.27	0.510
mmu-miR-99b*	-0.62	1.51	-2.75	0.526
mmu-miR-214	-0.07	0.18	-0.33	0.532
mmu-miR-338-3p	0.65	2.97	-1.67	0.540
mmu-miR-34c*	-0.10	0.26	-0.46	0.540
mmu-miR-214*	0.07	0.32	-0.18	0.541
mmu-miR-671-3p	0.08	0.38	-0.21	0.542
mmu-miR-21	-0.03	0.09	-0.15	0.547
mmu-let-7f	-0.04	0.10	-0.18	0.548
rno-miR-196c	0.25	1.14	-0.65	0.550
mmu-let-7e	-0.05	0.14	-0.25	0.568
mmu-miR-124	0.76	3.65	-2.14	0.568
snoRNA202	**-0.05**	**0.15**	**-0.25**	**0.571**
mmu-miR-16	-0.03	0.10	-0.16	0.577
mmu-miR-200a	0.16	0.81	-0.48	0.582
mmu-miR-15b	-0.04	0.13	-0.22	0.590
mmu-miR-145	0.05	0.23	-0.14	0.591

Supplementary Table S13 (cont.)

		95% CI of the difference		
MicroRNA Assay ID	**Mean Difference**	**Upper**	**Lower**	***P*-value**
mmu-miR-376b*	-0.24	0.73	-1.20	0.594
mmu-miR-744	-0.05	0.15	-0.25	0.601
mmu-miR-467d	0.43	2.21	-1.36	0.602
mmu-miR-99a	-0.05	0.17	-0.28	0.602
mmu-miR-23b	-0.07	0.21	-0.35	0.604
mmu-miR-141	-0.10	0.32	-0.52	0.605
mmu-miR-301a	0.06	0.32	-0.20	0.609
mmu-miR-146b	0.05	0.26	-0.16	0.615
mmu-miR-223	0.06	0.30	-0.19	0.618
mmu-miR-106b	-0.05	0.17	-0.26	0.634
mmu-miR-339-3p	-0.05	0.17	-0.26	0.643
mmu-miR-872	-0.07	0.28	-0.43	0.646
rno-miR-673	-0.14	0.51	-0.78	0.646
mmu-miR-196b	0.05	0.32	-0.21	0.652
mmu-miR-429	0.13	0.81	-0.56	0.679
mmu-miR-26b*	0.04	0.27	-0.19	0.681
mmu-miR-19a	0.04	0.24	-0.17	0.685
mmu-miR-7b	-0.12	0.56	-0.80	0.693
mmu-miR-142-5p	-0.03	0.14	-0.21	0.695
mmu-miR-340-5p	-0.04	0.16	-0.23	0.696
mmu-miR-374	0.04	0.24	-0.16	0.697
mmu-miR-676	0.04	0.27	-0.19	0.701
mmu-miR-93	-0.03	0.15	-0.22	0.704
rno-miR-204*	0.08	0.55	-0.39	0.709
mmu-miR-500	0.55	3.78	-2.68	0.710
mmu-let-7a	-0.04	0.22	-0.31	0.713
mmu-miR-101a	0.03	0.19	-0.13	0.717
mmu-let-7g	-0.03	0.13	-0.18	0.719
mmu-miR-134	0.07	0.48	-0.35	0.724
mmu-miR-99b	0.04	0.26	-0.19	0.726
mmu-miR-16*	-0.07	0.39	-0.53	0.727
mmu-miR-301b	0.04	0.30	-0.22	0.728
mmu-miR-805	-0.04	0.20	-0.27	0.739
rno-miR-339-3p	-0.03	0.19	-0.26	0.744
mmu-miR-706	-0.04	0.22	-0.30	0.747
mmu-miR-33*	-0.04	0.25	-0.34	0.753
mmu-miR-704	0.41	3.30	-2.47	0.753
mmu-miR-27b*	-0.07	0.43	-0.57	0.754
mmu-miR-204	0.02	0.18	-0.14	0.757
mmu-miR-673-5p	0.40	3.26	-2.46	0.757
U87	**-0.03**	**0.16**	**-0.21**	**0.759**
mmu-miR-125b*	-0.06	0.38	-0.50	0.763
mmu-miR-27a	0.03	0.23	-0.17	0.769
mmu-miR-185	0.02	0.21	-0.16	0.774
mmu-miR-26b	0.02	0.17	-0.13	0.774
mmu-miR-1	0.06	0.58	-0.45	0.784
mmu-miR-206	-0.18	1.37	-1.73	0.799
mmu-miR-150	-0.02	0.15	-0.19	0.801
mmu-miR-193	0.04	0.44	-0.35	0.805
mmu-miR-199a-3p	-0.02	0.15	-0.19	0.807
mmu-miR-142-3p	-0.02	0.19	-0.23	0.812
mmu-miR-181c	0.04	0.45	-0.37	0.816
mmu-miR-182	-0.05	0.43	-0.52	0.819
mmu-miR-139-5p	-0.02	0.14	-0.18	0.823

Supplementary Table S13 (cont.)

		95% CI of the difference		
MicroRNA Assay ID	**Mean Difference**	**Upper**	**Lower**	***P*-value**
mmu-miR-200b	-0.06	0.54	-0.67	0.824
mmu-miR-466d-3p	-0.03	0.25	-0.30	0.827
mmu-miR-22*	0.03	0.30	-0.24	0.828
mmu-miR-222	0.02	0.19	-0.16	0.845
mmu-miR-200c	0.03	0.38	-0.32	0.847
mmu-miR-24	-0.01	0.14	-0.17	0.852
mmu-miR-138	0.02	0.23	-0.19	0.863
mmu-miR-26a	-0.01	0.15	-0.17	0.874
mmu-miR-20a	0.01	0.13	-0.11	0.877
mmu-miR-138*	-0.04	0.65	-0.74	0.888
mmu-let-7d	-0.01	0.19	-0.22	0.896
mmu-miR-667	-0.17	2.75	-3.10	0.897
mmu-miR-328	-0.01	0.16	-0.18	0.900
mmu-miR-191	-0.01	0.19	-0.21	0.900
mmu-miR-872*	0.01	0.18	-0.16	0.907
mmu-miR-29c	-0.01	0.21	-0.24	0.909
mmu-miR-696	-0.02	0.32	-0.36	0.909
mmu-miR-376a	0.04	1.07	-0.98	0.928
mmu-miR-18a*	0.01	0.31	-0.29	0.940
mmu-miR-106a	0.01	0.19	-0.18	0.951
mmu-miR-491	-0.01	0.38	-0.39	0.974
mmu-let-7i	0.00	0.20	-0.21	0.975
mmu-miR-678	-0.03	2.67	-2.72	0.982

Supplementary Table S14 (Chapter 4): Association of MicroRNA expression and lifespan in mouse spleen tissue across 6 strains of different longevities

Data from mice of all ages, young mice only (6 months) and old mice only (20-22 months) are given separately. MicroRNAs significantly associated below the Bonferroni-corrected significance threshold ($p<0.005$) are shown in bold italics. *P*-values were determined from linear regression of log-transformed relative expression data.

	ALL MICE			**YOUNG MICE ONLY**			**OLD MICE ONLY**		
	Beta coefficient	**Std. Error**	***P*-value**	**Beta coefficient**	**Std. Error**	***P*-value**	**Beta coefficient**	**Std. Error**	***P*-value**
miR-192-5p	0.16	0.00	0.14	0.12	0.00	0.49	0.20	0.00	0.20
miR-203-3p	***-0.64***	***0.00***	***<0.001***	***-0.67***	***0.00***	***<0.001***	***-0.67***	***0.00***	***<0.001***
miR-224-5p	-0.09	0.00	0.44	-0.23	0.00	0.16	0.02	0.00	0.91
miR-297b-5p	0.16	0.00	0.15	0.14	0.00	0.41	0.18	0.00	0.22
miR-484	-0.07	0.00	0.55	-0.21	0.00	0.21	0.08	0.00	0.61
miR-592	0.16	0.00	0.15	0.08	0.00	0.65	0.23	0.00	0.13
miR-664-3p	***0.56***	***0.00***	***<0.001***	0.42	0.00	0.01	***0.75***	***0.00***	***<0.001***
miR-687	0.20	0.00	0.11	0.17	0.00	0.39	0.23	0.00	0.18
miR-708-5p	***0.50***	***0.00***	***<0.001***	0.37	0.00	0.02	***0.64***	***0.00***	***<0.001***
miR-327	-0.21	0.00	0.06	-0.38	0.00	0.02	-0.09	0.00	0.54

Supplementary Table S15 (Chapter 4): Sub analysis of the relationship between miRNA expression and median strain longevity in spleen samples from animals not included in the initial global analysis

Data from mice of all ages, young mice only (6 months) and old mice only (20-22 months) are given separately. MicroRNAs significantly associated below the Bonferroni-corrected significance threshold (p<0.005) are shown in bold italics. *P*-values were determined from linear regression of log-transformed relative expression data.

	ALL MICE			**YOUNG MICE ONLY**			**OLD MICE ONLY**		
	Beta coefficient	**Std. Error**	***P*-value**	**Beta coefficient**	**Std. Error**	***P*-value**	**Beta coefficient**	**Std. Error**	***P*-value**
miR-192-5p	0.08	0.00	0.50	-0.21	0.00	0.30	0.20	0.00	0.20
miR-203-3p	***-0.51***	***0.00***	***<0.001***	-0.10	0.00	0.64	***-0.70***	***0.00***	***<0.001***
miR-224-5p	0.17	0.00	0.16	***0.82***	***0.00***	***<0.001***	0.02	0.00	0.90
miR-297b-5p	0.11	0.00	0.38	-0.20	0.00	0.33	0.19	0.00	0.22
miR-484	0.12	0.00	0.30	0.31	0.00	0.12	0.08	0.00	0.61
miR-592	0.10	0.00	0.41	-0.38	0.00	0.06	0.22	0.00	0.15
miR-664-3p	***0.56***	***0.00***	***<0.001***	0.47	0.00	0.02	***0.75***	***0.00***	***<0.001***
miR-687	0.17	0.00	0.21	0.02	0.01	0.93	0.23	0.00	0.18
miR-708-5p	***0.41***	***0.00***	***<0.001***	-0.50	0.01	0.01	***0.64***	***0.00***	***<0.001***
rno-miR-327	-0.18	0.00	0.14	***-0.54***	***0.00***	***0.004***	-0.10	0.00	0.54

Supplementary Table S16 (Chapter 4): Association of MicroRNA expression and age in mouse spleen tissue across 6 strains of different longevities

Data from mice of all ages, 'Average-lived' mice only (<847.5 days) and 'Long-lived' mice only (>847.5 days) are given separately. MicroRNAs significantly associated below the Bonferroni-corrected significance threshold (p<0.005) are shown in bold italics. *P*-values were determined from linear regression of log-transformed relative expression data.

	ALL MICE			**AVERAGE-LIVED MICE ONLY**			**LONG-LIVED MICE ONLY**		
	Beta coefficient	**Std. Error**	***P*-value**	**Beta coefficient**	**Std. Error**	***P*-value**	**Beta coefficient**	**Std. Error**	***P*-value**
miR-192-5p	0.12	0.04	0.27	0.00	0.07	0.99	0.20	0.05	0.16
miR-203-3p	0.18	0.06	0.11	0.09	0.10	0.63	0.30	0.05	0.03
miR-224-5p	-0.01	0.11	0.95	-0.14	0.17	0.44	0.09	0.13	0.55
miR-297b-5p	-0.09	0.08	0.41	-0.10	0.15	0.58	-0.09	0.09	0.55
miR-484	0.10	0.04	0.35	0.04	0.06	0.81	0.14	0.05	0.33
miR-592	***0.44***	***0.05***	***<0.001***	0.37	0.07	0.03	***0.57***	***0.06***	***<0.001***
miR-664-3p	0.04	0.41	0.77	0.12	0.41	0.58	0.02	0.62	0.90
miR-687	0.26	0.08	0.02	0.12	0.17	0.49	***0.50***	***0.06***	***<0.001***
miR-708-5p	0.03	0.09	0.77	-0.05	0.17	0.78	0.13	0.08	0.38
rno-miR-327	-0.08	0.12	0.46	-0.07	0.22	0.72	-0.11	0.13	0.43

Supplementary Table S17 (Chapter 4): Analyses of potential interactions between mouse strain longevity and mouse age

Std. Error = standard error, 95% CI = 95% confidence intervals. Mouse strains were categorised for this analysis based on whether the median individual strain lifespan was above or below the median lifespan calculated across all strains, with 'Average-lived' being <847.5 days and 'Long-lived' >847.5 days. Young mice are 6 months and old mice are 20-22 months old. Statistically significant results are indicated in bold italic text.

Longevity:age interactions - microRNAs associated with lifespan					
MicroRNA	**Sub-category**	**β coefficient**	**Std. Error**	**95% CI**	***p*-value**
mmu-miR-203-3p	Average-lived/Young	0			
	Average-lived/Old	0.05	0.08	-0.11 to 0.21	0.55
	Long-lived/Young	-0.29	0.08	-0.44 to -0.13	***0.0004***
	Long-lived/Old	-0.17	0.08	-0.32 to -0.02	***0.03***
mmu-miR-664-3p	Average-lived/Young	0			
	Average-lived/Old	0.15	0.07	0.01 to 0.29	***0.04***
	Long-lived/Young	0.18	0.07	0.04 to 0.31	***0.01***
	Long-lived/Old	0.46	0.07	0.33 to 0.60	***6.59E-10***
mmu-miR-708-5p	Average-lived/Young	0			
	Average-lived/Old	0.12	0.12	-0.12 to 0.36	0.33
	Long-lived/Young	0.08	0.12	-0.15 to 0.31	0.49
	Long-lived/Old	0.31	0.11	0.09 to 0.53	***0.007***

Supplementary Table S18 (Chapter 4): Taqman® Low Density Array card contents

Assay names and unique assay IDs are given for all microRNAs tested using each array layout.

Rodent A Array v2.0					
Assay ID	**Assay Name**	**Assay ID**	**Assay Name**	**Assay ID**	**Assay Name**
000377	mmu-let-7a	002592	mmu-miR-291a-3p	002456	mmu-miR-503
000378	mmu-let-7b	002537	mmu-miR-291b-5p	002084	mmu-miR-504
000379	mmu-let-7c	002593	mmu-miR-292-3p	001655	mmu-miR-505
002283	mmu-let-7d	001794	mmu-miR-293	002521	mmu-miR-509-3p
002406	mmu-let-7e	001056	mmu-miR-294	002520	mmu-miR-509-5p
000382	mmu-let-7f	000189	mmu-miR-295	002549	mmu-miR-511
002282	mmu-let-7g	002101	mmu-miR-296-3p	002355	mmu-miR-532-3p
002221	mmu-let-7i	000527	mmu-miR-296-5p	001518	mmu-miR-532-5p
002222	mmu-miR-1	001626	mmu-miR-297b-5p	001286	mmu-miR-539
000437	mmu-miR-100	002480	mmu-miR-297c	001310	mmu-miR-540-3p
002253	mmu-miR-101a	002598	mmu-miR-298	002561	mmu-miR-540-5p
000439	mmu-miR-103	002112	mmu-miR-29a	001284	mmu-miR-542-3p
002465	mmu-miR-105	000413	mmu-miR-29b	002563	mmu-miR-542-5p
002459	mmu-miR-106a	000587	mmu-miR-29c	002376	mmu-miR-543
000442	mmu-miR-106b	000528	mmu-miR-301a	002550	mmu-miR-544
000443	mmu-miR-107	002600	mmu-miR-301b	001312	mmu-miR-546
000387	mmu-miR-10a	000529	mmu-miR-302a	002564	mmu-miR-547
002218	mmu-miR-10b	000531	mmu-miR-302b	001535	mmu-miR-551b
002245	mmu-miR-122	002558	mmu-miR-302c	002349	mmu-miR-574-3p
001182	mmu-miR-124	000535	mmu-miR-302d	002567	mmu-miR-582-3p
002199	mmu-miR-125a-3p	000417	mmu-miR-30a	002566	mmu-miR-582-5p
002198	mmu-miR-125a-5p	000602	mmu-miR-30b	001984	mmu-miR-590-5p
002378	mmu-miR-125b-3p	000419	mmu-miR-30c	002476	mmu-miR-598
000449	mmu-miR-125b-5p	000420	mmu-miR-30d	001960	mmu-miR-615-3p
002228	mmu-miR-126-3p	002223	mmu-miR-30e	002353	mmu-miR-615-5p
000451	mmu-miR-126-5p	000185	mmu-miR-31	002352	mmu-miR-652
000452	mmu-miR-127	002109	mmu-miR-32	002239	mmu-miR-654-3p
002216	mmu-miR-128a	002277	mmu-miR-320	002522	mmu-miR-654-5p
001184	mmu-miR-129-3p	001076	mmu-miR-322	002607	mmu-miR-665
000590	mmu-miR-129-5p	002227	mmu-miR-323-3p	001952	mmu-miR-666-5p
000454	mmu-miR-130a	002509	mmu-miR-324-3p	001949	mmu-miR-667
000456	mmu-miR-130b	000539	mmu-miR-324-5p	001947	mmu-miR-668
000457	mmu-miR-132	002510	mmu-miR-325	001683	mmu-miR-669a
002246	mmu-miR-133a	000543	mmu-miR-328	002020	mmu-miR-670
002247	mmu-miR-133b	000192	mmu-miR-329	002322	mmu-miR-671-3p
001186	mmu-miR-134	002230	mmu-miR-330	002327	mmu-miR-672
000460	mmu-miR-135a	000545	mmu-miR-331-3p	002021	mmu-miR-674
002261	mmu-miR-135b	002233	mmu-miR-331-5p	001941	mmu-miR-675-3p
002511	mmu-miR-136	002185	mmu-miR-335-3p	001940	mmu-miR-675-5p
001129	mmu-miR-137	000546	mmu-miR-335-5p	001959	mmu-miR-676
002284	mmu-miR-138	002532	mmu-miR-337-3p	001660	mmu-miR-677
002546	mmu-miR-139-3p	002515	mmu-miR-337-5p	001662	mmu-miR-679
002289	mmu-miR-139-5p	002252	mmu-miR-338-3p	001664	mmu-miR-680
001187	mmu-miR-140	002533	mmu-miR-339-3p	001666	mmu-miR-682
000463	mmu-miR-141	002257	mmu-miR-339-5p	001668	mmu-miR-683
000464	mmu-miR-142-3p	002259	mmu-miR-340-3p	001669	mmu-miR-684
002248	mmu-miR-142-5p	002258	mmu-miR-340-5p	001670	mmu-miR-685
002249	mmu-miR-143	002260	mmu-miR-342-3p	001672	mmu-miR-686
002278	mmu-miR-145	002527	mmu-miR-342-5p	001674	mmu-miR-687
000468	mmu-miR-146a	001063	mmu-miR-344	002341	mmu-miR-708
001097	mmu-miR-146b	002529	mmu-miR-345-3p	002457	mmu-miR-741
002262	mmu-miR-147	002528	mmu-miR-345-5p	002038	mmu-miR-742
000470	mmu-miR-148a	001064	mmu-miR-346	002469	mmu-miR-743a
000471	mmu-miR-148b	000426	mmu-miR-34a	002471	mmu-miR-743b-3p
000473	mmu-miR-150	002618	mmu-miR-34b-3p	002470	mmu-miR-743b-5p

Supplementary Table S18 (cont.)

Rodent A Array v2.0					
Assay ID	**Assay Name**	**Assay ID**	**Assay Name**	**Assay ID**	**Assay Name**
001190	mmu-miR-151-3p	000428	mmu-miR-34c	002324	mmu-miR-744
000475	mmu-miR-152	002530	mmu-miR-350	002027	mmu-miR-770-3p
001191	mmu-miR-153	001067	mmu-miR-351	000268	mmu-miR-7a
000477	mmu-miR-154	000554	mmu-miR-361	002555	mmu-miR-7b
002571	mmu-miR-155	002616	mmu-miR-362-3p	002029	mmu-miR-802
000389	mmu-miR-15a	001271	mmu-miR-363	002354	mmu-miR-871
000390	mmu-miR-15b	001020	mmu-miR-365	002264	mmu-miR-872
000391	mmu-miR-16	000555	mmu-miR-367	002356	mmu-miR-873
002308	mmu-miR-17	000557	mmu-miR-369-3p	002268	mmu-miR-874
000480	mmu-miR-181a	001021	mmu-miR-369-5p	002547	mmu-miR-875-3p
000482	mmu-miR-181c	002275	mmu-miR-370	002464	mmu-miR-876-3p
002599	mmu-miR-182	000564	mmu-miR-375	002463	mmu-miR-876-5p
002269	mmu-miR-183	001069	mmu-miR-376a	002540	mmu-miR-878-5p
000485	mmu-miR-184	002452	mmu-miR-376b	002472	mmu-miR-879
002271	mmu-miR-185	002450	mmu-miR-376c	002609	mmu-miR-881
002285	mmu-miR-186	000566	mmu-miR-377	002461	mmu-miR-883a-3p
001193	mmu-miR-187	001138	mmu-miR-379	002611	mmu-miR-883a-5p
002106	mmu-miR-188-3p	001071	mmu-miR-380-3p	002565	mmu-miR-883b-3p
002320	mmu-miR-188-5p	002601	mmu-miR-380-5p	000583	mmu-miR-9
002422	mmu-miR-18a	000571	mmu-miR-381	000430	mmu-miR-92a
002466	mmu-miR-18b	000572	mmu-miR-382	001090	mmu-miR-93
000489	mmu-miR-190	001767	mmu-miR-383	000186	mmu-miR-96
002299	mmu-miR-191	002603	mmu-miR-384-3p	000577	mmu-miR-98
000491	mmu-miR-192	002602	mmu-miR-384-5p	000435	mmu-miR-99a
002250	mmu-miR-193	002332	mmu-miR-409-3p	000436	mmu-miR-99b
002467	mmu-miR-193b	002331	mmu-miR-409-5p	002064	rno-miR-1
000493	mmu-miR-194	001274	mmu-miR-410	002078	rno-miR-17-3p
000494	mmu-miR-195	001610	mmu-miR-411	002048	rno-miR-190b
002215	mmu-miR-196b	002340	mmu-miR-423-5p	002049	rno-miR-196c
000497	mmu-miR-197	001516	mmu-miR-425	001315	rno-miR-207
002304	mmu-miR-199a-3p	001077	mmu-miR-429	002052	rno-miR-20b-3p
000498	mmu-miR-199a-5p	001979	mmu-miR-431	002077	rno-miR-219-1-3p
000395	mmu-miR-19a	001028	mmu-miR-433	002390	rno-miR-219-2-3p
000396	mmu-miR-19b	002604	mmu-miR-434-3p	000599	rno-miR-224
000502	mmu-miR-200a	002581	mmu-miR-434-5p	001328	rno-miR-327
002251	mmu-miR-200b	001029	mmu-miR-448	001329	rno-miR-333
002300	mmu-miR-200c	001030	mmu-miR-449a	001331	rno-miR-336
002578	mmu-miR-201	002539	mmu-miR-449b	002059	rno-miR-339-3p
001195	mmu-miR-202-3p	002303	mmu-miR-450a-5p	001344	rno-miR-343
000507	mmu-miR-203	001962	mmu-miR-450b-5p	001332	rno-miR-344-3p
000508	mmu-miR-204	001141	mmu-miR-451	002060	rno-miR-344-5p
000509	mmu-miR-205	001032	mmu-miR-452	002061	rno-miR-345-3p
001198	mmu-miR-207	002484	mmu-miR-453	001333	rno-miR-346
000511	mmu-miR-208	002455	mmu-miR-455	001334	rno-miR-347
002290	mmu-miR-208b	001081	mmu-miR-464	001335	rno-miR-349
000580	mmu-miR-20a	002040	mmu-miR-465a-3p	002063	rno-miR-351
001014	mmu-miR-20b	001082	mmu-miR-465a-5p	001320	rno-miR-377
000397	mmu-miR-21	002485	mmu-miR-465b-5p	001322	rno-miR-381
000512	mmu-miR-210	002516	mmu-miR-466h	001317	rno-miR-409-5p
001199	mmu-miR-211	002587	mmu-miR-467a	001343	rno-miR-421
002306	mmu-miR-214	001671	mmu-miR-467b	001345	rno-miR-450a
001200	mmu-miR-215	002517	mmu-miR-467c	002066	rno-miR-466b
002220	mmu-miR-216a	002518	mmu-miR-467d	002067	rno-miR-466c
002326	mmu-miR-216b	002568	mmu-miR-467e	001316	rno-miR-505
002556	mmu-miR-217	001085	mmu-miR-468	002051	rno-miR-532-5p
000521	mmu-miR-218	001086	mmu-miR-469	002065	rno-miR-543
000522	mmu-miR-219	002588	mmu-miR-470	002053	rno-miR-598-5p

Supplementary Table S18 (cont.)

Rodent A Array v2.0					
Assay ID	**Assay Name**	**Assay ID**	**Assay Name**	**Assay ID**	**Assay Name**
002468	mmu-miR-220	001821	mmu-miR-484	002054	rno-miR-673
000524	mmu-miR-221	001278	mmu-miR-486	002055	rno-miR-742
002276	mmu-miR-222	001285	mmu-miR-487b	002068	rno-miR-743b
002295	mmu-miR-223	001659	mmu-miR-488	001990	rno-miR-758
002553	mmu-miR-224	001302	mmu-miR-489	002057	rno-miR-760-5p
000399	mmu-miR-23a	001037	mmu-miR-490	002069	rno-miR-871
000400	mmu-miR-23b	001630	mmu-miR-491	002070	rno-miR-878
000402	mmu-miR-24	002519	mmu-miR-493	002072	rno-miR-881
000403	mmu-miR-25	002365	mmu-miR-494	000338	ath-miR159a
000405	mmu-miR-26a	001663	mmu-miR-495	001973	Mamm U6
000407	mmu-miR-26b	001953	mmu-miR-496	001230	snoRNA135
000408	mmu-miR-27a	001346	mmu-miR-497	001232	snoRNA202
000409	mmu-miR-27b	001352	mmu-miR-499	001712	U87
000411	mmu-miR-28	002606	mmu-miR-500	001727	Y1
002591	mmu-miR-290-3p	001651	mmu-miR-501-3p		

Rodent Array B					
Assay ID	**Assay Name**	**Assay ID**	**Assay Name**	**Assay ID**	**Assay Name**
002478	mmu-let-7a*	002498	mmu-miR-30b*	001642	mmu-miR-707
002479	mmu-let-7c-1*	002495	mmu-miR-31*	001646	mmu-miR-711
001178	mmu-let-7d*	002506	mmu-miR-322*	001961	mmu-miR-712*
002492	mmu-let-7g*	001060	mmu-miR-325*	001648	mmu-miR-713
002507	mmu-miR-101a*	001061	mmu-miR-326	001649	mmu-miR-715
002531	mmu-miR-101b	002481	mmu-miR-327	001652	mmu-miR-717
002572	mmu-miR-10b*	002136	mmu-miR-33*	001656	mmu-miR-718
002508	mmu-miR-125b*	001062	mmu-miR-330*	001673	mmu-miR-719
002229	mmu-miR-127*	002483	mmu-miR-343	001629	mmu-miR-720
002460	mmu-miR-130b*	002584	mmu-miR-34c*	001657	mmu-miR-721
001637	mmu-miR-133a*	002043	mmu-miR-374*	002034	mmu-miR-759
002512	mmu-miR-136*	002482	mmu-miR-376a*	002028	mmu-miR-762
002554	mmu-miR-138*	002451	mmu-miR-376b*	002033	mmu-miR-763
002513	mmu-miR-141*	002523	mmu-miR-376c*	002032	mmu-miR-764-3p
002514	mmu-miR-145*	001078	mmu-miR-433*	002031	mmu-miR-764-5p
002453	mmu-miR-146b*	002525	mmu-miR-450a-3p	002044	mmu-miR-804
002570	mmu-miR-150*	002582	mmu-miR-463*	002045	mmu-miR-805
002488	mmu-miR-15a*	002586	mmu-miR-466a-3p	002542	mmu-miR-872*
002489	mmu-miR-16*	002500	mmu-miR-466b-3-3p	002548	mmu-miR-877*
002543	mmu-miR-17*	002534	mmu-miR-466d-5p	002541	mmu-miR-878-3p
002270	mmu-miR-183*	001826	mmu-miR-467a*	002473	mmu-miR-879*
002574	mmu-miR-186*	001684	mmu-miR-467b*	002475	mmu-miR-881*
002490	mmu-miR-18a*	002569	mmu-miR-467e*	002231	mmu-miR-9*
002576	mmu-miR-191*	002589	mmu-miR-470*	002496	mmu-miR-92a*
002577	mmu-miR-193*	002560	mmu-miR-483*	001351	rno-miR-1*
002477	mmu-miR-196a*	001943	mmu-miR-485*	002074	rno-miR-125b*
001131	mmu-miR-199b*	002014	mmu-miR-488*	002075	rno-miR-135a*
002544	mmu-miR-19a*	002536	mmu-miR-503*	002058	rno-miR-148b-5p
002491	mmu-miR-20a*	002017	mmu-miR-592	002076	rno-miR-204*
002524	mmu-miR-20b*	002449	mmu-miR-673-3p	001336	rno-miR-20a*
002493	mmu-miR-21*	001956	mmu-miR-674*	002079	rno-miR-24-1*
002293	mmu-miR-214*	001958	mmu-miR-676*	002080	rno-miR-25*
002552	mmu-miR-218-1*	001675	mmu-miR-688	002082	rno-miR-29b-1*
002494	mmu-miR-24-2*	001677	mmu-miR-690	001339	rno-miR-352
002545	mmu-miR-28*	001678	mmu-miR-691	002081	rno-miR-379*
002538	mmu-miR-291b-3p	001679	mmu-miR-692	001354	rno-miR-382*
001055	mmu-miR-292-5p	002036	mmu-miR-693-3p	001353	rno-miR-489
002594	mmu-miR-293*	001681	mmu-miR-694	001323	rno-miR-664
002595	mmu-miR-294*	001627	mmu-miR-695	002056	rno-miR-743a
002454	mmu-miR-297a*	001628	mmu-miR-696	002062	rno-miR-7a*

Supplementary Table S18 (cont.)

Rodent Array B					
Assay ID	**Assay Name**	**Assay ID**	**Assay Name**	**Assay ID**	**Assay Name**
000600	mmu-miR-299*	001631	mmu-miR-697	002073	rno-miR-99a*
002497	mmu-miR-29b*	001632	mmu-miR-698	000338	ath-miR159a
000191	mmu-miR-300	001634	mmu-miR-700	001973	Mamm U6
002613	mmu-miR-300*	001635	mmu-miR-701	001230	snoRNA135
002615	mmu-miR-302a*	001636	mmu-miR-702	001232	snoRNA202
001307	mmu-miR-302b*	001639	mmu-miR-704	001712	U87
002557	mmu-miR-302c*	001641	mmu-miR-706	001727	Y1

Supplementary Table S19 (Chapter 4): MicroRNA assays used for targeted analysis

Assay names, IDs and miRBase/NCBI information are given for the assays used to follow up the ten most strongly associated microRNAs from the TaqMan® MicroRNA Array analysis. Endogenous control small RNA assays used for this analysis are shown in italics.

miRBase ID	Assay Name	Assay ID	miRBase/NCBI Accession Number
mmu-miR-192-5p	hsa-miR-192	000491	MIMAT0000517
mmu-miR-203-3p	hsa-miR-203	000507	MIMAT0000236
mmu-miR-224-5p	mmu-miR-224	002553	MIMAT0000671
mmu-miR-297b-5p	mmu-miR-297b	001626	MIMAT0003480
mmu-miR-484	hsa-miR-484	001821	MIMAT0003127
mmu-mir-592-5p	mmu-mir-592	002017	MIMAT0003730
mmu-miR-664-3p	rno-miR-664	001323	MIMAT0012774
mmu-miR-687	mmu-miR-687	001674	MIMAT0003466
mmu-miR-708-5p	mmu-miR-708	002341	MIMAT0004828
rno-miR-327	rno-miR-327	001328	MIMAT0000561
N/A	*snoRNA202*	*001232*	*AF357327*
N/A	*U6 snRNA*	*001973*	*NR_004394*
N/A	*U87*	*001712*	*AF272707*

Supplementary Table S20 (Chapter 4): mRNA assays used for predicted target analysis

Assay IDs and NCBI information are given for the assays used to follow up the genes predicted to be targeted by the candidate microRNAs as determined by the DIANA-miRPath analysis. Endogenous control assays used for this analysis are shown in italics.

Gene Symbol	Assay ID	NCBI Accession Number
Acvr2a	Mm01331097_m1	NM_007396.4
Dusp5	Mm01266106_m1	NM_001085390.1
Fgf7	Mm00433292_m1	NM_008008.4
Gabarapl1	Mm00457880_m1	NM_020590.4
Mmp9	Mm00442991_m1	NM_013599.3
Pten	Mm01212530_m1	NM_008960.2
Rps6ka3	Mm00455829_m1	NM_148945.2
Smad4	Mm01262405_m1	NM_008540.2
Zfhx3	Mm01240016_m1	NM_007496.2
Gusb	*Mm01197698_m1*	*NM_010368.1*
Idh3b	*Mm00504589_m1*	*NM_130884.4*

Supplementary Table S21 (Chapter 5): Taqman® Assays

Splicing factor target genes, assay IDs and qPCR software settings for each transcript included in the current study. Endogenous control genes used are shown in bold italics.

Target	Assay ID	Threshold	Baseline Start	Baseline End
Hnrnpa0	Mm03809085_s1	0.075	3	22
Hnrnpa1	Mm02528230_g1	0.098	3	18
Hnrnpa2b1	Mm01325931_g1	0.145	3	18
Hnrnpd	Mm01201314_m1	0.112	3	21
Hnrnph3	Mm01032120_g1	0.095	3	24
Hnrnpk	Mm01349462_m1	0.129	3	18
Hnrnpm	Mm00513070_m1	0.068	3	21
Hnrnpul2	Mm01230949_m1	0.114	3	21
Pnisr	Mm01219239_m1	0.052	3	20
Srsf1	Mm00557620_m1	0.123	3	21
Srsf2	Mm00448705_m1	0.040	3	20
Srsf3	Mm00786953_s1	0.044	3	23
Srsf6	Mm00471475_m1	0.074	3	21
Tra2b	Mm00833637_mH	0.031	3	21
Sf1	Mm00496060_m1	0.104	3	19
Sf3b1	Mm00473100_m1	0.044	3	19
Gusb	***Mm01197698_m1***	***0.092***	***3***	***21***
Idh3b	***Mm00504589_m1***	***0.112***	***3***	***18***
Ppia	***Mm03024003_g1***	***0.068***	***3***	***17***

Supplementary Table S22 (Chapter 5): Changes in splicing factor expression with long-term and short-term 40% DR in non-responder mice

Changes in splicing factor expression levels with long-term and short-term DR in brain, heart and kidney tissues from mice which display no change in lifespan under 40% DR conditions (TejJ89), by ANCOVA. A positive mean difference denotes an increase in expression levels under 40% DR conditions when compared to AL feeding. Transcripts showing nominal associations (p<0.05) are shown in italic and underlined. SE: standard error, 95% CI: 95% confidence intervals.

		Brain – Short-term DR					Brain – Long-term DR				
		Mean Difference	SE	*p*-value	95% CI lower	95% CI upper	Mean Difference	SE	*p*-value	95% CI lower	95% CI upper
Splicing Factors	*Hnrnpa0*	0.360	0.203	0.102	0.803	-0.083	0.188	0.208	0.383	0.641	-0.264
	Hnrnpa1	0.326	0.187	0.109	0.739	-0.086	-0.175	0.204	0.407	0.269	-0.619
	Hnrnpa2b1	0.029	0.192	0.882	0.447	-0.389	0.161	0.113	0.182	0.408	-0.086
	Hnrnpd	0.200	0.121	0.123	0.463	-0.063	0.194	0.121	0.136	0.459	-0.070
	Hnrnph3	-0.192	0.135	0.181	0.103	-0.487	-0.063	0.161	0.701	0.287	-0.413
	Hnrnpk	0.082	0.112	0.482	0.329	-0.165	-0.131	0.131	0.335	0.153	-0.416
	Hnrnpm	-0.220	0.211	0.318	0.240	-0.679	0.150	0.136	0.293	0.447	-0.147
	Hnrnpul2	0.027	0.121	0.830	0.291	-0.238	0.179	0.125	0.178	0.451	-0.094
	Pnisr	-0.181	0.161	0.284	0.171	-0.532	0.305	0.186	0.126	0.709	-0.099
	Srsf1	-0.257	0.235	0.294	0.254	-0.769	0.044	0.144	0.766	0.357	-0.270
	Srsf2	-0.130	0.168	0.456	0.237	-0.496	-0.157	0.186	0.414	0.248	-0.562
	Srsf3	0.283	0.137	0.063	0.584	-0.018	-0.252	0.197	0.225	0.177	-0.681
	Srsf6	*0.837*	*0.297*	*0.015*	*1.483*	*0.190*	-0.187	0.251	0.470	0.359	-0.734
	Tra2b	-0.190	0.133	0.179	0.100	-0.480	-0.188	0.100	0.085	0.030	-0.406
Core	*Sf1*	0.232	0.163	0.183	0.590	-0.127	-0.070	0.146	0.638	0.247	-0.388
	Sf3b1	-0.170	0.168	0.330	0.195	-0.536	-0.162	0.191	0.414	0.255	-0.578

		Heart – Short-term DR					Heart – Long-term DR				
		Mean Difference	SE	*p*-value	95% CI lower	95% CI upper	Mean Difference	SE	*p*-value	95% CI lower	95% CI upper
Splicing Factors	*Hnrnpa0*	-0.135	0.111	0.249	0.108	-0.378	0.077	0.161	0.642	0.430	-0.277
	Hnrnpa1	-0.115	0.146	0.448	0.204	-0.433	0.112	0.190	0.566	0.531	-0.306
	Hnrnpa2b1	0.135	0.158	0.411	0.480	-0.210	-0.205	0.121	0.119	0.062	-0.473
	Hnrnpd	0.115	0.104	0.292	0.341	-0.112	-0.029	0.117	0.810	0.228	-0.286
	Hnrnph3	0.000	0.114	0.997	0.247	-0.248	0.056	0.113	0.630	0.303	-0.192
	Hnrnpk	-0.065	0.153	0.681	0.269	-0.398	-0.156	0.157	0.340	0.189	-0.501
	Hnrnpm	-0.195	0.193	0.332	0.225	-0.615	-0.029	0.080	0.721	0.149	-0.208
	Hnrnpul2	0.003	0.104	0.980	0.230	-0.224	-0.096	0.196	0.632	0.334	-0.527
	Pnisr	0.023	0.102	0.826	0.244	-0.199	0.109	0.171	0.535	0.485	-0.266
	Srsf1	-0.020	0.297	0.948	0.627	-0.666	0.280	0.290	0.355	0.918	-0.358
	Srsf2	-0.109	0.131	0.423	0.176	-0.394	0.208	0.154	0.205	0.547	-0.132
	Srsf3	0.113	0.142	0.439	0.422	-0.195	0.318	0.171	0.091	0.695	-0.059
	Srsf6	0.143	0.210	0.511	0.601	-0.316	0.020	0.212	0.928	0.487	-0.448
	Tra2b	-0.086	0.093	0.375	0.117	-0.288	-0.091	0.143	0.541	0.229	-0.410
Core	*Sf1*	-0.239	0.190	0.232	0.174	-0.652	-0.219	0.213	0.327	0.250	-0.687
	Sf3b1	-0.021	0.175	0.905	0.363	-0.406	-0.048	0.214	0.826	0.423	-0.519

		Kidney – Short-term DR					Kidney – Long-term DR				
		Mean Difference	SE	*p*-value	95% CI lower	95% CI upper	Mean Difference	SE	*p*-value	95% CI lower	95% CI upper
Splicing Factors	*Hnrnpa0*	-0.371	0.176	0.064	0.027	-0.769	0.028	0.199	0.891	0.462	-0.406
	Hnrnpa1	0.263	0.143	0.096	0.581	-0.056	0.141	0.130	0.300	0.426	-0.143
	Hnrnpa2b1	-0.137	0.153	0.395	0.210	-0.483	0.117	0.145	0.436	0.435	-0.201
	Hnrnpd	-0.230	0.155	0.168	0.115	-0.575	*-0.196*	*0.086*	*0.041*	*-0.010*	*-0.383*
	Hnrnph3	-0.182	0.151	0.254	0.154	-0.519	0.088	0.174	0.624	0.467	-0.292
	Hnrnpk	-0.360	0.165	0.054	0.007	-0.727	-0.082	0.074	0.290	0.079	-0.242
	Hnrnpm	-0.047	0.213	0.829	0.428	-0.522	-0.129	0.090	0.178	0.067	-0.325
	Hnrnpul2	-0.101	0.256	0.703	0.469	-0.671	*-0.403*	*0.134*	*0.011*	*-0.112*	*-0.695*
	Pnisr	0.237	0.182	0.222	0.643	-0.169	-0.170	0.103	0.124	0.054	-0.394
	Srsf1	-0.148	0.141	0.316	0.165	-0.461	-0.016	0.100	0.874	0.202	-0.235
	Srsf2	0.316	0.191	0.128	0.740	-0.109	*0.299*	*0.102*	*0.012*	*0.521*	*0.077*
	Srsf3	-0.035	0.231	0.882	0.479	-0.549	0.154	0.165	0.367	0.513	-0.205
	Srsf6	-0.179	0.202	0.398	0.272	-0.630	0.093	0.133	0.500	0.383	-0.198
	Tra2b	-0.424	0.225	0.089	0.077	-0.925	-0.041	0.136	0.769	0.255	-0.336
Core	*Sf1*	*0.420*	*0.145*	*0.016*	*0.744*	*0.097*	0.178	0.132	0.202	0.465	-0.109
	Sf3b1	*0.400*	*0.151*	*0.025*	*0.737*	*0.063*	-0.092	0.137	0.514	0.206	-0.390

Supplementary Table S23 (Chapter 5): Changes in splicing factor expression with long-term and short-term 40% DR in positive responder mice

Changes in splicing factor expression levels with long-term and short-term DR in brain, heart and kidney tissues from mice which display lifespan extension under 40% DR conditions (TejJ89), by ANCOVA. A positive mean difference denotes an increase in expression levels under 40% DR conditions when compared to AL feeding. Transcripts showing nominal associations (p<0.05) are shown in italic and underlined, those which meet correction for multiple testing (p<0.0045) are shown in bold italic and underlined. SE: standard error, 95% CI: 95% confidence intervals.

		Brain – Short-term DR					Brain – Long-term DR				
		Mean Difference	SE	*p*-value	95% CI lower	95% CI upper	Mean Difference	SE	*p*-value	95% CI lower	95% CI upper
Splicing Factors	*Hnrnpa0*	-0.424	0.252	0.119	-0.974	0.126	***-0.954***	***0.235***	***0.002***	***-1.478***	***-0.429***
	Hnrnpa1	-0.240	0.187	0.223	-0.647	0.167	***1.554***	***0.389***	***0.004***	***0.658***	***2.450***
	Hnrnpa2b1	0.128	0.125	0.324	-0.143	0.400	*0.508*	*0.228*	*0.047*	*0.007*	*1.009*
	Hnrnpd	0.021	0.179	0.909	-0.370	0.412	0.360	0.204	0.106	-0.090	0.810
	Hnrnph3	0.085	0.135	0.542	-0.210	0.380	***-1.595***	***0.293***	***<0.001***	***-2.272***	***-0.918***
	Hnrnpk	-0.312	0.179	0.107	-0.703	0.079	***1.512***	***0.343***	***0.002***	***0.736***	***2.287***
	Hnrnpm	0.061	0.164	0.717	-0.296	0.418	-0.167	0.195	0.409	-0.597	0.262
	Hnrnpul2	0.039	0.134	0.777	-0.254	0.331	0.122	0.142	0.407	-0.190	0.435
	Pnisr	0.078	0.168	0.651	-0.287	0.443	0.024	0.268	0.929	-0.566	0.615
	Srsf1	0.316	0.214	0.166	-0.150	0.783	*-0.828*	*0.272*	*0.011*	*-1.427*	*-0.229*
	Srsf2	-0.187	0.139	0.202	-0.489	0.115	-0.510	0.390	0.220	-1.379	0.359
	Srsf3	*-0.433*	*0.128*	*0.005*	*-0.712*	*-0.154*	-1.020	0.507	0.079	-2.189	0.148
	Srsf6	*-0.674*	*0.220*	*0.010*	*-1.153*	*-0.195*	-0.742	0.363	0.065	-1.540	0.056
	Tra2b	0.100	0.091	0.290	-0.097	0.298	0.160	0.159	0.335	-0.189	0.510
Core	*Sf1*	*-0.290*	*0.126*	*0.040*	*-0.564*	*-0.016*	*-0.637*	*0.188*	*0.007*	*-1.055*	*-0.219*
	Sf3b1	*0.373*	*0.155*	*0.033*	*0.035*	*0.710*	*0.737*	*0.254*	*0.016*	*0.172*	*1.302*

		Heart – Short-term DR					Heart – Long-term DR				
		Mean Difference	SE	*p*-value	95% CI lower	95% CI upper	Mean Difference	SE	*p*-value	95% CI lower	95% CI upper
Splicing Factors	*Hnrnpa0*	-0.331	0.180	0.089	-0.720	0.058	0.091	0.158	0.574	-0.254	0.436
	Hnrnpa1	0.210	0.199	0.310	-0.219	0.639	-0.208	0.156	0.206	-0.548	0.132
	Hnrnpa2b1	-0.022	0.109	0.841	-0.257	0.212	*0.287*	*0.129*	*0.046*	*0.006*	*0.569*
	Hnrnpd	-0.017	0.115	0.884	-0.265	0.231	0.169	0.120	0.184	-0.092	0.431
	Hnrnph3	-0.123	0.086	0.173	-0.309	0.062	-0.007	0.157	0.964	-0.349	0.334
	Hnrnpk	0.234	0.191	0.244	-0.180	0.647	0.142	0.151	0.367	-0.188	0.471
	Hnrnpm	-0.149	0.293	0.621	-0.783	0.485	-0.127	0.137	0.372	-0.425	0.171
	Hnrnpul2	-0.126	0.151	0.420	-0.453	0.201	-0.266	0.195	0.197	-0.692	0.159
	Pnisr	*-0.402*	*0.135*	*0.011*	*-0.694*	*-0.110*	-0.156	0.177	0.396	-0.541	0.229
	Srsf1	-0.241	0.235	0.323	-0.748	0.266	0.004	0.269	0.988	-0.581	0.589
	Srsf2	0.171	0.178	0.353	-0.212	0.555	0.115	0.175	0.523	-0.266	0.496
	Srsf3	-0.103	0.135	0.458	-0.396	0.189	-0.051	0.131	0.704	-0.336	0.234
	Srsf6	-0.064	0.201	0.753	-0.498	0.369	*0.607*	*0.220*	*0.017*	*0.128*	*1.086*
	Tra2b	0.230	0.130	0.100	-0.051	0.511	0.220	0.181	0.247	-0.174	0.614
Core	*Sf1*	-0.147	0.155	0.361	-0.482	0.188	0.044	0.111	0.702	-0.198	0.285
	Sf3b1	0.323	0.300	0.301	-0.326	0.972	-0.160	0.166	0.355	-0.522	0.202

		Kidney – Short-term DR					Kidney – Long-term DR				
		Mean Difference	SE	*p*-value	95% CI lower	95% CI upper	Mean Difference	SE	*p*-value	95% CI lower	95% CI upper
Splicing Factors	*Hnrnpa0*	0.203	0.214	0.362	-0.264	0.669	0.152	0.088	0.108	-0.039	0.343
	Hnrnpa1	***-0.438***	***0.093***	***<0.001***	***-0.640***	***-0.237***	-0.332	0.216	0.150	-0.803	0.138
	Hnrnpa2b1	-0.158	0.085	0.086	-0.343	0.026	-0.205	0.196	0.315	-0.632	0.221
	Hnrnpd	0.063	0.087	0.483	-0.129	0.256	0.012	0.132	0.928	-0.276	0.301
	Hnrnph3	-0.085	0.075	0.277	-0.248	0.078	*-0.627*	*0.212*	*0.012*	*-1.088*	*-0.166*
	Hnrnpk	-0.025	0.066	0.715	-0.169	0.119	-0.020	0.150	0.898	-0.346	0.307
	Hnrnpm	*0.330*	*0.140*	*0.037*	*0.024*	*0.635*	0.098	0.195	0.625	-0.327	0.522
	Hnrnpul2	*-0.237*	*0.105*	*0.043*	*-0.465*	*-0.008*	-0.192	0.161	0.258	-0.545	0.162
	Pnisr	*-0.289*	*0.121*	*0.034*	*-0.552*	*-0.026*	***0.522***	***0.149***	***0.004***	***0.198***	***0.846***
	Srsf1	0.133	0.066	0.068	-0.012	0.278	*-0.189*	*0.057*	*0.006*	*-0.314*	*-0.064*
	Srsf2	0.069	0.101	0.509	-0.151	0.288	0.353	0.232	0.155	-0.153	0.859
	Srsf3	0.094	0.160	0.569	-0.256	0.444	-0.186	0.180	0.322	-0.578	0.206
	Srsf6	***0.692***	***0.144***	***<0.001***	***0.378***	***1.005***	0.054	0.175	0.763	-0.327	0.435
	Tra2b	*0.343*	*0.109*	*0.008*	*0.106*	*0.580*	-0.265	0.173	0.152	-0.641	0.112
Core	*Sf1*	0.064	0.115	0.592	-0.188	0.315	0.147	0.122	0.251	-0.118	0.413
	Sf3b1	*-0.327*	*0.150*	*0.049*	*-0.653*	*-0.001*	*0.328*	*0.151*	*0.050*	*0.000*	*0.656*

Supplementary Table S24 (Chapter 5): Changes in splicing factor expression with long-term and short-term 40% DR in negative responder mice

Changes in splicing factor expression levels with long-term and short-term DR in brain, heart and kidney tissue from mice which display lifespan reduction under 40% DR conditions (TejJ114), by ANCOVA. A positive mean difference denotes an increase in expression levels under 40% DR conditions when compared to AL feeding. Transcripts showing nominal associations (p<0.05) are shown in italic and underlined, those which meet correction for multiple testing (p<0.0045) are shown in bold italic and underlined. SE: standard error, 95% CI: 95% confidence intervals.

		Brain – Short-term DR					Brain – Long-term DR				
		Mean Difference	SE	*p*-value	95% CI lower	95% CI upper	Mean Difference	SE	*p*-value	95% CI lower	95% CI upper
Splicing Factors	*Hnrnpa0*	0.062	0.200	0.761	-0.373	0.497	0.258	0.332	0.453	-0.472	0.988
	Hnrnpa1	0.032	0.215	0.886	-0.436	0.499	-0.254	0.314	0.435	-0.937	0.430
	Hnrnpa2b1	*0.268*	*0.114*	*0.037*	*0.019*	*0.517*	*-0.437*	*0.153*	*0.014*	*-0.769*	*-0.104*
	Hnrnpd	0.093	0.116	0.436	-0.158	0.345	*-0.462*	*0.186*	*0.028*	*-0.867*	*-0.058*
	Hnrnph3	0.089	0.100	0.392	-0.129	0.307	*-0.342*	*0.151*	*0.043*	*-0.670*	*-0.013*
	Hnrnpk	-0.281	0.159	0.102	-0.627	0.065	-0.196	0.269	0.481	-0.781	0.390
	Hnrnpm	0.010	0.147	0.949	-0.310	0.329	0.163	0.255	0.535	-0.393	0.719
	Hnrnpul2	0.112	0.086	0.214	-0.074	0.298	-0.193	0.166	0.266	-0.554	0.168
	Pnisr	-0.008	0.174	0.965	-0.388	0.372	0.123	0.184	0.517	-0.278	0.524
	Srsf1	-0.247	0.317	0.453	-0.945	0.451	0.222	0.235	0.365	-0.291	0.734
	Srsf2	*0.348*	*0.157*	*0.046*	*0.007*	*0.689*	0.237	0.277	0.408	-0.366	0.840
	Srsf3	-0.334	0.184	0.094	-0.735	0.067	0.172	0.204	0.417	-0.273	0.616
	Srsf6	***-0.808***	***0.208***	***0.002***	***-1.262***	***-0.354***	0.261	0.149	0.105	-0.064	0.586
	Tra2b	-0.037	0.102	0.727	-0.259	0.186	0.156	0.189	0.427	-0.257	0.568
Core	*Sf1*	*-0.407*	*0.125*	*0.007*	*-0.680*	*-0.134*	-0.023	0.213	0.916	-0.487	0.441
	Sf3b1	0.417	0.213	0.074	-0.047	0.882	-0.009	0.340	0.979	-0.750	0.732

		Heart – Short-term DR					Heart – Long-term DR				
		Mean Difference	SE	*p*-value	95% CI lower	95% CI upper	Mean Difference	SE	*p*-value	95% CI lower	95% CI upper
Splicing Factors	*Hnrnpa0*	0.067	0.174	0.705	-0.312	0.447	*-0.344*	*0.099*	*0.005*	*-0.561*	*-0.127*
	Hnrnpa1	***0.407***	***0.113***	***0.004***	***0.161***	***0.653***	-0.236	0.170	0.189	-0.606	0.134
	Hnrnpa2b1	***-0.287***	***0.073***	***0.002***	***-0.448***	***-0.127***	0.258	0.151	0.114	-0.071	0.587
	Hnrnpd	***-0.316***	***0.087***	***0.003***	***-0.505***	***-0.127***	0.005	0.156	0.975	-0.334	0.344
	Hnrnph3	0.010	0.077	0.895	-0.158	0.178	-0.015	0.116	0.899	-0.268	0.238
	Hnrnpk	-0.006	0.165	0.971	-0.365	0.353	0.368	0.181	0.066	-0.028	0.763
	Hnrnpm	*0.567*	*0.187*	*0.011*	*0.158*	*0.975*	-0.221	0.249	0.393	-0.763	0.321
	Hnrnpul2	-0.202	0.135	0.159	-0.495	0.091	*0.275*	*0.126*	*0.049*	*0.001*	*0.550*
	Pnisr	0.060	0.166	0.724	-0.305	0.425	0.043	0.120	0.725	-0.218	0.304
	Srsf1	0.054	0.189	0.779	-0.357	0.465	-0.079	0.126	0.543	-0.353	0.196
	Srsf2	*0.460*	*0.166*	*0.017*	*0.099*	*0.821*	0.071	0.111	0.531	-0.170	0.313
	Srsf3	0.147	0.205	0.489	-0.301	0.594	-0.005	0.107	0.967	-0.240	0.231
	Srsf6	***-0.685***	***0.151***	***<0.001***	***-1.014***	***-0.355***	0.318	0.151	0.057	-0.012	0.648
	Tra2b	0.092	0.144	0.534	-0.221	0.405	0.338	0.195	0.109	-0.088	0.763
Core	*Sf1*	***-0.511***	***0.138***	***0.003***	***-0.812***	***-0.211***	-0.342	0.187	0.092	-0.750	0.065
	Sf3b1	-0.259	0.205	0.230	-0.705	0.188	-0.305	0.253	0.252	-0.857	0.247

		Kidney – Short-term DR					Kidney – Long-term DR				
		Mean Difference	SE	*p*-value	95% CI lower	95% CI upper	Mean Difference	SE	*p*-value	95% CI lower	95% CI upper
Splicing Factors	*Hnrnpa0*	0.147	0.195	0.466	-0.276	0.569	0.202	0.194	0.320	-0.225	0.630
	Hnrnpa1	-0.129	0.100	0.216	-0.345	0.086	*-0.325*	*0.125*	*0.025*	*-0.600*	*-0.050*
	Hnrnpa2b1	-0.105	0.129	0.433	-0.384	0.175	*-0.419*	*0.125*	*0.007*	*-0.698*	*-0.140*
	Hnrnpd	-0.095	0.098	0.350	-0.307	0.117	0.013	0.103	0.905	-0.214	0.239
	Hnrnph3	-0.122	0.111	0.293	-0.362	0.118	-0.345	0.201	0.120	-0.800	0.110
	Hnrnpk	0.198	0.128	0.146	-0.079	0.474	0.134	0.170	0.448	-0.240	0.507
	Hnrnpm	0.148	0.109	0.196	-0.087	0.384	-0.054	0.215	0.805	-0.527	0.419
	Hnrnpul2	*-0.314*	*0.135*	*0.037*	*-0.605*	*-0.022*	0.171	0.129	0.212	-0.113	0.454
	Pnisr	-0.261	0.144	0.094	-0.573	0.051	0.182	0.224	0.432	-0.310	0.674
	Srsf1	***0.285***	***0.073***	***0.002***	***0.128***	***0.442***	-0.015	0.081	0.857	-0.193	0.164
	Srsf2	0.151	0.139	0.297	-0.149	0.451	0.048	0.134	0.728	-0.247	0.343
	Srsf3	*0.456*	*0.140*	*0.006*	*0.155*	*0.758*	0.126	0.218	0.574	-0.354	0.606
	Srsf6	*0.449*	*0.177*	*0.025*	*0.066*	*0.832*	0.283	0.191	0.168	-0.139	0.704
	Tra2b	***0.487***	***0.119***	***0.001***	***0.228***	***0.746***	0.015	0.307	0.961	-0.660	0.691
Core	*Sf1*	***-0.495***	***0.104***	***<0.001***	***-0.720***	***-0.270***	0.173	0.145	0.257	-0.145	0.491
	Sf3b1	*-0.557*	*0.168*	*0.005*	*-0.919*	*-0.195*	0.223	0.204	0.297	-0.225	0.672

Supplementary Table S25 (Chapter 5): Splicing factor expression according to mouse strain

Differences in splicing factor expression between the lifespan extension (TejJ89) and lifespan reduction (TejJ114) responder strains under 40% DR by ANCOVA. A positive mean difference denotes higher expression levels in TejJ89 relative to TejJ114 under 40% DR conditions. Transcripts showing nominal associations (p<0.05) are shown in italic and underlined, those which meet correction for multiple testing (p<0.0045) are shown in bold italic and underlined. SE: standard error, 95% CI: 95% confidence intervals.

		Brain – Short-term DR					Brain – Long-term DR				
		Mean Difference	SE	*p*-value	95% CI lower	95% CI upper	Mean Difference	SE	*p*-value	95% CI lower	95% CI upper
Splicing Factors	*Hnrnpa0*	*-0.446*	*0.170*	*0.022*	*-0.816*	*-0.077*	*-1.150*	*0.358*	*0.011*	*-1.960*	*-0.340*
	Hnrnpa1	0.089	0.208	0.675	-0.364	0.542	*1.788*	*0.510*	*0.008*	*0.613*	*2.963*
	Hnrnpa2b1	-0.044	0.156	0.780	-0.384	0.295	***0.963***	***0.199***	***<0.001***	***0.526***	***1.400***
	Hnrnpd	0.032	0.127	0.808	-0.245	0.309	***0.825***	***0.215***	***0.003***	***0.351***	***1.300***
	Hnrnph3	-0.105	0.125	0.418	-0.377	0.168	***-1.289***	***0.314***	***0.003***	***-2.014***	***-0.565***
	Hnrnpk	0.102	0.160	0.534	-0.246	0.450	***1.691***	***0.411***	***0.003***	***0.761***	***2.621***
	Hnrnpm	-0.281	0.148	0.082	-0.604	0.041	-0.200	0.264	0.465	-0.780	0.381
	Hnrnpul2	-0.017	0.109	0.876	-0.254	0.220	*0.309*	*0.109*	*0.016*	*0.070*	*0.549*
	Pnisr	-0.119	0.160	0.471	-0.468	0.230	0.144	0.190	0.465	-0.274	0.562
	Srsf1	0.229	0.278	0.426	-0.377	0.836	*-0.881*	*0.294*	*0.012*	*-1.528*	*-0.234*
	Srsf2	***-0.533***	***0.133***	***0.002***	***-0.823***	***-0.243***	-0.801	0.371	0.056	-1.628	0.026
	Srsf3	-0.219	0.135	0.131	-0.513	0.076	*-1.281*	*0.431*	*0.018*	*-2.274*	*-0.288*
	Srsf6	-0.084	0.227	0.718	-0.578	0.410	***-1.180***	***0.286***	***0.002***	***-1.810***	***-0.550***
	Tra2b	0.008	0.103	0.940	-0.216	0.231	-0.119	0.143	0.424	-0.434	0.196
Core	*Sf1*	0.186	0.138	0.204	-0.115	0.487	***-0.687***	***0.184***	***0.004***	***-1.098***	***-0.276***
	Sf3b1	0.245	0.155	0.141	-0.094	0.584	0.715	0.398	0.103	-0.172	1.602

		Heart – Short-term DR					Heart – Long-term DR				
		Mean Difference	SE	*p*-value	95% CI lower	95% CI upper	Mean Difference	SE	*p*-value	95% CI lower	95% CI upper
Splicing Factors	*Hnrnpa0*	*-0.374*	*0.165*	*0.041*	*-0.731*	*-0.017*	*0.516*	*0.175*	*0.012*	*0.134*	*0.899*
	Hnrnpa1	-0.039	0.164	0.817	-0.393	0.316	-0.230	0.167	0.194	-0.593	0.134
	Hnrnpa2b1	0.194	0.130	0.162	-0.089	0.478	-0.015	0.108	0.893	-0.249	0.220
	Hnrnpd	***0.344***	***0.088***	***0.002***	***0.154***	***0.534***	0.107	0.121	0.393	-0.156	0.371
	Hnrnph3	-0.168	0.093	0.096	-0.369	0.034	-0.001	0.130	0.996	-0.284	0.283
	Hnrnpk	0.214	0.163	0.211	-0.138	0.566	-0.093	0.146	0.535	-0.412	0.225
	Hnrnpm	*-0.733*	*0.255*	*0.013*	*-1.283*	*-0.183*	0.159	0.243	0.526	-0.371	0.690
	Hnrnpul2	0.056	0.158	0.731	-0.286	0.397	***-0.572***	***0.134***	***0.001***	***-0.863***	***-0.282***
	Pnisr	*-0.457*	*0.183*	*0.028*	*-0.856*	*-0.058*	-0.248	0.139	0.099	-0.550	0.054
	Srsf1	*-0.338*	*0.144*	*0.035*	*-0.648*	*-0.028*	0.165	0.217	0.462	-0.307	0.636
	Srsf2	-0.224	0.173	0.219	-0.599	0.151	0.073	0.144	0.624	-0.241	0.386
	Srsf3	-0.248	0.152	0.126	-0.576	0.080	***0.359***	***0.093***	***0.002***	***0.156***	***0.561***
	Srsf6	*0.425*	*0.172*	*0.028*	*0.053*	*0.797*	*0.429*	*0.177*	*0.032*	*0.043*	*0.815*
	Tra2b	0.022	0.177	0.904	-0.361	0.404	0.034	0.156	0.834	-0.307	0.374
Core	*Sf1*	0.191	0.169	0.279	-0.175	0.557	*0.402*	*0.183*	*0.048*	*0.005*	*0.800*
	Sf3b1	*0.657*	*0.234*	*0.015*	*0.151*	*1.162*	0.008	0.231	0.974	-0.495	0.510

		Kidney – Short-term DR					Kidney – Long-term DR				
		Mean Difference	SE	*p*-value	95% CI lower	95% CI upper	Mean Difference	SE	*p*-value	95% CI lower	95% CI upper
Splicing Factors	*Hnrnpa0*	-0.013	0.208	0.950	-0.463	0.436	-0.264	0.153	0.115	-0.604	0.076
	Hnrnpa1	***-0.371***	***0.092***	***0.001***	***-0.569***	***-0.173***	-0.206	0.156	0.217	-0.554	0.142
	Hnrnpa2b1	-0.065	0.150	0.672	-0.389	0.259	-0.001	0.156	0.996	-0.354	0.352
	Hnrnpd	0.123	0.089	0.191	-0.070	0.316	-0.022	0.120	0.856	-0.289	0.245
	Hnrnph3	0.055	0.103	0.605	-0.169	0.278	-0.148	0.247	0.566	-0.718	0.422
	Hnrnpk	-0.151	0.132	0.274	-0.436	0.135	0.229	0.148	0.154	-0.101	0.559
	Hnrnpm	0.188	0.111	0.114	-0.051	0.427	0.193	0.237	0.435	-0.335	0.721
	Hnrnpul2	0.093	0.147	0.538	-0.224	0.410	-0.177	0.153	0.274	-0.518	0.164
	Pnisr	-0.059	0.149	0.698	-0.381	0.263	0.259	0.160	0.136	-0.097	0.614
	Srsf1	-0.174	0.086	0.065	-0.361	0.012	-0.089	0.100	0.394	-0.311	0.133
	Srsf2	-0.112	0.116	0.352	-0.362	0.138	0.282	0.224	0.236	-0.217	0.781
	Srsf3	*-0.280*	*0.115*	*0.030*	*-0.528*	*-0.033*	-0.006	0.234	0.979	-0.527	0.514
	Srsf6	0.279	0.186	0.157	-0.122	0.681	0.072	0.143	0.627	-0.247	0.390
	Tra2b	-0.059	0.090	0.525	-0.254	0.137	0.096	0.263	0.724	-0.491	0.682
Core	*Sf1*	***0.552***	***0.116***	***<0.001***	***0.301***	***0.802***	-0.031	0.112	0.785	-0.281	0.218
	Sf3b1	0.178	0.160	0.285	-0.167	0.524	-0.102	0.187	0.597	-0.520	0.315

Supplementary Table S26 (Chapter 5): Interactions between strain effects and 40% DR effects on splicing factor expression

Shown here are the interaction coefficients between strain effects and DR effects on splicing factor transcript expression. A positive coefficient denotes combinatorial effects contributing to higher expression levels in TejJ89 relative to TejJ114 under 40% DR conditions. Also shown are the postestimation marginal effects for each strain. Positive margins denote an increase in expression levels in the respective strain under 40% DR conditions when compared to AL feeding. Transcripts showing nominal associations (p<0.05) are shown in italic and underlined, those which meet correction for multiple testing (p<0.0045) are shown in bold italic and underlined. SE: standard error, 95% CI: 95% confidence intervals.

Brain – Short-term DR							
			Coefficient	**SE**	**95% CI lower**	**95% CI upper**	***p*-value**
Splicing Factors	*Hnrnpa0*	**Interaction coefficient**	-0.495	0.308	-1.128	0.138	0.120
		TejJ89 – Predictive margins	-0.407	0.148	-0.711	-0.103	
		TejJ114 – Predictive margins	0.056	0.149	-0.251	0.362	
	Hnrnpa1	**Interaction coefficient**	-0.175	0.289	-0.769	0.418	0.549
		TejJ89 – Predictive margins	-0.112	0.139	-0.397	0.172	
		TejJ114 – Predictive margins	-0.204	0.140	-0.491	0.083	
	Hnrnpa2b1	**Interaction coefficient**	-0.083	0.179	-0.452	0.285	0.646
		TejJ89 – Predictive margins	0.153	0.086	-0.024	0.330	
		TejJ114 – Predictive margins	0.198	0.087	0.020	0.377	
	Hnrnpd	**Interaction coefficient**	-0.026	0.211	-0.460	0.409	0.904
		TejJ89 – Predictive margins	0.048	0.101	-0.160	0.257	
		TejJ114 – Predictive margins	0.012	0.102	-0.199	0.222	
	Hnrnph3	**Interaction coefficient**	-0.055	0.170	-0.406	0.295	0.748
		TejJ89 – Predictive margins	0.087	0.082	-0.081	0.255	
		TejJ114 – Predictive margins	0.175	0.082	0.005	0.344	
	Hnrnpk	**Interaction coefficient**	-0.012	0.230	-0.485	0.462	0.960
		TejJ89 – Predictive margins	-0.278	0.111	-0.505	-0.051	
		TejJ114 – Predictive margins	-0.394	0.112	-0.624	-0.165	
	Hnrnpm	**Interaction coefficient**	0.019	0.212	-0.418	0.455	0.930
		TejJ89 – Predictive margins	-0.085	0.102	-0.294	0.125	
		TejJ114 – Predictive margins	0.189	0.103	-0.022	0.400	
	Hnrnpul2	**Interaction coefficient**	-0.081	0.155	-0.400	0.238	0.607
		TejJ89 – Predictive margins	0.080	0.074	-0.073	0.233	
		TejJ114 – Predictive margins	0.107	0.075	-0.048	0.261	
	Pnisr	**Interaction coefficient**	-0.002	0.257	-0.530	0.526	0.994
		TejJ89 – Predictive margins	0.075	0.123	-0.178	0.329	
		TejJ114 – Predictive margins	0.192	0.124	-0.064	0.448	
	Srsf1	**Interaction coefficient**	0.493	0.368	-0.265	1.251	0.193
		TejJ89 – Predictive margins	0.287	0.174	-0.072	0.646	
		TejJ114 – Predictive margins	0.110	0.175	-0.252	0.471	
	Srsf2	**Interaction coefficient**	*-0.491*	*0.206*	*-0.914*	*-0.067*	*0.025*
		TejJ89 – Predictive margins	*-0.254*	*0.099*	*-0.457*	*-0.051*	
		TejJ114 – Predictive margins	*0.305*	*0.100*	*0.100*	*0.510*	
	Srsf3	**Interaction coefficient**	-0.061	0.218	-0.509	0.387	0.782
		TejJ89 – Predictive margins	-0.548	0.105	-0.763	-0.333	
		TejJ114 – Predictive margins	-0.335	0.106	-0.552	-0.118	
	Srsf6	**Interaction coefficient**	0.249	0.320	-0.409	0.907	0.444
		TejJ89 – Predictive margins	-0.913	0.154	-1.228	-0.597	
		TejJ114 – Predictive margins	-0.850	0.155	-1.169	-0.532	
	Tra2b	**Interaction coefficient**	0.189	0.152	-0.123	0.502	0.224
		TejJ89 – Predictive margins	-0.049	0.073	-0.199	0.102	
		TejJ114 – Predictive margins	-0.038	0.074	-0.189	0.114	
Core Spliceosome	*Sf1*	**Interaction coefficient**	0.134	0.170	-0.215	0.482	0.439
		TejJ89 – Predictive margins	-0.276	0.081	-0.444	-0.109	
		TejJ114 – Predictive margins	-0.474	0.082	-0.643	-0.305	
	Sf3b1	**Interaction coefficient**	-0.012	0.260	-0.546	0.522	0.964
		TejJ89 – Predictive margins	0.485	0.125	0.229	0.741	
		TejJ114 – Predictive margins	0.212	0.126	-0.046	0.471	

Supplementary Table S26 (cont.)

Heart – Short-term DR							
			Coefficient	**SE**	**95% CI lower**	**95% CI upper**	***p*-value**
Splicing Factors	*Hnrnpa0*	**Interaction coefficient**	-0.407	0.242	-0.904	0.090	0.104
		TejJ89 – Predictive margins	-0.310	0.121	-0.560	-0.061	
		TejJ114 – Predictive margins	0.023	0.125	-0.233	0.279	
	Hnrnpa1	**Interaction coefficient**	-0.197	0.221	-0.651	0.258	0.383
		TejJ89 – Predictive margins	0.242	0.111	0.015	0.470	
		TejJ114 – Predictive margins	0.284	0.114	0.050	0.518	
	Hnrnpa2b1	**Interaction coefficient**	0.280	0.144	-0.016	0.575	0.063
		TejJ89 – Predictive margins	-0.019	0.071	-0.165	0.126	
		TejJ114 – Predictive margins	-0.281	0.078	-0.440	-0.121	
	Hnrnpd	**Interaction coefficient**	0.291	0.151	-0.018	0.600	0.064
		TejJ89 – Predictive margins	-0.017	0.075	-0.172	0.138	
		TejJ114 – Predictive margins	-0.371	0.077	-0.530	-0.212	
	Hnrnph3	**Interaction coefficient**	-0.148	0.127	-0.410	0.113	0.254
		TejJ89 – Predictive margins	-0.153	0.064	-0.284	-0.022	
		TejJ114 – Predictive margins	0.023	0.066	-0.111	0.158	
	Hnrnpk	**Interaction coefficient**	0.277	0.247	-0.230	0.785	0.272
		TejJ89 – Predictive margins	0.231	0.124	-0.023	0.486	
		TejJ114 – Predictive margins	0.068	0.127	-0.194	0.329	
	Hnrnpm	**Interaction coefficient**	*-0.750*	*0.339*	*-1.446*	*-0.054*	*0.036*
		TejJ89 – Predictive margins	*-0.176*	*0.170*	*-0.525*	*0.173*	
		TejJ114 – Predictive margins	*0.603*	*0.175*	*0.244*	*0.961*	
	Hnrnpul2	**Interaction coefficient**	0.059	0.196	-0.344	0.462	0.767
		TejJ89 – Predictive margins	-0.140	0.098	-0.342	0.063	
		TejJ114 – Predictive margins	-0.205	0.101	-0.412	0.003	
	Pnisr	**Interaction coefficient**	*-0.441*	*0.205*	*-0.864*	*-0.019*	*0.041*
		TejJ89 – Predictive margins	*-0.417*	*0.102*	*-0.626*	*-0.208*	
		TejJ114 – Predictive margins	*0.026*	*0.113*	*-0.206*	*0.259*	
	Srsf1	**Interaction coefficient**	-0.338	0.294	-0.942	0.267	0.262
		TejJ89 – Predictive margins	-0.270	0.148	-0.573	0.033	
		TejJ114 – Predictive margins	0.064	0.152	-0.247	0.375	
	Srsf2	**Interaction coefficient**	-0.275	0.233	-0.753	0.203	0.249
		TejJ89 – Predictive margins	0.183	0.117	-0.056	0.423	
		TejJ114 – Predictive margins	0.446	0.120	0.199	0.692	
	Srsf3	**Interaction coefficient**	-0.219	0.238	-0.708	0.270	0.366
		TejJ89 – Predictive margins	-0.113	0.120	-0.358	0.133	
		TejJ114 – Predictive margins	0.202	0.123	-0.050	0.454	
	Srsf6	**Interaction coefficient**	*0.584*	*0.248*	*0.074*	*1.093*	*0.026*
		TejJ89 – Predictive margins	*-0.131*	*0.125*	*-0.386*	*0.125*	
		TejJ114 – Predictive margins	*-0.576*	*0.128*	*-0.838*	*-0.314*	
	Tra2b	**Interaction coefficient**	0.138	0.189	-0.250	0.525	0.472
		TejJ89 – Predictive margins	0.198	0.095	0.004	0.392	
		TejJ114 – Predictive margins	0.205	0.097	0.006	0.404	
Core Spliceosome	*Sf1*	**Interaction coefficient**	0.335	0.203	-0.082	0.751	0.111
		TejJ89 – Predictive margins	-0.174	0.102	-0.383	0.035	
		TejJ114 – Predictive margins	-0.466	0.105	-0.681	-0.252	
	Sf3b1	**Interaction coefficient**	0.604	0.351	-0.117	1.324	0.097
		TejJ89 – Predictive margins	0.367	0.176	0.006	0.729	
		TejJ114 – Predictive margins	-0.354	0.181	-0.725	0.017	

Supplementary Table S26 (cont.)

Kidney – Short-term DR							
			Coefficient	**SE**	**95% CI lower**	**95% CI upper**	***p*-value**
Splicing Factors	*Hnrnpa0*	**Interaction coefficient**	0.051	0.280	-0.523	0.625	0.856
		TejJ89 – Predictive margins	0.196	0.142	-0.094	0.486	
		TejJ114 – Predictive margins	0.171	0.134	-0.104	0.445	
	Hnrnpa1	**Interaction coefficient**	*-0.310*	*0.132*	*-0.580*	*-0.039*	*0.027*
		TejJ89 – Predictive margins	*-0.496*	*0.067*	*-0.633*	*-0.359*	
		TejJ114 – Predictive margins	*-0.081*	*0.063*	*-0.210*	*0.049*	
	Hnrnpa2b1	**Interaction coefficient**	-0.054	0.153	-0.368	0.260	0.725
		TejJ89 – Predictive margins	-0.172	0.077	-0.331	-0.013	
		TejJ114 – Predictive margins	-0.112	0.073	-0.262	0.038	
	Hnrnpd	**Interaction coefficient**	0.152	0.131	-0.117	0.422	0.255
		TejJ89 – Predictive margins	0.036	0.069	-0.107	0.179	
		TejJ114 – Predictive margins	-0.082	0.062	-0.209	0.045	
	Hnrnph3	**Interaction coefficient**	0.033	0.136	-0.246	0.312	0.812
		TejJ89 – Predictive margins	-0.086	0.069	-0.227	0.055	
		TejJ114 – Predictive margins	-0.133	0.065	-0.266	0.000	
	Hnrnpk	**Interaction coefficient**	-0.226	0.146	-0.526	0.074	0.133
		TejJ89 – Predictive margins	-0.004	0.074	-0.155	0.148	
		TejJ114 – Predictive margins	0.171	0.070	0.028	0.314	
	Hnrnpm	**Interaction coefficient**	0.192	0.178	-0.173	0.558	0.290
		TejJ89 – Predictive margins	0.336	0.090	0.151	0.521	
		TejJ114 – Predictive margins	0.136	0.085	-0.039	0.311	
	Hnrnpul2	**Interaction coefficient**	0.088	0.177	-0.275	0.452	0.622
		TejJ89 – Predictive margins	-0.254	0.090	-0.438	-0.070	
		TejJ114 – Predictive margins	-0.349	0.085	-0.523	-0.175	
	Pnisr	**Interaction coefficient**	-0.029	0.183	-0.405	0.346	0.873
		TejJ89 – Predictive margins	-0.284	0.093	-0.474	-0.094	
		TejJ114 – Predictive margins	-0.251	0.088	-0.431	-0.072	
	Srsf1	**Interaction coefficient**	-0.159	0.105	-0.375	0.057	0.143
		TejJ89 – Predictive margins	0.127	0.053	0.018	0.237	
		TejJ114 – Predictive margins	0.280	0.050	0.177	0.383	
	Srsf2	**Interaction coefficient**	-0.077	0.178	-0.443	0.289	0.668
		TejJ89 – Predictive margins	0.079	0.090	-0.106	0.264	
		TejJ114 – Predictive margins	0.169	0.085	-0.006	0.344	
	Srsf3	**Interaction coefficient**	-0.363	0.204	-0.781	0.055	0.086
		TejJ89 – Predictive margins	0.119	0.103	-0.092	0.331	
		TejJ114 – Predictive margins	0.445	0.097	0.245	0.645	
	Srsf6	**Interaction coefficient**	0.238	0.225	-0.223	0.699	0.298
		TejJ89 – Predictive margins	0.744	0.114	0.511	0.978	
		TejJ114 – Predictive margins	0.444	0.107	0.224	0.664	
	Tra2b	**Interaction coefficient**	-0.145	0.156	-0.466	0.177	0.364
		TejJ89 – Predictive margins	0.382	0.078	0.222	0.542	
		TejJ114 – Predictive margins	0.461	0.078	0.301	0.621	
Core Spliceosome	*Sf1*	**Interaction coefficient**	***0.554***	***0.153***	***0.241***	***0.867***	***0.001***
		TejJ89 – Predictive margins	***0.091***	***0.077***	***-0.068***	***0.249***	
		TejJ114 – Predictive margins	***-0.488***	***0.073***	***-0.637***	***-0.338***	
	Sf3b1	**Interaction coefficient**	0.219	0.222	-0.236	0.674	0.332
		TejJ89 – Predictive margins	-0.346	0.112	-0.576	-0.115	
		TejJ114 – Predictive margins	-0.526	0.106	-0.744	-0.309	

Supplementary Table S26 (cont.)

			Brain – Long-term DR				
			Coefficient	**SE**	**95% CI lower**	**95% CI upper**	***p*-value**
Splicing Factors	*Hnrnpa0*	**Interaction coefficient**	*-1.057*	*0.408*	*-1.902*	*-0.213*	*0.016*
		TejJ89 – Predictive margins	*-0.941*	*0.212*	*-1.379*	*-0.503*	
		TejJ114 – Predictive margins	*0.134*	*0.197*	*-0.273*	*0.541*	
	Hnrnpa1	**Interaction coefficient**	***1.652***	***0.479***	***0.659***	***2.644***	***0.002***
		TejJ89 – Predictive margins	***1.478***	***0.296***	***0.865***	***2.091***	
		TejJ114 – Predictive margins	***-0.208***	***0.208***	***-0.639***	***0.223***	
	Hnrnpa2b1	**Interaction coefficient**	***0.896***	***0.258***	***0.365***	***1.426***	***0.002***
		TejJ89 – Predictive margins	***0.507***	***0.130***	***0.239***	***0.775***	
		TejJ114 – Predictive margins	***-0.408***	***0.120***	***-0.655***	***-0.161***	
	Hnrnpd	**Interaction coefficient**	*0.717*	*0.270*	*0.161*	*1.273*	*0.014*
		TejJ89 – Predictive margins	*0.385*	*0.136*	*0.104*	*0.666*	
		TejJ114 – Predictive margins	*-0.370*	*0.126*	*-0.629*	*-0.112*	
	Hnrnph3	**Interaction coefficient**	***-1.241***	***0.296***	***-1.855***	***-0.627***	***<0.001***
		TejJ89 – Predictive margins	***-1.536***	***0.183***	***-1.915***	***-1.156***	
		TejJ114 – Predictive margins	***-0.272***	***0.129***	***-0.539***	***-0.005***	
	Hnrnpk	**Interaction coefficient**	***1.632***	***0.421***	***0.760***	***2.504***	***0.001***
		TejJ89 – Predictive margins	***1.515***	***0.232***	***1.035***	***1.995***	
		TejJ114 – Predictive margins	***-0.063***	***0.180***	***-0.436***	***0.309***	
	Hnrnpm	**Interaction coefficient**	-0.164	0.326	-0.834	0.507	0.620
		TejJ89 – Predictive margins	-0.175	0.165	-0.514	0.164	
		TejJ114 – Predictive margins	-0.042	0.152	-0.354	0.271	
	Hnrnpul2	**Interaction coefficient**	0.376	0.210	-0.055	0.808	0.084
		TejJ89 – Predictive margins	0.096	0.106	-0.122	0.314	
		TejJ114 – Predictive margins	-0.239	0.098	-0.440	-0.038	
	Pnisr	**Interaction coefficient**	0.026	0.318	-0.629	0.681	0.936
		TejJ89 – Predictive margins	0.040	0.161	-0.291	0.371	
		TejJ114 – Predictive margins	-0.048	0.148	-0.353	0.257	
	Srsf1	**Interaction coefficient**	*-0.876*	*0.366*	*-1.629*	*-0.123*	*0.024*
		TejJ89 – Predictive margins	*-0.776*	*0.185*	*-1.157*	*-0.396*	
		TejJ114 – Predictive margins	*0.136*	*0.170*	*-0.214*	*0.487*	
	Srsf2	**Interaction coefficient**	-0.845	0.433	-1.738	0.049	0.063
		TejJ89 – Predictive margins	-0.504	0.237	-0.993	-0.014	
		TejJ114 – Predictive margins	0.247	0.198	-0.161	0.655	
	Srsf3	**Interaction coefficient**	*-1.204*	*0.449*	*-2.135*	*-0.274*	*0.014*
		TejJ89 – Predictive margins	*-0.976*	*0.272*	*-1.539*	*-0.412*	
		TejJ114 – Predictive margins	*0.224*	*0.184*	*-0.158*	*0.606*	
	Srsf6	**Interaction coefficient**	*-1.052*	*0.367*	*-1.807*	*-0.296*	*0.008*
		TejJ89 – Predictive margins	*-0.795*	*0.185*	*-1.176*	*-0.413*	
		TejJ114 – Predictive margins	*0.408*	*0.171*	*0.056*	*0.760*	
	Tra2b	**Interaction coefficient**	-0.064	0.239	-0.555	0.428	0.792
		TejJ89 – Predictive margins	0.163	0.121	-0.086	0.411	
		TejJ114 – Predictive margins	0.236	0.111	0.007	0.465	
Core Spliceosome	*Sf1*	**Interaction coefficient**	-0.481	0.274	-1.047	0.085	0.092
		TejJ89 – Predictive margins	-0.603	0.150	-0.914	-0.293	
		TejJ114 – Predictive margins	0.024	0.125	-0.235	0.282	
	Sf3b1	**Interaction coefficient**	0.665	0.422	-0.206	1.536	0.128
		TejJ89 – Predictive margins	0.658	0.224	1.120	0.000	
		TejJ114 – Predictive margins	-0.013	0.193	-0.412	0.386	

Supplementary Table S26 (cont.)

Heart – Long-term DR							
			Coefficient	**SE**	**95% CI lower**	**95% CI upper**	***p*-value**
Splicing Factors	*Hnrnpa0*	**Interaction coefficient**	0.368	0.199	-0.043	0.778	0.077
		TejJ89 – Predictive margins	-0.025	0.096	-0.222	0.172	
		TejJ114 – Predictive margins	-0.557	0.096	-0.754	-0.360	
	Hnrnpa1	**Interaction coefficient**	0.016	0.221	-0.437	0.470	0.941
		TejJ89 – Predictive margins	-0.395	0.108	-0.617	-0.172	
		TejJ114 – Predictive margins	-0.172	0.108	-0.394	0.051	
	Hnrnpa2b1	**Interaction coefficient**	0.019	0.191	-0.374	0.412	0.922
		TejJ89 – Predictive margins	0.238	0.094	0.045	0.431	
		TejJ114 – Predictive margins	0.258	0.094	0.065	0.451	
	Hnrnpd	**Interaction coefficient**	0.180	0.192	-0.215	0.574	0.358
		TejJ89 – Predictive margins	0.109	0.094	-0.084	0.303	
		TejJ114 – Predictive margins	0.019	0.094	-0.175	0.212	
	Hnrnph3	**Interaction coefficient**	-0.008	0.193	-0.406	0.390	0.968
		TejJ89 – Predictive margins	-0.052	0.095	-0.247	0.143	
		TejJ114 – Predictive margins	-0.036	0.095	-0.231	0.159	
	Hnrnpk	**Interaction coefficient**	-0.247	0.235	-0.730	0.236	0.303
		TejJ89 – Predictive margins	0.212	0.115	-0.025	0.450	
		TejJ114 – Predictive margins	0.284	0.115	0.047	0.521	
	Hnrnpm	**Interaction coefficient**	0.109	0.276	-0.458	0.675	0.696
		TejJ89 – Predictive margins	-0.068	0.135	-0.346	0.210	
		TejJ114 – Predictive margins	-0.235	0.135	-0.513	0.043	
	Hnrnpul2	**Interaction coefficient**	*-0.547*	*0.236*	*-1.033*	*-0.062*	*0.029*
		TejJ89 – Predictive margins	*-0.342*	*0.116*	*-0.581*	*-0.104*	
		TejJ114 – Predictive margins	*0.261*	*0.116*	*0.023*	*0.499*	
	Pnisr	**Interaction coefficient**	-0.228	0.207	-0.652	0.197	0.280
		TejJ89 – Predictive margins	-0.217	0.101	-0.426	-0.009	
		TejJ114 – Predictive margins	0.051	0.101	-0.157	0.259	
	Srsf1	**Interaction coefficient**	0.079	0.281	-0.499	0.657	0.780
		TejJ89 – Predictive margins	0.034	0.138	-0.250	0.318	
		TejJ114 – Predictive margins	-0.112	0.138	-0.396	0.171	
	Srsf2	**Interaction coefficient**	0.051	0.196	-0.351	0.453	0.796
		TejJ89 – Predictive margins	0.136	0.096	-0.062	0.333	
		TejJ114 – Predictive margins	0.070	0.096	-0.127	0.267	
	Srsf3	**Interaction coefficient**	-0.014	0.166	-0.357	0.329	0.934
		TejJ89 – Predictive margins	0.069	0.080	-0.096	0.233	
		TejJ114 – Predictive margins	-0.314	0.080	-0.478	-0.149	
	Srsf6	**Interaction coefficient**	0.303	0.253	-0.217	0.824	0.242
		TejJ89 – Predictive margins	0.710	0.124	0.454	0.965	
		TejJ114 – Predictive margins	0.266	0.124	0.011	0.521	
	Tra2b	**Interaction coefficient**	-0.089	0.257	-0.618	0.441	0.733
		TejJ89 – Predictive margins	0.352	0.126	0.092	0.612	
		TejJ114 – Predictive margins	0.307	0.126	0.047	0.566	
Core Spliceosome	*Sf1*	**Interaction coefficient**	0.411	0.225	-0.052	0.874	0.079
		TejJ89 – Predictive margins	0.073	0.111	-0.154	0.301	
		TejJ114 – Predictive margins	-0.307	0.110	-0.534	-0.080	
	Sf3b1	**Interaction coefficient**	0.109	0.298	-0.504	0.723	0.717
		TejJ89 – Predictive margins	-0.290	0.146	-0.591	0.011	
		TejJ114 – Predictive margins	-0.257	0.146	-0.558	0.044	

Supplementary Table S26 (cont.)

Kidney – Long-term DR							
			Coefficient	SE	95% CI lower	95% CI upper	*p*-value
Splicing Factors	*Hnrnpa0*	**Interaction coefficient**	-0.067	0.211	-0.501	0.368	0.755
		TejJ89 – Predictive margins	-0.016	0.108	-0.237	0.206	
		TejJ114 – Predictive margins	0.306	0.095	0.110	0.503	
	Hnrnpa1	**Interaction coefficient**	0.014	0.245	-0.490	0.519	0.954
		TejJ89 – Predictive margins	-0.486	0.125	-0.744	-0.229	
		TejJ114 – Predictive margins	-0.164	0.111	-0.392	0.064	
	Hnrnpa2b1	**Interaction coefficient**	0.184	0.239	-0.309	0.677	0.449
		TejJ89 – Predictive margins	-0.277	0.120	-0.524	-0.030	
		TejJ114 – Predictive margins	-0.300	0.112	-0.531	-0.069	
	Hnrnpd	**Interaction coefficient**	-0.045	0.170	-0.396	0.305	0.792
		TejJ89 – Predictive margins	0.064	0.087	-0.114	0.243	
		TejJ114 – Predictive margins	0.105	0.077	-0.053	0.264	
	Hnrnph3	**Interaction coefficient**	-0.336	0.284	-0.924	0.252	0.250
		TejJ89 – Predictive margins	-0.509	0.139	-0.796	-0.222	
		TejJ114 – Predictive margins	-0.414	0.149	-0.722	-0.107	
	Hnrnpk	**Interaction coefficient**	-0.146	0.218	-0.595	0.303	0.508
		TejJ89 – Predictive margins	0.162	0.111	-0.067	0.391	
		TejJ114 – Predictive margins	-0.050	0.099	-0.253	0.153	
	Hnrnpm	**Interaction coefficient**	0.106	0.280	-0.472	0.683	0.709
		TejJ89 – Predictive margins	0.202	0.143	-0.092	0.497	
		TejJ114 – Predictive margins	0.009	0.127	-0.251	0.270	
	Hnrnpul2	**Interaction coefficient**	-0.385	0.216	-0.831	0.061	0.087
		TejJ89 – Predictive margins	0.074	0.106	-0.145	0.294	
		TejJ114 – Predictive margins	0.259	0.093	0.067	0.452	
	Pnisr	**Interaction coefficient**	0.384	0.257	-0.145	0.913	0.147
		TejJ89 – Predictive margins	0.436	0.131	0.167	0.706	
		TejJ114 – Predictive margins	0.155	0.116	-0.084	0.394	
	Srsf1	**Interaction coefficient**	-0.212	0.107	-0.432	0.008	0.058
		TejJ89 – Predictive margins	-0.127	0.054	-0.239	-0.015	
		TejJ114 – Predictive margins	-0.012	0.048	-0.111	0.088	
	Srsf2	**Interaction coefficient**	0.365	0.296	-0.245	0.975	0.229
		TejJ89 – Predictive margins	0.218	0.151	-0.093	0.529	
		TejJ114 – Predictive margins	-0.076	0.134	-0.351	0.200	
	Srsf3	**Interaction coefficient**	-0.307	0.269	-0.862	0.248	0.265
		TejJ89 – Predictive margins	-0.062	0.137	-0.345	0.221	
		TejJ114 – Predictive margins	-0.068	0.122	-0.319	0.182	
	Srsf6	**Interaction coefficient**	-0.237	0.251	-0.754	0.279	0.353
		TejJ89 – Predictive margins	0.180	0.128	-0.083	0.444	
		TejJ114 – Predictive margins	0.093	0.113	-0.140	0.327	
	Tra2b	**Interaction coefficient**	-0.269	0.329	-0.946	0.408	0.421
		TejJ89 – Predictive margins	-0.072	0.168	-0.417	0.273	
		TejJ114 – Predictive margins	-0.173	0.149	-0.479	0.133	
Core Spliceosome	*Sf1*	**Interaction coefficient**	-0.049	0.180	-0.421	0.322	0.787
		TejJ89 – Predictive margins	0.154	0.092	-0.036	0.343	
		TejJ114 – Predictive margins	0.176	0.082	0.008	0.344	
	Sf3b1	**Interaction coefficient**	0.114	0.250	-0.400	0.629	0.651
		TejJ89 – Predictive margins	0.170	0.127	-0.092	0.432	
		TejJ114 – Predictive margins	0.281	0.113	0.048	0.513	

Supplementary Table S27 (Chapter 6): Taqman® Low Density Array card contents

Splicing factor target genes, assay IDs and qPCR software settings for each transcript included on the Taqman® Low Density Array cards. Endogenous control genes used are shown in bold italics.

Target	Assay ID	Threshold	Baseline Start	Baseline End
HNRNPA0	Hs00246543_s1	0.315	9	21
HNRNPA1	Hs01656228_s1	0.377	9	24
HNRNPA2B1	Hs00242600_m1	0.270	9	18
HNRNPD	Hs01086914_g1	0.249	4	21
HNRNPH3	Hs01032113_g1	0.345	3	21
HNRNPK	Hs00829140_s1	0.360	3	21
HNRNPM	Hs00246018_m1	0.234	3	22
HNRNPUL2	Hs00859848_m1	0.470	3	21
AKAP17A	Hs00946624_m1	0.145	9	22
PNISR	Hs00369090_m1	0.305	3	19
SRSF1	Hs00199471_m1	0.191	3	20
SRSF2	Hs00427515_g1	0.092	3	24
SRSF3	Hs00751507_s1	0.195	3	22
SRSF6	Hs00607200_g1	0.293	3	22
SRSF7	Hs00196708_m1	0.217	3	20
TRA2B	Hs00907493_m1	0.165	3	21
IMP3	Hs00251000_s1	0.259	3	23
LSM14A	Hs00385941_m1	0.146	3	21
LSM2	Hs01061967_g1	0.191	3	23
SF3B1	Hs00202782_m1	0.424	3	20
18S	***Hs99999901_s1***	***0.189***	***2***	***6***
GUSB	***Hs00939627_m1***	***0.249***	***8***	***22***
IDH3B	***Hs00199382_m1***	***0.249***	***3***	***22***
PPIA	***Hs04194521_s1***	***0.332***	***3***	***23***

Supplementary Table S28 (Chapter 6): Associations of splicing factor expression with decline in corrected MMSE score as a continuous measure

Relationships of splicing factor expression levels with decline in corrected MMSE score by multivariate linear regression. β-coefficients represent change in log expression per unit change in MMSE score. Transcripts showing nominally statistically significant associations (p<0.05) are shown in italic and underlined. Those which satisfy Bonferroni correction for multiple testing (p<0.0083) are shown in bold italic and underlined.

MMSE: DECLINE IN TEST SCORE (n = 296)						
		β-coefficient	**SE**	***p*-value**	**95% CI lower**	**95% CI upper**
Splicing Factors	*HNRNPA0*	*-0.003*	*0.001*	*0.019*	*-0.006*	*-0.001*
	HNRNPA1	-0.001	0.002	0.476	-0.005	0.002
	HNRNPA2B1	0.000	0.001	0.783	-0.003	0.002
	HNRNPD	0.000	0.001	0.917	-0.003	0.003
	HNRNPH3	-0.001	0.002	0.577	-0.004	0.002
	HNRNPK	-0.001	0.002	0.488	-0.005	0.002
	HNRNPM	***-0.005***	***0.002***	***0.006***	***-0.008***	***-0.001***
	HNRNPUL2	-0.002	0.002	0.137	-0.005	0.001
	AKAP17A	-0.005	0.003	0.077	-0.011	0.001
	PNISR	0.001	0.001	0.359	-0.002	0.004
	SRSF1	-0.001	0.001	0.176	-0.003	0.001
	SRSF2	-0.001	0.003	0.612	-0.006	0.004
	SRSF3	0.001	0.002	0.732	-0.004	0.005
	SRSF6	-0.003	0.002	0.076	-0.007	0.000
	SRSF7	0.001	0.001	0.375	-0.002	0.004
	TRA2B	0.002	0.002	0.222	-0.001	0.006
Core Spliceosome	*IMP3*	0.002	0.001	0.190	-0.001	0.005
	LSM14A	0.000	0.002	0.964	-0.003	0.003
	LSM2	0.004	0.002	0.111	-0.001	0.008
	SF3B1	0.001	0.002	0.717	-0.003	0.004

Supplementary Table S29 (Chapter 6): Further analysis of associations of splicing factor expression found with decline in MMSE score

Relationships of splicing factor expression levels with different subsets of the cohort by multivariate linear regression. β-coefficients represent change in log expression per unit change in MMSE score. Transcripts showing nominally statistically significant associations (p<0.05) are shown in italic and underlined. Those which satisfy Bonferroni correction for multiple testing (p<0.0083) are shown in bold italic and underlined.

SPLICING FACTORS ASSOCIATED WITH DECLINE IN MMSE SCORE							
AKAP17A		**n**	**β-coefficient**	**SE**	***p*-value**	**95% CI Lower**	**95% CI upper**
Full cohort		296	-0.005	0.003	0.077	-0.011	0.001
FU3 MMSE score >=28		174	-0.012	0.007	0.070	-0.025	0.001
FU3 Age >= 70		178	-0.005	0.004	0.133	-0.013	0.002
Non-decliners removed		260	*-0.008*	*0.004*	*0.036*	*-0.015*	*-0.001*
Full cohort - categorised	Mild decline	103	-0.017	0.025	0.486	-0.066	0.031
	Severe decline	13	***-0.153***	***0.056***	***0.007***	***-0.264***	***-0.041***
HNRNPA0		**n**	**β-coefficient**	**SE**	***p*-value**	**95% CI Lower**	**95% CI upper**
Full cohort		296	*-0.003*	*0.001*	*0.019*	*-0.006*	*-0.001*
FU3 MMSE score >=28		174	*-0.007*	*0.003*	*0.010*	*-0.012*	*-0.002*
FU3 Age >= 70		178	*-0.004*	*0.002*	*0.028*	*-0.007*	*0.000*
Non-decliners removed		260	***-0.004***	***0.002***	***0.007***	***-0.008***	***-0.001***
Full cohort - categorised	Mild decline	103	0.004	0.011	0.702	-0.018	0.026
	Severe decline	13	***-0.083***	***0.025***	***0.001***	***-0.133***	***-0.033***
HNRNPM		**n**	**β-coefficient**	**SE**	***p*-value**	**95% CI Lower**	**95% CI upper**
Full cohort		296	***-0.005***	***0.002***	***0.006***	***-0.008***	***-0.001***
FU3 MMSE score >=28		174	*-0.009*	*0.003*	*0.011*	*-0.016*	*-0.002*
FU3 Age >= 70		178	*-0.005*	*0.002*	*0.011*	*-0.009*	*-0.001*
Non-decliners removed		260	***-0.006***	***0.002***	***0.005***	***-0.009***	***-0.002***
Full cohort - categorised	Mild decline	103	-0.010	0.013	0.454	-0.036	0.016
	Severe decline	13	***-0.082***	***0.031***	***0.008***	***-0.143***	***-0.022***

Supplementary Table S30 (Chapter 6): Correlation between different splicing factor expression levels

Pearson correlations of relationships between expression levels of all splicing factors measured.

	HNRNPA0	HNRNPA1	HNRNPA2B1	HNRNPD	HNRNPH3	HNRNPK	HNRNPM	HNRNPUL2	AKAP17A	PNISR	SRSF1	SRSF2	SRSF3	SRSF6	SRSF7	TRA2B	IMP3	LSM14A	LSM2	SF3B1
HNRNPA0	1																			
HNRNPA1	0.161	1																		
HNRNPA2B1	-0.228	-0.026	1																	
HNRNPD	-0.021	-0.043	0.028	1																
HNRNPH3	-0.214	-0.096	0.281	0.189	1															
HNRNPK	-0.188	-0.352	0.039	0.221	0.338	1														
HNRNPM	0.282	-0.049	-0.012	-0.031	-0.292	0.028	1													
HNRNPUL2	0.226	-0.034	0.062	0.393	0.366	0.201	0.143	1												
AKAP17A	0.239	-0.117	0.096	-0.246	-0.180	0.131	0.440	-0.047	1											
PNISR	-0.330	0.045	0.027	0.074	0.419	0.126	-0.317	-0.023	-0.270	1										
SRSF1	0.107	0.152	-0.133	-0.154	0.108	-0.229	-0.164	0.011	-0.241	0.131	1									
SRSF2	0.080	0.005	-0.189	-0.134	-0.353	-0.017	0.243	0.009	0.179	-0.188	0.071	1								
SRSF3	-0.493	-0.125	0.007	-0.149	-0.030	0.186	-0.205	-0.401	-0.078	0.361	-0.077	-0.038	1							
SRSF6	0.126	0.024	0.143	-0.159	-0.224	-0.216	0.005	-0.143	0.076	-0.308	0.045	-0.025	-0.269	1						
SRSF7	-0.241	0.158	-0.060	-0.179	-0.140	-0.368	-0.218	-0.204	-0.369	0.107	0.195	0.035	0.232	-0.019	1					
TRA2B	-0.386	0.107	0.018	-0.192	-0.068	-0.193	-0.369	-0.369	-0.289	0.176	0.058	-0.103	0.451	-0.026	0.498	1				
IMP3	-0.080	0.131	-0.318	-0.090	-0.312	-0.362	-0.125	-0.327	-0.292	-0.068	0.064	0.015	0.246	0.013	0.326	0.318	1			
LSM14A	0.149	-0.126	0.109	-0.020	0.238	-0.181	-0.095	0.362	-0.071	-0.135	0.185	-0.264	-0.507	0.125	-0.174	-0.280	-0.239	1		
LSM2	-0.126	0.120	-0.171	-0.186	-0.337	-0.296	-0.088	-0.441	0.024	-0.104	-0.057	-0.015	-0.006	0.076	0.134	0.156	0.265	-0.050	1	
SF3B1	-0.344	-0.195	-0.049	0.014	0.476	0.260	-0.441	0.009	-0.421	0.505	0.229	-0.257	0.426	-0.287	0.158	0.302	-0.114	0.036	-0.258	1

Supplementary Table S31 (Chapter 6): Associations of splicing factor expression with alternate measures of cognitive ability

Relationships between expression levels of splicing factors implicated in decline in MMSE score and results of the Trail Making Test A, Trail Making Test B and the Purdue Pegboard Test, by multivariate linear regression. For the Trail Making Tests, β-coefficients represent change in log expression per minute increased time taken to complete the tests. For the Purdue Pegboard Test, β-coefficients represent change in log expression per unit change in total number of pegs placed on the board. Transcripts showing nominally statistically significant associations (p<0.05) are shown in italic and underlined. Those which satisfy Bonferroni correction for multiple testing (p<0.0083) are shown in bold italic and underlined.

ASSOCIATIONS WITH INCREASE IN TIME TO COMPLETE TRAIL MAKING TEST A							
AKAP17A		**n**	**β-coefficient**	**SE**	***p*-value**	**95% CI Lower**	**95% CI upper**
Full cohort		268	*0.057*	*0.022*	*0.009*	*0.014*	*0.099*
FU3 Lowest quintile removed		224	*0.067*	*0.031*	*0.035*	*0.005*	*0.128*
FU3 Age >= 70		151	*0.070*	*0.027*	*0.010*	*0.017*	*0.124*
Non-decliners removed		247	***0.074***	***0.025***	***0.004***	***0.024***	***0.123***
Full cohort - categorised	Mild decline	21	0.048	0.045	0.289	-0.041	0.136
	Severe decline	57	-0.049	0.031	0.117	-0.110	0.012
HNRNPA0		**n**	**β-coefficient**	**SE**	***p*-value**	**95% CI Lower**	**95% CI upper**
Full cohort		268	***0.028***	***0.009***	***0.004***	***0.009***	***0.046***
FU3 Lowest quintile removed		224	*0.033*	*0.013*	*0.015*	*0.007*	*0.059*
FU3 Age >= 70		151	*0.029*	*0.011*	*0.014*	*0.006*	*0.051*
Non-decliners removed		247	***0.031***	***0.011***	***0.005***	***0.009***	***0.052***
Full cohort - categorised	Mild decline	21	-0.013	0.020	0.506	-0.053	0.026
	Severe decline	57	*-0.027*	*0.014*	*0.044*	*-0.054*	*-0.001*
HNRNPM		**n**	**β-coefficient**	**SE**	***p*-value**	**95% CI Lower**	**95% CI upper**
Full cohort		268	0.012	0.011	0.299	-0.010	0.033
FU3 Lowest quintile removed		224	0.020	0.016	0.214	-0.012	0.051
FU3 Age >= 70		151	0.021	0.012	0.092	-0.003	0.046
Non-decliners removed		247	0.024	0.013	0.064	-0.001	0.049
Full cohort - categorised	Mild decline	21	0.015	0.023	0.506	-0.030	0.060
	Severe decline	57	-0.005	0.016	0.770	-0.036	0.027

Supplementary Table S31 (cont.)

ASSOCIATIONS WITH INCREASE IN TIME TO COMPLETE TRAIL MAKING TEST B

AKAP17A		**n**	**β-coefficient**	**SE**	***p*-value**	**95% CI Lower**	**95% CI upper**
Full cohort		179	0.034	0.025	0.174	-0.015	0.083
FU3 Lowest quintile removed		159	0.015	0.031	0.636	-0.047	0.077
FU3 Age > 70		67	-0.007	0.042	0.863	-0.097	0.082
Non-decliners removed		160	0.019	0.030	0.523	-0.040	0.078
Full cohort - categorised	Mild decline	52	0.028	0.035	0.422	-0.041	0.097
	Severe decline	37	-0.001	0.045	0.982	-0.089	0.088
HNRNPA0		**n**	**β-coefficient**	**SE**	***p*-value**	**95% CI Lower**	**95% CI upper**
Full cohort		179	0.011	0.011	0.315	-0.011	0.033
FU3 Lowest quintile removed		159	0.002	0.013	0.894	-0.024	0.027
FU3 Age > 70		67	-0.013	0.018	0.463	-0.051	0.024
Non-decliners removed		160	0.005	0.012	0.672	-0.019	0.030
Full cohort - categorised	Mild decline	52	0.002	0.015	0.909	-0.028	0.031
	Severe decline	37	-0.032	0.019	0.084	-0.069	0.004
HNRNPM		**n**	**β-coefficient**	**SE**	***p*-value**	**95% CI Lower**	**95% CI upper**
Full cohort		179	*0.026*	*0.012*	*0.036*	*0.002*	*0.051*
FU3 Lowest quintile removed		159	0.021	0.015	0.182	-0.010	0.051
FU3 Age >= 70		67	0.010	0.019	0.629	-0.032	0.051
Non-decliners removed		160	0.016	0.015	0.288	-0.014	0.045
Full cohort - categorised	Mild decline	52	0.006	0.017	0.749	-0.029	0.040
	Severe decline	37	*-0.051*	*0.022*	*0.022*	*-0.095*	*-0.007*

ASSOCIATIONS WITH DECLINE IN TOTAL NUMBER OF PEGS PLACED IN PURDUE PEGBOARD TEST

AKAP17A		**n**	**β-coefficient**	**SE**	***p*-value**	**95% CI Lower**	**95% CI upper**
Full cohort		257	*-0.005*	*0.002*	*0.012*	*-0.008*	*-0.001*
FU3 Lowest quintile removed		212	-0.004	0.002	0.079	-0.008	0.000
FU3 Age > 70		141	***-0.009***	***0.003***	***0.002***	***-0.015***	***-0.004***
Non-decliners removed		204	-0.005	0.003	0.060	-0.010	0.000
Full cohort - categorised	Mild decline	87	*-0.062*	*0.027*	*0.024*	*-0.116*	*-0.008*
	Severe decline	48	*-0.094*	*0.035*	*0.008*	*-0.164*	*-0.024*
HNRNPA0		**n**	**β-coefficient**	**SE**	***p*-value**	**95% CI Lower**	**95% CI upper**
Full cohort		257	*-0.002*	*0.001*	*0.047*	*-0.003*	*0.000*
FU3 Lowest quintile removed		212	-0.001	0.001	0.101	-0.003	0.000
FU3 Age > 70		141	***-0.004***	***0.001***	***0.002***	***-0.006***	***-0.001***
Non-decliners removed		204	***-0.003***	***0.001***	***0.002***	***-0.005***	***-0.001***
Full cohort - categorised	Mild decline	87	-0.004	0.012	0.751	-0.027	0.020
	Severe decline	48	*-0.035*	*0.015*	*0.025*	*-0.065*	*-0.004*
HNRNPM		**n**	**β-coefficient**	**SE**	***p*-value**	**95% CI Lower**	**95% CI upper**
Full cohort		257	*-0.002*	*0.001*	*0.044*	*-0.004*	*0.000*
FU3 Lowest quintile removed		212	-0.002	0.001	0.073	-0.004	0.000
FU3 Age >= 70		141	-0.002	0.001	0.081	-0.005	0.000
Non-decliners removed		204	-0.002	0.001	0.242	-0.004	0.001
Full cohort - categorised	Mild decline	87	-0.001	0.014	0.926	-0.029	0.027
	Severe decline	48	-0.021	0.019	0.259	-0.058	0.016

Supplementary Table S32 (Chapter 6): Correlations between trajectories in phenotypic test scores

Pearson correlations of relationships between calculated change variables for the different cognitive and physical measures used in the current study. Part a. shows correlations seen between the cognitive measures and part b. the physical measures.

a.

	MMSE: DECLINE IN TEST SCORE	TMT-A: INCREASE IN TIME TO COMPLETE	TMT-B: INCREASE IN TIME TO COMPLETE	PURDUE PEGBOARD: DECLINE IN TOTAL NUMBER OF PEGS PLACED
MMSE: DECLINE IN TEST SCORE	1			
TMT-A: INCREASE IN TIME TO COMPLETE	-0.381	1		
TMT-B: INCREASE IN TIME TO COMPLETE	-0.188	0.322	1	
PURDUE PEGBOARD: DECLINE IN TOTAL NUMBER OF PEGS PLACED	0.295	-0.329	-0.157	1

b.

	MEAN HAND-GRIP STRENGTH: DECLINE IN EXERTED FORCE (kg)	EPESE SPPB: DECLINE IN COMPOSITE SCORE	400m FAST WALK: DECLINE IN CALCULATED SPEED (m/s)
MEAN HAND-GRIP STRENGTH: DECLINE IN EXERTED FORCE (kg)	1		
EPESE SPPB: DECLINE IN COMPOSITE SCORE	0.217	1	
400m FAST WALK: DECLINE IN CALCULATED SPEED (m/s)	0.265	0.357	1

Supplementary Table S33 (Chapter 6): Associations of splicing factor expression with mean hand-grip strength as a continuous measure

Relationships of splicing factor expression levels with mean hand-grip strength by multivariate linear regression. β-coefficients represent change in log expression per Kg change in mean hand-grip strength. Transcripts showing nominally statistically significant associations (p<0.05) are shown in italic and underlined.

MEAN HAND-GRIP – DECLINE (n = 285)						
		β-coefficient	**SE**	***p*-value**	**95% CI lower**	**95% CI upper**
Splicing Factors	*HNRNPA0*	0.001	0.001	0.664	-0.002	0.003
	HNRNPA1	0.000	0.002	0.885	-0.003	0.003
	HNRNPA2B1	-0.002	0.001	0.134	-0.004	0.001
	HNRNPD	0.002	0.001	0.198	-0.001	0.004
	HNRNPH3	0.001	0.001	0.667	-0.002	0.003
	HNRNPK	0.001	0.002	0.333	-0.002	0.004
	HNRNPM	-0.002	0.001	0.256	-0.004	0.001
	HNRNPUL2	0.002	0.001	0.111	0.000	0.005
	AKAP17A	*-0.006*	*0.003*	*0.023*	*-0.011*	*-0.001*
	PNISR	0.000	0.001	0.707	-0.002	0.003
	SRSF1	-0.001	0.001	0.480	-0.002	0.001
	SRSF2	0.001	0.002	0.771	-0.004	0.005
	SRSF3	0.000	0.002	0.932	-0.004	0.004
	SRSF6	-0.001	0.002	0.469	-0.004	0.002
	SRSF7	0.001	0.001	0.547	-0.002	0.003
	TRA2B	-0.002	0.002	0.278	-0.005	0.001
Core Spliceosome	*IMP3*	0.001	0.001	0.672	-0.002	0.003
	LSM14A	0.000	0.001	0.759	-0.002	0.003
	LSM2	0.000	0.002	0.876	-0.004	0.004
	SF3B1	0.002	0.001	0.179	-0.001	0.005

Supplementary Table S34 (Chapter 6): Further analysis of associations of splicing factor expression found with decline in mean hand-grip strength

Relationships of splicing factor expression levels with different subsets of the cohort by multivariate linear regression. β-coefficients represent change in log expression per Kg change in mean hand-grip strength. Transcripts showing nominally statistically significant associations (p<0.05) are shown in italic and underlined. Those which satisfy Bonferroni correction for multiple testing (p<0.0083) are shown in bold italic and underlined.

ASSOCIATIONS WITH DECLINE IN MEAN HAND-GRIP STRENGTH							
AKAP17A		**n**	**β-coefficient**	**SE**	***p*-value**	**95% CI Lower**	**95% CI upper**
Full cohort		285	*-0.006*	*0.003*	*0.023*	*-0.011*	*-0.001*
Mean FU3 hand-grip >= EWGSOP cutoffs		204	*-0.007*	*0.003*	*0.035*	*-0.013*	*0.000*
FU3 Age >= 70		169	***-0.011***	***0.004***	***0.008***	***-0.018***	***-0.003***
Non-decliners removed		229	-0.005	0.004	0.190	-0.012	0.002
Full cohort - categorised	Mild decline	74	-0.026	0.029	0.370	-0.084	0.031
	Severe decline	52	-0.053	0.031	0.094	-0.115	0.009

Supplementary Table S35 (Chapter 6): Associations of splicing factor expression with alternate measures of physical ability

Relationships between expression levels of splicing factors implicated in decline in mean hand-grip strength and physical performance as measured by the Epidemiologic Studies of the Elderly – Short Physical Performance Battery (EPESE SPPB) and a timed 400m fast walk, by multivariate linear regression. For the EPESE SPPB, β-coefficients represent change in log expression per unit decline in composite score. For the 400m fast walk, β-coefficients represent change in log expression per unit decline in speed calculated in m/s. Transcripts showing nominally statistically significant associations (p<0.05) are shown in italic and underlined. Those which satisfy Bonferroni correction for multiple testing (p<0.0083) are shown in bold italic and underlined.

ASSOCIATIONS WITH DECLINE IN EPESE SPPB COMPOSITE SCORE

AKAP17A		**n**	**β-coefficient**	**SE**	***p*-value**	**95% CI Lower**	**95% CI upper**
Full cohort		276	*-0.011*	*0.006*	*0.048*	*-0.022*	*0.000*
FU3 Lowest quintile removed		216	-0.002	0.009	0.810	-0.020	0.016
FU3 Age >= 70		160	*-0.014*	*0.007*	*0.042*	*-0.027*	*-0.001*
Non-decliners removed		244	-0.012	0.006	0.068	-0.024	0.001
Full cohort - categorised	Mild decline	61	0.028	0.031	0.356	-0.032	0.089
	Severe decline	46	*-0.087*	*0.034*	*0.011*	*-0.155*	*-0.020*

ASSOCIATIONS WITH DECLINE IN CALCULATED SPEED (m/s) DURING 400m FAST WALK

AKAP17A		**n**	**β-coefficient**	**SE**	***p*-value**	**95% CI Lower**	**95% CI upper**
Full cohort		206	*-0.252*	*0.101*	*0.013*	*-0.451*	*-0.053*
FU3 Lowest quintile removed		183	*-0.277*	*0.112*	*0.015*	*-0.499*	*-0.055*
FU3 Age >= 70		93	-0.172	0.182	0.348	-0.539	0.194
Non-decliners removed		194	-0.189	0.117	0.109	-0.421	0.043
Full cohort - categorised	Mild decline	126	-0.053	0.034	0.118	-0.120	0.014
	Severe decline	39	-0.084	0.046	0.068	-0.174	0.006

Supplementary Data

Supplementary Data S1 (Chapter 3): Tissue collection procedure for the mouse strain comparison study

Mice were housed in duplex "shoebox" cages. Two to three days prior to sacrifice and tissue collection, mouse cages were moved from the mouse room to the procedure room. All the mice from one pen (n = 4–5 mice) were sacrificed within 1–6 minutes of initial disturbance of the home cage. The mice in the remaining pen of the home cage were returned to the mouse room and sacrificed 2–4 weeks later. Each mouse to be sacrificed was removed from its cage and immediately euthanized by CO2 asphyxiation. As soon as the mouse stopped breathing and did not exhibit a reflex to a foot pinch, it was bled by cardiac puncture. The liver, spleen, kidneys and heart were removed in that order. Next, the skin sample, thigh muscle and thymus were removed. Portions of liver, spleen, kidney, skin, heart, and skeletal muscle were placed into RNAlater (SigmaAldrich) and immediately frozen in liquid nitrogen; the remainder of each tissue was placed in Cryo-tubes and frozen directly in liquid nitrogen. Four technicians participated in the dissection of each mouse to minimize the time from death to freezing the tissue (less than 2 minutes for liver, and less than 3 minutes for each of the remaining tissues). All tissues were stored at –80° C.

Supplementary Data S2 (Chapter 3): Assay identifiers and sequence details for qRT–PCR assays used in this study.

Splicing factors

Transcript	TaqMan® Assay
Hnrnpa0	Mm03809085_s1
Hnrnpa1	Mm01303205_g1
Hnrnpa2b1	Mm01325931_g1
Hnrnpd	Mm01201314_m1
Hnrnph3	Mm01032120_g1
Hnrnpk	Mm01349462_m1
Hnrnpm	Mm00513070_m1
Hnrnpul2	Mm01230949_m1
Sf3b1	Mm00473100_m1
Sfrs18	Mm01219239_m1
Srsf1	Mm00557620_m1
Srsf2	Mm00448705_m1
Srsf3	Mm00786953_s1
Srsf6	Mm00471475_m1
Tra2b	Mm00833637_mH

Supplementary Data S2 (cont.)

Spleen

Isoform Target(s) - UCSC ID	**Assay Name**	Forward Primer	Reverse Primer	Probe
uc009pme.2 ; uc009pmd.2	**ATM_13**	CGACCTGGGTTTGCATTGG	GTGCTAGACTCATGGTTTAAGATTTCAGA	CCTCACCGCTGCATTC
uc012gtj.1	**ATM_2**	TGCTCTGCAGTGTCTAAGAAACAG	TGCCCTTACTCAACTCTTCAACTTC	TTTCACCCTGGCATATCG
uc008toi.1	**CDKN2A_1**	GCCGCACCGGAATCCT	AAGAGCTGCTACGTGAACGT	CCCATCATCATCACCTGGTC
uc008toh.1	**CDKN2A_2**	CAACGCCCCGAACTCTTTC	AAGAGCTGCTACGTGAACGT	CCCGATTCAGGTGATGAT
uc008yrw.1	**CHEK2_1**	AAGAGACGAATACATCATGTCAAAAACTCT	CACTTTCTGACATGTCTTCCTCTCAA	ACACGCACCACTTCCA
uc008yrx.1	**CHEK2_2**	TGAGTAACAACTCTGAAATCGCACTT	CACTTTCTGACATGTCTTCCTCTCAA	ACACGCACCACTTTAT
uc007bju.2	**FN1_1**	CCCTACTACACTGACACAGCAA	GTGTCTGGACCGATATTGGTGAAT	ACGGCTGTCCCTCCTC
uc007bjv.2 ; uc007bjy.2	**FN1_25**	AGCCCCTGATTGGGAGGAA	GTCATACCCAGGGTTGGTGAT	AAGACAGTTCAAAAGACCC
uc008pvj.3	**LMNA_1**	GACGACGAGGATGGAGAAGAG	CGTGAGCGCAGGTTGTACT	CCGTGGTTCCCACTGCA
uc008pvj.3 ; uc008pvl.3	**LMNA_13**	GTGCGTGAGGAGTTCAAGGA	CTGCGCAGCCAACAAGTC	AAGGCTCGCAACACCA
uc008pvk.3	**LMNA_2**	AAGGCCTTGCTCTCTCTGG	CTGCGCAGCCAACAAGTC	CTTGGTGTTGCGGCCCT
uc007vyh.2	**MYC_1**	GGATTTCCTTTGGGCGTTGGA	GGTCATAGTTCCTGTTGGTGAAGTT	AACCCCGACAGCCACG
uc007vyh.2 ; uc007vyg.2 ; uc007vyi.1	**MYC_123**	CTAGTGCTGCATGAGGAGACA	ACAGACACCACATCAATTTCTTCCT	CAGCGACTCTGAAGAAG
uc007jql.2 ; uc007jqm.2 ; uc007jqn.2	**TRP53_134**	GCAGGGTGTCACGCTTCT	TCCGACTGTGACTCCTCCAT	CAGTCATCCAGTCTTCG
uc011xww.1	**TRP53_2**	GCAGGGTGTCACGCTTCT	GCTTCAGGCTTTTCTTGGATTTTCT	ACTGGCCGCTTCTC
uc007jqm.2	**TRP53_3**	GTTAAAGGATGCCCATGCTACAGA	AGTTTGGGCTTTCCTCCTTGATC	TCCAGCCTCCAGCCTAG
uc007rjg.1	**VCAN_1**	CCAAGTTCCACCCTGACATAAATGT	GGATGACCACTTACAATCATATCACTCA	ATCGACCTGTCTTGTTTTC
uc011zck.1 ; uc007rji.2	**VCAN_23**	CCAAGTTCCACCCTGACATAAATGTTTATATTAT	CGTTGAGGCATGGGTTTGTTTTG	ACAGGACCTGATCTCTG

Supplementary Data S2 (cont.)

Muscle

Isoform Target(s) - UCSC ID	**Assay Name**	Forward Primer	Reverse Primer	Probe
uc012cdt.1	**IL1B_1**	TGAAAGCTCTCCACCTCAATGG	GCTCATGGAGAATATCACTGGAGAAA	TCAACCAACAAGACTCCTC
uc008mht.1	**IL1B_2**	GTTCCTGAACTCAACTGTGAAATGC	CGTCAACTTCAAAGAACAGGTCATT	TCATCACTGTCAAAAGGTG
uc008mht.1 ; uc008mhu.1	**IL1B_23**	GACAGTGATGAGAATGACCTGTTCT	AGCCCAGGTCAAAGGTTTGG	AAGCAGCCCTTCATCTTT
uc008wuu.1 ; uc008wuv.1	**IL6_12**	TCAATTCCAGAAACCGCTATGAAGT	GTCCCAAGAAGGCAACTGGAT	TCTGCAAGAGACTTCC
uc008wuu.1 ; uc008wuw.1	**IL6_13**	GCCAGAGTCCTTCAGAGAGATACA	GCTTATCTGTTAGGAGAGCATTGGA	TCAACCAAGAGGTAAAAGA
uc008rly.1 ; uc012cyg.1 ; uc008rlx.1	**NFKB1_145**	GCATTCTGACCTTGCCTATCTACAA	CCTGGCGGATGATCTCCTT	CTCTGTCTGTGAGTTGCC
uc008rly.1 ; uc008rlx.1	**NFKB1_15**	GAGCCTCTAGTGAGAAGAACAAGAA	TTTGCAGGCCCCACATAGTT	ACAGGTCAAAATTTGC
uc012cyf.1	**NFKB1_2**	CTGCTCCTTCTAAAACTCTCATGGA	TCTCCACACCACTGTCACAGA	CCCGGAGTTCATCTCAT
uc008rlw.1 ; uc012cyg.1 ; uc008rlx.1	**NFKB1_345**	TCTGCCTCTCTCGTCTTCCT	TCTCCACACCACTGTCACAGA	CCCGGAGTTCATCTATG
uc012cyg.1	**NFKB1_4**	GAGCCTCTAGTGAGAAGAACAAGAA	GCCCCACATAGTTGCAAATCTG	CAGGTCAAAAGGCCCC
uc012cyg.1 ; uc008rlx.1	**NFKB1_45**	GGAAACTAGTGAACCGAAACCCTTT	GCGTTTCCTTTGCACTTCCT	CCCTGAAATCAAAGACAAAG
uc007axy.1	**STAT1_1**	GGAGCTGGACAGTAAAGTCAGAAAT	CTCTTCGCCACACCATTGG	TCACCTTCATGACTTGATCC
uc007axy.1 ; uc007axz.1 ; uc007aya.2	**STAT1_134**	CCTGCGTGCAGTGAGTGA	GCCGGCTCAGGGTATGG	CTGAAACGACTGGCTCTCA
uc007ayd.2 ; uc007axz.1 ; uc007aya.2 ; uc007ayb.2	**STAT1_2345**	CTCTTAGCTTTGAAACCCAGTTGTG	AGATCACCACGACAGGAAGAGA	TTGACCTGGAGACCACC

Supplementary Data S2 (cont.)

Muscle

Isoform Target(s) - UCSC ID	**Assay Name**	Forward Primer	Reverse Primer	Probe
uc007ayd.2 ; uc007aya.2 ; uc007ayb.2 ; uc007ayc.2	**STAT1_2456**	CGAACTGGATACATCAAGACTGAGT	GTTGTCTGTGGTCTGAAGTCTAGAA	CTGTGTCTGAAGTCCACCC
uc007ayb.2	**STAT1_5**	GCAGAGAGATTTGCCCAGACT	GCCGGCTCAGGGTATGG	CAGAGCTGAAACGATCACT
uc007ayc.2	**STAT1_6**	CTCTTATCCTGCCGTTCTCACTTC	GCCGGCTCAGGGTATGG	TAGGTCGTTTCAGCTCTGC
uc008cgr.2 ; uc012arb.2	**TNF_12**	CACGCTCTTCTGTCTACTGAACTT	CTGATGAGAGGGAGGCCATTTG	AAGGGATGAGAAGTTCC
uc008cgr.2 ; uc008cgs.2	**TNF_13**	CAAAATTCGAGTGACAAGCCTGTAG	GCTGCTCCTCCACTTGGT	CACGTCGTAGCAAACC
uc012arb.2	**TNF_2**	GCCTCCCTCTCATCAGTTCTATG	CCAGCTGCTCCTCCACTT	CACACTCACAAACCACC
uc008cgs.2	**TNF_3**	CACGCTCTTCTGTCTACTGAACTTC	TCTGGGCCATAGAACTGATGAGA	CCATTTGGGAACTCATCC

Supplementary Data S3 (Chapter 3): Alternatively expressed isoforms captured by quantitative real-time PCR assays.

Additional information describing precisely which alternatively expressed isoforms of analysed genes are captured by each probe set.

ATM

Atm-1,3
uc009pme.2
uc009pmd.2
Atm-2
uc012gtj.1

CDKN2A

Cdkn2a-1
uc008toi.1
Cdkn2a-2
uc008toh.1

CHEK2

Chek2-1
uc008yrw.1
Chek2-2
uc008yrx.1

FN1

Fn1-1
uc007bju.2
Fn1-2,5
uc007bjv.2
uc007bjy.2

LMNA

Lmna-1
uc008pvj.3
Lmna-1,3
uc008pvj.3
uc008pvl.3

MYC

Myc-1
uc007vyh.2
Myc-1,2,3
uc007vyh.2
uc007vyg.2
uc007vyi.1

TRP53

Trp53-1,3,4
uc007jql.2
uc007jqm.2
uc007jqn.2
Trp53-2
uc011xww.1
Trp53-3
uc007jqm.2

VCAN

Vcan-1
uc007rjg.1
Vcan-2
uc011zck.1

IL1B

Il1b-2
uc008mht.1
Il1b-2,3
uc008mht.1
uc008mhu.1

IL6

IL6-1,2
uc008wuu.1
uc008wuv.1
Il6-1,3
uc008wuu.1
uc008wuw.1

NFKB1

Nfkb1-1,4,5
uc008rly.1
uc012cyg.1
uc008rlx.1
Nfkb1-1,5
uc008rly.1
uc008rlx.1
Nfkb1-2
uc012cyf.1
Nfkb1-3,4,5
uc008rlw.1
uc012cyg.1
uc008rlx.1
Nfkb1-4,5
uc012cyg.1
uc008rlx.1

STAT1

Stat1-1
uc007axy.1
Stat1-3,4
uc007axz.1
uc007aya.2
Stat1-2,3,4,5
uc007ayd.2
uc007axz.1
uc007aya.2
uc007ayb.2
Stat1-2,4,5,6
uc007ayd.2
uc007aya.2
uc007ayb.2
uc007ayc.2
Stat1-5
uc007ayb.2
Stat1-6
uc007ayc.2

TNF

Tnf-1,2
uc008cgr.2
uc012arb.2
Tnf-1,3
uc008cgr.2
uc008cgs.2
Tnf-3
uc008cgs.2

Appendices

Appendix 1: Publications

Chapter 3

Aging Cell (2016) **15**, pp903–913 Doi: 10.1111/acel.12499

Changes in the expression of splicing factor transcripts and variations in alternative splicing are associated with lifespan in mice and humans

Benjamin P. Lee,[1] Luke C. Pilling,[2] Florence Emond,[1] Kevin Flurkey,[3] David E. Harrison,[3] Rong Yuan,[3†] Luanne L. Peters,[3] George A. Kuchel,[4] Luigi Ferrucci,[5] David Melzer[2,4] and Lorna W. Harries[1]

[1]RNA-Mediated Mechanisms of Disease, [2]Epidemiology and Public Health, Institute of Biomedical and Clinical Sciences, University of Exeter Medical School, University of Exeter, Devon, UK
[3]The Jackson Laboratory Nathan Shock Centre of Excellence in the Basic Biology of Aging, Bar Harbor, ME, USA
[4]UConn Centre on Aging, University of Connecticut Health Centre, Farmington, CT, USA
[5]National Institute on Aging, Baltimore, MD, USA

Summary

Dysregulation of splicing factor expression and altered alternative splicing are associated with aging in humans and other species, and also with replicative senescence in cultured cells. Here, we assess whether expression changes of key splicing regulator genes and consequent effects on alternative splicing are also associated with strain longevity in old and young mice, across 6 different mouse strains with varying lifespan (A/J, NOD.B10Sn-H2^b/J, PWD.Phj, 129S1/SvlmJ, C57BL/6J and WSB/EiJ). Splicing factor expression and changes to alternative splicing were associated with strain lifespan in spleen and to a lesser extent in muscle. These changes mainly involved hnRNP splicing inhibitor transcripts with most changes more marked in spleens of young animals from long-lived strains. Changes in spleen isoform expression were suggestive of reduced cellular senescence and retained cellular proliferative capacity in long-lived strains. Changes in muscle isoform expression were consistent with reduced pro-inflammatory signalling in longer-lived strains. Two splicing regulators, *HNRNPA1* and *HNRNPA2B1*, were also associated with parental longevity in humans, in the InCHIANTI aging study. Splicing factors may represent a driver, mediator or early marker of lifespan in mouse, as expression differences were present in the young animals of long-lived strains. Changes to alternative splicing patterns of key senescence genes in spleen and key remodelling genes in muscle suggest that correct regulation of alternative splicing may enhance lifespan in mice. Expression of some splicing factors in humans was also associated with parental longevity, suggesting that splicing regulation may also influence lifespan in humans.

Key words: isoforms; lifespan; longevity; mouse; mRNA splicing; splicing factors.

Introduction

Aging is a dynamic, multisystem process, which is highly heterogeneous in humans with some people surviving disease-free until advanced age whilst others succumb to age-related conditions in mid-life. The factors underlying individual lifespan are currently unclear, but increasing our understanding of determinants of longevity and 'healthspan' are key aims for the future.

Correct expression and regulation of genes is critical for maintenance of cellular and organismal function. Alternative splicing, the process by which single genes can make multiple gene products in an adaptive and reactive fashion is a key part of this process (Cartegni *et al.*, 2002). Indeed, breakdown in the regulation of mRNA splicing is a prominent feature in many age-related diseases such as Alzheimer's disease, Parkinson's disease and several tumour types (Scuderi *et al.*, 2014; Danan-Gotthold *et al.*, 2015; Lisowiec *et al.*, 2015; Lu *et al.*, 2015). This may indicate that defects in the splicing machinery may cause the cellular response to stress to be less specific, with effects on cellular resiliency and accumulation of DNA damage. We have previously identified deregulation of splicing factor expression and alternative splicing as a key factor in normal human and cellular aging (Harries *et al.*, 2011; Holly *et al.*, 2013). Alternatively expressed isoforms also demonstrate tissue-specific differences in aging, as they do for many other phenomena (Holly *et al.*, 2013). Splicing factors themselves demonstrate high species conservation (Barbosa-Morais *et al.*, 2006), whereas patterns of alternative splicing are partially determined by genetic differences and may be species specific. Splicing patterns show drastically more interspecies variability than gene expression with only 50% of alternatively expressed isoforms being conserved between species (Barbosa-Morais *et al.*, 2012). Alternatively regulated splice sites demonstrating temporal, spatial or reactive expression are less likely to show species conservation (Garg & Green, 2007).

Several splicing factors have been suggested to be involved in organismal lifespan. The pre-mRNA processing factor 19 homologue (SNEV) protein, important for spliceosome assembly and mRNA processing, has been shown to suppress cellular senescence and suppress apoptosis when phosphorylated by the ataxia-telangiectasia (ATM) kinase in endothelial cells (Dellago *et al.*, 2012). The DNA damage protein ATM also appears to be an important regulator of splicing factor expression in our previous work, since targeted gene knockdown of the *ATM* gene resulted in increased levels of splicing factor expression in fibroblasts (Holly *et al.*, 2013). There is also evidence from systemic models. A network-based model of genes altered by calorific restriction across 17 tissues in mice revealed that the largest and most responsive

Correspondence
Prof. Lorna W. Harries, University of Exeter Medical School, University of Exeter, Barrack Road, Exeter EX2 5DW, UK. Tel.: +44-1392-406773; fax: +44-1392-406767; e-mail: L.W.Harries@exeter.ac.uk
Prof. David Melzer, University of Exeter Medical School, University of Exeter, Barrack Road, Exeter EX2 5DW, UK. Tel.: +44-1392-406753; fax: +44-1392-406767; e-mail: D.Melzer@exeter.ac.uk
[†]Present address: Geriatric Research Division Department of Internal Medicine Southern Illinois University School of Medicine Springfield IL USA

Accepted for publication *22 May 2016*

gene regulatory module was associated with mRNA processing, with a disproportionally large number of genes being involved in splicing, metabolism, processing and biosynthesis of mRNA (Swindell, 2009). Finally, a study of the relationship between copy number variation (CNV) and longevity in humans revealed that lifespan-associated CNVs were preferentially located in or near genes encoding proteins involved in splicing control. This led them to conclude that genetic variation that disrupts the processes of alternative splicing may have long-term effects on lifespan (Glessner *et al.*, 2013).

The study of inbred strains of mice has proven fruitful in uncovering factors associated with lifespan, as for other phenotypes. The Jackson Laboratory has characterized 30 strains of mice, for aging and longevity-related traits (Yuan *et al.*, 2009, 2011). Initial work with this resource identified that plasma IGF1 levels were related to lifespan in rodents (Yuan *et al.*, 2009). This collection, together with the associated repository of mouse phenome data, represents a rich resource (Bogue *et al.*, 2014). Here, we have harnessed this resource to assess the contribution of regulation of alternative splicing to longevity in mice.

We have systematically assessed the expression of splicing factors previously demonstrated to be altered in human aging in relation to lifespan in six mouse strains of different longevities. Our study design is illustrated in Fig. 1. Splicing factor expression and alternative splicing of key genes are associated with lifespan in mouse spleen tissue and to a lesser extent in mouse muscle, suggesting that aging effects may be driven by immune tissues. Some strain differences in expression are most marked in the young mice, suggesting that they may represent determinants or early markers of longevity rather than representing secondary effects of aging. We also identified differences in expression levels of alternatively expressed isoforms of key aging genes indicative of reduced cellular senescence, maintained cellular proliferative capacity (spleen) and reduced pro-inflammatory signalling (muscle) in long-lived mouse strains. Two splicing factors, *HNRNPA2B1* and *HNRNPA1,* were also associated with parental longevity in a large population study of aging, suggesting that regulation of splicing may also be involved in lifespan in human populations.

Results

Splicing factor transcript expression is associated with lifespan in mouse spleen and to a lesser extent in muscle tissues

We assessed splicing factors that we have previously demonstrated to be altered in human aging in relation to lifespan in 6 mouse strains of different longevities and in samples from both old and young mice as in Fig. 1. The expression of 8/15 and 3/15 splicing factors was associated with strain lifespan in mouse spleen and muscle tissue, respectively.

In spleen, we found associations between strain lifespan and the expression of the *Hnrnpa1, Hnrnpa2b1, Hnrnpk, Hnrnpm, Hnrnpul2, Sf3b1, Srsf3* and *Tra2β* genes (beta coefficients −0.40, −0.26, −0.32, −0.31, −0.22, −0.13 and −0.36; $P = 0.01$, 0.02, 0.003, 0.003, 0.04, 0.05, 0.02 and 0.02, respectively; Fig. 2A, Table S1). When an analysis was carried out to assess interactions between strain lifespan and mouse age, we found effects in both young and old mice of long-lived strains for all associated genes except *Hnrnpul2*. In the case of *Hnrnpa1* and *Hnrnpa2b1* genes, these differences were more marked in the young mice of long-lived strains (beta coefficients −0.14 and −0.19, $P = 0.001$ and < 0.0001 in the young long-lived mice compared with −0.09 and −0.12; $P = 0.01$ and 0.02 for the old long-lived mice for *Hnrnpa1* and *Hnrnpa2b1,* respectively; Table S9). For *Srsf3*, the associations between

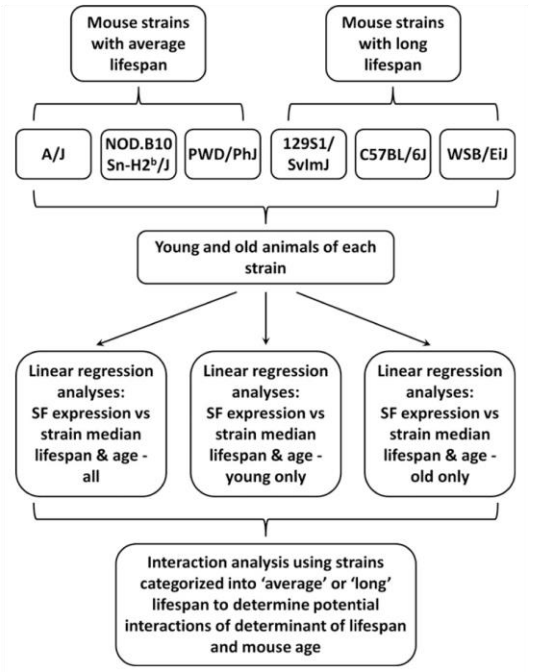

Fig. 1 Schematic of study design. This figure shows the experimental strategy employed to assess the effects of strain longevity and mouse age on the expression of an *a priori* panel of splicing factors (SFs).

splicing factor expression/age and splicing factor expression/strain median lifespan appear to be comparable, whereas for *Tra2β*, our data suggest that the effects of age are stronger than those of lifespan (Table S9). The majority (5/8) of the splicing factors demonstrating association of expression differences with lifespan belonged to the hnRNP class of splicing inhibitors, with only 2 splicing activators (*Srsf3* and *Tra2β*) showing expression changes with lifespan. The remaining associated splicing factor, *Sf3b1,* encodes a component of the U2 snRNP in the core spliceosome complex, rather than a splicing regulator. When data were assessed by binary logistic regression to allow for nonlinearity of response, all but one (*Hnrnpul2*) of the splicing regulators associated with lifespan in spleen remained associated with median strain lifespan (Table S10).

Fewer splicing factors were associated with strain lifespan in muscle tissue (Fig. 2B, Table S2). *Hnrnpa0* expression was found to be positively correlated with long life (beta coefficient 0.36; $P = 0.01$), whereas *Hnrnpd* and *Srsf3* transcripts both demonstrated reduced expression (beta coefficients −0.24 and −0.40; $P = 0.03$ and 0.02, respectively). Interaction analysis revealed that the *Srsf3* effect was again driven by effects in the young animals of the long-lived strains (beta coefficient −0.14, $P = 0.01$ in the young long-lived mice compared with beta coefficient −0.05, $P = 0.28$ in the old long-lived mice; Table S9). Again 2/3 lifespan-associated splicing factors represented hnRNP splicing inhibitors rather than SRSF splicing activators. When data were assessed by binary logistic regression to allow for nonlinearity of response, all of the splicing regulators associated with lifespan in muscle remained associated with median strain lifespan (Table S11). Effects were tissue

specific, with little overlap between lifespan-associated splicing factors in spleen and those in muscle, with only *Srsf3* common to both data sets.

Alternatively spliced genes demonstrate longevity-associated isoform changes in mouse spleen and muscle tissue

In spleen, we found splicing differences in association with lifespan for 4/8 genes tested (Fig. 3A; Table S3). Both uc008toi.1 and uc008toh.1 transcripts encoding p16INK4A and p14ARF isoforms of the *Cdkn2a* gene were expressed at lower levels in the long-lived strains (beta coefficients −0.43 and −0.59; $P = 0.002$ and < 0.0001 for uc008toi.1 [p16INK4A] and uc008toh.1 [p14ARF], respectively). Analysis of the interaction of strain longevity and mouse age revealed that although the effects on *Cdkn2a* isoform expression increased with age as expected in both average-lived and long-lived mice, the increase in expression was much less marked in the old long-lived mice than in old mice of average lifespan (beta coefficients 0.44 and 0.50, $P = <0.0001$ and < 0.0001 for the old average-lived mice compared with beta coefficients 0.22 and 0.27, $P = 0.01$ and 0.001 for the old long-lived mice; Table S9).

We also found expression of the uc007bju.2 isoform only of the *Fn1* gene to be increased in the long-lived strains (beta coefficient 0.25, $P = 0.02$). There is increased expression of the long isoform of the *Trp53* gene encoding full-length p53 (uc007jql.2/uc007jqn.2), but reduced expression of the truncated *p53AS* isoforms (uc011xww.1/uc007jqm.2; beta coefficients 0.41 and −0.35, $P = 0.009$ and 0.03 for full-length *Trp53* and truncated *p53AS* isoforms, respectively). Assessment of the interaction between strain longevity and mouse age revealed that expression of the full-length p53 isoform is only significantly increased in the young animals of long-lived strains (in comparison with young animals of short-lived strains $P = 0.004$; the older animals were not significantly different to young short-lived strains $P > 0.05$) and that diminished expression of p53AS was only significantly decreased in the

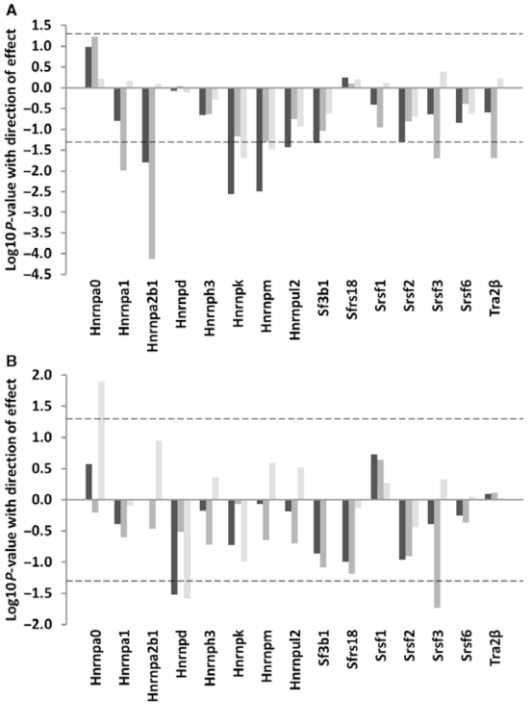

Fig. 2 Splicing factor expression according to mouse lifespan. This plot illustrates association between median lifespan and slicing factor expression in total RNA from spleen (A) or muscle (B) tissues in mice of 6 strains of different longevities, as assessed by linear regression against median strain lifespan. The identity of specific splicing factors is given on the *x*-axis. The log10 *P*-values for associations between lifespan and splicing factor expression from mice of strains with different lifespans and of different ages are given on the *y*-axis. Direction of effect is also indicated; data appearing above the zero line on the *y*-axis represent positive associations, whilst data appearing below the zero line represent negative associations. Analysis including all animals in the sample is given by dark grey bars, in young animals only by medium grey bars and in old animals only by light grey bars. The dotted line refers to a *P*-value cut-off for statistical significance of $P = 0.05$.

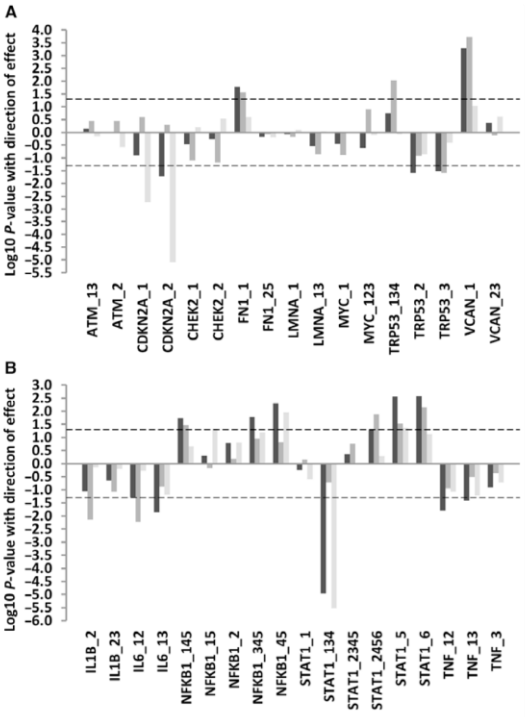

Fig. 3 The expression of alternative isoforms of key genes according to mouse lifespan. This plot illustrates association between median lifespan and the expression of alternatively expressed isoforms of key genes in total RNA from spleen (A) or muscle (B) tissues in mice of 6 strains of different longevities as assessed by linear regression against median strain lifespan. The identity of specific splicing factors is given on the *x*-axis. The log10 *P*-values for associations between lifespan and splicing factor expression from mice of strains with different lifespans and of different ages are given on the *y*-axis. Direction of effect is also indicated; data appearing above the zero line on the *y*-axis represent positive associations, whilst data appearing below the zero line represent negative associations. Analysis including all animals in the sample is given by dark grey bars, in young animals only by medium grey bars and in old animals only by light grey bars. The dotted line refers to a *P*-value cut-off for statistical significance of $P = 0.05$.

old animals of long-lived strains ($P = 0.009$, in comparison with young animals of short-lived strains; other groups were $P > 0.05$, Table S9). Finally, expression of the full-length uc007rjg.1 isoform of the *Vcan* gene is upregulated (beta coefficient 0.34, $P = 0.001$).

In mouse muscle, expression of isoforms of all five genes tested in relation to lifespan was altered (Fig. 3B, Table S4). First, expression of the full-length uc008mht.1 isoform of the *Il1b* gene was reduced in the long-lived strains (beta coefficient −0.46, $P = 0.007$), whilst the intron-retained uc008mhu.1 *Il1b* isoform was unaffected. Interaction analysis revealed that this difference was limited to the young mice of the long-lived strains ($P = 0.004$ for young long-lived mice compared with $P = 0.34$ for the old long-lived mice). Expression levels of the intron-retained uc008wuv.1 and full-length uc008wuw.1 isoforms of the *Il6* gene were also reduced (beta coefficient −0.48, $P = 0.006$ and −0.28, $P = 0.01$, respectively). Interaction analyses revealed that the effects on the intron-retained isoform were significant in the young long-lived mice only ($P = 0.04$ for young long-lived mice compared with $P = 0.72$ for old long-lived mice; Table S9).

Expression of the uc012cyg.1/uc008rlx.1 isoforms which encode the long full-length forms of the *Nfkb1* gene was greater in long-lived strains (beta coefficient 0.31, $P = 0.005$). No difference was seen in the expression of the noncoding truncated uc012cyf.1 *Nfkb1* isoform. Isoform usage for the *Stat1* gene in long-lived strains differed; the uc007axz.1 and uc007aya.2 isoforms of *Stat1* that both encode 'variant 2' of the STAT1 protein demonstrated diminished expression in the long-lived strains (beta coefficients −0.63, $P = <0.0001$), whereas the *Stat1* uc007ayc.2 isoform encoding 'variant 1' demonstrated increased expression in the long-lived strains (beta coefficient 0.46, $P = 0.007$). Interaction analysis revealed that the decrease in *Stat1* variant 2 expression was present only in the old long-lived mice ($P = 0.01$ in old long-lived mice compared with $P = 0.28$ in the young long-lived mice; Table S9). The greater *Stat1* variant 1 expression was driven by effects in the young long-lived mice ($P = 0.03$ in young long-lived mice compared with $P = 0.95$ in old long-lived mice). Transcript uc007ayb.2, encoding *Stat1* 'variant 3', was also upregulated (beta coefficient 0.33, $P = 0.005$) although this was seen in both young and old animals of long-lived strains. Finally, expression of both the uc012arb.2 and uc008cgs.2 isoforms of the *Tnf* gene which encode TNF variants 1 and 2 were reduced in muscle (beta coefficients −0.27 and −0.18, $P = 0.02$ and 0.04 for uc012arb.2 and uc008cgs.2, respectively). Interaction analyses revealed that the effect for *Tnf* variant 1 is most marked in the old long-lived animals ($P = 0.008$ in the old long-lived animals compared with $P = 0.05$ in the young long-lived animals, Table S9).

Few splicing factors are associated with age in mouse spleen and muscle tissues

Associations between mouse age and splicing factor expression were less marked than those seen for strain longevity (Fig. 4A,B, Tables S5 and S6). In spleen, we found reduced expression of the *Hnrnpa2b1, Srsf1, Srsf3* and *Tra2β* transcripts in old mice (beta coefficients −0.46, −0.34, −0.45 and −0.53; $P = 0.005$, 0.05, 0.007 and 0.008, respectively). Effects on *Srsf1*, *Srsf3* and Tra2*β* expression were evident in old animals of both average-lived and long-lived strains, but interaction analysis revealed that the age-associated difference in *Hnrnpa2b1* expression was most marked in the old animals of strains of average lifespan (beta coefficients −0.11, $P = 0.02$ in the old long-lived animals compared to beta coefficient −0.13 $P = <0.0001$ in the old average-lived animals). Age-associated changes to splicing factor expression were much less evident in muscle tissue, with only *Hnrnpa1* demonstrating increased expression (beta coefficient 0.22, $P = 0.05$). Analysis of cluster patterns for age revealed considerable inter- and intrastrain heterogeneity in splicing factor expression (Fig. S1).

Alternatively expressed isoforms demonstrate differential expression with age in mouse spleen and muscle tissue

Despite the small numbers of splicing factors demonstrating age-associated differences in splicing factor expression, we noted differences in alternative splicing in both spleen and muscle from aged mice (Fig. 5A,B, Tables S7 and S8).

In mouse spleen, we identified increased expression of both uc008-toi.1 and uc008toh.1 transcripts encoding p16INK4A and p14ARF isoforms of the *Cdkn2a* gene in the old animals as expected (beta coefficients 0.40 and 0.53, $P = <0.0001$ and $0 < 0.0001$, respectively). Interaction analyses revealed the age-associated increase in both *Cdkn2a*

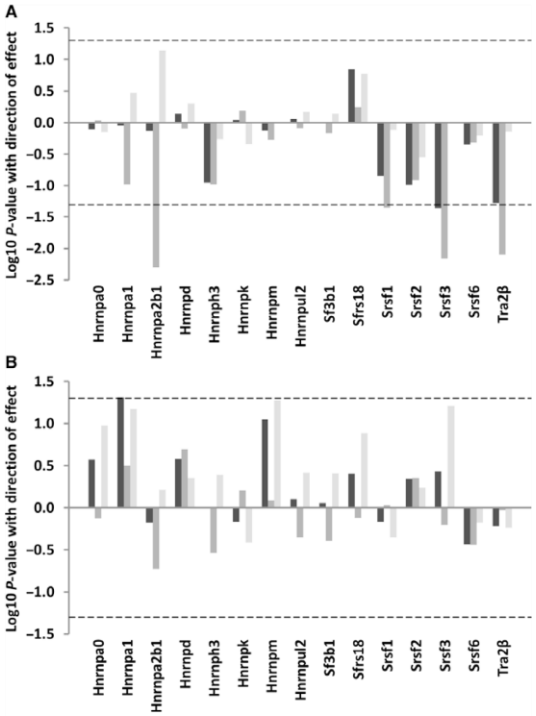

Fig. 4 Splicing factor expression according to mouse age. This plot illustrates association between age and splicing factor expression in total RNA from spleen (A) or muscle (B) tissues in young (6 months) vs. old (20–22 months) mice. The identity of specific splicing factors is given on the *x*-axis. The log10 *P*-values for associations between age and splicing factor expression from mice of different ages and of different strains are given on the *y*-axis. Direction of effect is also indicated; data appearing above the zero line on the *y*-axis represent positive associations, whilst data appearing below the zero line represent negative associations. Analysis including all animals in the sample is given by dark grey bars, in animals of average-lived strains only by medium grey bars and in long-lived animals only by light grey bars. The dotted line refers to a *P*-value cut-off for statistical significance of $P = 0.05$.

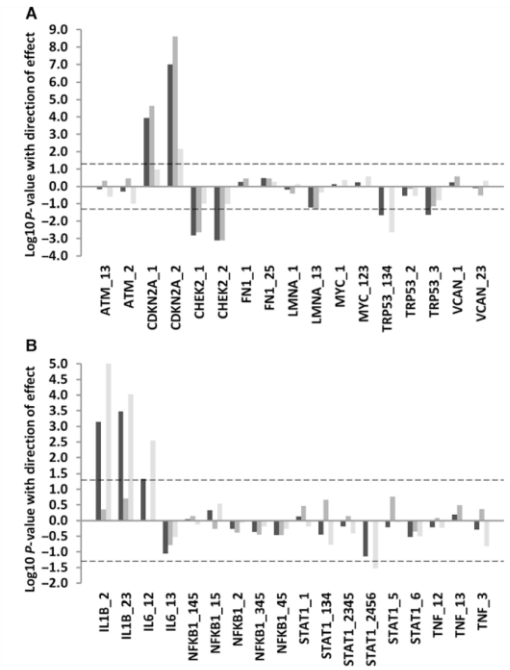

Fig. 5 The expression of alternative isoforms of key genes according to mouse age. This plot illustrates association between the expression of age and the expression of alternatively expressed isoforms of key genes in total RNA from spleen (A) or muscle (B) tissues in young (6 months) vs. old (20–22 months) mice. The identity of isoforms is given on the *x*-axis. The log10 *P*-values for associations between age and the expression of alternative isoforms from mice of different ages and of different strains are given on the *y*-axis. Direction of effect is also indicated; data appearing above the zero line on the *y*-axis represent positive associations, whilst data appearing below the zero line represent negative associations. Analysis including all animals in the sample is given by dark grey bars, in animals of average-lived strains only by medium grey bars and in long-lived animals only by light grey bars. The dotted line refers to a *P*-value cut-off for statistical significance of $P = 0.05$.

isoforms to be significantly reduced in old animals of long-lived strains as described above. We also identified decreased expression of both uc008yrw.1 (full length) and uc008yrx.1 (exon skipped) isoforms of the *Chek2* gene with increasing age (beta coefficients −0.33 and −0.35, $P = 0.02$ and 0.01, respectively). Interaction analyses between mouse age and strain longevity revealed that reduced expression of the full-length *Chek2* isoform was more marked in the old animals of the long-lived strains (beta coefficient −0.26, $P = <0.0001$ in the old long-lived animals compared with beta coefficient −0.24, $P = 0.003$ in the old average-lived animals; Table S9). *Trp53* isoforms also demonstrated effects with age in mouse spleen. With age, there was a reduction in levels of transcripts encoding both full-length p53 (uc007jql.2/uc007jqn.2) and also those encoding the truncated alternatively spliced p53AS (uc007jqm.2) isoform (beta coefficients −0.24 and −0.24, $P = 0.02$ and 0.03, respectively).

In mouse muscle, we found increased expression of both the full-length (uc008mht.1) and the intron-inclusion (uc008mhu.1) *Il1b* transcripts with age (beta coefficients 0.37 and 0.39, $P = 0.001$ and < 0.0001). The old animals also demonstrated elevated expression of the uc008wuv.1 isoform of the *Il6* gene, which contains a retention of intron 4 relative to the consensus transcript (beta coefficient 0.44, $P = 0.003$). Old animals also demonstrated reduction of uc007ayd.2, uc007aya.2, uc007ayb.2 and uc007ayc.2 isoforms of the *Stat1* gene, with the effects on uc007aya.2 being revealed by interaction analysis between mouse age and strain lifespan to be present exclusively in the old animals of long-lived strains (beta coefficient −0.17, $P = 0.01$; Table S9).

The expression of some splicing factors is associated with parental longevity in a large human population

We examined the expression of 15 splicing factors identified through the mouse work described in this study and previous analyses (Holly *et al.*, 2013) and determined that 2 genes, *HNRNPA2B1* and *HNRNPA1*, demonstrated associations of their expression with parental longevity, as defined in Dutta *et al.* (2013a) in the human InCHIANTI population study as well as in mice (Table 1). *HNRNPA2B1* transcripts demonstrated increased expression in the offspring of long-lived parents (beta coefficients 0.12, $P = 0.017$), whereas *HNRNPA1* demonstrated reduced expression in the offspring of long-lived parents (beta coefficient −0.09; $P = 0.035$, respectively; Table 1). *Hnrnpa1* demonstrates reduced expression in association with longevity in both man and mouse, whereas *Hnrnpa2b1* shows elevated expression with longevity in people, but reduced expression with longevity in mice.

Genetic variation within Hnrnpa2b1 and Hnrnpa1 that is discrepant between strains is unlikely to contribute to differences in gene expression

We have carried out a bioinformatic analysis of the potential for genetic variation that is discrepant between strains of mice to affect the regulation of the *Hnrnpa2b1* and *Hnrnpa1* genes. These genes were selected because their expression is associated with longevity in both mouse and man. The *Hnrnpa2b1* gene harbours 14 genetic variants that are discordant between strains. Two of these variants, rs51031918 and rs252413833, are associated with changes to the binding efficiencies of SRSF2 and SRSF5 splicing enhancers (see Table S12). These changes are, however, very subtle and may not adversely affect SRSF2 or SRSF5 binding. Similarly, two *Hnrnpa1* variants (rs32398879 and rs50030666) are discordant between the strains. One of these, rs50030666, lies in a cassette exon which is intronic in some *Hnrnpa1* isoforms, but coding in others (see Table S12). The coding change causes the substitution of glycine residue for a similarly sized serine residue with equivalent charge. No other predicted effects of genetic variation on transcription factor binding, RNA regulatory elements (A-rich elements, C to U RNA editing sites or microRNA binding sites) were identified for any variant studied.

Discussion

Splicing factor expression has been shown to be conclusively associated with chronological age in humans (Harries *et al.*, 2011) and also with cellular senescence in multiple human primary cell lines in culture (Holly *et al.*, 2013), indicating that these factors may be linked with cellular plasticity and adaptability during the aging process. Here, we have assessed the potential relationships between splicing factor expression and alternative splicing with strain longevity across 6 mouse strains of variable medium to long lifespans, in both young and old animals. We also assessed associations between splicing factor expression and parental longevity in the offspring of long-lived parents in humans.

Table 1 Associations between splicing factor expression and parental longevity in humans (the InCHIANTI population)

Gene name	Probe Id	Beta coefficient	95% Confidence intervals		*P*-value
HNRNPA2B1	ILMN_1886493	0.116	0.020	0.212	**0.017**
HNRNPA1	ILMN_1676091	−0.091	−0.176	−0.006	**0.035**
HNRNPA2B1	ILMN_2369682	0.088	0.002	0.175	**0.044**
TRA2B	ILMN_1742798	0.092	−0.001	0.186	0.051
HNRNPA1	ILMN_1661346	0.069	−0.004	0.143	0.065
SRSF1	ILMN_1795341	0.082	−0.008	0.171	0.073
HNRNPD	ILMN_2321451	0.088	−0.010	0.186	0.078
HNRNPK	ILMN_1701753	−0.066	−0.176	0.043	0.232
HNRNPUL2	ILMN_2072091	0.076	−0.053	0.205	0.246
HNRNPK	ILMN_2378048	0.060	−0.058	0.178	0.319
SRSF18	ILMN_2161357	0.068	−0.072	0.209	0.341
HNRNPUL2	ILMN_1810327	0.055	−0.066	0.176	0.374
HNRNPA1	ILMN_2220283	0.034	−0.051	0.119	0.432
SRSF2	ILMN_1696407	0.047	−0.074	0.167	0.446
HNRNPD	ILMN_1751368	−0.034	−0.137	0.068	0.511
SRSF6	ILMN_1697469	0.033	−0.077	0.143	0.552
SRSF6	ILMN_1754304	0.030	−0.078	0.138	0.585
HNRNPA0	ILMN_1753279	−0.035	−0.164	0.095	0.598
HNRNPA1	ILMN_1663447	−0.034	−0.168	0.101	0.624
HNRNPA1	ILMN_1720745	0.025	−0.080	0.131	0.637
HNRNPM	ILMN_2385173	−0.029	−0.161	0.103	0.668
SRSF6	ILMN_1805371	−0.026	−0.149	0.096	0.673
SF3B1	ILMN_1712347	−0.022	−0.151	0.107	0.738
SF3B1	ILMN_1705151	0.017	−0.091	0.125	0.754
HNRNPM	ILMN_1745385	−0.016	−0.119	0.086	0.756
HNRNPA1	ILMN_2175075	−0.012	−0.126	0.102	0.838
SRSF3	ILMN_2389582	0.004	−0.118	0.125	0.951

The relationship of parental longevity with expression of 15 unique splicing factors in 405 individuals by multivariate linear regression. Genes demonstrating significant associations at $P = <0.05$ are indicated in bold underlined text.

We have found that over half of the splicing factors tested are associated with longevity in mouse spleen, and to a lesser extent in mouse muscle and that these changes are accompanied by alterations to the profile of selected alternatively expressed isoforms in both tissues. Two splicing factors, *HNRNPA1* and *HNRNPA2B1,* also showed evidence of an association with parental longevity in humans. These results, to our knowledge, represent the first link between the regulation of alternative splicing and inherited longevity traits in mammals.

In spleen, 7/8 splicing factors tested demonstrated associations with strain longevity in both young and old animals, with effects being predominant in the young animals of longer-lived strains suggesting that these differences in splicing factor expression are not the end result of aging processes as such, but rather may represent fundamental differences in factor expression that drive or contribute to the aging process. It is possible that changes happening early on in life may set the scene for future longevity, which is an interesting concept given that several genes such as *Foxo1,* known to be associated with extended lifespan, are developmental genes (Lunetta *et al.*, 2007). It is very difficult to predict what the consequence of these changes will be to the overall level or pattern of splicing in long-lived mice or humans, since splice site choice at any given exon: intron junction is determined by the balance of activators and repressors, and that this balance is individually determined for each splice site in each gene (Cartegni *et al.*, 2002). However, diminished splicing factor expression may be beneficial in younger animals, since both SRSF and hnRNP splicing factors are known to have oncogenic features (Gautrey *et al.*, 2015; Goncalves & Jordan, 2015; Guo *et al.*, 2015). Lower splicing factor expression in younger animals may thus protect against an earlier death from malignancy.

We also found clear evidence to suggest tissue specificity of effect which is very common in studies of splicing with 8/15 (53%) splicing factors showing associations with strain longevity in spleen, but only 3/15 (20%) in muscle. It would be interesting to determine whether the splicing events targeted by these sets of splicing factors also show associations between median strain lifespan and splice site usage, but such analysis would be very difficult due to degeneracy of splicing factor binding sites, potential for compensation by other splicing factors and the fact that splice site usage is dependent on the balance of enhancers and silencers rather than on the binding of a specific splicing factor *per se*. The pattern of longevity-associated splicing regulator transcripts showed little overlap between the spleen and muscle data sets, with only changes to *Srsf3* expression being common to both tissues. This is in line with our previous findings, as we have previously shown that although fibroblasts and endothelial cells that have undergone *in vitro* senescence both show deregulation of splicing factors, the patterns of precisely which regulators are altered show quite marked differences between cell types (Holly *et al.*, 2013). Spleen is a lymphoid organ, consisting of large numbers of white blood cells. Most of the transcripts extracted from spleen will arise from B cells, T cells and mononuclear phagocytes. Our findings may thus reflect the hypothesis that aging of the immune system is one of the drivers of development of aging phenotypes (Franceschi & Campisi, 2014). It should also be considered that the preponderance of splicing factor expression changes in spleen compared with muscle could also reflect an accelerated rate of aging and more extensive tissue modification in spleen compared to muscle. White blood cells are also highly heterogeneous, reactive and proliferative but relatively unspecialized compared to the highly differentiated nonproliferative muscle cells. It may be that muscle requires less adaptive response than spleen cells, since it has a defined and tightly regulated function with less need to respond to environmental challenge.

Previous work from our group has identified that offspring of long-lived parents may have better health (Dutta *et al.*, 2013a,b). In the current study, two of the associations between splicing factor expression and longevity were also seen in RNA samples derived from the peripheral blood of participants in the InCHIANTI study (Ferrucci *et al.*, 2000), where we found relationships between expression of the *HNRNPA2B1* and *HNRNPA1* transcripts and parental longevity. *HNRNPA2B1* demonstrated increased expression in blood RNA from people with at least one long-lived parent, whereas parental longevity (as a continuous trait reflecting the combined age at death of both parents) was associated with lower *HNRNPA1* expression (Table 1). *Hnrnpa1* is also downregulated with greater lifespan in mouse splenocytes, but the *HNRNPA2B1* effect in humans is reversed compared to what we observe in the mice. This may be because the association between *Hnrnpa2b1* expression and longevity is most marked in the young animals of the long-lived strains, and our human subjects are mostly elderly, with a mean age of approximately 75 years (Harries *et al.*, 2011). Interestingly, both *Hnrnpa2b1* and *Hnrnpa1* are known to be determinants of lifespan in *Drosophila* species, by virtue of their regulation of the TDB-43 protein (Romano *et al.*, 2014). TDB-43 is crucial in fruit flies for correct splicing and regulation of mRNA stability and is associated with amyotrophic lobar sclerosis and frontotemporal lobar degeneration in humans (Neumann *et al.*, 2007; Kim *et al.*, 2013). Mutations have also been described in age-related diseases such as Alzheimer's, Parkinson's and Huntington's diseases (Baloh, 2011). Recent studies have shown that the action of TDB-43 relies on its ability to tether hnRNPA2B1 and hnRNPA1

proteins, and disruption or abolition of this association dramatically reduces lifespan in *Drosophila* (Romano *et al.*, 2014).

The consequences of altered splicing in spleen give a broad picture of altered expression and processing of genes involved in reduced cell senescence, superior DNA repair and retained cellular proliferative capacity in the long-lived strains. Old animals of long-lived strains of mice expressed reduced amounts of *Cdkn2a* isoforms compared with old animals of average-lived strains. *Cdkn2a* is an important marker of cellular senescence (Tominaga, 2015) and ablation of *Cdkn2a* expression reverses aging phenotypes in klotho mice (Sato *et al.*, 2015), indicating that old animals of long-lived strains may have lower levels of senescent cells. Young animals of longer-lived strains also expressed profiles of *Trp53* isoforms consistent with enhanced transcription and cell growth properties compared to young animals of average-lived strains, since they express higher levels of full-length p53 and lower levels of truncated p53AS which is thought to have antagonistic function (Wu *et al.*, 1997; Almog *et al.*, 2000; Huang *et al.*, 2002). Altered splicing of inflammatory genes involved in muscle remodelling produces a picture consistent with lower levels of pro-inflammatory signalling by virtue of lower levels of *Il1b* and *Il6* expression in young animals and reduced *Tnf* signalling in the older animals of long-lived strains.

We saw fewer associations of splicing factor expression with chronological age than we expected based on our previous human data. Our previous work suggests that splicing factor expression is strongly associated with age in humans and with cellular senescence in human cell models (Harries *et al.*, 2011; Holly *et al.*, 2013). In our human work, the per-year age-related changes in splicing factor expression were also relatively small (beta coefficients ranging from −0.01 to 0.005) (Holly *et al.*, 2013), which may explain why strong effects were not seen in the current mouse study where our sample numbers were much smaller. There is also considerable interstrain heterogeneity for most splicing factors; the young animals of one strain may express lower basal levels of splicing factors than the older animals of another and effects of aging may thus be difficult to detect in small numbers of samples (Fig. S1). These data suggest that the associations of splicing factor expression with longevity across strains may actually be considerably larger than effects of age alone on splicing factor expression within strains. Again, most changes seen in this study were seen in spleen, which is consistent with a key role in senescence for immune-mediated drivers of aging and aging phenotypes.

The limitations of our study include the relatively small sample sizes, restriction of our analyses to a small number of tissues, and the fact that we have assessed splicing patterns only at the mRNA level. Gene expression is a highly variable parameter in biological systems, so future experiments are likely to need larger sample sizes and assessment of potential effects in other tissue types, as well as assessment of effects on protein levels. Although the genes tested were selected *a priori* and therefore do not require adjustment for multiple testing, one must recognize that this does not entirely remove the possibility of false positives. It must also be considered that differences in splicing factor and isoform expression may arise not only from changes in the amount of transcription, but also from differences in the relative stabilities of different isoforms. These changes may form part of the mechanistic basis for our associations, as we would not expect stability changes unrelated to longevity to associate statistically with strain median lifespan. Finally, in the human follow up work described here, we were also restricted by the availability of expression data for all interesting splicing factors on the array and the likelihood that any effects were likely to be moderate on a per-year basis as they were in our previous human age data. This is likely to have reduced our power in the human study, and thus further work in larger populations is now required to definitively explore this possibility in human subjects.

Another potential caveat is that the splicing factor expression differences we have discovered in this study reflect other strain differences that are unrelated to longevity. Whilst this is a possibility, the links between splicing factor expression and aging in humans and other animals are well documented from our previous work (Harries *et al.*, 2011; Holly *et al.*, 2013) and that of other groups (Meshorer & Soreq, 2002). Our observation that the lifespan-associated expression changes relating to *Hnnrpa2b1* and *Hnrnpa1* we observe in mice are also translatable to humans is also supportive of our conclusions. More broadly, the importance of splicing factors in determination of lifespan is also suggested by studies of the effects of calorific restriction in mice (Swindell, 2009) and studies of the relationship between copy number variant (CNV) polymorphisms and longevity in humans (Glessner *et al.*, 2013).

Some of the genetic differences between strains may actually contribute mechanistically to the differences in strain median lifespan. To that effect, we carried out a bioinformatic analysis on the potential for genetic variation discordant between strains to lead to gene regulation differences for *Hnrnpa2b1* and *Hnrnpa1*, where we also found effects in man. We discovered some minor changes to the bioinformatically predicted strength of SRSF2 and SRSF5 binding within *Hnrnpa2b1* and a potential amino acid change for an alternatively expressed isoform of *Hnrnpa1*. Although these predictions are interesting, the predicted effects of the changes on *Hnrnpa2b1* or *Hnrnpa1* expression or activity are likely to be slight. The splicing effects cause only a slight alteration to predicted binding efficiency of SRSF2 or SRSF5, and the coding change involves the substitution of a serine for a glycine in an alternatively spliced cassette exon of *Hnrnpa1,* which may not comprise the major isoform at this locus. These amino acids are in any case of similar size and charge and may not cause much change to protein functionality. It is likely the effects on median strain longevity arise from multiple changes in many genes.

To be able to assign definitive causality for a role for splicing factors as determinants of longevity, it would be necessary to carry out detailed functional experiments *in vivo* and *in vitro*, which could form the basis for future studies. Such studies could comprise constitutive or conditional knockout or overexpression studies in animal models followed by assessment of effects on lifespan, or *in vitro* manipulation of splicing factor levels followed by investigation of effects on cellular senescence. Such an approach has previously been employed for the *Hnrnpa1* and *Hnrnpa2b1* genes where upregulation of the *Hnrnpa1* gene or the *Hnrnpa2* isoform of the *Hnrnpa2b1* gene in mouse hepatocarcinoma cells was shown to cause activation of the RAS-MAPK-ERK pathway (Shilo *et al.*, 2014). This is potentially important since a recent study has shown that activation of the RAS-ERK-ETS pathway is a key determinant of lifespan in Drosophila species (Slack *et al.*, 2015).

Both *in vivo* and *in vitro* studies to moderate the levels or activity of splicing factors in relation to longevity would not be without caveat. Splice site choice is a complex phenomenon and relies upon the balance of splicing activators or silencers, rather than the activity of a single splicing factor *per se* (Cartegni *et al.*, 2002). This finding, together with observations that exon and intron splicing enhancers and silencers often cluster near splice sites, raises the possibility of compensation between splicing regulatory factors. Selective modulation of a single splicing factor may not then show direct effects on longevity, effects would most probably only be noted after knockdown or overexpression of multiple splicing factors which would have technical challenges both *in vitro* and *in vivo*.

This study reports the first evidence of a link between expression of splicing regulator genes and strain lifespan in mice, together with data in support of potential roles for *HNRNPA1* and *HNRNPA2B1* in parental longevity in humans. We hypothesize that an influence of splicing factor expression on longevity may be mediated by slower immune aging and a protection from malignancy in the young mice of long-lived strains by virtue of restricting expression of SR and hnRNP proteins which have oncogenic potential in young animals. Both of the splicing factor transcripts demonstrating reduced expression in the old long-lived mice belonged to the hnRNP class of splicing regulators, indicating that these mice may have less inhibition of splice site usage and be better able to maintain splicing, and therefore cellular plasticity into older age. The changes in splicing factor expression in the spleen are accompanied by changes in alternatively spliced genes indicative of reduced cell senescence, superior DNA repair and retained cellular proliferative capacity, and changes in splicing factor expression in muscle are indicative of lower pro-inflammatory signalling. Our data highlight the importance of regulation of mRNA processing in determination of lifespan and suggest that splicing factors may provide novel points of intervention for future therapies to reduce disease burden in old age. Moreover, since some of these strains (e.g. C57BL/6J, A/J) are commonly used for the creation and cross-breeding of genetically modified mice, strain-specific alterations in alternative splicing could account for unexpected contributions to the final phenotype arising from the genetic background.

Experimental procedures

Mouse strains used for analysis

Strains were chosen on the basis of differential lifespan (A/J, NOD.B10Sn-H2^{b}/J, PWD.Phj, 129S1/SvlmJ, C57BL/6J and WSB/EiJ; see Table 2 for lifespan details) that were measured in a longitudinal study (Yuan *et al.*, 2009, 2011, 2012) at Jackson Laboratory Nathan Shock Center of Excellence in the Basic Biology of Aging. Strains with extremely short lifespans (median lifespan less than 600 days) were excluded on the basis that a short lifespan may be associated with significant comorbidities. Characteristics of the mice and the numbers of animals used in each category are given in Table 2. All mice used in this study were male. All tissues were obtained from the mice of a cross-sectional study that was conducted at the same period of time and in the same mouse room with the longitudinal study. Animal housing conditions have been fully described previously (Yuan *et al.*, 2009, 2012). Briefly, mice were fed *ad libitum* an autoclaved pellet diet with 6% fat and acidified water (pH 2.8–3.1). Animals were kept on a 12:12-h light/dark cycle at 50% relative humidity at 21–23 °C, in a restricted access specific pathogen-free barrier facility. Mice were housed four animals per pen in individually ventilated polycarbonate cages supplied with HEPA-filtered air and were tested quarterly for (and were free of) common viral, bacterial and mycoplasmal species. Mice were inspected daily and excluded if ill. At 6 or 20/22 months of age, mice were euthanized by CO_2 asphyxiation, followed by blood collection via cardiac puncture and cervical dislocation. A detailed description of the tissue collection procedure is given in Data S1. Immediately after death, spleen and quadriceps muscle tissues were excised and snap-frozen in vapour-phase liquid nitrogen for storage within 5 min of collection. Tissues were stored at −80 °C.

Splicing factor candidate genes for analysis

An *a priori* list of splicing factor candidate genes were chosen on the basis that they were associated with human aging in populations and in primary human cell lines that had undergone *in vitro* senescence in our previous work (Harries *et al.*, 2011; Holly *et al.*, 2013). The list of genes included the positive regulatory splicing factors *Srsf1, Srsf2, Srsf3, Srsf6, Srsf18* and *Tra2β*, the negative regulatory splicing inhibitors *Hnrnpa0, Hnrnpa1, Hnrnpa2b1, Hnrnpd, Hnrnph3, Hnrnpk, Hnrnpm, Hnrnpul2* and the *Sf3b1* subunit of the U2 spliceosome snRNP, which we have previously shown to be associated with age-related altered DNA methylation (Holly *et al.*, 2014). Assays were obtained in custom TaqMan low-density array (TLDA) format from Life Technologies (Foster City, CA, USA). Assay Identifiers are given in Data S1.

Alternatively spliced target genes in spleen

Genes were chosen for assessment of alternative splicing in spleen on the basis of potential roles in cellular senescence (*Cdkn2a*), cell cycle regulation (*Trp53*, *Myc*), extracellular matrix (*Fn1, Vcan*) or DNA damage response (*Atm, Chek2*), since these genes may also be important in

Table 2 Characteristics of mouse strains used in this study

Strain	Strain Median lifespan (days)*	Strain Max Age (days)	Longevity class	N Young	N Old
A/J	623	785	Average lifespan	Spleen – 7 Muscle – 8	Spleen – 7 Muscle – 7
NOD.B10Sn-H2^{b}/J	696	954	Average lifespan	Spleen – 4 Muscle – 4	Spleen – 6 Muscle – 6
PWD.PhJ	813	956	Average lifespan	Spleen – 5 Muscle – 4	Spleen – 6 Muscle – 6
129S1/SvlmJ	882	1044	Long-lived	Spleen – 10 Muscle – 4	Spleen – 10 Muscle – 10
C57BL/6J	901	1061	Long-lived	Spleen – 10 Muscle – 10	Spleen – 8 Muscle – 9
WSB/EiJ	1005	1213	Long-lived	Spleen – 5 Muscle – 5	Spleen – 10 Muscle – 10

*Strain Max Age = the mean of the longest lived 20% within each strain. Data for median and maximum lifespans are given in Yuan *et al.* (2011) from a longitudinal study that was performed in conjunction with the cross-sectional study described in the present paper.
The mean lifespan and the maximum lifespan (20% longest lived) are given for each strain used in this study. All mice used in this study were male. Young mice were 6 months old, and old mice were 20–22 months old. Muscle tissue was taken from the quadriceps.

determination of lifespan. We designed TaqMan quantitative real-time PCR assays to identify specific isoforms or groups of isoforms (if large numbers of common regions rendered the design of specific probes impossible). Assays were obtained in custom TaqMan low-density array (TLDA) format from Life Technologies. Assay Identifiers are given in Data S2. A list of transcripts captured by each assay are given in Data S3.

Alternatively spliced target genes in muscle

Genes were selected for analysis of alternative splicing in muscle on the basis of potential roles in inflammatory processes relating to muscle remodelling since we have shown in our previous work that these processes are key determinants of muscle strength in older humans (Harries *et al.*, 2012; Blackwell *et al.*, 2015). Our gene list included isoforms of the *Il1b, Il6, Nfkb1, Stat1* and *Tnf* genes. As above, TaqMan quantitative real-time PCR assays were designed to identify specific isoforms or groups of isoforms (if large numbers of common regions rendered the design of specific probes impossible). Assays were obtained in custom TaqMan low-density array (TLDA) format from Life Technologies. Assay Identifiers are given in Data S2.

RNA extraction and reverse transcription

Tissue samples were removed from storage and placed in 1 mL TRI Reagent® solution supplemented with the addition of 10 mM $MgCl_2$ to aid recovery of microRNAs for future analysis (Kim *et al.*, 2012). Samples were then completely homogenized (15mins for spleen samples, 30mins for muscle samples) using a bead mill (Retsch Technology GmbH, Haan, Germany). Phase separation was carried out using chloroform. Total RNA was precipitated from the aqueous phase by means of an overnight incubation at −20 °C with isopropanol. RNA pellets were then ethanol-washed twice and resuspended in RNase-free dH2O. RNA quality and concentration was assessed by Nanodrop spectrophotometry (Wilmington, DE, USA). Complementary DNA (cDNA) was then reverse-transcribed from 100 ng total RNA using the Invitrogen VILO cDNA synthesis kit (Life Technologies) in 20 μL reactions according to manufacturer's instructions.

Quantitative real-time PCR and data analysis

Quantitative RT–PCRs were performed on the ABI 7900HT platform (Life Technologies) on the TaqMan low-density array (TLDA) platform. Cycling conditions were 50 °C for 2 min, 94.5 °C for 10 min and 50 cycles of 97 °C for 30 s and 57.9 °C for 1 min. The reaction mixes included 50 μL TaqMan® Universal PCR Mastermix II (no AmpErase® UNG) (Life Technologies), 30 μL dH2O and 20 μL cDNA template. 100 μL reaction solution was dispensed into the TLDA card chamber and centrifuged twice for 1 min at 216 × g to ensure distribution of solution to each well. The expression of transcripts in each sample was measured in duplicate replicates. The comparative Ct technique was used to calculate the expression of each test transcript (28). Expression was assessed relative to the global mean of expression and normalized to the median level of expression for each individual transcript. Data were log-transformed to ensure normal distribution of data. Associations of transcript expression were assessed by linear regression against age, or lifespan as appropriate. Associations of transcript expression with mouse age were assessed in all animals and in animals of average-lived or long-lived strains individually, and associations of transcript expression with strain lifespan were assessed in all animals and in young and old groups individually. We also assessed the effect of potential nonlinearity of response for the splicing factor genes in spleen and muscle by a secondary analysis using binary logistic regression on data split by the median lifespan of all the strains. These statistical analyses were carried out using SPSS v.22 (IBM, North Castle, NY, USA). Interaction between strain longevity and mouse age was assessed using data categorized into average-lived or long-lived on the basis of interstrain median lifespan and was carried out in STATA v.14 (StataCorp, College Station, TX, USA).

Gene expression cluster analysis for heterogeneity of splicing factor expression with age

The expression of each gene was z-transformed to be on the scale of standard deviations from the mean, and then the expression values for each gene were plotted against the corresponding sample to generate a heat map. Hierarchical clustering methods were used to group similar expression profiles together. This analysis was done using the 'HEATMAP.2' package in R statistical software package v3.1.1 (Vienna, Austria).

Association between splicing factor expression and parental longevity in the InCHIANTI population

The participants in the InCHIANTI study aged 65+ years were categorized based on the age at death of their parents, the parental longevity score (PLS). Participants (total $n = 405$) were classified as either 'two short-lived parents' ($n = 17$), 'one short- and one intermediate-lived parent' ($n = 140$), 'two intermediate-lived parents' ($n = 190$) or 'any long-lived parents' ($n = 58$). Short-, intermediate- and long-lived cut-offs were calculated separately for mothers and fathers based on the normal distribution of age at death in the cohort, as described in Dutta *et al.* (2013a). The cut-offs for mothers were as follows: short-lived (49–72 years), intermediate-lived (72–95 years) and long-lived (> 95 years); mothers aged < 49 years at death were classed as premature and excluded. The cut-offs for fathers were: short-lived (52–67 years), intermediate-lived (68–89 years) and long-lived (> 89 years); fathers aged < 52 years at death were classed as premature and excluded.

To assess the association between the gene expression levels of the 15 splicing factor genes in whole blood as defined in our previous work (Holly *et al.*, 2013) and parental longevity score, linear regression models were carried out using R statistical software package v3.1.1 (Vienna, Austria), with gene expression as the dependent variable. Models were adjusted for age, sex, waist circumference, highest education level attained, smoking (pack-years), study site, batches and cell counts (neutrophils, monocytes, basophils, eosinophils and whole white blood cell count). Gene expression data were rank-normalized prior to analysis to remove any skew.

Bioinformatic assessment of potential regulatory effects of genetic variation within Hnrnpa2b1 and Hnrnpa1 genes

To assess the potential for genetic variation to contribute to splicing factor expression differences that we observe between strains, we have carried out a detailed examination of the strain-discordant genetic differences in the splicing factor genes *Hnrnpa2b1* and *Hnrnpa1,* which demonstrate links with longevity in both mouse and man. Complete genome sequence data were available for 4 of the strains we have used in our analysis (C57BL/6J, 129S1/SvImJ, A/J and WSB/EiJ). SNPs discordant between strains were examined for evidence of effects on gene regulation by a variety of bioinformatic approaches. Firstly, SNPs located in the 5′ UTR of the *Hnrnpa2b1* or *Hnrnpa1* genes were assessed for

position relative to known transcription factor binding sites using REGRNA2.0 (http://regrna2.mbc.nctu.edu.tw/), an integrated web server tool that allows screening for potential regulatory elements. Secondly, intronic SNPs were assessed for their ability to interrupt exon and intron splicing enhancer and silencer loci using REGRNA2.0 and ESEFINDER (http://rulai.cshl.edu/cgi-bin/tools/ESE3/esefinder.cgi?process=home), a specific tool for the identification of splicing regulatory elements. Finally, sequences in the 3′ untranslated region were screened for ability to disrupt elements with potential to disrupt elements important for mRNA stability (A-rich elements, C to U RNA editing sites and miRNA binding sites) using REGRNA2.0.

Acknowledgments

The authors would like to acknowledge the Wellcome Trust (grant number WT097835MF LWH, DM), and NIH-NIA grant number AG038070 to The Jackson Laboratory for providing the funding for this study. We would also like to acknowledge the contributions of Federica Bighi and John Watt for technical assistance. The authors have no conflict of interest to disclose.

Author contributions

BL carried out laboratory work, analysis and contributed to the manuscript, LCP contributed the statistical assessment of parental longevity in the human samples. FE contributed technical assistance and analysis. KF advised on selection and mouse strains and analytical approaches. RY and LP designed and managed the initial mouse lifespan study, identified genetic differences in *Hnrnpa2b1* and *Hnrnpa1* discordant between strains and contributed to the manuscript. DEH codirected the Jackson laboratory Nathan Shock Centre of Excellence in the Basic Biology of Aging at the time this work was performed, and was instrumental in facilitating the mouse collection and animal husbandry facilities used in this study. GAK contributed to and reviewed the manuscript. LF provided access to the InCHIANTI study data. DM comanaged the study and reviewed the manuscript. LWH managed the study, interpreted the data and wrote the manuscript.

References

Almog N, Goldfinger N, Rotter V (2000) p53-dependent apoptosis is regulated by a C-terminally alternatively spliced form of murine p53. *Oncogene* **19**, 3395–3403.

Baloh RH (2011) TDP-43: the relationship between protein aggregation and neurodegeneration in amyotrophic lateral sclerosis and frontotemporal lobar degeneration. *FEBS J.* **278**, 3539–3549.

Barbosa-Morais NL, Carmo-Fonseca M, Aparicio S (2006) Systematic genome-wide annotation of spliceosomal proteins reveals differential gene family expansion. *Genome Res.* **16**, 66–77.

Barbosa-Morais NL, Irimia M, Pan Q, Xiong HY, Gueroussov S, Lee LJ, Slobodeniuc V, Kutter C, Watt S, Colak R, Kim T, Misquitta-Ali CM, Wilson MD, Kim PM, Odom DT, Frey BJ, Blencowe BJ (2012) The evolutionary landscape of alternative splicing in vertebrate species. *Science* **338**, 1587–1593.

Blackwell J, Harries LW, Pilling LC, Ferrucci L, Jones A, Melzer D (2015) Changes in CEBPB expression in circulating leukocytes following eccentric elbow-flexion exercise. *J. Physiol. Sci.* **65**, 145–150.

Bogue MA, Peters LL, Paigen B, Korstanje R, Yuan R, Ackert-Bicknell C, Grubb SC, Churchill GA, Chesler EJ (2014) Accessing data resources in the mouse phenome database for genetic analysis of murine life span and health span. *J. Gerontol. A Biol. Sci. Med. Sci.* **71**, 170–177.

Cartegni L, Chew SL, Krainer AR (2002) Listening to silence and understanding nonsense: exonic mutations that affect splicing. *Nat. Rev. Genet.* **3**, 285–298.

Danan-Gotthold M, Golan-Gerstl R, Eisenberg E, Meir K, Karni R, Levanon EY (2015) Identification of recurrent regulated alternative splicing events across human solid tumors. *Nucleic Acids Res.* **43**, 5130–5144.

Dellago H, Khan A, Nussbacher M, Gstraunthaler A, Lammermann I, Schosserer M, Muck C, Anrather D, Scheffold A, Ammerer G, Jansen-Durr P, Rudolph KL, Voglauer-Grillari R, Grillari J (2012) ATM-dependent phosphorylation of SNEVhPrp19/hPso4 is involved in extending cellular life span and suppression of apoptosis. *Aging (Albany NY)* **4**, 290–304.

Dutta A, Henley W, Robine JM, Langa KM, Wallace RB, Melzer D (2013a) Longer lived parents: protective associations with cancer incidence and overall mortality. *J. Gerontol. A Biol. Sci. Med. Sci.* **68**, 1409–1418.

Dutta A, Henley W, Robine JM, Llewellyn D, Langa KM, Wallace RB, Melzer D (2013b) Aging children of long-lived parents experience slower cognitive decline. *Alzheimers Dement.* **10**, S315–322.

Ferrucci L, Bandinelli S, Benvenuti E, Di Iorio A, Macchi C, Harris TB, Guralnik JM (2000) Subsystems contributing to the decline in ability to walk: bridging the gap between epidemiology and geriatric practice in the InCHIANTI study. *J. Am. Geriatr. Soc.* **48**, 1618–1625.

Franceschi C, Campisi J (2014) Chronic inflammation (inflammaging) and its potential contribution to age-associated diseases. *J. Gerontol. A Biol. Sci. Med. Sci.* **69**(Suppl 1), S4–S9.

Garg K, Green P (2007) Differing patterns of selection in alternative and constitutive splice sites. *Genome Res.* **17**, 1015–1022.

Gautrey H, Jackson C, Dittrich AL, Browell D, Lennard T, Tyson-Capper A (2015) SRSF3 and hnRNP H1 regulate a splicing hotspot of HER2 in breast cancer cells. *RNA Biol.* **12**, 1139–1151.

Glessner JT, Smith AV, Panossian S, Kim CE, Takahashi N, Thomas KA, Wang F, Seidler K, Harris TB, Launer LJ, Keating B, Connolly J, Sleiman PM, Buxbaum JD, Grant SF, Gudnason V, Hakonarson H (2013) Copy number variations in alternative splicing gene networks impact lifespan. *PLoS One* **8**, e53846.

Goncalves V, Jordan P (2015) Posttranscriptional regulation of splicing factor SRSF1 and its role in cancer cell biology. *Biomed. Res. Int.* **2015**, 287048.

Guo J, Jia J, Jia R (2015) PTBP1 and PTBP2 impaired autoregulation of SRSF3 in cancer cells. *Sci. Rep.* **5**, 14548.

Harries LW, Hernandez D, Henley W, Wood AR, Holly AC, Bradley-Smith RM, Yaghootkar H, Dutta A, Murray A, Frayling TM, Guralnik JM, Bandinelli S, Singleton A, Ferrucci L, Melzer D (2011) Human aging is characterized by focused changes in gene expression and deregulation of alternative splicing. *Aging Cell* **10**, 868–878.

Harries LW, Pilling LC, Hernandez LD, Bradley-Smith R, Henley W, Singleton AB, Guralnik JM, Bandinelli S, Ferrucci L, Melzer D (2012) CCAAT-enhancer-binding protein-beta expression in vivo is associated with muscle strength. *Aging Cell* **11**, 262–268.

Holly AC, Melzer D, Pilling LC, Fellows AC, Tanaka T, Ferrucci L, Harries LW (2013) Changes in splicing factor expression are associated with advancing age in man. *Mech. Ageing Dev.* **134**, 356–366.

Holly AC, Pilling LC, Hernandez D, Lee BP, Singleton A, Ferrucci L, Melzer D, Harries LW (2014) Splicing factor 3B1 hypomethylation is associated with altered SF3B1 transcript expression in older humans. *Mech. Ageing Dev.* **135**, 50–56.

Huang H, Kaku S, Knights C, Park B, Clifford J, Kulesz-Martin M (2002) Repression of transcription and interference with DNA binding of TATA-binding protein by C-terminal alternatively spliced p53. *Exp. Cell Res.* **279**, 248–259.

Kim YK, Yeo J, Kim B, Ha M, Kim VN (2012) Short structured RNAs with low GC content are selectively lost during extraction from a small number of cells. *Mol. Cell* **46**, 893–895.

Kim HJ, Kim NC, Wang YD, Scarborough EA, Moore J, Diaz Z, MacLea KS, Freibaum B, Li S, Molliex A, Kanagaraj AP, Carter R, Boylan KB, Wojtas AM, Rademakers R, Pinkus JL, Greenberg SA, Trojanowski JQ, Traynor BJ, Smith BN, Topp S, Gkazi AS, Miller J, Shaw CE, Kottlors M, Kirschner J, Pestronk A, Li YR, Ford AF, Gitler AD, Benatar M, King OD, Kimonis VE, Ross ED, Weihl CC, Shorter J, Taylor JP (2013) Mutations in prion-like domains in hnRNPA2B1 and hnRNPA1 cause multisystem proteinopathy and ALS. *Nature* **495**, 467–473.

Lisowiec J, Magner D, Kierzek E, Lenartowicz E, Kierzek R (2015) Structural determinants for alternative splicing regulation of the MAPT pre-mRNA. *RNA Biol.* **12**, 330–342.

Lu ZX, Huang Q, Park JW, Shen S, Lin L, Tokheim CJ, Henry MD, Xing Y (2015) Transcriptome-wide landscape of pre-mRNA alternative splicing associated with metastatic colonization. *Mol. Cancer Res.* **13**, 305–318.

Lunetta KL, D'Agostino RB Sr, Karasik D, Benjamin EJ, Guo CY, Govindaraju R, Kiel DP, Kelly-Hayes M, Massaro JM, Pencina MJ, Seshadri S, Murabito JM (2007) Genetic correlates of longevity and selected age-related phenotypes: a genome-wide association study in the Framingham Study. *BMC Med. Genet.* **8**(Suppl 1), S13.

Meshorer E, Soreq H (2002) Pre-mRNA splicing modulations in senescence. *Aging Cell* **1**, 10–16.
Neumann M, Igaz LM, Kwong LK, Nakashima-Yasuda H, Kolb SJ, Dreyfuss G, Kretzschmar HA, Trojanowski JQ, Lee VM (2007) Absence of heterogeneous nuclear ribonucleoproteins and survival motor neuron protein in TDP-43 positive inclusions in frontotemporal lobar degeneration. *Acta Neuropathol.* **113**, 543–548.
Romano M, Buratti E, Romano G, Klima R, Del Bel Belluz L, Stuani C, Baralle F, Feiguin F (2014) Evolutionarily conserved heterogeneous nuclear ribonucleoprotein (hnRNP) A/B proteins functionally interact with human and Drosophila TAR DNA-binding protein 43 (TDP-43). *J. Biol. Chem.* **289**, 7121–7130.
Sato S, Kawamata Y, Takahashi A, Imai Y, Hanyu A, Okuma A, Takasugi M, Yamakoshi K, Sorimachi H, Kanda H, Ishikawa Y, Sone S, Nishioka Y, Ohtani N, Hara E (2015) Ablation of the p16(INK4a) tumour suppressor reverses ageing phenotypes of klotho mice. *Nat. Commun.* **6**, 7035.
Scuderi S, La Cognata V, Drago F, Cavallaro S, D'Agata V (2014) Alternative splicing generates different parkin protein isoforms: evidences in human, rat, and mouse brain. *Biomed. Res. Int.* **2014**, 690796.
Shilo A, Ben Hur V, Denichenko P, Stein I, Pikarsky E, Rauch J, Kolch W, Zender L, Karni R (2014) Splicing factor hnRNP A2 activates the Ras-MAPK-ERK pathway by controlling A-Raf splicing in hepatocellular carcinoma development. *RNA* **20**, 505–515.
Slack C, Alic N, Foley A, Cabecinha M, Hoddinott MP, Partridge L (2015) The Ras-Erk-ETS-signaling pathway is a drug target for longevity. *Cell* **162**, 72–83.
Swindell WR (2009) Genes and gene expression modules associated with caloric restriction and aging in the laboratory mouse. *BMC Genom.* **10**, 585.
Tominaga K (2015) The emerging role of senescent cells in tissue homeostasis and pathophysiology. *Pathobiol. Aging Age Relat. Dis.* **5**, 27743.
Wu Y, Huang H, Miner Z, Kulesz-Martin M (1997) Activities and response to DNA damage of latent and active sequence-specific DNA binding forms of mouse p53. *Proc. Natl Acad. Sci. USA* **94**, 8982–8987.
Yuan R, Tsaih SW, Petkova SB, Marin de Evsikova C, Xing S, Marion MA, Bogue MA, Mills KD, Peters LL, Bult CJ, Rosen CJ, Sundberg JP, Harrison DE, Churchill GA, Paigen B (2009) Aging in inbred strains of mice: study design and interim report on median lifespans and circulating IGF1 levels. *Aging Cell* **8**, 277–287.
Yuan R, Peters LL, Paigen B (2011) Mice as a mammalian model for research on the genetics of aging. *ILAR J.* **52**, 4–15.
Yuan R, Meng Q, Nautiyal J, Flurkey K, Tsaih SW, Krier R, Parker MG, Harrison DE, Paigen B (2012) Genetic coregulation of age of female sexual maturation and lifespan through circulating IGF1 among inbred mouse strains. *Proc. Natl Acad. Sci. USA* **109**, 8224–8229.

Supporting Information

Additional Supporting Information may be found online in the supporting information tab for this article:

Fig. S1 Interstrain heterogeneity of splicing factor expression according to mouse age in mouse strains of different lifespan.

Table S1 Splicing factor expression in mouse spleen tissue by lifespan, across 6 strains of different longevities.

Table S2 Splicing factor expression in mouse muscle tissue by lifespan, across 6 strains of different longevities.

Table S3 Alternative isoform expression in mouse spleen tissue by lifespan, across 6 strains of different longevities.

Table S4 Alternative isoform expression in mouse muscle tissue by lifespan, across 6 strains of different longevities.

Table S5 Splicing factor expression in mouse spleen tissue by age in young (6 months) and old (20–22 months) mice.

Table S6 Splicing factor expression in mouse muscle tissue by age in young (6 months) and old (20–22 months) mice.

Table S7 Alternative isoform expression in mouse spleen tissue by age in young (6 months) and old (20–22 months) mice.

Table S8 Alternative isoform expression in mouse muscle tissue by age in young (6 months) and old (20–22 months) mice.

Table S9 Analyses of potential interactions between mouse strain longevity and mouse age.

Table S10 Splicing factor expression in mouse spleen tissue by lifespan, across 6 strains of different longevities by binary logistic regression.

Table S11 Splicing factor expression in mouse muscle tissue by lifespan, across 6 strains of different longevities by binary logistic regression.

Table S12 Genetic variation within the mouse Hnrnpa2b1 and Hnrnpa1 genes and its predicted effect on gene regulation.

Data S1 Detailed tissue collection protocol.

Data S2 Assay identifiers and sequence details for qRT–PCR assays used in this study.

Data S3 Alternatively expressed isoforms captured by quantitative real-time PCR assays. Microsoft word file. Additional information describing precisely which alternatively expressed isoforms of analysed genes are captured by each probe set.

www.nature.com/scientificreports

OPEN

MicroRNAs miR-203-3p, miR-664-3p and miR-708-5p are associated with median strain lifespan in mice

Received: 18 November 2016
Accepted: 10 February 2017
Published: 17 March 2017

Benjamin P. Lee[1], Ivana Burić[1], Anupriya George-Pandeth[1], Kevin Flurkey[2], David E. Harrison[2], Rong Yuan[2,†], Luanne L. Peters[2], George A. Kuchel[3], David Melzer[3,4] & Lorna W. Harries[1]

MicroRNAs (miRNAs) are small non-coding RNA species that have been shown to have roles in multiple processes that occur in higher eukaryotes. They act by binding to specific sequences in the 3' untranslated region of their target genes and causing the transcripts to be degraded by the RNA-induced silencing complex (RISC). MicroRNAs have previously been reported to demonstrate altered expression in several aging phenotypes such as cellular senescence and age itself. Here, we have measured the expression levels of 521 small regulatory microRNAs (miRNAs) in spleen tissue from young and old animals of 6 mouse strains with different median strain lifespans by quantitative real-time PCR. Expression levels of 3 microRNAs were robustly associated with strain lifespan, after correction for multiple statistical testing (miR-203-3p [β-coefficient = −0.6447, $p = 4.8 \times 10^{-11}$], miR-664-3p [β-coefficient = 0.5552, $p = 5.1 \times 10^{-8}$] and miR-708-5p [β-coefficient = 0.4986, $p = 1.6 \times 10^{-6}$]). Pathway analysis of binding sites for these three microRNAs revealed enrichment of target genes involved in key aging and longevity pathways including mTOR, FOXO and MAPK, most of which also demonstrated associations with longevity. Our results suggests that miR-203-3p, miR-664-3p and miR-708-5p may be implicated in pathways determining lifespan in mammals.

Although lifestyle and environmental factors are the major influences on lifespan, inherited factors remain important, with approximately 25% of the variation in lifespan attributable to genetics[1,2]. This is reflected in the observation that children of longer-lived parents have lower levels of age-related disease, lower all-cause mortality and greater life expectancy than those with shorter-lived parents[3,4]. In addition to the contribution of 'conventional' genetics, there is increasing evidence that epigenetic factors such as DNA methylation, histone modifications, and fine tuning of gene expression by small non-coding RNA regulators such as microRNAs (miRNAs) may also contribute significantly to aging and longevity[5,6].

MicroRNAs (miRNAs) are short, non-coding RNAs that regulate mRNA expression[7]. Targets are recognized by virtue of sequence complementarity between specific sequences in the 3' untranslated region (3' UTR) of mRNA transcripts. Once bound, miRNAs act to either repress translation of the mRNA or target it for degradation. A single miRNA can target multiple mRNAs and many mRNAs have multiple miRNA binding sites in their 3' UTR[8]. In this manner, miRNAs have the capacity to regulate complex networks such as those implicated in aging and longevity[9]. Several of the 'hallmarks' of aging[10] including cellular senescence and genomic instability have been shown to be associated with multiple miRNAs[11]. Moreover, in several cases, individual miRNAs (or families of miRNAs) are associated with more than one of these processes[11]. Nevertheless, while several studies have implicated miRNAs in

[1]RNA-mediated mechanisms of Disease, Institute of Biomedical and Clinical Sciences, University of Exeter Medical School, University of Exeter, Devon, UK. [2]The Jackson Laboratory Nathan Shock Center of Excellence in the Basic Biology of Aging, Bar Harbor, Maine, USA. [3]UConn Centre on Aging, University of Connecticut Health Centre, Farmington, Connecticut, USA. [4]Epidemiology and Public Health, Institute of Biomedical and Clinical Sciences, University of Exeter Medical School, University of Exeter, Devon, UK. [†]Present Address: Geriatric Research Division, Department of Internal Medicine, Southern Illinois University School of Medicine, Springfield, IL, USA. Correspondence and requests for materials should be addressed to L.W.H. (email: L.W.Harries@exeter.ac.uk)

MicroRNA Assay ID	Mean Difference	95% CI of the difference		*p*-value
		Upper	Lower	
mmu-miR-297b-5p	***4.29***	***4.53***	***4.05***	***1.64×10^{-11}***
mmu-miR-708	***0.47***	***0.59***	***0.36***	***5.80×10^{-6}***
mmu-miR-224	***−0.97***	***−0.63***	***−1.30***	***0.0001***
mmu-miR-203	***−0.55***	***−0.35***	***−0.75***	***0.0002***
rno-miR-327	***−3.70***	***−2.33***	***−5.07***	***0.0002***
mmu-miR-664	0.46	0.66	0.27	*0.0005*
mmu-miR-592	0.50	0.73	0.27	*0.0008*
mmu-miR-484	0.33	0.49	0.17	*0.001*
mmu-miR-687	5.02	7.58	2.46	*0.002*
mmu-miR-192	0.31	0.47	0.15	*0.002*

Table 1. MicroRNAs with strongest association between expression and lifespan in spleen tissue from young mice of shortest-lived and longest-lived strains (A/J and WSB/EiJ respectively). MicroRNAs significantly associated below the Bonferroni-corrected significance threshold ($p < 0.0002$) are shown in bold italics. The ten most strongly associated microRNAs followed up in the targeted analysis are shown in italics. *P*-values were determined using independent sample t-tests on log-transformed relative expression data from TaqMan® MicroRNA Array cards.

prediction of lifespan in *C. elegans*[12–14], less is known about their potential role in mammalian lifespan. Identification of determinants of longevity is a key aim in identifying biomarkers of healthy aging.

Inbred strains of mice, with very well defined phenotypic characteristics and fully characterized genetics have proved a useful tool in understanding complex phenotypes such as aging[15–17]. In the present study, we assessed the potential role of miRNAs in longevity using spleen tissue from 6 inbred strains of mice of different median strain lifespans[15–17]. These mice have median strain lifespans ranging from 623 days to 1005 days and as a result we have previously used them for our studies of the factors influencing lifespan[17,18]. We carried out a high-throughput screen of 521 miRNAs in the young animals of the 2 strains at the extremes of the lifespan range, to identify candidate miRNAs associated with longer lifespan. We then tested for associations between median strain lifespan and the expression of the emerging miRNAs in young and old mice of all 6 strains, to determine whether these were robust associations. We found that 3 miRNAs, miR-203-3p, miR-664-3p and miR-708-5p, were all associated with lifespan in these mice. Subsequent bioinformatic analyses of pathways predicted to be targeted by these miRNAs included several that are known to be involved in determining lifespan e.g. FoxO[19], mTOR[20] and stem cell pluripotency pathways. Furthermore, genes predicted to be targeted by these miRNAs also show evidence of associations with median strain longevity. Our results suggest that differential regulation of key aging and longevity pathways by miRNAs may underpin some of the phenotypic variation in lifespan in mammals.

Results

High-throughput MicroRNA Arrays. We carried out a near-global, high throughput screen of expression of 521 miRNAs in spleen samples of young animals culled at 6 months of age from the 2 mouse strains from our collection showing the most marked divergence in lifespan (A/J; 623 days and WSB/EiJ; 1005 days) by qRT-PCR using TaqMan® MicroRNA Array cards. 279 miRNAs were found to be expressed above the limit of detection and of these, 5 (miR-297b-5p, miR-708-5p, miR-224-5p, miR-203-3p and miR-327) were shown to be differentially expressed between average-lived and long-lived strains after correction for multiple testing (significance cutoff: $p < 0.0002$). Five additional miRNAs (miR-664-3p, miR-592-5p, miR-484, miR-687 and miR-192-5p) showed expression differences which were close to significance (significance cut-off: $p < 0.002$). The results for these 10 miRNAs are summarized in Table S1. See Supplementary Table S1 for results of the full analysis.

Targeted microRNA Expression. We then measured the expression levels of the 10 miRNAs demonstrating significant or near significant associations with median strain lifespan in spleen samples from both young and old animals of all 6 mouse strains. We found that 3 miRNAs; miR-203-3p, miR-664-3p and miR-708-5p were associated with median strain lifespan (Supplementary Table S2). These 3 miRNAs were also associated with strain median lifespan in a replication sub analysis excluding all animals included in the discovery analysis (Supplementary Table S3). Analysis of expression in relation to age of the animals revealed that miR-203-3p was not significantly associated with age whereas both miR664-3p and miR-708-5p were positively associated (see Supplementary Table S4). This finding led us to perform an analysis to detect interactions between miRNA expression, age, and median strain lifespan, results of which are given in Supplementary Table S5.

MicroRNA miR-203-3p showed significantly reduced expression in both young and old animals of strains of longer lifespan when considered separately, as well as in the analysis of old and young animals of different median strain lifespans combined, after correction for multiple testing (β-coefficients $= -0.64$, -0.67 and -0.67; $p = 4.78 \times 10^{-11}$, 3.60×10^{-6} and 4.74×10^{-7} for all, young and old analyses respectively, see Supplementary Table S2 and Fig. 1a–c). Interaction analysis revealed no significant difference between young and old animals of average-lifespan strains (β-coefficient $= -0.05$; SE $= 0.08$; $p = 0.55$, see Supplementary Table S5 and Fig. 2). However, significant expression differences were seen between strains of average lifespan and long lifespan, with the most marked differences occurring in the young animals of long-lived strains (β-coefficient $= -0.29$;

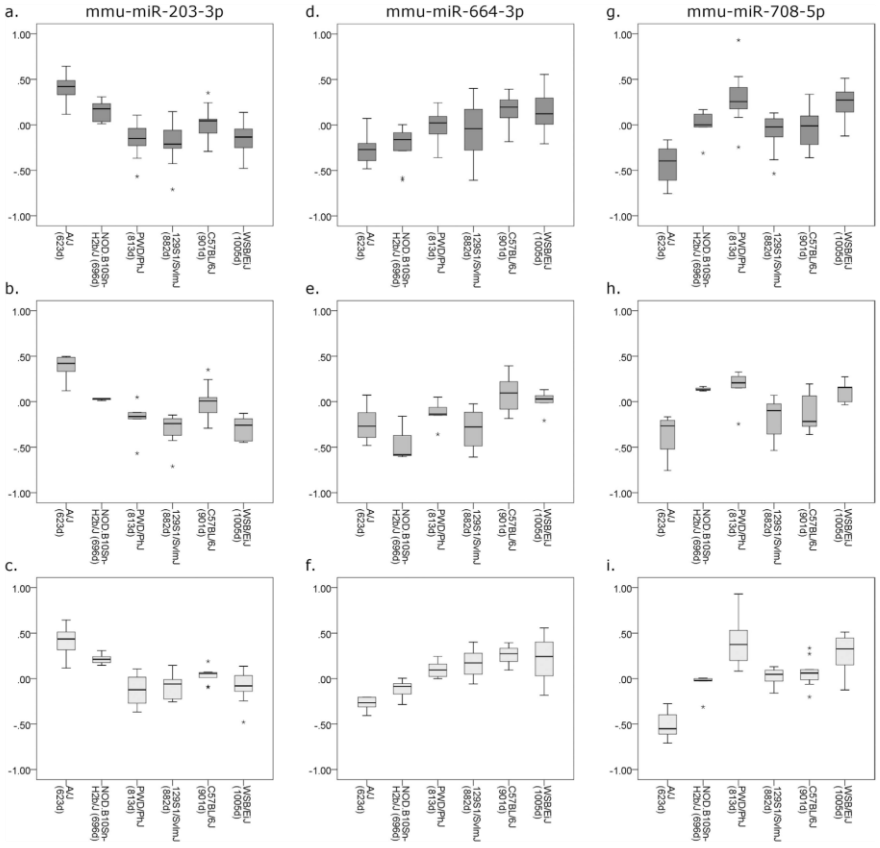

Figure 1. MicroRNA expression against lifespan as measured in targeted assessment of all available mouse strains. Box-and-whisker plots of relative microRNA expression for the 3 microRNAs found to be significantly associated with strain lifespan in the targeted assessment. Strains and median lifespan in days are given on the x-axis, while the y-axis shows mean log-transformed relative expression. Dark grey boxes show data for all mice analyzed, mid-grey boxes show data for young mice only and light grey boxes show data for old mice only. (**a**,**b** and **c**) expression data for miR-203-3p; (**d**,**e** and **f**) miR-664-3p; (**g**,**h** and **i**) miR-708-5p.

SE = 0.08; $p = 0.004$ compared with β-coefficient = −0.17; SE = 0.08; $p = 0.03$ in the old animals of long-lived strains, see Supplementary Table S5 and Fig. 2).

Conversely, miR-664-3p demonstrated increased expression in strains of longer lifespan in both old and young animals, after correction for multiple testing (β-coefficient = 0.56, $p = 5.12 \times 10^{-8}$, see Supplementary Table S2 and Fig. 1d). When expression was analyzed in young animals only, a trend was observed but this did not meet multiple testing criteria (β-coefficient = 0.42, $p = 0.008$, see Supplementary Table S2 and Fig. 1e) while in the analysis of old animals only, a significant association with lifespan was seen (β-coefficient = 0.75, $p = 3.93 \times 10^{-9}$, see Supplementary Table S2 and Fig. 1f). Analysis of strain lifespan and age interactions for miR-664-3p showed significant differences in expression between young and old animals of average lifespan (β-coefficient = 0.15; $p = 0.04$, see Supplementary Table S5 and Fig. 2). Significant differences were also apparent when comparing expression of miR-664-3p between strains of average lifespan and long lifespan, although the effect was much more marked in the old animals of long-lived strains (β-coefficient = 0.18; $p = 0.01$ in young long-lived animals compared with β-coefficient = 0.46; $p = 6.59 \times 10^{-10}$, see Supplementary Table S5 and Fig. 2).

MicroRNA miR-708-5p also showed increased expression in strains of longer lifespan in the combined analysis of old and young animals, after correction for multiple testing (β-coefficient = 0.50; $p = 1.61 \times 10^{-6}$, see

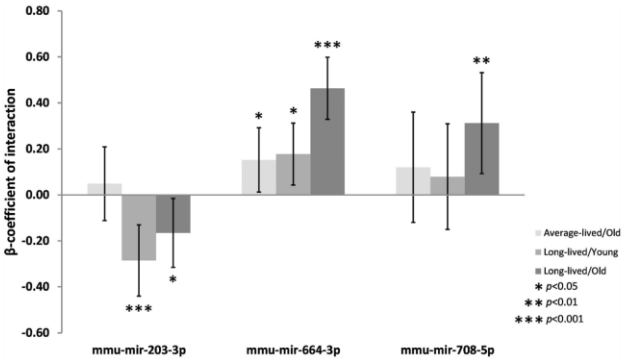

Figure 2. Longevity: Age interactions for microRNAs significantly associated with strain lifespan. This graph shows the relative expression changes in all mouse strains, categorized based on whether the median individual strain lifespan was above or below the median lifespan calculated across all strains, with 'Average-lived' being <847.5 days and 'Long-lived' >847.5 days. Young mice are 6 months and old mice are 20–22 months old. All changes are shown in relation to the young animals of the average-lived strains. Average-lived/old mice are shown in light grey, long-lived/young in mid-grey and long-lived/old animals in dark grey. Error bars denote the 95% confidence intervals and statistical significance is indicated by stars, where: $*p < 0.05$, $**p < 0.01$ and $***p < 0.001$.

Supplementary Table S2 and Fig. 1g). Again, when expression was analyzed in young animals only, a trend was observed that did not meet multiple testing criteria (β-coefficient = 0.36; $p = 0.02$, see Supplementary Table S2 and Fig. 1h) while the analysis of old animals only showed a significant association with lifespan (β-coefficient = 0.64, $p = 2.70 \times 10^{-6}$, see Supplementary Table S2 and Fig. 1i). Interaction analysis for miR-708-5p showed no significant difference in expression between young and old animals of average lifespan (β-coefficient = 0.12; $p = 0.33$, see Supplementary Table S5 and Fig. 2). Significant differences were observed between average-lived and long-lived strains, but these were only present in the old animals (β-coefficient = 0.08; $p = 0.49$ in young long-lived animals compared with β-coefficient = 0.31; $p = 0.007$ in the old animals of long-lived strains, see Supplementary Table S5 and Fig. 2).

Pathways Analysis. The lifespan effects of miR-203-3p, miR-664-3p and miR-708-5p are probably mediated by altered regulation of their target genes. We therefore used a gene set enrichment bioinformatic prediction approach specialized for miRNA targets[21] to determine the biochemical and functional pathways that are enriched for genes targeted by the 3 microRNAs significantly associated with strain lifespan. We identified 15 pathways that were predicted to be enriched in miR-203-3p, miR-664-3p or miR-708-5p target genes, many of which are known to be associated with aging or longevity (see Table 2). Prominent pathways targeted by all 3 miRNAs include the 'FoxO signalling pathway (mmu04068)' and 'mTOR signalling pathway (mmu04150)', which contain 16 and 11 genes with predicted miR-203-3p, miR-664-3p and miR-708-5p binding sites (FDR-adjusted p-values = 0.02 and 0.01 respectively). Also predicted to be enriched for miR-203-3p, miR-664-3p and miR-708-5p binding sites are the 'Pathways in cancer (mmu05200)' pathway, the 'MAPK signalling pathway (mmu04010), the 'signalling pathways regulating pluripotency of stem cells (mmu04550)' pathway and the 'TGF-beta signalling pathway (mmu04350)', with 33, 26, 14 and 10 genes targeted respectively (FDR-adjusted p-values = 0.03, 0.005, 0.05 and 0.0001 respectively). To provide empirical evidence that the genes identified to lie within these pathways also showed associations with longevity, we characterized the expression of selected target genes in relation to median strain lifespan. We identified that the 7/9 of these target genes were indeed associated with longevity in the mouse spleen samples (Table 3).

Discussion

Even once the effects of lifestyle and environment are considered, conventional genetics cannot account for all of the variation in mammalian lifespan and other factors, such as epigenetic regulation of key genes, have also been suggested to play a role. Here we show that three miRNAs; miR-203-3p, miR-664-3p and miR-708-5p, are significantly associated with strain lifespan in mouse spleen.

The expression of miR-203-3p was negatively correlated with longer lifespan. Although effects were seen in both young and old animals of long-lived strains, the most marked effects were noted in the young animals, suggesting that modulated expression of this miRNA may be a determining factor in longevity rather than simply a consequence of advancing age. Elevated levels of miR-203-3p have previously been shown to suppress "stemness" in mouse keratinocytes with several studies finding that higher levels of miR-203-3p expression promote terminal differentiation, repress proliferation and induce senescence in human melanoma cells[22–24]. This microRNA has

KEGG Pathway	*p*-value	Number of genes	Number of miRNAs
Pathways in cancer (mmu05200)	0.03	33	3
MAPK signalling pathway (mmu04010)	0.005	26	3
FoxO signalling pathway (mmu04068)	0.016	16	3
Transcriptional misregulation in cancer (mmu05202)	0.03	15	3
Signalling pathways regulating pluripotency of stem cells (mmu04550)	0.05	14	3
Thyroid hormone signalling pathway (mmu04919)	0.002	12	2
mTOR signalling pathway (mmu04150)	0.01	11	3
Long-term potentiation (mmu04720)	0.01	11	3
TGF-beta signalling pathway (mmu04350)	0.0001	10	3
Long-term depression (mmu04730)	0.002	10	2
Chronic myeloid leukaemia (mmu05220)	0.02	9	3
Amphetamine addiction (mmu05031)	0.02	8	2
Thyroid hormone synthesis (mmu04918)	0.0004	6	3
ECM-receptor interaction (mmu04512)	0.023	6	2
Glycosphingolipid biosynthesis - lacto and neolacto series (mmu00601)	1.46×10^{-9}	4	2

Table 2. Pathways affected by longevity-associated microRNAs. DIANA-mirPath v3.0 software[21] was used to determine pathways targeted by the microRNAs associated with strain lifespan, using predicted targets from the DIANA-microT-CDS v5.0 algorithm. Pathways are listed in order of the number of genes which are predicted to interact with these microRNAs.

also been shown to be up-regulated in senescence in human *in vitro* models using WI-38 human diploid fibroblast cells[25] and human melanoma cells[26]. The p63 and caveolin genes are known to be targets of miR-203-3p[27]. p63 is a member of the p53 family of transcription factors and the absence of expression of one of its isoforms, TAp63, has been shown to lead to senescence and premature aging of epidermal and dermal precursors[28]. Caveolin is thought to have a tumor-suppressor function at early stages of malignant transformation[29], to contribute to immune senescence[30] and the ability of aged cells to respond to oxidative stress[31]. Our finding of reduced miR-203-3p expression in long-lived mouse strains may be indicative of a phenotype in which cells have greater proliferative and adaptive capacity alongside a reduced propensity to become senescent, all of which could create favorable conditions for increased longevity. miR-203 was also one of the miRNAs demonstrated to be inversely associated with lifespan in a longitudinal study of human serum samples from the Baltimore Longitudinal Study of Aging (BLSA)[32].

Conversely, expression of miR-664-3p showed a positive correlation with longer lifespan in our data. In contrast to miR-203-3p, the changes we noted were most evident in the old animals of the long-lived strains, suggesting that increased expression of miR-664-3p may be a later life effect on longevity. In comparison with miR-203-3p, miR-664-3p has not been extensively studied, with conflicting conclusions having been drawn by different research groups. It has been linked to both pro- and anti-proliferative action in different tumor types[33,34], which complicates any attempts at prediction of putative function in terms of longevity. However, elevated hsa-miR-664 expression has been noted in human blood samples from nonagenarians and centenarians compared with samples from younger individuals[35], indicating that in human populations, the expression of this miRNA also correlates with longevity.

MicroRNA miR-708-5p was also positively correlated with longer lifespan. Again, the changes we noted were most evident in the old animals of the long-lived strains, suggesting that increased expression of miR-708-5p may also be a later life effect on longevity. In human cells, hsa-miR-708 has been shown to have a tumor-suppressor function in several human cancer types[36–38]. Reduced expression of hsa-miR-708 expression has also been seen in blood taken from old individuals in comparison to young individuals[39]. In our data, elevated, rather than decreased miR-708-5p expression was found to be associated with longer lifespan. This may be partially explained if the effects on miR-708-5p expression reflect a balance between protection from malignancy and maintained proliferative capacity.

The effects of altered miRNA expression on median strain lifespan will be mediated by altered regulation of their target genes. Gene set enrichment analysis using the DIANA miRPath webtool[21] reveals 15 pathways that are enriched for miR-203-3p, miR-664-3p and miR-708-5p target genes. The expression of the majority of the genes entriched for longevity-associated miRNA binding sites also demonstrated associations with longevity (Table 3). Although not all of these relationships were entirely straightforward in terms of the direction of effect one would predict based on expression differences of the specific miRNAs, this is to be expected, since transcripts will be targeted by many miRNAs in addition to the one tested, and several of our candidates are targeted by multiple miRNAs, often with antagonistic relationships with longevity. For example, *Zfhx3*, in the 'pluripotency of stem cells' pathway is targeted by both mmu-miR-203-3p and mmu-664-3p, one of which is negatively associated with lifespan and the other positively. MicroRNAs have also been previously reported to ber associated with both positive and negative associations with the expression of their target genes[40].

Most notable amongst the pathways we found were FoxO signalling, mTOR, MAPK signaling, pathways regulating pluripotency of stem cells, TGF-beta signaling and pathways involved in cancer. FoxO is well known to be involved in the regulation of lifespan, with strong evidence that alterations in proteins in this pathway can

Predicted Target Gene	KEGG Pathway	MicroRNA	ALL MICE			YOUNG MICE ONLY			OLD MICE ONLY		
			Beta coefficient	Std. Error	*P*-value	Beta coefficient	Std. Error	*P*-value	Beta coefficient	Std. Error	*P*-value
Acvr2a	Signalling pathways regulating pluripotency of stem cells (mmu04550)	mmu-miR-664-3p	−0.12	0.00	0.26	−0.38	0.00	***0.01***	0.19	0.00	0.19
Dusp5	MAPK signalling pathway (mmu04010)	mmu-miR-203-3p	−0.17	0.00	0.11	−0.37	0.00	***0.02***	0.03	0.00	0.84
Fgf7	Pathways in cancer (mmu05200)	mmu-miR-664-3p	−0.08	0.00	0.48	−0.24	0.00	0.14	0.11	0.00	0.45
	MAPK signalling pathway (mmu04010)										
Gabarapl1	FoxO signalling pathway (mmu04068)	mmu-miR-203-3p	−0.12	0.00	0.26	−0.48	0.00	***0.001***	0.29	0.00	***0.05***
Mmp9	Pathways in cancer (mmu05200)	mmu-miR-664-3p	0.45	0.00	***<0.001***	0.35	0.00	***0.02***	0.59	0.00	***<0.001***
Pten	FoxO signalling pathway (mmu04068)	mmu-miR-664-3p	0.18	0.00	0.09	−0.17	0.00	0.29	0.40	0.00	***0.004***
	mTOR signalling pathway (mmu04150)										
	Pathways in cancer (mmu05200)										
Rps6ka3	mTOR signalling pathway (mmu04150)	mmu-miR-664-3p	0.07	0.00	0.54	−0.16	0.00	0.31	0.31	0.00	***0.03***
	MAPK signalling pathway (mmu04010)										
Smad4	Pathways in cancer (mmu05200)	mmu-miR-664-3p	−0.36	0.00	***<0.001***	−0.38	0.00	***0.02***	−0.41	0.00	***0.004***
	FoxO signalling pathway (mmu04068)										
	Signalling pathways regulating pluripotency of stem cells (mmu04550)										
Zfhx3	Signalling pathways regulating pluripotency of stem cells (mmu04550)	mmu-miR-664-3p	0.03	0.00	0.80	−0.02	0.00	0.90	0.03	0.00	0.82
		mmu-miR-203-3p									

Table 3. Association of predicted target mRNA expression and lifespan in mouse spleen tissue across 6 strains of different longevities. Data from mice of all ages, young mice only (6 months) and old mice only (20–22 months) are given separately. For each gene, the associated pathway is given, along with the microRNA predicted to target the transcript. mRNAs significantly associated below the significance threshold ($p < 0.05$) are shown in bold italics. *P*-values were determined from linear regression of log-transformed relative expression data.

radically increase lifespan in several model organisms as well as humans, while mTOR inhibition has also been shown to increase lifespan in several species, from yeast to mice[41]. The observation that many of the pathways implicated contain genes that are known to control shared outcomes such as apoptosis, cell cycle regulation, differentiation, proliferation, cell survival, autophagy and DNA repair adds strength to the hypothesis that miR-203-3p, miR-664-3p and miR-708-5p may have functionality in terms of longevity. Our group has previously shown that other aspects of RNA processing and regulation are important in aging and longevity in humans, in animal models and *in vitro*[17,42,43]. The results of the present study provide further evidence that post-transcriptional control of mRNA expression is a key factor in the aging process and determination of lifespan.

The use of mouse tissues from very well characterized inbred strains is a strength of our study and allows us to be precise about the genetics and phenotypes associated with each strain, and allows assessment of median strain lifespan with some confidence. Spleen is an appropriate tissue for analysis, given the known role of the immune system and inflammation as drivers of aging[44]. However, our study cannot comment on the potential tissue-specificity of the effects we have seen and may not be representative of mechanism elsewhere in the organism. We also recognize that there are both strain-specific and age-related differences in the cellular composition of the spleen. While strain differences in the cell types found in mouse spleen are apparent, the kinetics of change of cell composition with age are similar at different stages of life in separate mouse strains where this has been measured[45]. It must also be mentioned that there is a relatively large amount of inter-individual cell-type variation, in some cases more pronounced than the inter-strain variability[45,46]. Unfortunately, data on splenic cellular composition for the strains used in this paper are not available, however while we cannot definitively state that all of our findings are not linked to age-related cell-type changes in the splenic make-up, the associations that are present only in the young mice are far less likely to be influenced by such changes. Our use of a wide-spectrum discovery phase in a limited sample set, followed by targeted validation and replication of results in a larger inclusive cohort ensures robust results, but we recognize that for some of the mouse strains analyzed, low numbers of samples may have affected the statistical power to detect more subtle changes. The use of pathways analysis also allows a larger 'systems'-based assessment of the effects of deregulation of modules of miRNAs in determination of longevity. Of course, it must be recognized that these results are from an *in silico* predictive algorithm and are not necessarily indicative of actual interactions *in vivo* or *in vitro*. Finally, it is possible that the effects we see may derive from differences between the strains unrelated to longevity. However, evidence suggests that there are links between both miR-664-3p and miR-203-3p and lifespan in human studies[32,35], suggesting that unrelated strain differences alone probably do not account for our observations, at least for these microRNAs.

In conclusion, we present evidence that three miRNAs, miR-203-3p, miR-664-3p and miR-708-5p are robustly associated with median strain lifespan in 6 well-characterized inbred strains of mice, and that both early life (miR-203-3p) and later life (miR-664-3p and miR-708-5p) changes in their expression may modulate the expression of target genes in several very well-known aging and longevity pathways. These studies demonstrate the importance of miRNAs in determination of mammalian longevity and raise the possibility that they may have utility as biomarkers of healthy aging in the future.

Strain	Strain Median Lifespan (days)	Strain Maximum Age (days)	Longevity Category	n Young (6 months)	n Old (20/22 months)
A/J	623	785	Average lifespan	7	6
NOD.B10Sn-H2^{b}/J	696	954	Average lifespan	3	6
PWD/PhJ	813	956	Average lifespan	5	6
129S1/SvImJ	882	1044	Long-lived	8	8
C57BL/6J	901	1061	Long-lived	10	9
WSB/EiJ	1005	1213	Long-lived	5	10

Table 4. Mouse strains and characteristics. Median lifespan and maximum age (average of longest-surviving 20% of animals) are given for each strain in the present study. All mice used were male.

Methods

Mouse tissue used in the study. Samples of spleen tissue were obtained from mice of six strains (A/J, NOD.B10Sn-H2^{b}/J, PWD/PhJ, 129S1/SvImJ, C57BL/6 J and WSB/EiJ), selected for having variable life expectancy (see Table 4 for details of lifespan, numbers of animals used in each category and their respective characteristics). Median lifespan was measured in a longitudinal study[16,47] at Jackson Laboratory Nathan Shock Center of Excellence in the Basic Biology of Aging. All tissues used in the present study were taken from male animals which were part of a cross sectional study being run at the same time, in the same mouse room as the longitudinal study mentioned above. All experiments were carried out in accordance with National Institutes of Health Laboratory Animal Care Guidelines and was approved by the Animal Care and Use Committee (ACUC) of The Jackson Laboratory. Details of mouse strains used and animal husbandry have been previously published[17]. Spleen tissue was excised immediately after death, placed into RNA-later storage solution (Sigma-Aldrich, St. Louis, MO, USA) and snap-frozen in vapor phase liquid nitrogen for storage within 5 minutes of collection.

MicroRNA candidate transcripts for analysis. To determine which microRNA transcripts to assess for association with longevity, an initial high-throughput array analysis was performed to measure the expression of a wide spectrum of microRNAs. In an attempt to ensure the best possible chance of detecting differences with lifespan, the arrays were run using all available samples from young animals (sacrificed at 6 months old) of A/J and WSB/EiJ, the two strains at either extreme of lifespan (623 days for A/J and 1005 days for WSB/EiJ). The top 10 most significantly associated microRNAs from this analysis were followed up with targeted microRNA expression experiments in old and young animals from all 6 strains.

RNA Extraction. Tissue samples were removed from RNA-later storage solution and placed in 1 mL TRI Reagent® Solution (Thermo Fisher, Waltham, MA, USA) supplemented with the addition of 10 mM $MgCl_2$ to aid recovery of microRNAs[48]. Samples were then completely homogenized for 15 mins in a bead mill (Retsch Technology GmbH, Haan, Germany). Phase separation was carried out using chloroform. Total RNA was precipitated from the aqueous phase by means of an overnight incubation at −20 °C with isopropanol. RNA pellets were then ethanol-washed twice and re-suspended in RNase-free dH2O. RNA quality and concentration was assessed by NanoDrop spectrophotometry (NanoDrop, Wilmington, DE, USA).

High-throughput MicroRNA Arrays. *MegaPlex Reverse Transcription.* 400ng of RNA per reaction was reverse transcribed using the TaqMan® MicroRNA Reverse Transcription Kit and Megaplex™ RT Primers, Rodent Pool Set v3.0 (Thermo Fisher, Waltham, MA, USA) in separate reactions for Pool A and Pool B, according to the manufacturer's instructions.

MicroRNA Array qRT-PCR. Expression of a wide spectrum of microRNAs was measured using Quantitative RT-PCR, performed on the ABI 7900HT platform (Thermo Fisher, Waltham, MA, USA), using both TaqMan® Rodent MicroRNA A Array v2.0 and TaqMan® Rodent MicroRNA Array B cards (Thermo Fisher, Waltham, MA, USA). Supplementary Table S6 lists the 521 unique microRNAs tested using this approach. Reaction mixes included 415 µl Taqman® Universal PCR Master Mix II (no AmpErase® UNG) (Thermo Fisher, Waltham, MA, USA), 407.5 µl dH_2O and 7.5 µl cDNA template from Pool A or Pool B Megaplex™ reverse transcriptions as appropriate. 100 µl of reaction solution for each sample was dispensed into all chambers of an array card (again, A or B accordingly), then centrifuged twice for 1 minute at 1000 rpm to ensure distribution of solution to each well. Amplification conditions were 50 °C for 2 minutes, 94.5 °C for 10 minutes, followed by 50 cycles of 97 °C for 30 seconds and 57.9 °C for 1 minute.

Targeted MicroRNA Expression. *Multiplex Reverse Transcription.* 60 ng of RNA per reaction was reverse transcribed using the TaqMan® MicroRNA Reverse Transcription Kit and RT primers provided with the TaqMan® MicroRNA Assays detailed in Supplementary Table S7 (Thermo Fisher, Waltham, MA, USA). Each reaction contained 1 µl each of all the RT primers of the microRNAs to be analyzed, 1 mM dNTPs (with dTTP), 100 U MultiScribe™ Reverse Transcriptase, 1X Reverse Transcription Buffer, 7.6U RNase Inhibitor and dH_2O to a final volume of 30 µl. The thermal profile for the reactions was 16 °C for 30 minutes, 42 °C for 30 minutes, 85 °C for 5 minutes and a final hold at 4 °C.

Individual microRNA qRT-PCR. MicroRNA expression was measured using Quantitative RT-PCR, performed on the ABI 7900HT platform (Thermo Fisher, Waltham, MA, USA), using the TaqMan® MicroRNA Assays detailed in Supplementary Table S7 (Thermo Fisher, Waltham, MA, USA). Reactions were run in triplicate on 384-well plates, using one assay per plate containing all samples. Each reaction included 2.5 µl TaqMan® Universal Master Mix II (no AmpErase® UNG) and 0.25 µl TaqMan® MicroRNA Assay (Thermo Fisher, Waltham, MA, USA), 0.5 µl cDNA (multiplex reverse transcribed as indicated above) and dH_2O to a final volume of 5 µl. Amplification conditions were a single cycle of 95 °C for 10 minutes, followed by 50 cycles of 95 °C for 15 seconds and 60 °C for 1 minute.

Interaction analysis. Analyses of interactions between mouse age and strain longevity were carried out for the three significantly associated microRNAs using data categorized based on whether the median individual strain lifespan was above or below the median lifespan calculated across all strains, with 'average-lived' being < 847.5 days and 'long-lived' >847.5 days (see Table 2 for details). Interaction terms for the relationship between age and median strain longevity were included. Analyses were carried out in STATA 14 (StataCorp, College Station, TX, USA).

Pathway analysis. Pathway analysis was carried out with DIANA-miRPath v3.0[21], using predicted microRNA targets from the DIANA-microT-CDS v5.0 algorithm[49] and Gene Ontology genesets derived from KEGG. The *p*-value threshold was set to 0.05 and MicroT threshold to 0.8.

Predicted target mRNA candidates for analysis. Target genes for validation were selected based on the MiTG scores taken from the DIANA-microT-CDS v5.0 algorithm[49]. We elected to assess the two genes with the highest MiTG score from each of the three pathways with the highest numbers of genes predicted to be targeted by the microRNAs in question; 'Pathways in cancer' (mmu05200), 'MAPK signalling pathway' (mmu04010) and 'FoxO signalling pathway' (mmu04068). We also decided to assess the two genes with the highest MiTG score from the 'mTOR signalling pathway' (mmu04150) and 'Signalling pathways regulating pluripotency of stem cells' (mmu04550), as these were likely to be of interest in relation to lifespan. One other gene was picked (*Smad4*), as it is the only one to be present in 3 of the 5 pathways we had elected to pursue and is also present in 5 of the 15 pathways identified from DIANA-miRPath[21].

Predicted Target mRNA Expression. *Reverse Transcription.* 200 ng of RNA per reaction was reverse transcribed using the SuperScript® VILO™ cDNA Synthesis Kit (Thermo Fisher, Waltham, MA, USA) in 20 µl reactions, according to the manufacturer's instructions. Each cDNA was then diluted with 10 µl of water to give sufficient volume to carry out the necessary qPCR reactions.

Predicted target mRNA qRT-PCR. Predicted target mRNA expression was measured using Quantitative RT-PCR, performed on the QuantStudio 12 K Flex platform (Thermo Fisher, Waltham, MA, USA), using the TaqMan® Gene Expression Assays detailed in Supplementary Table S8 (Thermo Fisher, Waltham, MA, USA). Reactions were run in triplicate on 384-well plates, using one assay per plate containing all samples. Each reaction included 2.5 µl TaqMan® Universal Master Mix II (no AmpErase® UNG) and 0.25 µl TaqMan® Gene Expression Assay (Thermo Fisher, Waltham, MA, USA), 0.5 µl cDNA (reverse transcribed as indicated above) and dH_2O to a final volume of 5 µl. Amplification conditions were a single cycle of 95 °C for 10 minutes, followed by 40 cycles of 95 °C for 15 seconds and 60 °C for 1 minute.

Relative quantification. In all experiments described here, the ΔΔCt method was used to calculate relative expression levels of the microRNAs tested[50]. Expression was assessed relative to the global mean of the 279 expressed microRNAs and normalized to the mean level of expression of each individual transcript in the shorter lifespan animals (A/J) for the high-throughput microRNA arrays. Data were log transformed to ensure normal distribution and differences in expression were tested with independent t-tests, using SPSS v22 (IBM, North Castle, NY, USA). For the targeted microRNA experiments, expression was assessed relative to the mean expression of three endogenous control small RNA species (snoRNA202, U6 snRNA and U87 snRNA) and normalized to the median level of expression for each individual transcript across all samples. Data were log10 transformed to ensure normal distribution. For the predicted target mRNA experiments, expression was assessed relative to the mean expression of two endogenous control genes (*Gusb* and *Idh3b*) and normalized to the median level of expression for each individual transcript across all samples. Data were log10 transformed to ensure normal distribution.

Statistical approach. Associations between both miRNA and mRNA target expression and median strain lifespan were assessed using linear regression. The relationships between these parameters were assessed in both young and old animals of all 6 strains. We also assessed the relationship between median strain lifespan and miRNA expression in the animals not originally tested in the global analysis, to comprise an independent replication. Regressions were carried out using SPSS v22 (IBM, North Castle, NY, USA).

References

1. Herskind, A. M. *et al.* The heritability of human longevity: a population-based study of 2872 Danish twin pairs born 1870–1900. *Human genetics* **97,** 319–323 (1996).
2. vB Hjelmborg, J. *et al.* Genetic influence on human lifespan and longevity. *Human genetics* **119,** 312–321 (2006).
3. Dutta, A. *et al.* Longer lived parents: protective associations with cancer incidence and overall mortality. *J Gerontol A Biol Sci Med Sci* **68,** 1409–1418 (2013).
4. Dutta, A. *et al.* Aging children of long-lived parents experience slower cognitive decline. *Alzheimers Dement* **10,** S315–322 (2014).
5. Ben-Avraham, D. Epigenetics of aging. *Advances in experimental medicine and biology* **847,** 179–191 (2015).

6. Taormina, G. & Mirisola, M. G. Longevity: epigenetic and biomolecular aspects. *Biomolecular concepts* **6,** 105–117 (2015).
7. Gregory, R. I., Chendrimada, T. P., Cooch, N. & Shiekhattar, R. Human RISC couples microRNA biogenesis and posttranscriptional gene silencing. *Cell* **123,** 631–640 (2005).
8. Lim, L. P. *et al.* Microarray analysis shows that some microRNAs downregulate large numbers of target mRNAs. *Nature* **433,** 769–773 (2005).
9. Inukai, S. & Slack, F. MicroRNAs and the genetic network in aging. *Journal of molecular biology* **425,** 3601–3608 (2013).
10. Lopez-Otin, C., Blasco, M. A., Partridge, L., Serrano, M. & Kroemer, G. The hallmarks of aging. *Cell* **153,** 1194–1217 (2013).
11. Harries, L. W. MicroRNAs as Mediators of the Ageing Process. *Genes* (*Basel*) 5, 656–670 (2014).
12. Boulias, K. & Horvitz, H. R. The C. elegans microRNA mir-71 acts in neurons to promote germline-mediated longevity through regulation of DAF-16/FOXO. *Cell metabolism* **15,** 439–450 (2012).
13. Pincus, Z., Smith-Vikos, T. & Slack, F. J. MicroRNA Predictors of Longevity in Caenorhabditis elegans. *PLoS genetics* **7,** e1002306 (2011).
14. Vora, M. *et al.* Deletion of microRNA-80 Activates Dietary Restriction to Extend C. elegans Healthspan and Lifespan. *PLoS genetics* **9,** e1003737 (2013).
15. Yuan, R., Peters, L. L. & Paigen, B. Mice as a mammalian model for research on the genetics of aging. *ILAR J* **52,** 4–15 (2011).
16. Yuan, R. *et al.* Aging in inbred strains of mice: study design and interim report on median lifespans and circulating IGF1 levels. *Aging Cell* **8,** 277–287 (2009).
17. Lee, B. P. *et al.* Changes in the expression of splicing factor transcripts and variations in alternative splicing are associated with lifespan in mice and humans. *Aging Cell* **15,** 903–913 (2016).
18. Bogue, M. A. *et al.* Accessing Data Resources in the Mouse Phenome Database for Genetic Analysis of Murine Life Span and Health Span. *J Gerontol A Biol Sci Med Sci* (2014).
19. Martins, R., Lithgow, G. J. & Link, W. Long live FOXO: unraveling the role of FOXO proteins in aging and longevity. *Aging cell* **15,** 196–207 (2016).
20. Lamming, D. W. Inhibition of the Mechanistic Target of Rapamycin (mTOR)-Rapamycin and Beyond. *Cold Spring Harbor perspectives in medicine* **6** (2016).
21. Vlachos, I. S. *et al.* DIANA-miRPath v3.0: deciphering microRNA function with experimental support. *Nucleic acids research* **43,** W460–466 (2015).
22. Yi, R., Poy, M. N., Stoffel, M. & Fuchs, E. A skin microRNA promotes differentiation by repressing 'stemness'. *Nature* **452,** 225–229 (2008).
23. Lena, A. M. *et al.* miR-203 represses 'stemness' by repressing DeltaNp63. *Cell death and differentiation* **15,** 1187–1195 (2008).
24. Jackson, S. J. *et al.* Rapid and widespread suppression of self-renewal by microRNA-203 during epidermal differentiation. *Development* (*Cambridge, England*) **140,** 1882–1891 (2013).
25. Marasa, B. S. *et al.* MicroRNA profiling in human diploid fibroblasts uncovers miR-519 role in replicative senescence. *Aging* **2,** 333–343 (2010).
26. Noguchi, S. *et al.* Anti-oncogenic microRNA-203 induces senescence by targeting E2F3 protein in human melanoma cells. *The Journal of biological chemistry* **287,** 11769–11777 (2012).
27. Ørom, U. A. *et al.* MicroRNA-203 regulates caveolin-1 in breast tissue during caloric restriction. *Cell Cycle* **11,** 1291–1295 (2012).
28. Su, X. *et al.* TAp63 prevents premature aging by promoting adult stem cell maintenance. *Cell stem cell* **5,** 64–75 (2009).
29. Shatz, M. & Liscovitch, M. Caveolin-1: a tumor-promoting role in human cancer. *International journal of radiation biology* **84,** 177–189 (2008).
30. Lim, J. S. *et al.* Flagellin-dependent TLR5/caveolin-1 as a promising immune activator in immunosenescence. *Aging Cell* **14,** 907–915 (2015).
31. Volonte, D., Liu, Z., Shiva, S. & Galbiati, F. Caveolin-1 controls mitochondrial function through regulation of m-AAA mitochondrial protease. *Aging* (*Albany NY*) **8,** 2355–2369 (2016).
32. Smith-Vikos, T. *et al.* A serum miRNA profile of human longevity: findings from the Baltimore Longitudinal Study of Aging (BLSA). *Aging* **8,** 2971–2987 (2016).
33. Ding, Z. *et al.* Loss of MiR-664 Expression Enhances Cutaneous Malignant Melanoma Proliferation by Upregulating PLP2. *Medicine* (*Baltimore*) **94,** e1327 (2015).
34. Zhu, H., Miao, M. H., Ji, X. Q., Xue, J. & Shao, X. J. miR-664 negatively regulates PLP2 and promotes cell proliferation and invasion in T-cell acute lymphoblastic leukaemia. *Biochem Biophys Res Commun* **459,** 340–345 (2015).
35. ElSharawy, A. *et al.* Genome-wide miRNA signatures of human longevity. *Aging cell* **11,** 607–616 (2012).
36. Li, G. *et al.* MicroRNA-708 is downregulated in hepatocellular carcinoma and suppresses tumor invasion and migration. Biomedicine & pharmacotherapy=Biomedecine & pharmacotherapie **73,** 154–159 (2015).
37. Yang, J. *et al.* Metformin induces ER stress-dependent apoptosis through miR-708-5p/NNAT pathway in prostate cancer. *Oncogenesis* **4,** e158 (2015).
38. Baer, C. *et al.* Epigenetic silencing of miR-708 enhances NF-kappaB signaling in chronic lymphocytic leukemia. *International journal of cancer. Journal international du cancer* **137,** 1352–1361 (2015).
39. Noren Hooten, N. *et al.* microRNA Expression Patterns Reveal Differential Expression of Target Genes with Age. *PloS one* **5,** e10724 (2010).
40. Song, R., Liu, Q., Liu, T. & Li, J. Connecting rules from paired miRNA and mRNA expression data sets of HCV patients to detect both inverse and positive regulatory relationships. *BMC Genomics* **16** Suppl 2, S11 (2015).
41. Kenyon, C. J. The genetics of ageing. *Nature* **464,** 504–512 (2010).
42. Harries, L. W. *et al.* Human aging is characterized by focused changes in gene expression and deregulation of alternative splicing. *Aging Cell* **10,** 868–878 (2011).
43. Holly, A. C. *et al.* Changes in splicing factor expression are associated with advancing age in man. *Mech Ageing Dev* **134,** 356–366 (2013).
44. Franceschi, C. & Campisi, J. Chronic inflammation (inflammaging) and its potential contribution to age-associated diseases. *J Gerontol A Biol Sci Med Sci* **69** Suppl 1, S4–9 (2014).
45. Pinchuk, L. M. & Filipov, N. M. Differential effects of age on circulating and splenic leukocyte populations in C57BL/6 and BALB/c male mice. *Immunity & ageing: I & A* **5,** 1–1 (2008).
46. Connoy, A. C., Trader, M. & High, K. P. Age-related changes in cell surface and senescence markers in the spleen of DBA/2 mice: a flow cytometric analysis. *Experimental gerontology* **41,** 225–229 (2006).
47. Yuan, R. *et al.* Genetic coregulation of age of female sexual maturation and lifespan through circulating IGF1 among inbred mouse strains. *Proc Natl Acad Sci USA* **109,** 8224–8229 (2012).
48. Kim, Y. K., Yeo, J., Kim, B., Ha, M. & Kim, V. N. Short structured RNAs with low GC content are selectively lost during extraction from a small number of cells. *Mol Cell* **46,** 893–895 (2012).
49. Paraskevopoulou, M. D. *et al.* DIANA-microT web server v5.0: service integration into miRNA functional analysis workflows. *Nucleic acids research* **41,** W169–173 (2013).
50. Livak, K. J. & Schmittgen, T. D. Analysis of relative gene expression data using real-time quantitative PCR and the 2(-Delta Delta C(T)) Method. *Methods* (*San Diego, Calif.*) **25,** 402–408 (2001).

Acknowledgements

This work was funded by the Wellcome Trust (grant number WT097835MF to D. Melzer and L.W. Harries), and the NIH-NIA (grant number AG038070 to The Jackson Laboratory). The authors would like to thank Miss Florence Emond for technical assistance.

Author Contributions

B.P.L., I.B., A.G.P. carried out and interpreted the experiments. K.F. contributed to collection and characterization of samples. D.H.E. co-directs the Jackson laboratory Nathan Shock Centre of Excellence in the Basic Biology of Aging, and was instrumental in facilitating the mouse collection and animal husbandry facilities used in this study. R.Y. and L.P. designed and managed the initial mouse lifespan study and contributed to the manuscript. B.P.L. also co-wrote the manuscript. G.A.K. and D.M. contributed to and reviewed the manuscript. L.W.H. managed the study, interpreted the data, and co-wrote the manuscript.

Additional Information

Supplementary information accompanies this paper at http://www.nature.com/srep

Competing Interests: The authors declare no competing financial interests.

How to cite this article: Lee, B. P. *et al.* MicroRNAs miR-203-3p, miR-664-3p and miR-708-5p are associated with median strain lifespan in mice. *Sci. Rep.* **7**, 44620; doi: 10.1038/srep44620 (2017).

Publisher's note: Springer Nature remains neutral with regard to jurisdictional claims in published maps and institutional affiliations.

Biogerontology
https://doi.org/10.1007/s10522-019-09819-0

RESEARCH ARTICLE

The transcript expression levels of *HNRNPM*, *HNRNPA0* and *AKAP17A* splicing factors may be predictively associated with ageing phenotypes in human peripheral blood

Benjamin P. Lee · Luke C. Pilling · Stefania Bandinelli · Luigi Ferrucci · David Melzer · Lorna W. Harries

Received: 8 May 2019 / Accepted: 24 June 2019

Abstract Dysregulation of splicing factor expression is emerging as a driver of human ageing; levels of transcripts encoding splicing regulators have previously been implicated in ageing and cellular senescence both in vitro and in vivo. We measured the expression levels of an a priori panel of 20 age- or senescence-associated splicing factors by qRT-PCR in peripheral blood samples from the InCHIANTI Study of Aging, and assessed longitudinal relationships with human ageing phenotypes (cognitive decline and physical ability) using multivariate linear regression. *AKAP17A, HNRNPA0* and *HNRNPM* transcript levels were all predictively associated with severe decline in MMSE score ($p = 0.007$, 0.001 and 0.008 respectively). Further analyses also found expression of these genes was associated with a performance decline in two other cognitive measures; the Trail Making Test and the Purdue Pegboard Test. *AKAP17A* was nominally associated with a decline in mean hand-grip strength ($p = 0.023$), and further analyses found nominal associations with two other physical ability measures; the Epidemiologic Studies of the Elderly-Short Physical Performance Battery and calculated speed (m/s) during a timed 400 m fast walking test. These data add weight to the hypothesis that splicing dyregulation may contribute to the development of some ageing phenotypes in the human population.

Keywords Splicing factors · Cognitive decline · Biomarkers

Electronic supplementary material The online version of this article (https://doi.org/10.1007/s10522-019-09819-0) contains supplementary material, which is available to authorized users.

B. P. Lee · L. W. Harries (✉)
Institute of Biomedical and Clinical Sciences, University of Exeter College of Medicine and Health, RILD Building, RD&E NHSFT Campus, Barrack Rd, Exeter EX2 5DW, UK
e-mail: L.W.Harries@exeter.ac.uk

L. C. Pilling · D. Melzer
Epidemiology and Public Health, University of Exeter College of Medicine and Health, RILD Building, RD&E NHSFT Campus, Barrack Rd, Exeter EX2 5DW, UK

S. Bandinelli
Geriatric Unit, USL Toscana Centro, 50122 Florence, Italy

L. Ferrucci
National Institute on Aging, Clinical Research Branch, Harbor Hospital, Baltimore, MD 21225, USA

Published online: 10 July 2019

Introduction

There is an intimate relationship between stress responses and successful ageing (Kourtis and Tavernarakis 2011) yet the ability to respond appropriately to stressful environments and to maintain systemic homeostasis declines with age in multiple species (Kirkland et al. 2016; Schorr et al. 2018;

Varadhan et al. 2008). Cellular responses to external and internal stressors are mediated at the level of genomic plasticity, in particular at the level of the transcriptome. Several mechanisms are known to play a part in the diversity of response, including transcriptional regulation at the level of polymerase activity (Chen et al. 2018), post-transcriptional regulation (Harvey et al. 2017), epigenetics (Guillaumet-Adkins et al. 2017) and genomic landscape (Winick-Ng and Rylett 2018). Alternative splicing comprises a key part of the homeostatic response to stress (Disher and Skandalis 2007; Martinez and Lynch 2013; Mastrangelo et al. 2012), and dysregulation of this process is now emerging as a new and important driver of cellular ageing (Harries et al. 2011; Holly et al. 2013; Latorre and Harries 2017). Over 95% of genes are capable of producing more than one mRNA product under different conditions and alternatively-expressed mRNAs can have profoundly different temporal or spatial expression patterns, or demonstrate major differences in functionality (Celotto and Graveley 2001; Grumont and Gerondakis 1994; Pan et al. 2008).

Alternative splicing decisions are made by a series of trans-acting splicing regulatory proteins termed splicing factors. These are the Serine Arginine-rich (SR) family of splicing factors which usually, but not exclusively, promote splice site usage, and the heterogeneous nuclear ribonucleoprotein (HNRNP) family of splicing factors which are usually, but not exclusively, associated with inhibition of splice site usage (Cartegni et al. 2002). SR proteins and HNRNPs bind to exon/intron splicing enhancer (ESE/ISE) or silencer (ESS/ISS) elements in the vicinity of the splice sites and the balance of activators and inhibitors at any given splice site regulates splice site usage (Smith and Valcarcel 2000). The expression levels of splicing regulators is known to be associated with ageing; of seven gene ontology pathways robustly associated with age in a large cross-sectional population study of human ageing, six were directly involved in mRNA splicing processes (Harries et al. 2011). Splicing factor expression is also associated with lifespan in mice and humans (Lee et al. 2016).

We have previously observed disruption of splicing factor expression in human senescent cells (Holly et al. 2013; Latorre et al. 2018b), and demonstrated that experimental manipulation of splicing factor expression is capable of inducing rescue from the senescent cell phenotype (Latorre et al. 2017, 2018a, c). Although we have demonstrated epidemiological links with ageing itself, and reversal of cellular senescence in vitro, evidence that the phenomena we observe in vitro is linked with downstream ageing phenotypes is lacking. In this study, we addressed this question by measurement of the expression of an a priori panel of age- and senescence-related splicing factor genes in human peripheral blood mRNA from the InCHIANTI study of Aging. We used samples from two follow-up visits (FU3; 2007–2010 and FU4; 2012–2014) of the InCHIANTI study of Aging, and related their expression to changes in recorded measures of two important human ageing phenotypes; cognitive and physical function. We initially used the Mini Mental State Exam (MMSE) score and mean hand-grip strength to identify putative associations between splicing factor expression and changes in cognitive or physical ability respectively. We then assessed expression of these transcripts against other cognitive and physical measures available in the dataset. In each case, a set of sub-analyses were also performed to test the robustness of the findings.

We found that the expression of three splicing factor genes, *HNRNPM*, *HNRNPA0* and *AKAP17A* may be predictive for change in in this population; all three genes were associated with cognitive decline as measured by the Mini-Mental State Examination (MMSE), Trail-Making Tests part A and B (TMT A/B), and the Purdue Pegboard Test (PPT). *AKAP17A* was also associated with a decline in physical ability as measured by hand-grip strength, the Epidemiologic Studies of the Elderly-Short Physical Performance Battery (EPESE-SPPB) and calculated speed during a timed 400 m fast walking test. Our data suggest that age-associated dysregulation of splicing factor expression in ageing humans may contribute to the development of downstream ageing outcomes.

Methods

InCHIANTI cohort and selection of participants

The InCHIANTI study of Aging is a population study of ageing (Ferrucci et al. 2000). Participants undertook detailed assessment of health and lifestyle parameters at baseline, and again at three subsequent follow-ups

(FU2; 2004–2006, FU3; 2007–2010 and FU4; 2012–2014). The present study used participants from the third and fourth follow-up visits (FU3 and FU4). RNA samples and clinical/phenotypic data were already available for 698 participants at FU3. The collection of the FU4 samples and data comprise part of this study. During the FU4 interviews in 2012/13, blood and clinical/phenotypic data were collected from 455 study participants. These data were cross-checked against RNA samples and clinical/phenotypic data already held from FU3, to ensure that sample and phenotypic data was available from both collections. 393 individuals fitted these criteria, of which nine died shortly after the FU4 visit and so were excluded from the analysis. From the remaining 384 eligible samples, 300 were randomly selected from the cohort to be analysed for expression of splicing factor genes. Anthropometric parameters and blood cell subtypes in FU4 were measured as previously (Ferrucci et al. 2000).

Splicing factor candidate genes for analysis

An a priori list of splicing factor candidate genes were chosen based on associations we had documented with human ageing in multiple populations and in senescent primary human cell lines in our previous work (Harries et al. 2011; Holly et al. 2013; Latorre et al. 2017). We have also found associations of components of this gene set with lifespan in both mice and humans (Lee et al. 2016). The list of genes included the positive regulatory splicing factors *AKAP17A*, *SRSF1*, *SRSF2*, *SRSF3*, *SRSF6*, *SRSF7*, *PNISR* and *TRA2B*, the negative regulatory splicing inhibitors *HNRNPA0*, *HNRNPA1*, *HNRNPA2B1*, *HNRNPD*, *HNRNPH3*, *HNRNPK*, *HNRNPM*, *HNRNPUL2* and the *IMP3*, *LSM14A*, *LSM2* and *SF3B1* core components of the spliceosome. Expression assays were obtained in custom TaqMan® low-density array (TLDA) format (ThermoFisher, Waltham, MA, USA). Assay Identifiers are given in Supplementary Table S1.

RNA collection and extraction

2.5 ml of peripheral blood was collected from each participant into PAXgene Blood RNA Tubes (IVD) (PreAnalytiX GmbH, Hombrechtikon, Switzerland). Blood tubes were then treated according to the manufacturer's instructions and subsequently cold-chain shipped to the UK. RNA extractions were then carried out using the PAXgene Blood mRNA Kit (Qiagen, Hilden, Germany), according to manufacturer's instructions. Samples were assessed for RNA quality and quantity by Nanodrop spectrophotometry (NanoDrop, Wilmington, DE, USA).

Reverse transcription and quantitative RT-PCR

100 ng of total RNA was reverse transcribed using SuperScript® VILO™ cDNA Synthesis Kit (ThermoFisher, Waltham, MA, USA) in 20 µl reactions, according to the manufacturer's instructions. 20 µl cDNA (reverse transcribed as indicated above) was added to 50 µl TaqMan® Universal Master Mix II, no UNG (ThermoFisher, Waltham, MA, USA) and 30 µl RNase-free dH_2O, then loaded onto TaqMan® Low-Density Array 384-Well Microfluidic cards. 100µL reaction solution was dispensed into each TLDA card chamber and the card centrifuged twice for 1 min at $216 \times g$ to ensure distribution of solution to each well. The expression of transcripts in each sample was measured in duplicate replicates. Cards were run on the 7900HT Fast Real-Time PCR System (ThermoFisher, Waltham, MA, USA). Amplification conditions were as follows: a single cycle of 50 °C for 2 min, a single cycle of 94.5 °C for 10 min followed by 40 cycles of 97 °C for 30 s and 59.7 °C for 1 min.

Data preparation

SDS files were uploaded to the ThermoFisher Cloud (ThermoFisher, Waltham, MA, USA) and analysed using the Relative Quantification qPCR App encompassed within the software (https://www.thermofisher.com/uk/en/home/cloud.html). This platform was used to manually set Baseline and Threshold for each assay (see Supplementary Table S1 for values) and to ensure there were no apparent outliers before further analysis. One sample was excluded at this stage as expression data was missing for all genes measured. Output was imported into Excel (Microsoft, Redmond, WA, USA) and the C_T values used for analysis using the comparative C_T method. The most stable genes for use as endogenous controls were determined from the raw data using the RefFinder webtool (Xie et al. 2012), which returned the geometric mean value across all genes measured as the most stable control, and thus the

most appropriate for the ΔC_T normalisation step. Expression was then calculated relative to the median expression for each individual transcript. Data were log transformed to ensure normal distribution. Outlier detection was performed in SPSS (IBM, Armonk, NY, USA). Univariate outliers were identified using standardised z-scores, with any individual measures for each gene falling outside the cut-off (set at three standard deviations from the mean) being discarded. Multivariate outliers were identified using a regression model with Mahalanobis distance as an output, followed by comparison of the calculated Mahalanobis distances with the critical χ^2 value for the dataset (Rasmussen 1988). One sample for which the Mahalanobis distance exceeded the critical χ^2 was discarded, leaving a total of n = 298 samples to take forward for statistical testing. The characteristics of this final subset of participants are summarised in Table 1.

Phenotypic outcomes for analysis

The current study analysed the associations of splicing factor gene expression at FU3 with the following cognitive phenotypic outcomes; MMSE score, Trail-Making-Test (TMT A&B) and Purdue Pegboard Test (as measures of cognitive function), along with hand-grip strength, EPESE-SPPB composite score and calculated speed during a 400 m fast walk (as measures of physical ability).

MMSE score was measured at both FU3 and FU4 using the standard test, after which the data was corrected to adjust for incomplete tests. This was calculated using the score attained as a proportion of the maximum possible points for the parts of the test that were completed. Decline in MMSE score was calculated by subtracting the score at FU4 from the score at FU3. Time taken to complete the Trail-Making-Tests part A and B were measured in seconds at both FU3 and FU4 using the standard tests. Decline in performance on the tests was calculated by subtracting the score at FU4 from the score at FU3. Decline in seconds was then converted to a decline in fractions of a minute prior to analysis. The Purdue Pegboard Test was administered as standard (although data for the assembly portion of the test was not available), and scores for number of pegs placed in the board for right-hand, left-hand and both-hands were summed to give a total number of pegs placed during the test. Decline in performance on the test was calculated by subtracting the total number of pegs placed at FU4 from the total number of pegs placed at FU3.

Hand-grip strength was measured in kilograms at both FU3 and FU4 using a dynamometer, with two separate measurements taken for each hand. Mean hand-grip strength was used for the analyses in this study, and was calculated as the mean of all 4 hand-grip strength measurements across both hands. Decline in mean hand-grip strength was calculated by subtracting the measurement at FU4 from the measurement at FU3. The EPESE-SPPB was administered and scored as described elsewhere (Guralnik et al. 1994), and a composite score generated from the sub-scores of the three activities performed: repeated chair-stand, standing balance and 4 m normal pace walk. Decline in performance was calculated by subtracting the composite score at FU4 from the composite score at FU3. The 400 m fast walk was performed by completing 20 laps of a 20 m circuit with a maximum of two stops if the subject required. Speed in m/s was calculated over the entire distance (any individuals who did not complete the test were excluded from further analysis), and decline in performance was calculated by subtracting the speed at FU4 from the speed at FU3.

Sub-analyses for robustness testing

For all phenotypes, any associations found in the full cohort were then tested for robustness through four sub-analyses on different subsets of the data.

First, individuals with the lowest initial scores (at FU3) were excluded from the analysis, to avoid confounding due to the inclusion of participants already on a trajectory to decline. For MMSE score, the cut-off was set at $\geq$28, as a score above 28 is clearly indicative of a lack of cognitive impairment. In the case of mean hand-grip strength, the cut-offs used were those previously reported as a consensus definition of sarcopenia by The European Working Group on Sarcopenia in Older People (EWGSOP) (Cruz-Jentoft et al. 2010), i.e. $<$ 20 kg for females and $<$ 30 kg for males. For all the other phenotypes analysed, the dataset at FU3 was divided into quintiles, with the lowest scoring quintile being excluded from this sub-analysis.

Table 1 Participant details

(A)

	Follow-up 3		Follow-up 4	
	n	%	n	%
Participants	298	100	298	100
Age (years)				
30–39	21	7.05	11	3.69
40–49	31	10.40	28	9.40
50–59	31	10.40	28	9.40
60–69	35	11.74	34	11.41
70–79	111	37.25	38	12.75
80–89	67	22.48	142	47.65
90–100	2	0.67	17	5.70
Gender				
Male	136	45.64	136	45.64
Female	162	54.36	162	54.36
Pack years smoked (lifetime)				
None	159	53.36	No	Data
< 20	79	26.51	No	Data
20–39	44	14.76	No	Data
40 +	16	5.37	No	Data
Site				
Greve	140	46.98	140	46.98
Bagno a Ripoli	158	53.02	158	53.02
Education level attained				
Nothing	28	9.4	24	8.05
Elementary	121	40.6	125	41.95
Secondary	51	17.11	59	19.80
High school	46	15.44	58	19.46
Professional school	33	11.07	11	3.69
University or equivalent	19	6.38	21	7.05

(B)

	Follow-up 3				Follow-up 4			
	Mean	Std. dev.	Min	Max	Mean	Std. dev.	Min	Max
Age (years)	67.69	15.68	30.00	94.00	72.92	15.68	35.00	100.00
BMI	26.97	4.27	15.01	42.99	26.86	4.42	13.39	41.19
White blood cell count (n, K/μl)	6.39	1.60	2.10	13.00	6.16	1.72	2.30	16.59
Neutrophils (%)	56.61	8.61	26.20	81.20	56.50	9.23	22.20	88.40
Lymphocytes (%)	31.56	8.04	9.80	59.90	32.47	8.70	8.30	63.30
Monocytes (%)	8.08	2.22	3.70	21.30	7.36	2.28	1.60	24.40
Eosinophils (%)	3.19	2.20	0.00	21.50	3.21	2.02	0.00	13.00
Basophils (%)	0.55	0.20	0.10	1.30	0.47	0.29	0.00	2.10

Table 1 continued

(C)

	n	Follow-up 3				Follow-up 4			
		Mean	Std. dev.	Min	Max	Mean	Std. dev.	Min	Max
Corrected MMSE score	296	27.22	3.18	14.00	30.00	25.71	5.11	0.00	30.00
TMT-A (mins)	268	0.91	0.62	0.23	5.00	1.13	0.83	0.25	5.00
TMT-B (mins)	179	1.56	1.02	0.47	5.00	1.91	1.19	0.52	5.00
PPT (total pegs placed)	257	64.77	13.38	26	98	61.60	16.45	17	103
Mean hand-grip strength (Kg)	285	29.67	12.28	10.00	70.75	28.11	12.14	5.00	65.50
EPESE-SPPB (composite score)	276	11.10	1.59	0	12	10.09	2.95	0	12
400 m fast walk speed (m/s)	206	1.41	0.25	0.73	2.18	1.26	0.29	0.47	2.03

Characteristics of the InCHIANTI participants used in the present study. Panel A shows summary of non-clinical details, panel B shows summary results of clinical/laboratory tests and panel C shows summary results of phenotypic measures used for analysis

Second, an analysis was carried out using only the eldest participants aged ≥ 70 years at FU3 to exclude any potential confounding effects from younger participants. Declining cognitive and physical ability are predominantly features of ageing, and measures such as mean hand-grip strength and MMSE are likely to perform poorly in measuring change of function in young, non-compromised individuals.

Third, some individuals measured showed an apparent improvement in performance over time between FU3 and FU4, which may reflect a degree of measurement error. To test this, we first calculated an allowed error of 5% (as a fraction of the total range of change measured), then removed any individuals with scores showing an increase greater than the allowed error between the follow-ups, for each phenotype.

Finally, participants were categorised into mild or severe decline classes, to assess whether the associations seen were specific to either group of individuals. Decline in MMSE score was categorised for sub-analysis as follows; 'No decline' (score change of -1 to $+7$, based on a 5% allowable error calculated as described above), 'Mild decline' (-2 to -8), and 'Severe decline' (-9 to -22). While opinion differs as to what amounts to a significant rate of change in MMSE during cognitive decline, we chose to classify a severe decline as a drop in MMSE score of >3 per annum on average, based on information from several previous studies (Clark et al. 1999; Hensel et al. 2007; McCarten et al. 2004). Analysis of categorised MMSE decline was carried out using the 'No decline' class as the comparator.

Decline in mean hand-grip strength was categorised as follows; quintiles of change in mean hand-grip were calculated separately for males and females, after which the respective 20% of males and females displaying the largest decline in mean hand-grip strength were together designated as the 'Severe decline' class (mean hand-grip change of -3.75 kg to -22 kg). The remainder of the cohort was divided into 'No decline' (-1 kg to $+15.5$ kg, based on a 5% allowable error calculated as described above) and 'Mild decline' (-1.25 kg to -6 kg) categories. Analysis of categorised mean hand-grip strength decline was carried out using the 'No decline' class as the comparator.

For all other measures used for analysis, categorisation was carried out by dividing using the cohort into quintiles based on the change in score, and the quintile with the greatest decline in performance designated as the 'Severe decline' class. The remainder of the cohort was divided into 'No decline' and 'Mild decline' classes using the same method as described above for MMSE and mean hand-grip strength. Analysis of categorised variables was carried out using the 'No decline' class as the comparator in all cases.

Statistical analysis

Associations of gene expression with cognitive and physical phenotype measures were assessed using

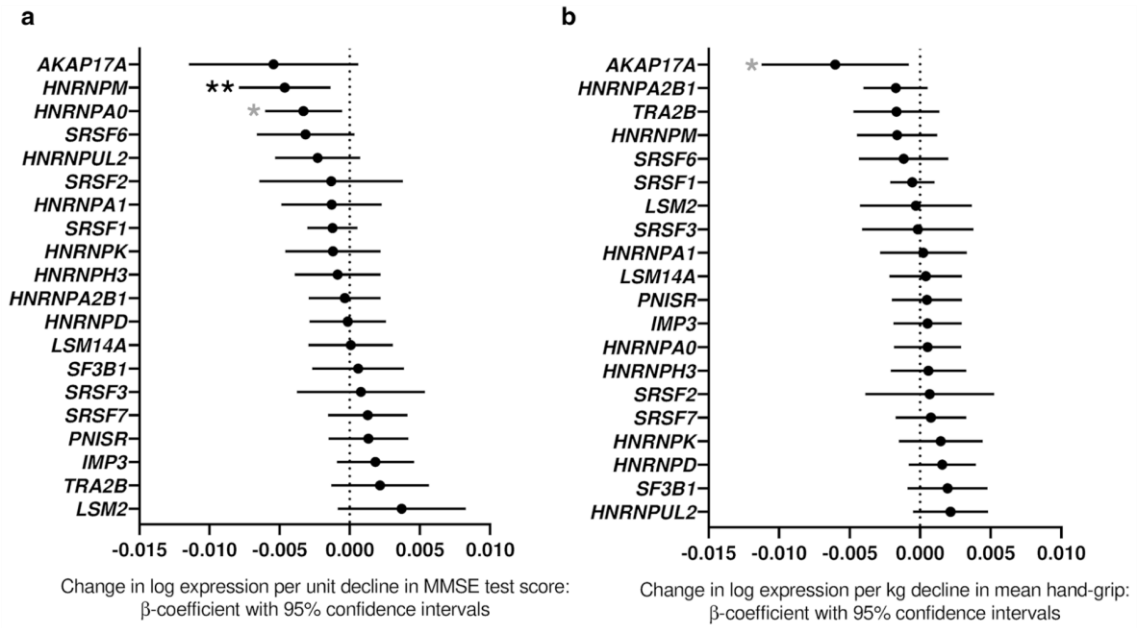

Fig. 1 Associations of splicing factor expression with MMSE score. Forest plots showing splicing factor expression in relation to **a** decline in corrected MMSE scores and **b** mean hand-grip strength in the InCHIANTI human ageing cohort. Individual splicing factors are indicated on the *y-axis* while β-coefficients of change in log expression per unit change in measurements are given on the *x-axis*. Positive values denote an increase in expression with larger decline in score while negative values denote a decrease in expression with larger decline in score. Error bars denote 95% confidence intervals, significance is shown using stars as follows: $*p < 0.05$, $**p < 0.01$. Stars indicated in black denote associations which meet multiple testing thresholds, while those in grey represent nominal associations

multivariate linear regression models. All models were adjusted for age, sex, BMI, smoking (lifetime pack-years), highest education level attained, study site, TLDA batch and cell counts (neutrophils, lymphocytes, monocytes, eosinophils and overall white blood cell count). Regressions were carried out in STATA SE v15.1 (StataCorp, College Station, TX, USA). Pearson correlation tests were carried out in SPSS (IBM, Armonk, NY, USA) to assess relationships between splicing factor expression levels, phenotypic measures and established biomarkers of ageing.

Results

AKAP17A, HNRNPA0 and HNRNPM transcript levels are associated with change in MMSE score

MMSE is a commonly used measure of cognitive decline (Clark et al. 1999; Hensel et al. 2007; McCarten et al. 2004). *HNRNPM* expression showed a significant association with decline in MMSE score in the entire cohort (β-coefficient -0.005, $p = 0.006$), with *HNRNPA0* also showing a nominal association (β-coefficient -0.003, $p = 0.019$). In both cases individuals with lower expression levels at the early time-point (FU3) had subsequently experienced a greater drop in MMSE score (Fig. 1a, Supplementary Table S2). The remaining splicing factor genes did not demonstrate associations between MMSE and expression.

To test the robustness of our findings we carried out four sub-analyses. Similar sub-analyses were also used on all other associations found in the present study and full details can be found in the Methods. In brief, regression models were repeated on the following subsets of data: firstly we removed individuals with low starting scores, secondly only individuals over 70 years of age were included, thirdly any individuals showing an increase in performance over time were

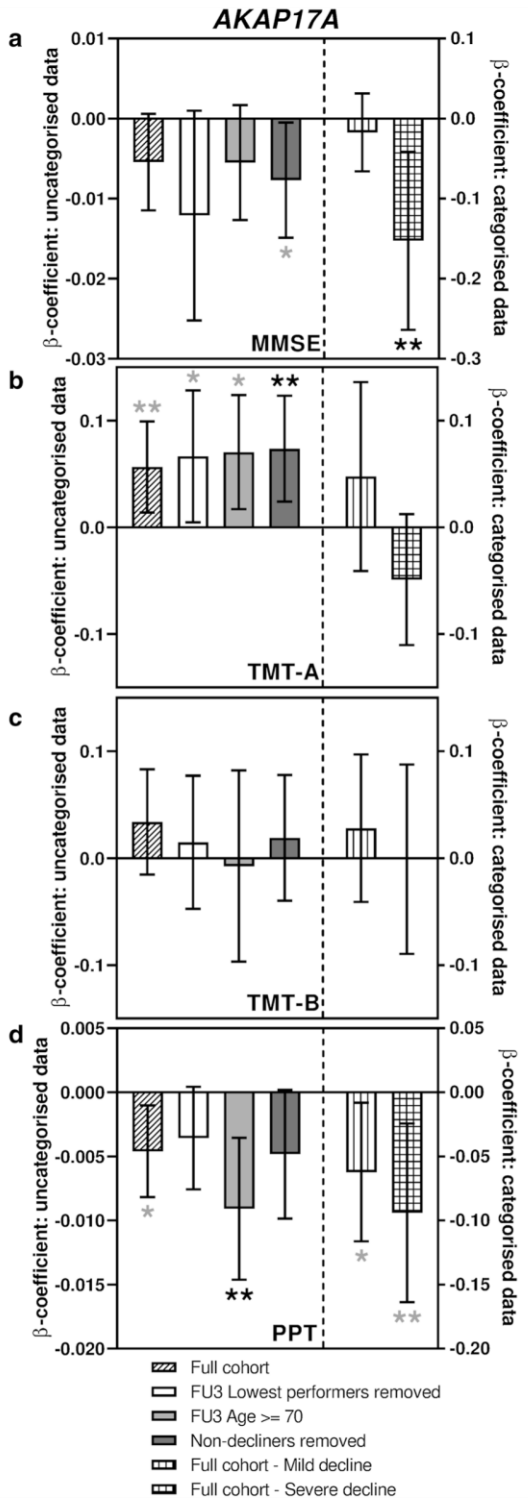

◀**Fig. 2** Sub-analyses of *AKAP17A* associations with measures of cognitive function. Bar charts showing the associations between expression of *AKAP17A* and change in performance in tests of cognitive function. **a** shows associations with MMSE score, **b** shows associations with TMT-A, **c** shows associations with TMT-B and **d** shows associations with PPT. Different sub-analyses are plotted separately as indicated in the figure legend. Error bars denote 95% confidence intervals, significance is shown using stars as follows: $*p < 0.05$, $**p < 0.01$. Stars indicated in black denote associations which meet multiple testing thresholds, while those in grey represent nominal associations

excluded, and finally participants were categorised into 'mild' or 'severe' decline classes.

Although *AKAP17A* showed only a trend with MMSE decline in the initial analysis, the observation that it had the largest β-coefficient, coupled with a suggestive *p* value of 0.077 merited its inclusion in these further analyses. As can be seen in Figs. 2a, 3a and 4a (Supplementary Table S3), both *HNRNPA0* and *HNRNPM* remained at least nominally associated with decline in MMSE score across all sub-analyses, and significantly associated with severe decline in the categorised analysis. *AKAP17A* on the other hand was only nominally associated with decline in MMSE in the sub-analysis excluding the individuals displaying an apparent improvement over time, but in the categorised analysis a significant association was also seen between *AKAP17A* expression and severe decline.

To assess whether these findings represent independent effects or could be driven by co-ordinate expression of the three genes, we carried out correlation analysis. Correlations between the three genes in question were only moderate (R values: *HNRNPA0* & *HNRNPM*: 0.282, *HNRNPA0* & *AKAP17A*: 0.239, *HNRNPM* & *AKAP17A*: 0.440 (Supplementary Table S4).

Expression of HNRNPA0, HNRNPM and AKAP17A transcripts are also associated with two other measures of cognitive ability

The Trail Making Test (TMT) is another widely used test for cognitive assessment which addresses visual scanning, graphomotor speed and executive function (Llinas-Regla et al. 2017). Figures 2b, c, 3b, c and 4b, c (Supplementary table S5) show *AKAP17A* and

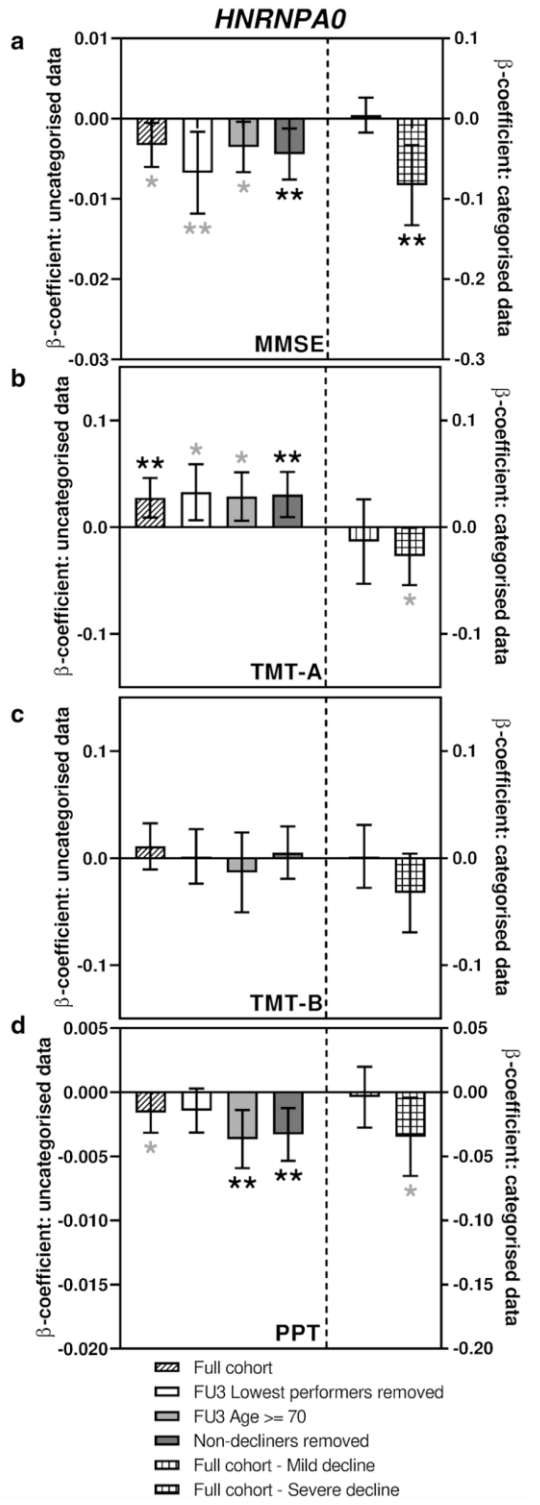

◀**Fig. 3** Sub-analyses of *HNRNPA0* associations with measures of cognitive function. Bar charts showing the associations between expression of *HNRNPA0* and change in performance in tests of cognitive function. **a** shows associations with MMSE score, **b** shows associations with TMT-A, **c** shows associations with TMT-B and **d** shows associations with PPT. Different sub-analyses are plotted separately as indicated in the figure legend. Error bars denote 95% confidence intervals, significance is shown using stars as follows: $*p < 0.05$, $**p < 0.01$. Stars indicated in black denote associations which meet multiple testing thresholds, while those in grey represent nominal associations

HNRNPA0 transcript levels were at least nominally associated with increased time to complete TMT-A, both in the full cohort (β-coefficients 0.057 and 0.028, $p = 0.009$ and 0.004 for *AKAP17A* and *HNRNPA0* respectively) and in all sub-analyses with the exception of the categorised analysis for *AKAP17A*. *HNRNPM* expression was nominally associated with increased time to complete TMT-B, but only in the full cohort (β-coefficient 0.026, $p = 0.036$) and categorised analyses. In all cases, lower expression levels were associated with an increase in the time taken to complete the test (i.e. a decline in performance).

The Purdue Pegboard Test (PPT) was originally developed as a tool to evaluate fine manual dexterity but has since been used for assessments of cognitive function (Brown et al. 1993; Zakzanis et al. 1998). As shown in Figs. 2d, 3d and 4d (Supplementary table S5), all three transcripts were nominally associated with a performance decline in the full cohort (β-coefficients − 0.005, − 0.002 and − 0.002, $p = 0.012$, 0.047 and 0.044 for *AKAP17A*, *HNRNPA0* and *HNRNPM* respectively). While *AKAP17A* and *HNRNPA0* transcript levels were found to be significantly associated with performance decline in some of the sub-analyses, *HNRNPM* showed no such further associations.

Pearson correlations were also carried out to assess relationships between the aspects of cognition being measured by MMSE, TMT and PPT. Correlations between the measures were relatively weak (R values range from − 0.381 to 0.322, see Supplementary Table S6a).

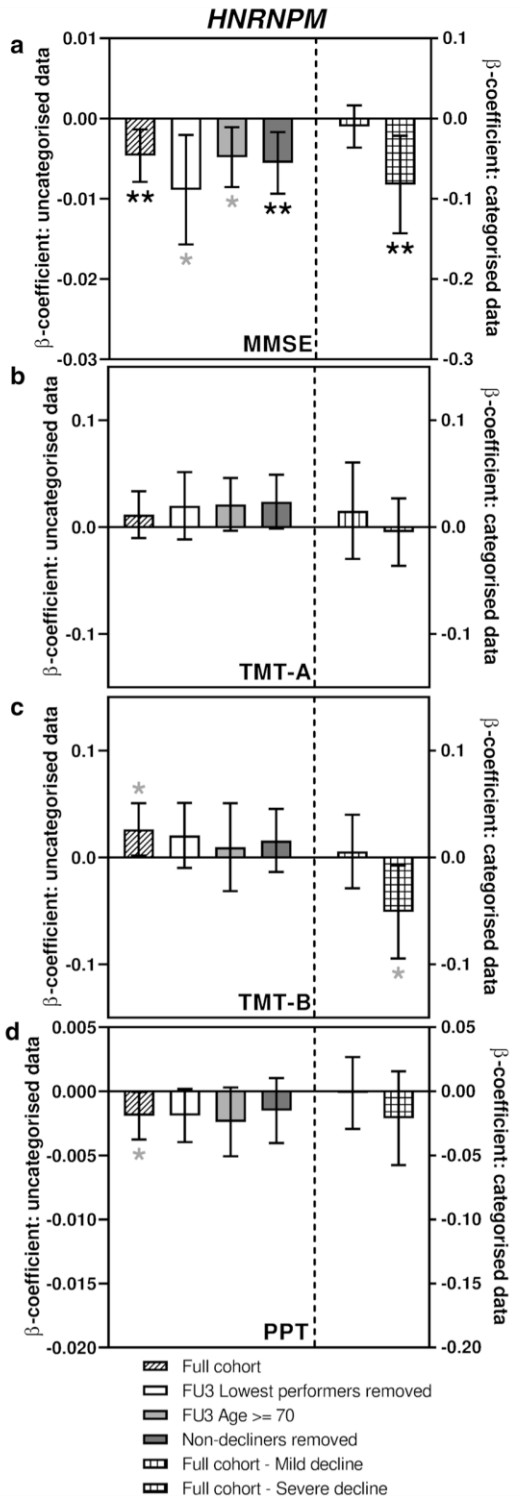

◀**Fig. 4** Sub-analyses of *HNRNPM* associations with measures of cognitive function. Bar charts showing the associations between expression of *HNRNPM* and change in performance in tests of cognitive function. **a** shows associations with MMSE score, **b** shows associations with TMT-A, **c** shows associations with TMT-B and **d** shows associations with PPT. Different sub-analyses are plotted separately as indicated in the figure legend. Error bars denote 95% confidence intervals, significance is shown using stars as follows: $*p < 0.05$, $**p < 0.01$. Stars indicated in black denote associations which meet multiple testing thresholds, while those in grey represent nominal associations

Expression of AKAP17A transcript is associated with mean hand-grip strength

Hand-grip strength, a measure of muscle weakness, is a useful indicator of physical functioning and health-related quality of life in the elderly (Bohannon 2015). Of the transcripts tested, only *AKAP17A* transcript levels were nominally associated with decline in hand-grip strength between FU3 and FU4 (β-coefficient − 0.006, $p = 0.023$) (Fig. 1b, Supplementary Table S7). As shown in Fig. 5a (Supplementary Table S8), robustness testing of this finding revealed one nominal and one significant association in the sub-analyses, and no associations with the categorised data.

Expression of AKAP17A transcript is also associated with two other measures of physical ability

The Epidemiologic Studies of the Elderly-Short Physical Performance Battery (EPESE-SPPB) is a validated measure of lower body function and is predictive of several important health outcomes, including mortality (Pavasini et al. 2016). *AKAP17A* expression was found to be nominally associated with decline in the EPESE-SPPB composite score (β-coefficient − 0.011, $p = 0.048$), and as can be seen in Fig. 5b (Supplementary Table S9), subsequent testing showed it also to be nominally associated in two of the sub-analyses.

Another measure of physical ability that was available in the data set was the calculated speed (m/s) during a timed 400 m fast walking test. Once again, *AKAP17A* expression was found to be nominally associated with decline in walking speed (β-

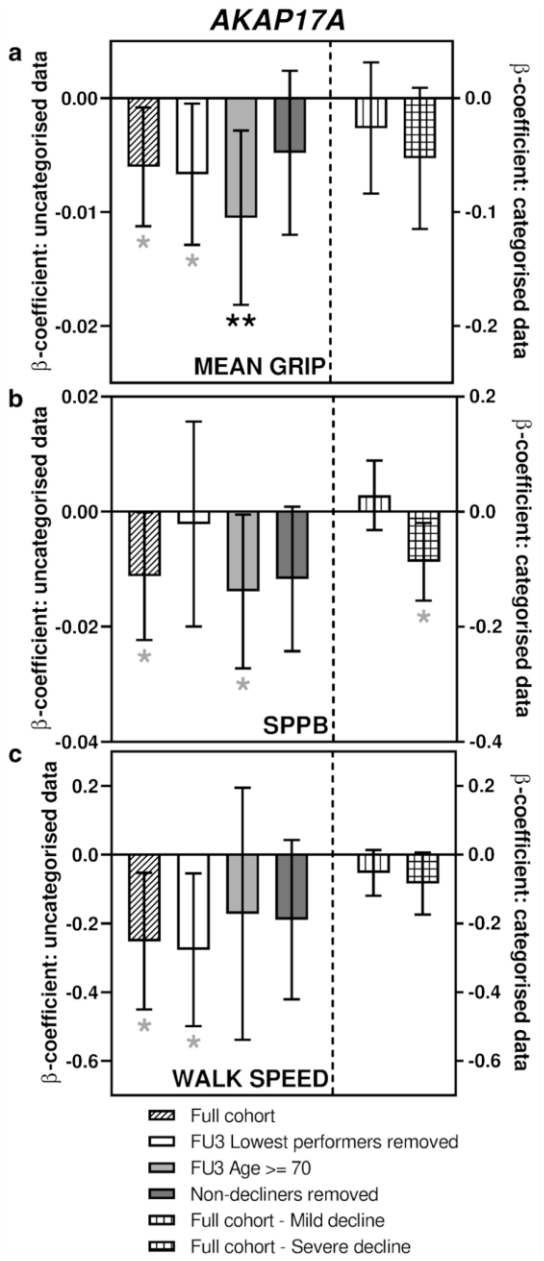

◀**Fig. 5** Sub-analyses of *AKAP17A* associations with measures of physical ability. Bar charts showing the associations between expression of *AKAP17A* and change in performance in tests of physical ability. **a** shows associations with mean hand-grip strength, **b** shows associations with the EPESE-SPPB composite score and **c** shows associations with calculated speed (m/s) during a 400 m fast walking test. Different sub-analyses are plotted separately as indicated in the figure legend. Error bars denote 95% confidence intervals, significance is shown using stars as follows: $*p < 0.05$, $**p < 0.01$. Stars indicated in black denote associations which meet multiple testing thresholds, while those in grey represent nominal associations

coefficient − 0.252, $p = 0.013$). Figure 5c (Supplementary Table S9) shows that this nominal association only held true in one sub-analysis.

Finally, Pearson correlations were carried out to assess relationships between the aspects of physical ability being measured. Again, correlations between the measures were relatively weak (R values range from 0.217 to 0.357, see Supplementary Table S6b).

HNRNPA0, *HNRNPM* and *AKAP17A* transcripts show correlations with known biomarkers of ageing

To test whether these transcripts might share expression patterns with levels of recognised biomarkers of ageing (Xia et al. 2017), where such measures were available in our dataset, we carried out Pearson correlations between transcript expression levels and measurements of interleukin-6 (IL-6), albumin and total erythrocyte numbers. Significant correlations were found between: *AKAP17A* expression and IL-6 levels (R value = 0.144, p = 0.013); *HNRNPA0* expression and both IL-6 and erythrocyte number (R values = − 0.200 and 0.115, p = 0.001 and 0.048 respectively); *HNRNPM* expression and albumin levels (R value = − 0.137, p = 0.018).

Discussion

The human genome is equipped with mechanisms to generate transcriptomic diversity from a relatively small DNA complement (Nilsen and Graveley 2010). This transcriptomic diversity underpins our ability to respond appropriately to internal and external environmental challenges, while the failure of such cellular stress responses contributes to ageing itself and to age-related diseases (Kourtis and Tavernarakis 2011). Alternative splicing is one of the major mechanisms for generation of such diversity (Kelemen et al. 2013), and is regulated by the combinatorial binding of a set of trans-acting activating and inhibitory proteins

termed splicing factors to *cis*- sequence control elements (Smith and Valcarcel 2000). Dysregulation of splicing factor expression occurs with human ageing at the epidemiological and cellular levels (Harries et al. 2011; Holly et al. 2013), and is also associated with longevity in animal models (Lee et al. 2016). These changes are drivers of cellular ageing, since restoration of splicing factor levels is able to reverse multiple senescence phenotypes in aged human cells in vitro (Latorre et al. 2017, 2018a, c). In the work described here, we provide evidence that changes in splicing factor expression are not only present in in vitro data, but may also contribute to the development of downstream ageing phenotypes in older people. We report predictive associations between the transcript expression levels of three splicing factor genes, *HNRNPM*, *HNRNPA0* and *AKAP17A* with several ageing phenotypes in a human population study, the InCHIANTI study of Aging (Ferrucci et al. 2000).

HNRNPM, *HNRNPA0* and *AKAP17A* transcript levels were predictively associated with a decline in MMSE score as well as a decline in performance on the Trail-Making Test parts A & B and the Purdue Pegboard Test. Associations between transcript expression of all three genes and ageing phenotypes were strongest in the individuals with severe cognitive decline as measured by MMSE. It is possible that these three splicing factors are not independently associated with the traits in question, but correlations between them are only moderate. *HNRNPM* and *HNRNPA0* encode splicing inhibitor proteins that have roles in determining the splicing patterns of several genes with relevance to brain physiology. TDP-43 is one of the major proteins involved with Amyotrophic lateral sclerosis (ALS) and Frontotemporal Dementia (FTD) in humans (Orr 2011). HNRNPM and HNRNPA0 are both known to interact with TDP-43 (Couthouis et al. 2011), and mutations in other HNRNPs have been described in patients with ALS (Calini et al. 2013). In *Drosophila* species, depletion of the fly homologue of *HNRNPM* (*Rump*) is associated with loss of neuronal dendritic terminal branches; a phenotype that could be partially restored by the addition of a Rump transgene (Xu et al. 2013). HNRNPM has also been demonstrated to directly regulate alternative splicing of the dopamine receptor 2 (*DRD2*) gene, whereby it inhibits the inclusion of exon 6 (Park et al. 2011). *DRD2* splice variants have previously been implicated with schizophrenia and impaired cognitive function in humans (Cohen et al. 2016; Kaalund et al. 2014). Similarly, increased protein expression of HNRNPA0 in hippocampus has been shown to be associated with memory formation and consolidation in mice (Ferreira et al. 2016). *AKAP17A*, otherwise known as *SFSR17A*, is an X-linked gene encoding a splicing regulatory factor that also has roles in targeting protein kinase A anchoring protein to splicing factor compartments (Jarnaess et al. 2009). It is a poorly characterised gene, but has been previously associated with the development of Alzheimer's disease; sequences deriving from this gene appear twice amongst probes that best differentiate Alzheimer's disease brain samples from controls (Lunnon et al. 2013).

AKAP17A was also found to be associated with decline over time in measures of physical function, although the sporadic nature of replication of this association in the sub-analyses suggests that either this finding is less robust, or the measurements themselves are more subject to variation. No functional role for *AKAP17A* has previously been reported in relation to muscle function.

Although the changes reported here represent changes in peripheral blood, similar changes to splicing regulation have been reported in senescent cell lines from other, less accessible tissues (Latorre et al. 2017, 2018b). Splicing factor expression is ubiquitous, although changes in the exact composition of the splicing factor milieu will occur from tissue to tissue. We postulate that the expression patterns of splicing factors in peripheral blood may at least partly reflect changes in less accessible tissues. We previously demonstrated that senescence-related changes in splicing factor expression in endothelial cells and cardiomyocytes are preserved in human peripheral blood, and resultant changes in the alternative splicing of the *VEGFA* gene are associated with incident and prevalent coronary artery disease (Latorre et al. 2018b). Both cognitive decline and deterioration in muscle strength also have a significant inflammatory component (Harries et al. 2012; Marottoli et al. 2017).

Our study has several strengths; the use of a longitudinal population study has allowed some assessment of causality of effect. Placed in the context of the known dysregulation of splicing factor expression in human and animal ageing, their associations with longevity in both animals and humans (Heintz et al. 2017; Lee et al. 2016) and the observation that

correction of splicing factor levels is sufficient to reverse senescence phenotypes in vitro (Latorre et al. 2017) suggests that these changes may be a driver of ageing rather than an effect. The data presented here suggest that the presence of dysregulated splicing factor transcripts before the emergence of overt disease in peripheral blood may contribute to the development of age-related phenotypes such as cognitive decline. Our finding that expression of these transcripts correlate with established biomarkers of ageing is also suggestive that they may be indicative of future outcomes. Our study is not without limitations however; we have only assessed splicing factor expression at the level of the mRNA transcript for reasons of practicality. It is possible that processes such as post-transcriptional regulation of mRNA transcripts or altered protein kinetics may also contribute and would not be identified in our study. However, the observation of phenotypic changes in senescent cells in vitro strongly suggests that these changes may also occur at the protein level. Our study cohort is also relatively small in comparison to some resources. It is however exquisitely well characterised and features longitudinal waves of samples which many other studies do not. These observations require replication in an additional dataset in the future. However, we have measures from two waves of the study, which although they comprise the same people, represent completely separate sample collection, sample handling and analytical subsets.

We recognise that although an adjustment for multiple testing has been applied at the level of phenotype (i.e. accounting for six measurements) throughout this study, there remains a risk of Type I error in the results presented by using a significance level of $p = 0.0083$ as the corrected threshold. However, the genes tested represented an a priori list on the basis of known associations with age or cellular senescence (Harries et al. 2011; Holly et al. 2013), and we show here that although moderate, correlations do exist between splicing factor expression levels as well as between the measured phenotypic outcomes (Supplementary Tables S4 and S6), all of which complicate a sensible implementation of multiple testing criteria. It is also possible that the statistical power of this study may be limited given the number of samples and the observed effect sizes, leading to potential inflation of Type II error. Therefore, either Bonferroni or Benjamini–Hochberg correction for both the number of genes and phenotypes seem likely to be overly stringent for this dataset, however the issue of multiple testing persists, so without independent validation of the findings presented here, we must be conservative with any interpretation of these results.

We present here evidence to suggest that expression levels of *HNRNPM*, *HNRNPA0* and *AKAP17A* genes may be associated with cognitive decline, whilst *AKAP17A* levels may be associated with decline in physical performance in a human population. These findings suggest that the age-related splicing factor changes we have previously reported in vitro and in vivo may contribute to the development of downstream ageing phenotypes in older humans. Given validation of these findings in an independent data set, splicing factor expression could comprise a relatively non-invasive biomarker of cognitive decline or physical ability in the future, which could be assessed from samples collected from routine screening of the vulnerable people in the population.

Acknowledgements The authors acknowledge the technical assistance of Federica Bighi and Robert Morse for help with the RNA extractions. We are also grateful to Eleonora Talluri for collection of RNA samples and anthropometric/clinical data. This work was funded by the Velux Stiftung Foundation (Grant Number 822) and supported in part by the Intramural Research Program of the NIH, National institute on Aging. The authors declare no competing interests.

Author contributions LH managed the project, designed the experiments and co-wrote the manuscript. BL coordinated and performed experiments, performed the data analysis and co-wrote the manuscript. LP carried out cross-checks during cohort selection, advised on statistical techniques and reviewed the manuscript. SB oversaw participant interviews and sample collection. LF provided access to the InCHIANTI cohort and NIA resources. DM contributed to data analysis and reviewed the manuscript.

Compliance with ethical standards

Ethical approval Ethical approval was granted by the Instituto Nazionale Riposo e Cura Anziani institutional review board in Italy. Methods were carried out in accordance with the relevant guidelines and regulations.

Informed consent Informed consent was obtained from all participants.

References

Bohannon RW (2015) Muscle strength: clinical and prognostic value of hand-grip dynamometry. Curr Opin Clin Nutr Metab Care 18:465–470. https://doi.org/10.1097/MCO.0000000000000202

Brown RG, Jahanshahi M, Marsden CD (1993) The execution of bimanual movements in patients with Parkinson's, Huntington's and cerebellar disease. J Neurol Neurosurg Psychiatry 56:295–297. https://doi.org/10.1136/jnnp.56.3.295

Calini D et al (2013) Analysis of hnRNPA1, A2/B1, and A3 genes in patients with amyotrophic lateral sclerosis. Neurobiol Aging 34:2695.e2611. https://doi.org/10.1016/j.neurobiolaging.2013.05.025

Cartegni L, Chew SL, Krainer AR (2002) Listening to silence and understanding nonsense: exonic mutations that affect splicing. Nat Rev Genet 3:285–298

Celotto AM, Graveley BR (2001) Alternative splicing of the Drosophila Dscam pre-mRNA is both temporally and spatially regulated. Genetics 159:599–608

Chen FX, Smith ER, Shilatifard A (2018) Born to run: control of transcription elongation by RNA polymerase II. Nat Rev Mol Cell Biol 19:464–478. https://doi.org/10.1038/s41580-018-0010-5

Clark CM et al (1999) Variability in annual Mini-Mental State Examination score in patients with probable Alzheimer disease: a clinical perspective of data from the Consortium to Establish a Registry for Alzheimer's Disease. Arch Neurol 56:857–862

Cohen OS et al (2016) A splicing-regulatory polymorphism in DRD2 disrupts ZRANB2 binding, impairs cognitive functioning and increases risk for schizophrenia in six Han Chinese samples. Mol Psychiatry 21:975–982. https://doi.org/10.1038/mp.2015.137

Couthouis J et al (2011) A yeast functional screen predicts new candidate ALS disease genes. Proc Natl Acad Sci USA 108:20881–20890. https://doi.org/10.1073/pnas.1109434108

Cruz-Jentoft AJ et al (2010) Sarcopenia: European consensus on definition and diagnosis: report of the European Working Group on Sarcopenia in older people. Age Ageing 39:412–423. https://doi.org/10.1093/ageing/afq034

Disher K, Skandalis A (2007) Evidence of the modulation of mRNA splicing fidelity in humans by oxidative stress and p53. Genome 50:946–953

Ferreira E, Shaw DM, Oddo S (2016) Identification of learning-induced changes in protein networks in the hippocampi of a mouse model of Alzheimer's disease. Transl Psychiatry 6:e849. https://doi.org/10.1038/tp.2016.114

Ferrucci L, Bandinelli S, Benvenuti E, Di Iorio A, Macchi C, Harris TB, Guralnik JM (2000) Subsystems contributing to the decline in ability to walk: bridging the gap between epidemiology and geriatric practice in the InCHIANTI study. J Am Geriatr Soc 48:1618–1625

Grumont RJ, Gerondakis S (1994) Alternative splicing of RNA transcripts encoded by the murine p105 NF-kappa B gene generates I kappa B gamma isoforms with different inhibitory activities. Proc Natl Acad Sci USA 91:4367–4371

Guillaumet-Adkins A, Yanez Y, Peris-Diaz MD, Calabria I, Palanca-Ballester C, Sandoval J (2017) Epigenetics and oxidative stress in aging. Oxid Med Cell Longev 2017:9175806. https://doi.org/10.1155/2017/9175806

Guralnik JM et al (1994) A short physical performance battery assessing lower extremity function: association with self-reported disability and prediction of mortality and nursing home admission. J Gerontol 49:M85–94

Harries LW et al (2011) Human aging is characterized by focused changes in gene expression and deregulation of alternative splicing. Aging Cell 10:868–878. https://doi.org/10.1111/j.1474-9726.2011.00726.x

Harries LW et al (2012) CCAAT-enhancer-binding protein-beta expression in vivo is associated with muscle strength. Aging Cell 11:262–268. https://doi.org/10.1111/j.1474-9726.2011.00782.x

Harvey R, Dezi V, Pizzinga M, Willis AE (2017) Post-transcriptional control of gene expression following stress: the role of RNA-binding proteins. Biochem Soc Trans 45:1007–1014. https://doi.org/10.1042/bst20160364

Heintz C et al (2017) Splicing factor 1 modulates dietary restriction and TORC1 pathway longevity in *C. elegans*. Nature 541:102–106. https://doi.org/10.1038/nature20789

Hensel A, Angermeyer MC, Riedel-Heller SG (2007) Measuring cognitive change in older adults: reliable change indices for the Mini-Mental State Examination. J Neurol Neurosurg Psychiatry 78:1298–1303. https://doi.org/10.1136/jnnp.2006.109074

Holly AC, Melzer D, Pilling LC, Fellows AC, Tanaka T, Ferrucci L, Harries LW (2013) Changes in splicing factor expression are associated with advancing age in man. Mech Ageing Dev 134:356–366. https://doi.org/10.1016/j.mad.2013.05.006

Jarnaess E et al (2009) Splicing factor arginine/serine-rich 17A (SFRS17A) is an A-kinase anchoring protein that targets protein kinase A to splicing factor compartments. J Biol Chem 284:35154–35164. https://doi.org/10.1074/jbc.m109.056465

Kaalund SS et al (2014) Contrasting changes in DRD1 and DRD2 splice variant expression in schizophrenia and affective disorders, and associations with SNPs in post-mortem brain. Mol Psychiatry 19:1258–1266. https://doi.org/10.1038/mp.2013.165

Kelemen O, Convertini P, Zhang Z, Wen Y, Shen M, Falaleeva M, Stamm S (2013) Function of alternative splicing. Gene 514:1–30. https://doi.org/10.1016/j.gene.2012.07.083

Kirkland JL, Stout MB, Sierra F (2016) Resilience in aging mice. J Gerontol A 71:1407–1414. https://doi.org/10.1093/gerona/glw086

Kourtis N, Tavernarakis N (2011) Cellular stress response pathways and ageing: intricate molecular relationships. EMBO J 30:2520–2531. https://doi.org/10.1038/emboj.2011.162

Latorre E, Harries LW (2017) Splicing regulatory factors, ageing and age-related disease. Ageing Res Rev 36:165–170. https://doi.org/10.1016/j.arr.2017.04.004

Latorre E et al (2017) Small molecule modulation of splicing factor expression is associated with rescue from cellular senescence. BMC Cell Biol 18:31. https://doi.org/10.1186/s12860-017-0147-7

Latorre E, Ostler EO, Faragher RGA, Harries LW (2018a) FOXO1 and ETV6 genes may represent novel regulators of splicing factor expression in cellular senescence. FASEB J 33:1086–1097

Latorre E, Pilling LC, Lee BP, Bandinelli S, Melzer D, Ferrucci L, Harries LW (2018b) The VEGFA156b isoform is dysregulated in senescent endothelial cells and may be associated with prevalent and incident coronary heart disease. Clin Sci (Lond) 132:313–325. https://doi.org/10.1042/cs20171556

Latorre E, Torregrossa R, Wood ME, Whiteman M, Harries LW (2018c) Mitochondria-targeted hydrogen sulfide attenuates endothelial senescence by selective induction of splicing factors HNRNPD and SRSF2. Aging (Albany NY) 10:1666–1681. https://doi.org/10.18632/aging.101500

Lee BP et al (2016) Changes in the expression of splicing factor transcripts and variations in alternative splicing are associated with lifespan in mice and humans. Aging Cell 15:903–913. https://doi.org/10.1111/acel.12499

Llinas-Regla J, Vilalta-Franch J, Lopez-Pousa S, Calvo-Perxas L, Torrents Rodas D, Garre-Olmo J (2017) The trail making test. Assessment 24:183–196. https://doi.org/10.1177/1073191115602552

Lunnon K et al (2013) A blood gene expression marker of early Alzheimer's disease. J Alzheimers Dis 33:737–753. https://doi.org/10.3233/JAD-2012-121363

Marottoli FM, Katsumata Y, Koster KP, Thomas R, Fardo DW, Tai LM (2017) Peripheral inflammation, apolipoprotein E4, and amyloid-beta interact to induce cognitive and cerebrovascular dysfunction. ASN Neuro. https://doi.org/10.1177/1759091417719201

Martinez NM, Lynch KW (2013) Control of alternative splicing in immune responses: many regulators, many predictions, much still to learn. Immunol Rev 253:216–236. https://doi.org/10.1111/imr.12047

Mastrangelo AM, Marone D, Laido G, De Leonardis AM, De Vita P (2012) Alternative splicing: enhancing ability to cope with stress via transcriptome plasticity. Plant Sci 185–186:40–49. https://doi.org/10.1016/j.plantsci.2011.09.006

McCarten JR, Rottunda SJ, Kuskowski MA (2004) Change in the mini-mental state exam in Alzheimer's disease over 2 years: the experience of a dementia clinic. J Alzheimers Dis 6:11–15

Nilsen TW, Graveley BR (2010) Expansion of the eukaryotic proteome by alternative splicing. Nature 463:457–463. https://doi.org/10.1038/nature08909

Orr HT (2011) FTD and ALS: genetic ties that bind. Neuron 72:189–190. https://doi.org/10.1016/j.neuron.2011.10.001

Pan Q, Shai O, Lee LJ, Frey BJ, Blencowe BJ (2008) Deep surveying of alternative splicing complexity in the human transcriptome by high-throughput sequencing. Nat Genet 40:1413–1415

Park E et al (2011) Regulatory roles of heterogeneous nuclear ribonucleoprotein M and Nova-1 protein in alternative splicing of dopamine D2 receptor pre-mRNA. J Biol Chem 286:25301–25308. https://doi.org/10.1074/jbc.m110.206540

Pavasini R et al (2016) Short Physical Performance Battery and all-cause mortality: systematic review and meta-analysis. BMC Med 14:215. https://doi.org/10.1186/s12916-016-0763-7

Rasmussen JL (1988) Evaluating outlier identification tests: Mahalanobis D squared and Comrey Dk. Multivar Behav Res 23:189–202. https://doi.org/10.1207/s15327906mbr2302_4

Schorr A, Carter C, Ladiges W (2018) The potential use of physical resilience to predict healthy aging. Pathobiol Aging Age Relat Dis 8:1403844. https://doi.org/10.1080/20010001.2017.1403844

Smith CW, Valcarcel J (2000) Alternative pre-mRNA splicing: the logic of combinatorial control. Trends Biochem Sci 25:381–388

Varadhan R, Seplaki CL, Xue QL, Bandeen-Roche K, Fried LP (2008) Stimulus-response paradigm for characterizing the loss of resilience in homeostatic regulation associated with frailty. Mech Ageing Dev 129:666–670. https://doi.org/10.1016/j.mad.2008.09.013

Winick-Ng W, Rylett RJ (2018) Into the fourth dimension: dysregulation of genome architecture in aging and Alzheimer's disease. Front Mol Neurosci 11:60. https://doi.org/10.3389/fnmol.2018.00060

Xia X, Chen W, McDermott J, Han JJ (2017) Molecular and phenotypic biomarkers of aging. F1000Res 6:860. https://doi.org/10.12688/f1000research.10692.1

Xie F, Xiao P, Chen D, Xu L, Zhang B (2012) miRDeepFinder: a miRNA analysis tool for deep sequencing of plant small RNAs. Plant Mol Biol. https://doi.org/10.1007/s11103-012-9885-2

Xu X, Brechbiel JL, Gavis ER (2013) Dynein-dependent transport of nanos RNA in Drosophila sensory neurons requires Rumpelstiltskin and the germ plasm organizer Oskar. J Neurosci 33:14791–14800. https://doi.org/10.1523/JNEUROSCI.5864-12.2013

Zakzanis KK, Leach L, Freedman M (1998) Structural and functional meta-analytic evidence for fronto-subcortical system deficit in progressive supranuclear palsy. Brain Cogn 38:283–296. https://doi.org/10.1006/brcg.1998.1036

Appendix 2: Copyright Permissions

ELSEVIER: LICENSE FOR FIGURE 1.2
TERMS AND CONDITIONS AVAILABLE ON REQUEST
Viewed: Dec 14, 2019

This Agreement between Mr. Benjamin Lee ("You") and Elsevier ("Elsevier") consists of your license details and the terms and conditions provided by Elsevier and Copyright Clearance Center.

License Number	4716101122519
License date	Nov 25, 2019
Licensed Content Publisher	Elsevier
Licensed Content Publication	Cell
Licensed Content Title	The Hallmarks of Aging
Licensed Content Author	Carlos López-Otín,Maria A. Blasco,Linda Partridge,Manuel Serrano,Guido Kroemer
Licensed Content Date	Jun 6, 2013
Licensed Content Volume	153
Licensed Content Issue	6
Licensed Content Pages	24
Start Page	1194
End Page	1217
Type of Use	reuse in a thesis/dissertation
Portion	figures/tables/illustrations
Number of figures/tables/illustrations	1
Format	both print and electronic
Are you the author of this Elsevier article?	No
Will you be translating?	No
Title	Changes in RNA regulatory processes during mammalian ageing
Institution name	University of Exeter
Expected presentation date	Dec 2019
Portions	Figure 1
Requestor Location	Mr. Benjamin Lee RILD Building RD&E NHSFT Campus Barrack Road Exeter, Devon EX2 5DW United Kingdom Attn: Mr. Benjamin Lee
Publisher Tax ID	GB 494 6272 12
Total	0.00 GBP

ELSEVIER: LICENSE FOR FIGURE 1.5
TERMS AND CONDITIONS AVAILABLE ON REQUEST
Viewed: Dec 14, 2019

This Agreement between Mr. Benjamin Lee ("You") and Elsevier ("Elsevier") consists of your license details and the terms and conditions provided by Elsevier and Copyright Clearance Center.

License Number	4725501326983
License date	Dec 10, 2019
Licensed Content Publisher	Elsevier
Licensed Content Publication	Cell
Licensed Content Title	Alternative Splicing: New Insights from Global Analyses
Licensed Content Author	Benjamin J. Blencowe
Licensed Content Date	Jul 14, 2006
Licensed Content Volume	126
Licensed Content Issue	1
Licensed Content Pages	11
Start Page	37
End Page	47
Type of Use	reuse in a thesis/dissertation
Portion	figures/tables/illustrations
Number of figures/tables/illustrations	1
Format	both print and electronic
Are you the author of this Elsevier article?	No
Will you be translating?	No
Title	Changes in RNA regulatory processes during mammalian ageing
Institution name	University of Exeter
Expected presentation date	Dec 2019
Portions	Figure 2. AS Events in Metazoan Transcripts
Requestor Location	Mr. Benjamin Lee RILD Building RD&E NHSFT Campus Barrack Road Exeter, Devon EX2 5DW United Kingdom Attn: Mr. Benjamin Lee
Publisher Tax ID	GB 494 6272 12
Total	0.00 USD

ELSEVIER: LICENSE FOR FIGURE 1.7
TERMS AND CONDITIONS AVAILABLE ON REQUEST
Viewed: Dec 14, 2019

This Agreement between Mr. Benjamin Lee ("You") and Elsevier ("Elsevier") consists of your license details and the terms and conditions provided by Elsevier and Copyright Clearance Center.

License Number	4727031227944
License date	Dec 13, 2019
Licensed Content Publisher	Elsevier
Licensed Content Publication	Trends in Cell Biology
Licensed Content Title	Does Longer Lifespan Mean Longer Healthspan?
Licensed Content Author	Malene Hansen,Brian K. Kennedy
Licensed Content Date	Aug 1, 2016
Licensed Content Volume	26
Licensed Content Issue	8
Licensed Content Pages	4
Start Page	565
End Page	568
Type of Use	reuse in a thesis/dissertation
Portion	figures/tables/illustrations
Number of figures/tables/illustrations	1
Format	both print and electronic
Are you the author of this Elsevier article?	No
Will you be translating?	No
Title	Changes in RNA regulatory processes during mammalian ageing
Institution name	University of Exeter
Expected presentation date	Dec 2019
Portions	Figure 1
Requestor Location	Mr. Benjamin Lee RILD Building RD&E NHSFT Campus Barrack Road Exeter, Devon EX2 5DW United Kingdom Attn: Mr. Benjamin Lee
Publisher Tax ID	GB 494 6272 12
Total	0.00 USD

American Association for Clinical Chemistry, Inc: License for Figure 2.2

Terms and Conditions available on request

This is a License Agreement between Mr. Benjamin Lee ("You") and American Association for Clinical Chemistry, Inc ("Publisher") provided by Copyright Clearance Center ("CCC"). The license consists of your order details, the terms and conditions provided by American Association for Clinical Chemistry, Inc, and the CCC terms and conditions.

Order Date
16-Dec-2019
Order license ID
1009297-1
ISSN
1530-8561
Type of Use
Republish in a thesis/dissertation
Publisher
P.B. HOEBER,
Portion
Chart/graph/table/figure
Licensed Content
Publication Title
Clinical chemistry
Author/Editor
HighWire Press., American Association for Clinical Chemistry.
Date
01/01/1955
Language
English
Country
United States of America
Rightsholder
American Association for Clinical Chemistry, Inc
Publication Type
e-Journal
URL
http://www.clinchem.org/
Request Details
Portion Type
Chart/graph/table/figure
Number of charts / graphs / tables / figures requested
1
Format (select all that apply)
Print, Electronic
Who will republish the content?
Academic institution
Duration of Use
Life of current edition
Lifetime Unit Quantity
Up to 499
Rights Requested
Main product
Distribution
Worldwide
Translation
Original language of publication
Copies for the disabled?
No
Minor editing privileges?
No
Incidental promotional use?
No
Currency
GBP

New Work Details
Title
Changes in RNA regulatory processes during mammalian ageing
Instructor name
Prof. L. W. Harries
Institution name
University of Exeter
Expected presentation date
2019-12-23

Additional Details
Order reference number
N/A
The requesting person / organization to appear on the license
Mr. Benjamin Lee
Reuse Content Details
Title, description or numeric reference of the portion(s)
Figure 1
Editor of portion(s)
N/A
Volume of serial or monograph
Vol 46, No. 1
Page or page range of portion
p25
Title of the article/chapter the portion is from
5′ Nuclease Assays for the Loci CCR5-+/Δ32, CCR2-V64I, and SDF1-G801A Related to Pathogenesis of AIDS
Author of portion(s)
HighWire Press.; American Association for Clinical Chemistry.
Issue, if republishing an article from a serial
N/A
Publication date of portion
2000-01-01